# CHARACTERISTICS AND IMPLICATIONS OF EARTHQUAKE-INDUCED SEDIMENTARY DEFORMATION FEATURES (SEISMITES) IN THE GREEN RIVER FORMATION (EOCENE), WYOMING, COLORADO, AND UTAH, USA

A Thesis Submitted to the College of
Graduate Studies and Research
in Partial Fulfillment of the Requirements
for the Degree of Doctor of Philosophy
in the Department of Geological Sciences,
University of Saskatchewan,
Saskatoon

By

BALÁZS TÖRŐ

## PERMISSION TO USE

In presenting this thesis in partial fulfillment of the requirements for a Postgraduate degree from the University of Saskatchewan, I agree that the Libraries of this University may make it freely available for inspection. I further agree that permission for copying of this thesis in any manner, in whole or in part, for scholarly purposes may be granted by the professor or professors who supervised my thesis work or, in their absence, by the Head of the Department of Geological Sciences or the Dean of the College of Graduate Studies and Research, in which my thesis work was done. It is understood that any copying or publication or use of this thesis or parts thereof for financial gain shall not be allowed without my written permission. It is also understood that due recognition shall be given to me and to the University of Saskatchewan in any scholarly use which may be made of any material in my thesis.

Requests for permission to copy or to make other uses of materials in this thesis in whole or part should be addressed to:

Head of the Department of Geological Sciences
University of Saskatchewan
114 Science Place
Saskatoon, Saskatchewan, S7N 5E2
CANADA

## ABSTRACT

Lacustrine sediments of the Green River Formation were deposited during Eocene (53-45 Ma) in interconnected foreland basins along the Front Range of the Rocky Mountains across an area of > 62 150 $km^2$ in present-day Wyoming, Colorado and Utah, USA. These deposits are up to 2 km thick, dominated by finely laminated carbonate mudstones. Deposition was taken place in an active tectonic setting during the late-stage activity of the Laramide Orogeny and the Sevier Fold and Thrust Belt. Sedimentary deformation structures are widespread in these deposits and despite the large number of geological studies devoted to the stratigraphy, they are poorly understood.

The principal aim of this thesis was to explore and document previously overlooked or unrecognized deformation structures through field observations of exceptional outcrops in Wyoming, Colorado and Utah. This work represents the first detailed study on such features in the Green River Formation, the best-documented ancient lake systems worldwide.

The investigation of outcrops revealed an unparalleled suite of sedimentary deformation structures in all the sub-basins, in a variety of depositional settings. These include convolute lamination, load structures, folds, hybrid brittle–ductile features, sedimentary dikes, microfaults, fluid-escape features, oil shale breccias, and mass-transport deposits. They occur in numerous laterally extensive deformed horizons, mainly in laminated carbonates, that could be traced and correlated laterally for >25 km. Their morphological attributes, lateral extent, and recurrence at different stratigraphic levels, along with the low-energy and low-gradient sedimentary environment and the active tectonic setting, indicate that they were induced by ancient syndepositional earthquakes and can be interpreted as ‘seismites’. This study has demonstrated that these structures can be used to infer tectonically active periods and to refine the paleotectonic history of the area. The reinterpretation of features previously described as the result of desiccation helped to better understand the depositional setting of the Green River Formation. Moreover, the occurrence of seismites was related to synchronous changes in basin evolution for the first time, implying that many abrupt changes in the history of the Green River Formation were tectonically, rather than climatically, driven. Clearly, seismites should be more widely utilized to recognize the contribution of tectonics on basin history.

## ACKNOWLEDGEMENTS

First and foremost, I would like to express my gratitude to my graduate supervisors, B.R. Pratt and R.W. Renaut, for the opportunity to pursue this project and their guidance throughout my Ph.D. degree. I am truly grateful for their insightful advice and endless patience during our numerous discussions.

I am immensely thankful to S. Dasgupta, E. Wiens, and J.J. Scott (Mount Royal University) for field assistance and eye-opening conversations on several aspects of my Ph.D. I owe special thanks to Blaine Novakovski for the preparation of thin sections, and I am grateful for the technical help I received from Tom Bonli and Jim Rosen at the University of Saskatchewan. I would like to thank A. Aase (Fossil Butte National Monument), H.P. Buchheim (Loma Linda University), David Keighley (University of New Brunswick), M. Vanden Berg (Utah Geological Survey), K. Tänavsuu-Milkeviciene (Statoil ASA), A.R. Carroll (University of Wisconsin, Madison), Tim Lowenstein and J. Pietras (Binghamton University), and M.E. Smith (North Arizona University) for their advice on field sites and valuable insights on the geology of the Green River Formation. I am thankful to the members of my advisory committee, M.G. Mángano, L.A. Buatois, E. Robertson and J. Merriam for their encouragements and feedbacks. Finally, I would like to thank Krisztina Pandur, my family, and my friends for their support and patience throughout my time at the University of Saskatchewan.

I am grateful for Enefit American Oil for giving permission to study their box cut at Evacuation Creek. I gratefully acknowledge the Natural Science and Engineering Research Council of Canada for the Discovery Grants awarded to B.R. Pratt and R.W. Renaut, and the University of Saskatchewan for the Dean's Graduate Scholarship I received. Additional funds for this research, which include travel and research grants from the Geological Society of America, the American Association of Petroleum Geologists, the Society for Sedimentary Geology (SEPM), and the International Association of Sedimentologists, were also greatly appreciated.

## TABLE OF CONTENTS

## LIST OF TABLES

## LIST OF FIGURES

# CHAPTER 1
# INTRODUCTION

## 1.1 Background

### *1.1.1 Synsedimentary Deformation – Theoretical Background*

Synsedimentary deformation features are sedimentary structures that form at the sediment–water interface or under shallow burial depth in unconsolidated to semi-consolidated sediments with low shear resistance (Maltman, 1984; Maltman and Bolton, 2003). Decrease of yield strength is generally reached by thixotropic behavior, liquefaction, and/or fluidization in the unconsolidated sediment (Allen, 1982; Owen, 1987). Because the style of deformation depends on the applied stresses and the initial sediment rheology, synsedimentary deformation includes a wide range of *in situ* features that demonstrate ductile, brittle–ductile, and brittle responses as well (e.g., Montenat et al., 2007).

Deformation can be triggered by several processes (e.g., overloading, wave action, earthquakes) (G. Owen et al., 2011). However, the final morphology and size of the deformed structure depends on the driving forces (e.g., density contrast, unequal loading), the areal extent and thickness of the rheologically susceptible sediment, and less so on the trigger agent (Owen, 1987, 2003; Moretti and Ronchi, 2011). Accordingly, recognition of the trigger mechanism is complex, it relies on criteria that are not yet well established, and many commonly used criteria are unreliable, non-diagnostic, or difficult to apply (e.g., Sims, 1975; Leeder, 1987; Pope et al., 1997; Jones and Omoto, 2000; Montenat et al., 2007; G. Owen et al., 2011).

Because sand-rich sediments have the highest susceptibility to liquefaction (Tsuchida and Hayashi, 1971; Obermeier, 1996), synsedimentary deformation features can be found in all kind of depositional environments and they are most frequently reported from siliciclastic sand-rich deposits (e.g., Lowe, 1975; Allen, 1982; Owen, 1987). Deformation features in carbonates and mudstones (marine or lacustrine) are less studied. The mechanical behaviour of carbonates is fundamentally different from siliciclastics, and, thus, the type of deformation structures are distinctive (e.g., Weaver and Jeffcoat, 1978; Plaziat et al., 1990; Pratt, 1994, 1998a, b, 2002b; Pope et al., 1997; Kahle, 2002; Onasch and Kahle, 2002; Bachmann and Aref, 2005; El Taki and Pratt, 2012). Although fine grained particles (silt, clay, lime mud, and organics) potentially

influence plasticity or cohesion, their effects on liquefaction potential is poorly understood (e.g., Ishihara, 1993). Consequently, the relatively small number of studies from carbonates and various mudstones makes finding analogues and studying deformation mechanisms difficult in such settings.

### *1.1.2 Synsedimentary Deformation – Implications*

The analysis of sedimentary deformation features can be an integral part of the depositional history because they provide insight into syn- to early post-depositional physical processes, sediment rheology and diagenesis, hydrodynamic conditions, and, occasionally, the paleoslope in the basin (Mills, 1983; van Loon and Brodzikowski, 1987; van Loon, 1992). For example, 'mudcracks' imply subaerial exposure and desiccation that may be later used to reconstruct the depositional history of an area.

Seismites are indicative of synsedimentary tectonic activity and they provide information about the location, timing, and intensity of the movements of nearby structural elements (e.g., Sims, 1973; El-Isa and Mustafa, 1986; Pratt, 1994, 2001; Moretti, 2000; Migowski et al., 2004; Marco and Agnon, 2005; Thomas et al., 2006; Rodríguez-López et al., 2007; Fortuin and Dabrio, 2008; El Taki and Pratt, 2012). Syndepositional tectonism, in turn, potentially influences the hydrology, hydrogeology, watershed geology, accommodation, biology, and spring activity within a basin (Tweddle and Crossley, 1991; Paz and Rossetti, 2005, 2006; Carrillo et al., 2006; B.R. Owen et al., 2011; Lee et al., 2013).

The common heterolithic nature of sediments deposited in lacustrine environments gives them high susceptibility to deformation and the low-gradient, quiet-water environment tends to eliminate other triggering mechanisms (e.g., overloading, storm waves), and increases the potential for preservation (Sims, 1975; Renaut and Gierlowski-Kordesch, 2010). As a result, there is a large number of studies describing seismites in lacustrine successions (e.g., Sims, 1973, 1975; Hempton and Dewey, 1983; Seilacher, 1984; Plint, 1985; El-Isa and Mustafa, 1986; Anand and Jain, 1987; Davenport and Ringrose, 1987; Scott and Price, 1988; Ringrose, 1989; Karlin and Abella, 1992; van Loon et al., 1995; Alfaro et al., 1997; Rodríguez-Pascua et al., 2000; Becker et al., 2002; Leroy et al., 2002; Bowman et al., 2004; Migowski et al., 2004; Weidlich and Bernecker, 2004; Moretti and Sabato, 2007; Schnellmann et al., 2007; Beck, 2011; Koç Taşgin et

al., 2011; Strasser et al., 2013). Despite the extensive literature on seismites in modern or ancient lacustrine (or marine) deposits, a direct linkage between deformed intervals and changes in lake-character has yet to be achieved and, thus, they represent an untapped opportunity to better understand the role of tectonics in basin evolution.

### *1.1.3 Lacustrine Deposits as Paleoseismological Archives*

Most lakes develop in relatively short-lived sedimentary basins, but their isolation and typically low-energy settings mean that they often preserve high-resolution archives of paleoenvironmental change, including evidence of former climate, geomorphology, hydrology, and tectonic milieu (Cohen, 2003; Renaut and Gierlowski-Kordesch, 2010). Although climate and tectonics are equally important controlling factors of lake-basin types (overfilled, balanced-fill, underfilled: Carroll and Bohacs, 1999), changes in lake character are typically considered as the result of climatic change, and the tectonic record is rarely exploited.

Earthquake-induced sedimentary deformation features ("seismites": Seilacher, 1969, 1984) provide a powerful tool for interpreting the contribution and importance of tectonic events in the evolution of lacustrine systems. Additionally, lacustrine sediments have rheologies that are ideal for recording seismic events of large-magnitude (Sims, 1975; Ricci Lucchi, 1995), and there is increasing interest in understanding the processes of sedimentary deformation (G. Owen et al., 2011). Consequently, seismites have been extensively reported from lake basins (e.g., Moretti and Sabato, 2007; Beck, 2011), and widely used in paleoseismological studies in recent deposits (e.g., Waldmann et al., 2010; Strasser et al., 2013). Nevertheless, the potential of seismites to provide insight into the tectonic evolution of an area is unexplored in ancient deposits.

### *1.1.4 The Green River Formation*

Lacustrine sediments of the Green River Formation were deposited in interconnected foreland basins east of the Sevier Fold and Thrust Belt in the central Rocky Mountain region during the early to middle Eocene (53 Ma – 43 Ma) (Dickinson et al., 1988; Smith et al. 2008) (Fig. 1.1., 1.2). The Green River Formation represents one of the best-documented ancient lake systems and has long been a type example for understanding lacustrine depositional systems (Bradley, 1929, 1930; Eugster and Surdam, 1973; Carroll and Bohacs, 1999).

Lacustrine sediments were deposited in three, temporarily connected lakes, "Fossil Lake" (Fossil Basin, SW Wyoming), "Lake Gosuite" (greater Green River Basin, SW Wyoming and NW Colorado), and "Lake Uinta" (Piceance Creek Basin, NW Colorado and Uinta Basin, NE Utah) (Fig. 1.1). These comprise siliciclastic, evaporitic and carbonate-rich lake-margin to profundal strata locally up to 2 km thick (e.g., Bradley, 1931, 1964; Roehler, 1993; Smith et al., 2008). The Green River lakes have been interpreted as permanent and stratified (e.g., Bradley, 1964; Bradley and Eugster, 1969; Desborough, 1978; Johnson, 1981) or playa-type lakes (e.g., Eugster and Surdam, 1973; Eugster and Hardie, 1975; Lundell and Surdam, 1975; Cole and Picard, 1978; Moncure and Surdam, 1980). Others have noted that both may be applicable but at different times (e.g., Boyer 1982; Moncure and Surdam, 1980; Smith et al., 2008; Davis et al., 2009).

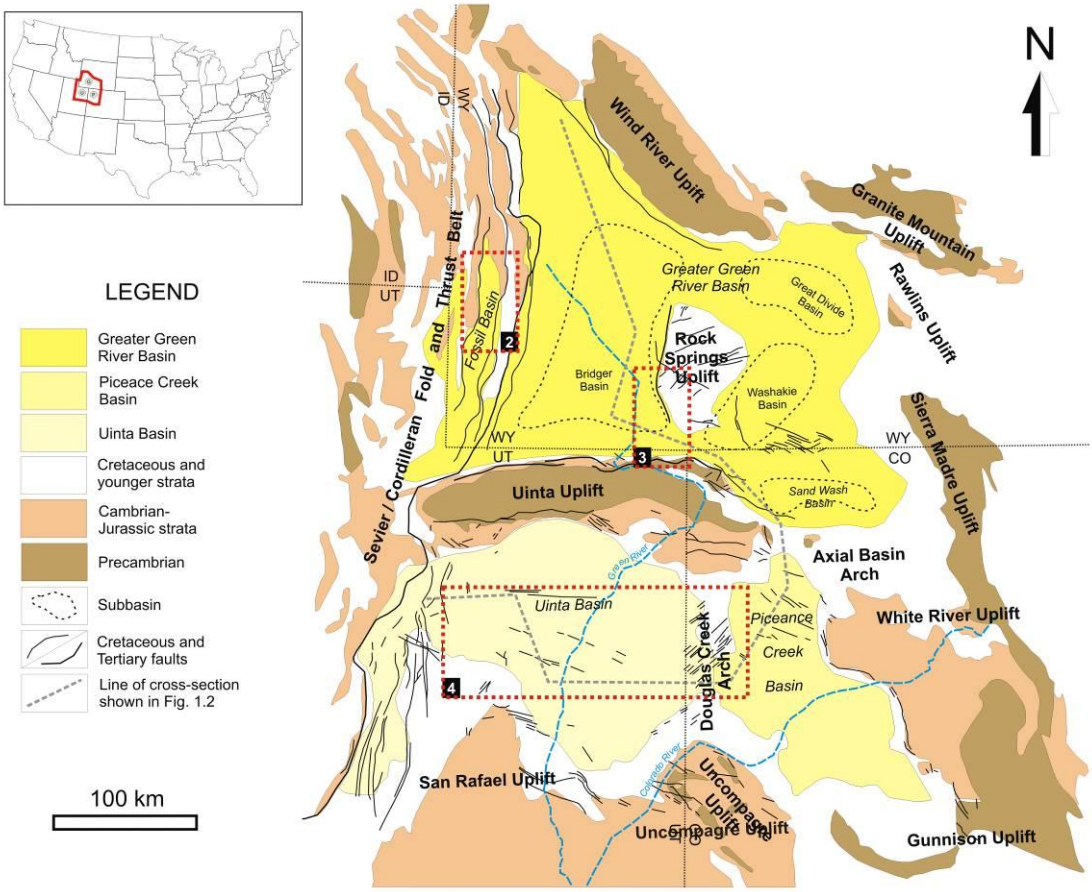


**Figure 1.1** Map of the Green River basins of SW Wyoming, NW Colorado and NE Utah (modified after Smith et al., 2008; Johnson et al., 2010a, b), with the main structural elements (uplifts and faults) and approximate studied locations of Chapter 2, 3, 4 (red rectangles with dashed border). Cross section across the basins (Fig. 1.2) is marked with grey dashed line.

These lake basins were characterized by a gently dipping slope (0.01–0.5°; e.g., Bradley, 1964; Lundell and Surdam, 1975; Surdam and Wolfbauer, 1975; Roehler et al., 1988, Roehler, 1990; Buchheim, 1994a), with gradients decreasing rapidly to nearly horizontal towards the basin center and an inferred water depth of ~ 20–100 m (Bradley, 1926, 1929; Roehler, 1965, 1990). Steeper gradients >1° may have been existed in the alluvial–fluvial settings closer to the uplifts. The lakes were always interfingering with the surrounding alluvial/fluvial sediments and were hydrologically connected during periods of higher lake level (e.g., Bradley, 1931; Roehler, 1974; Surdam and Stanley 1980; Smith et al., 2008). Nevertheless, the sub-basins evolved separately, influenced by the local geographical and geological setting, which resulted in a unique sedimentary record for each basin (Smith et al., 2008) (Fig. 1.2).

These basins formed in a mid-latitude (35° N) setting with an overall warm temperate to sub-tropical climate (Roehler, 1993; Wilf, 2000). The time of deposition overlapped with the warmest period of the Cenozoic, the Early Eocene Climatic Optimum (EECO; ~ 52–50 Ma: Zachos et al., 2001, 2008). Early Eocene abrupt global-warming events (hyperthermals: Zachos et al., 2008) potentially influenced weathering, sediment production rates, precipitation intensity, and seasonality (Birgenheier and Vanden Berg, 2011).

Tectonic movements along basement-cored uplifts and arches that formed during the Laramide Orogeny influenced the basin shape, gradients, geomorphology, and drainage pattern (Roehler, 1992; Carroll et al., 2006, 2008; Pietras and Carroll, 2006; Smith et al., 2008; Davis et al., 2009). Consequently, salinity, areal extent and types of sedimentary deposits varied throughout the history of the lakes as expressed by distinct facies associations, stratal stacking patterns, and changing lake-basin types (Smith et al., 2008).

Despite the known syndepositional tectonic activity along the structures within the basins and along their margins, and the large number of geological studies devoted to the stratigraphy, the study of deformation features is an unexplored part of the geology of the Green River Formation. Moreover, deformation structures were mostly overlooked or misinterpreted in previous studies. The term ‘mudcrack’, for example, is extensively used in the literature to describe features from littoral to profundal deposits, and taken as evidence for subaerial exposure irrespective of the host facies, morphology, mode of preservation (positive epirelief, positive hyporelief, or negative epirelief), and the characteristics of their infill.

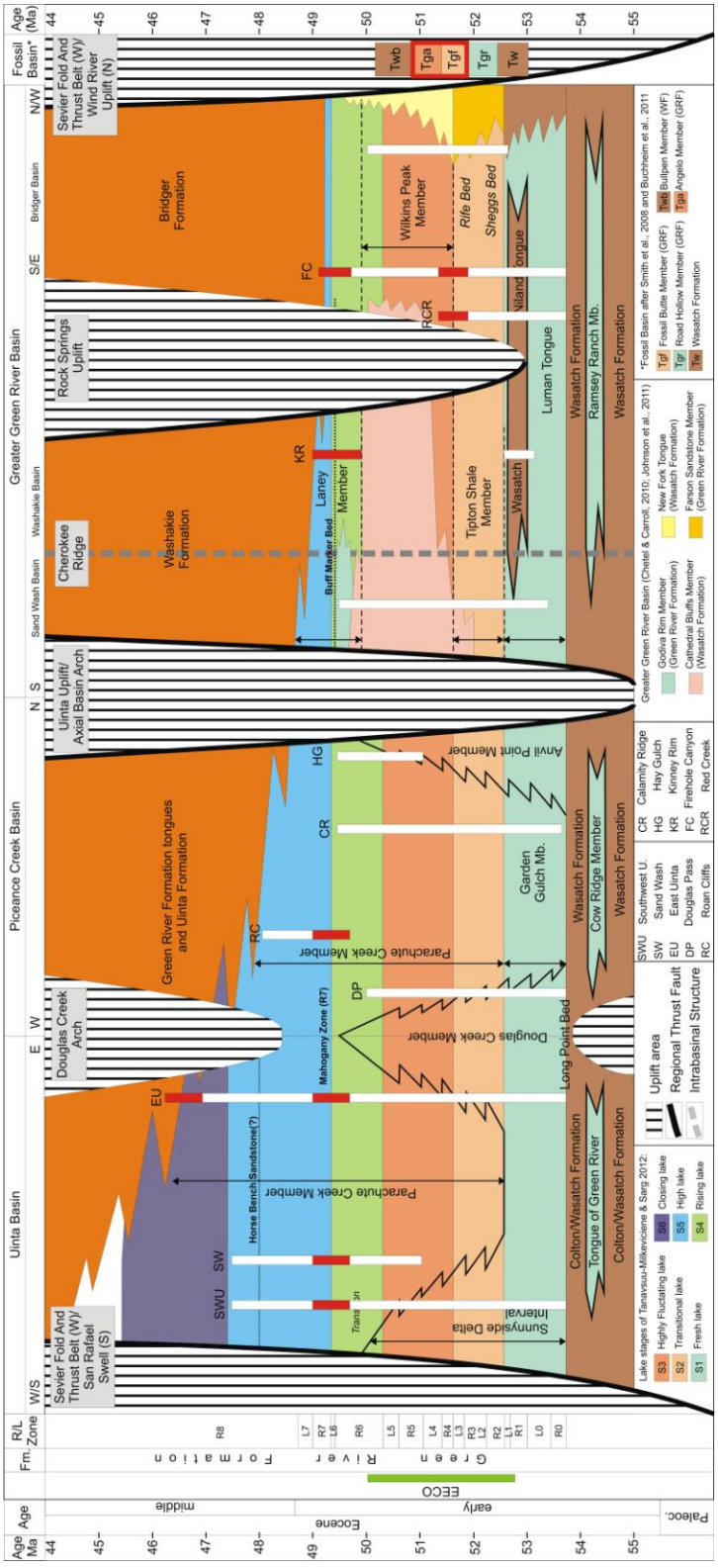


**Figure 1.2** Main structural elements, simplified stratigraphy and correlation of the Greater Green River, Piceance Creek and Uinta basins (modified after Smith et al., 2008; Chetel and Carroll, 2010; Tänavsuu-Milkeviciene and Sarg, 2011), with the main studied locations and stratigraphic intervals (white/red rectangles).

## 1.2 Research Objectives

The Green River Formation was chosen to perform a systematic study of sedimentary features related to earthquakes, as (1) sedimentary deformations were not studied in detail in previous studies; (2) deformation features can be studied on extensive outcrops across a large area which aids correlation, (3) lacustrine sediments were deposited in a tectonically active setting, (4) lake history is characterized by frequent changes in lateral extent of the ancient lakes, along with changing lake chemistry and alkalinity, and (5) it has well-established stratigraphic framework, in which the linkage between deformed intervals as evidences for syndepositional tectonic movements and changes in lake evolution can be studied.

Thus, this study represents the first attempt to examine sedimentary deformation features in this well-studied geological setting. The main objectives are:

- the identification of previously unknown or overlooked deformation features;
- the detailed description and classification of the deformation features based on macroscopic and microscopic observations;
- the determination of the processes responsible for their genesis and the timing of deformation relative to shallow burial in order to expand our knowledge on the controlling factors of sediment deformation in fine-grained lacustrine deposits, particularly in lacustrine carbonates;
- the identification of potential trigger mechanisms based on the relationship between depositional facies and the occurrence of synsedimentary deformation to establish diagnostic criteria to identify different trigger agents;
- the reinterpretation of previously neglected deformation features that may challenge previous interpretations regarding the depositional environment of the strata and overall basin evolution;
- the correlation of deformation features across the studied areas (if possible) and to study their stratigraphic and geographic distribution to provide data on their temporal and spatial occurrence;

- to assess the implications of earthquake-induced structures refine the paleotectonic history of nearby fault systems or uplifts to understand the tectonic control on lake character and how syndepositional tectonism might have affected sedimentation and lake chemistry.

### 1.3 Thesis Outline

The thesis is organized into five chapters. Chapter 1 provides an introduction to the thesis, including background information on the processes and implications of sedimentary deformation features and the geology of the Eocene Green River Formation. Chapter 1 also provides the main thesis objectives and overview of the thesis, as well as the thesis organization. The three discussion chapters (Chapters 2 to 4) each represent a separate manuscript focusing on case studies of how the research objectives outlined above were applied in various depositional and tectonic settings from different parts of the Green River system. These locations were chosen based on available geological information, and the quality and accessibility of outcrops. The manuscripts were reformatted for inclusion in the thesis.

Chapter 2 investigates the characteristics of sedimentary deformation features in the lacustrine carbonates of the Fossil Basin in southwestern Wyoming, and gives insight into the their origin and the role of tectonic activity in the Sevier Fold and Thrust Belt on basin evolution. This study is currently 'in press' in *Journal of Sedimentary Research*. Chapter 3 reports laterally extensive deformation features from the boundary of the balanced-fill Tipton and underfilled Wilkins Peak Members of the Bridger Basin in southwestern Wyoming, and provides implications for tectonically-induced regional changes in lake character related to movements along the Uinta and Wind River uplifts. This chapter was published in *Terra Nova* (Törő et al., 2015). Chapter 4 focuses on sedimentary deformation features preserved in the lacustrine and fluvial deposits of the Uinta and Piceance Creek basins in Utah and Colorado in order to establish criteria for recognizing trigger agents in various depositional settings and lithologies, and, ultimately, to refine the paleotectonic history of nearby structures. This chapter was submitted for publication to a special paper of the *Utah Geological Association*. Certain aspects of the latter study were published in a separate manuscript (Keighley et al., in press) that is not included in this thesis.

Finally, Chapter 5 discusses the relationship of individual discussion chapters to the thesis as a whole and provides a summary of the major conclusions.

# CHAPTER 2

# EOCENE PALEOSEISMIC RECORD OF THE GREEN RIVER FORMATION, FOSSIL BASIN, WYOMING, U.S.A. – IMPLICATIONS OF SYNSEDIMENTARY DEFORMATION STRUCTURES IN LACUSTRINE CARBONATE MUDSTONES

Törő, B., and Pratt, B.R., in press. Eocene paleoseismic record in the Green River Formation, Fossil Basin, Wyoming, U.S.A. – implications of synsedimentary deformation structures in lacustrine carbonate mudstones: Journal of Sedimentary Research.

## 2.1 Abstract

Laterally extensive intervals containing sedimentary deformation features are identified in outcrops of lacustrine deposits of the Eocene (~ 52–51 Ma) Green River Formation in Fossil Basin, southwestern Wyoming. Fossil Basin is the smallest of the paleo-lakes in the Green River system and is located in the Sevier Fold and Thrust Belt, which was tectonically active during deposition. Deformation structures include convolute lamination, load structures, hybrid brittle–ductile features, sedimentary dikes, microfaults, fluid-escape features such as cusps and pipes, oil shale breccias, and mass-transport deposits. In most cases these structures are hosted by finely laminated, variably organic-rich carbonate mudstones that accumulated in a low-energy profundal lacustrine environment. Deformed intervals range from a few centimeters to 5 m in thickness and are bounded above and below by undeformed strata of the same facies, which demonstrates the early post-depositional timing of deformation. The distribution of these features indicates a primary control exerted by sediment rheology, resulting from variation in grain size, clay and organic content, and degree of lithification, which in turn were governed by the depositional environment and early diagenesis.

Based on their morphological attributes, lateral extent, and recurrence at different stratigraphic levels, along with their sedimentary environment and the tectonic setting of the basin, the deformation structures are interpreted to be ‘seismites’, i.e., the result of stresses induced by syndepositional earthquakes, and other potential trigger agents are rejected. Moreover, stratigraphic relationships indicate that these small-scale deformation features as well as the mass-transport deposits, formed on a virtually flat lake floor, ruling out instability caused by the gravitational regime. Syndepositional deformation in Fossil Basin points to tectonic

activity along the nearby Absaroka and/or Hogsback thrusts and related fault systems. Seismites point to possible tectonic forcing as a mechanism for changes in bathymetry and sedimentation in the Green River Formation and, consequently, demonstrate their potential for elucidating the tectonic history of other lacustrine and marine basins.

## 2.2 Introduction

Synsedimentary deformation features form in unconsolidated to semi-cohesive deposits with zero to low shear resistance, and are the result of thixotropic behavior, liquefaction, fluidization, folding, and rupturing due to external forces acting on the sediment (Mills, 1983; Owen, 1987). Deformation occurs essentially instantaneously at some point after deposition, but before significant burial and diagenesis (e.g., Maltman, 1984, 1994; Maltman and Bolton, 2003). The susceptibility of the sediment, its response to various stresses and, thus, the style of deformation — ductile, mixed brittle–ductile, brittle, or injection into dikes — are controlled by the rheological properties of the sediment (e.g., Pratt, 1998b, 2001; Spalluto et al., 2007; El Taki and Pratt, 2012). Rheology in turn is governed by various factors like porosity, fluid content, grain size, grain morphology, presence or absence of low-permeability layers, or the degree of lithification (e.g., Obermeier, 1996).

Liquidization (*sensu* Allen, 1982) can be triggered by several processes, including overloading by rapid sedimentation and cyclic stresses induced by storm waves and earthquakes. Brittle failure can be induced by cyclic shear stresses as well as those caused by gravity-related movement (i.e., slumping or collapse). The final morphology and size of the deformation structure depend on the driving forces and the areal extent and thickness of the rheologically susceptible sediment (Owen, 1996b). Accordingly, determination of the trigger mechanism relies on criteria that are not yet widely agreed upon (Sims 1975; Seilacher 1984; Pratt 1998a, b; Jones and Omoto, 2000; Wheeler, 2002; Montenat et al., 2007; G. Owen et al., 2011; Hurst et al., 2011).

Synsedimentary deformation features are commonly reported from siliciclastic strata, mainly in sediments of sand size or with relatively high sedimentation rates (e.g., Lowe 1975; Allen, 1982; Obermeier, 1996). Mudstones, especially carbonate mudstone, also host a variety of deformation features (e.g., Plaziat et al., 1990; Pratt, 1994, 1998a, b; Pope et al., 1997; Rodríguez-Pascua et al., 2000; Kahle, 2002; Onasch and Kahle, 2002; Ettensohn et al., 2011; El

Taki and Pratt, 2012), but the effects of fines (silt- and clay-sized carbonate particles, clay and organic matter) on the rheological properties of sediment and how they control the nature of the deformation structures are not well understood (Tsuchida and Hayasi, 1971; Lowe, 1975; Owen, 1987; Ishihara, 1993; Obermeier, 1996; Pratt, 2001, 2011). High organic content may well result in increase of sensitivity and plasticity, similar to that seen with organic-rich marine (e.g., Grimm and Orange, 1997) or lacustrine deposits (Larsson, 1990; Becker et al., 2002). With respect to carbonate sediments, there are no widely accepted models of seismogenic deformation and experimental analogs are relatively few (Weaver and Jeffcoat, 1978).

Deformation features related to earthquake-induced shaking, i.e. "seismites" (Seilacher, 1969, 1984), are indicative of synsedimentary tectonism. As a result, these features can provide information about the location, timing, and intensity of the movements of near-field structural elements (e.g., Weidlich and Bernecker, 2004; Marco and Agnon, 2005; El Taki and Pratt, 2012). The commonly heterolithic nature of lacustrine sediments gives them a high susceptibility to seismogenic deformation because of their variable rheological properties (e.g., Rodríguez-Pascua et al., 2000; Moretti and Sabato, 2007). Deposition in an overall quiet-water environment eliminates other trigger agents and increases the potential for preservation (Renaut and Gierlowski-Kordesch, 2010). These conditions make the lacustrine deposits ideal candidates to examine seismogenic features. Ultimately, seismites can be used to provide evidence for the contribution of tectonics versus climate in the evolution of lacustrine conditions, where tectonic activity might have had an impact on local or regional paleohydrology and sedimentation (e.g., Carrillo et al., 2006; Beck et al., 2007; R.B. Owen et al., 2011).

The Eocene Green River Formation in western USA is one of the best-documented ancient lacustrine systems (Bradley, 1929, 1931, 1964; Eugster and Surdam, 1973; Carroll and Bohacs, 1999; Smith et al., 2008). Although syndepositional tectonic activity along the structures around and within the basins is known to have occurred (e.g., Smith et al., 2008) and despite the many studies that have been devoted to the stratigraphy and sedimentology, the presence of sedimentary deformation features has been recognized only in passing. This study is the first attempt to examine deformation features in detail in order to determine their origin and to integrate them into the interpretation of the depositional and tectonic history.

We focus on laterally extensive deformed intervals from laminated lacustrine carbonates of Fossil Basin, part of the larger Green River paleo-lake system, cropping out in southwestern

Wyoming, emphasizing: (1) the processes responsible for their genesis; (2) the timing of deformation relative to shallow burial; (3) the stratigraphic distribution and their correlation across the study area; (4) the determination of potential trigger mechanisms; and (5) their significance in the geological evolution of the region.

## 2.3 Geological and Stratigraphic Framework

### *2.3.1 Regional Geological Setting*

Lacustrine sediments of the Green River Formation were deposited during the early to middle Eocene (54–43 Ma) across a large area east of the Sevier Fold and Thrust Belt in the central Rocky Mountain region (Dickinson et al., 1988; Smith et al., 2008). These carbonate-rich sediments were formed in three, intermittently connected lakes: "Fossil Lake" (Fossil Basin, southwestern Wyoming); "Lake Gosiute" (greater Green River Basin, southwestern Wyoming and northwestern Colorado); and "Lake Uinta" (Piceance Creek Basin and Uinta Basin, northwestern Colorado and northeastern Utah, respectively) (Fig. 2.1A). These lake basins formed in mid latitudes (~ 35° N), in a humid subtropical to warm-temperate climate (Roehler, 1993; Wilf, 2000). The interval of deposition overlaps with the early Eocene Climate Optimum (~ 52–50 Ma), the warmest time of the Cenozoic (Zachos et al., 2008). The basins are surrounded and separated from one another by basement-cored uplifts and arches that formed during the Laramide orogeny, and they were variably active from Cretaceous through Eocene time (e.g., Dickinson et al., 1988; DeCelles, 1994, 2004; Johnston and Yin, 2001; Bader, 2008, 2009). Tectonic movements along these structures flanking and within the paleo-lake system influenced the shape of the lake basins, surface drainage and paleohydrology, topographic gradients and, as a consequence, the sedimentation of the Green River Formation as a whole (e.g., Surdam and Stanley, 1980; Steidtmann et al., 1983; Roehler, 1992; Rhodes et al., 2002; Carroll et al., 2006, 2008; Pietras and Carroll, 2006; Smith et al., 2008, 2014a; Davis et al., 2008, 2009; Chetel and Carroll, 2010; Doebbert et al., 2010).

### *2.3.2 Fossil Basin*

Fossil Basin is a small intermontane basin situated in the Sevier Fold and Thrust Belt (Fig. 2.1B, C), which was variably active during lacustrine deposition (Rubey et al., 1975; Dorr and Gingerich, 1980; Lamerson, 1982; Dickinson et al., 1988; Coogan, 1992). It is elongated in the

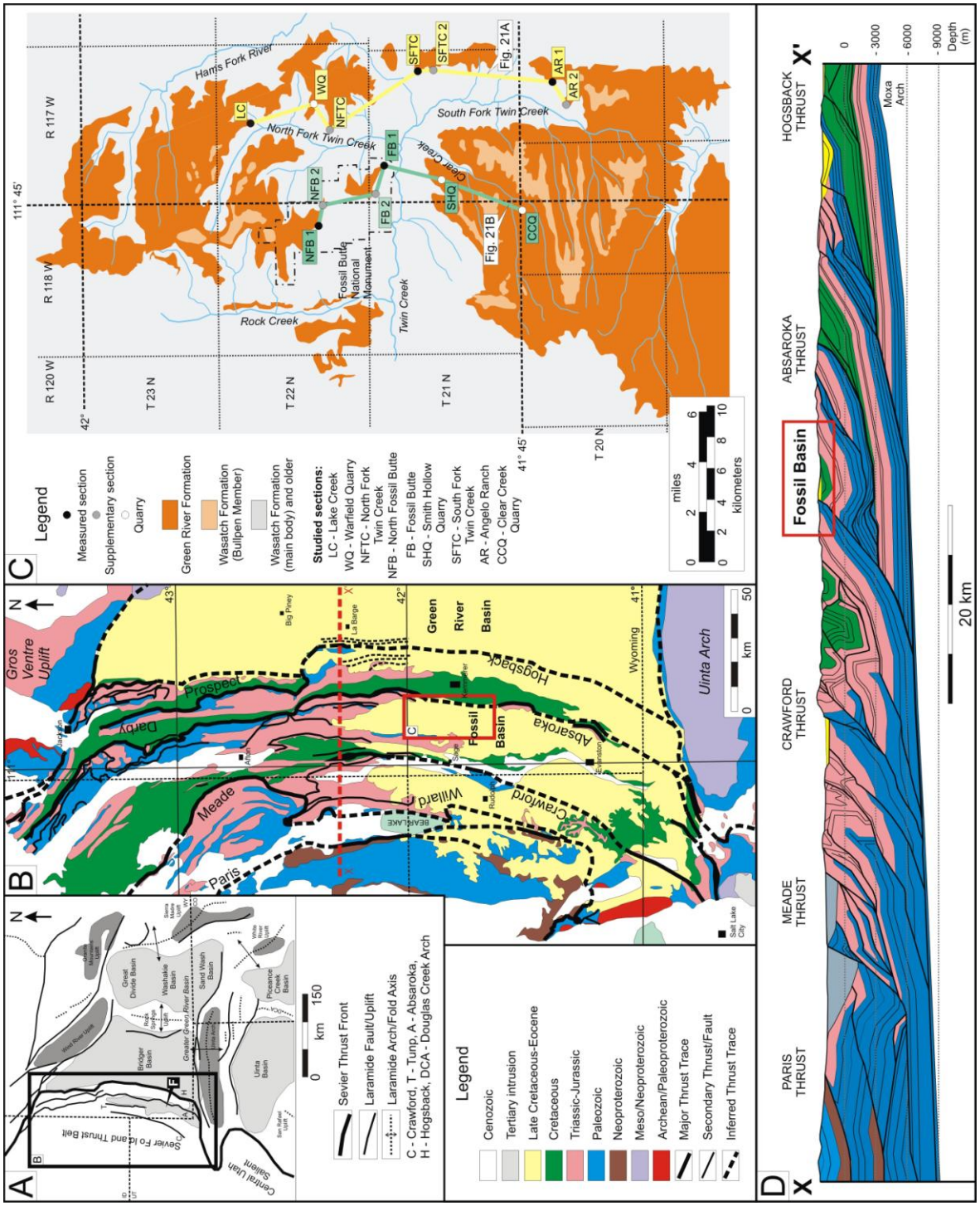


**Figure 2.1** A) Map of the Green River system of Wyoming, Colorado and Utah, and the basin-bounding uplifts (modified after Smith et al., 2008), with Fossil Basin (F). B) Location of Fossil Basin within the Sevier Fold and Thrust Belt, southwestern Wyoming, and location of the structure section (X–X') shown in Part D) Simplified geological map of northern Fossil Basin (after Buchheim and Eugster, 1998), showing location of studied sections and cross sections (Fig. 2.21). D) Structure section X–X' across northern part of Fossil Basin (after Yonkee and Weil, 2010).

north–south direction, and is approximately 95 km long and 55 km wide (Buchheim et al., 2011). The eastern boundary of the basin is about 20 km west of the front of the Sevier Fold and Thrust Belt, and the basin is located 3 to 6 km above the main thrusts (Yonkee and Weil, 2010) (Fig. 2.1D). The basin infill is up to 120 m thick, and there are facies changes over kilometer-scale distances (Fig. 2.2A, B) (Oriel and Tracey, 1970; Rubey et al., 1975; M'Gonigle and Dover, 1992; Buchheim, 1994a, b; Buchheim and Eugster, 1998; Biaggi and Buchheim, 1999; Buchheim et al., 2011). The basin was connected to Lake Gosiute and the greater Green River Basin via its southeastern corner (Buchheim et al., 2011).

### *2.3.3 Lithofacies and Stratigraphy*

The lacustrine Green River Formation is underlain, surrounded, and overlain by alluvial–fluvial siliciclastic deposits of the Wasatch Formation (Fig. 2.2A). Buchheim et al. (2011) split the Green River Formation into three members, which represent three distinct phases in the evolution of Fossil Basin: a floodplain-like, overfilled stage (Road Hollow Member), a balanced-fill stage (Fossil Butte Member), and an underfilled, hypersaline–alkaline stage (Angelo Member). During the early history of the lake the depocenter was located in the southern part, and it gradually shifted northward through time. The depositional slope of Fossil Basin was as low as 40 cm/km or 0.023°, and sediments record lake-margin to lake-center environments under an alkaline chemistry with fluctuating salinity (Buchheim, 1994a, b). The main facies include nearshore and deltaic sandstone, siltstone and claystone, and nearshore to offshore carbonate mudstone consisting of organic-poor bioturbated micrite, deeper-water laminated organic-poor or organic-rich laminated micrite or dolomicrite ("oil shale"), and minor structureless dolomicrite (Buchheim, 1994a, b; Buchheim and Eugster, 1998) (Fig. 2.2B). In general, the amount of bioturbation decreases basinward and indistinctly laminated bioturbated carbonates grade into finely laminated micrites with high organic content. Sedimentation was relatively slow because carbonate minerals precipitated from the water column due to mixing of the lake water with Ca-rich fluvial inflow; lamination is laterally continuous, and frequent mass-wasting deposits like turbidites are absent. Sedimentation rate was somewhat higher towards the margins, which resulted in thicker and more numerous laminae. Tuff layers and other marker beds aid stratigraphic correlation. The latter include the informal "lower oil shale bed", "sandwich beds", the "K-spar tuff", and the "purple oil shale" (Buchheim and Eugster, 1998).

The ~ 50 m thick interval comprising cliff-forming carbonates of the Fossil Butte Member and lower part of the Angelo Member was studied in detail (Fig. 2.2A). Deposition below the storm wave base is implied by the absence of shallow-water indicators, including ripple cross-lamination, root casts, and true desiccation cracks. Observations were made on cliff exposures and four quarry faces (Figs. 2.1C, 2.2B). Bedding-plane exposures are relatively rare due to the nature of the terrain and weathering. About 20 large-format thin sections were prepared from key samples.

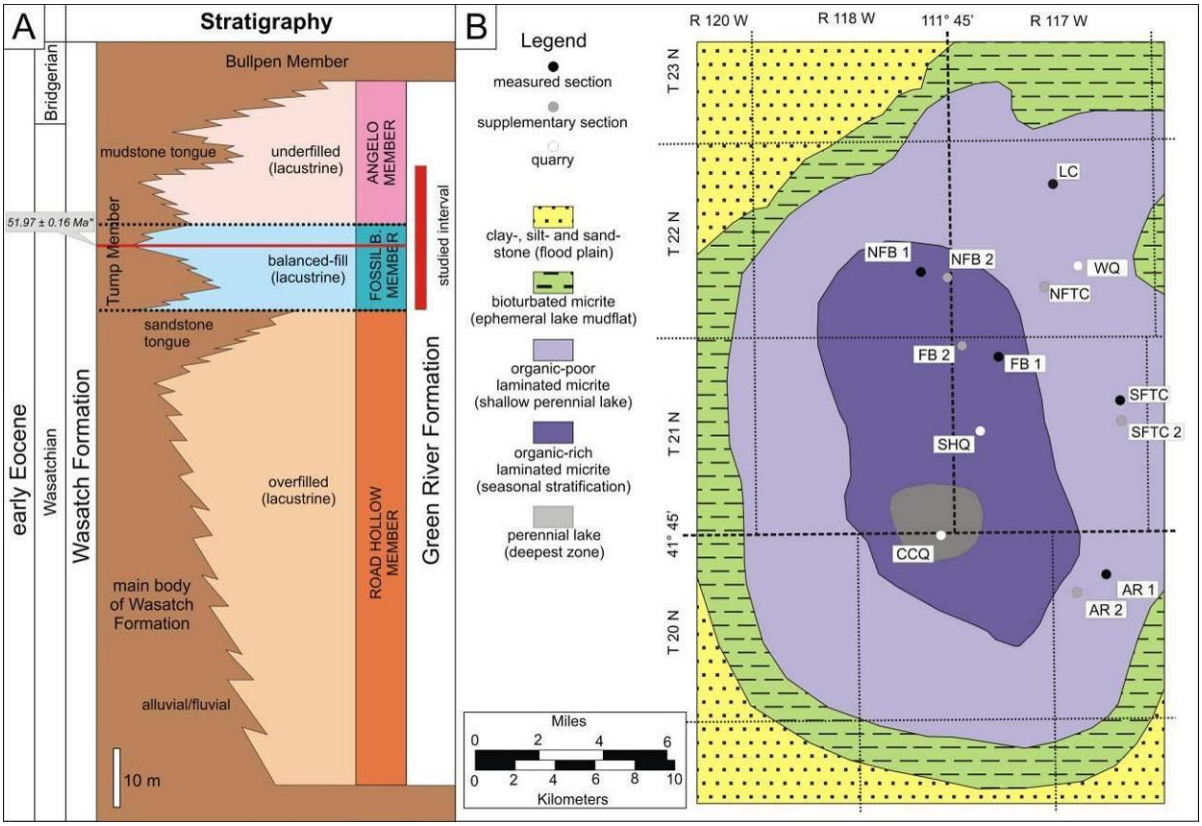


**Figure 2.2** A) Generalized stratigraphy and depositional environment of the Green River Formation and associated formations in Fossil Basin (modified after Buchheim et al., 2011). The alluvial–fluvial Wasatch Formation underlies, interfingers with, grades into, and overlies the lacustrine Green River Formation. Lacustrine conditions transitioned from overfilled (sediment and water supply > accommodation) through balance-filled (sediment and water supply ≈ accommodation) to underfilled (sediment and water supply < accommodation), reflecting changing climatic and tectonic influences (Carroll and Bohacs, 1999). $^{40}Ar/^{39}Ar$ date of 51.97 ± 0.16 Ma for the K-spar tuff from Smith et al. (2010). B) Studied sections and paleoenvironments of Fossil paleo-lake during time of lower Fossil Butte Member (after Buchheim and Eugster, 1998).

## 2.4 Deformation Features

### *2.4.1 Classification*

Classification schemes have been based on morphology (e.g., Rossetti, 1999; Rodríguez-Pascua et al., 2000; Owen, 2003), inferred genesis (e.g., Owen, 1987; van Loon, 2009; Hurst et al., 2011), or both (e.g., Lowe, 1975; Mills, 1983; Alfaro et al., 1997; Montenat et al., 2007). However, existing classifications either concentrate only on those in siliciclastic sediments and do not capture the full range of structures including brittle and compound brittle–ductile responses and sediment injection, or are focused on large-scale features and overlook ones at the millimeter to centimeter scale, such as "molar-tooth structure", "syneresis cracks", certain fracture and vein arrays, and some types of breccias (Pratt, 1998a, b, 2002b; Kahle, 2002; El Taki and Pratt, 2012). The variety of deformation features in the Fossil Basin succession is grouped into nine categories named from a combination of morphology and genesis: convolute lamination, load structures, brittle–ductile features, sedimentary dikes, fluid-escape cusps, fluid-escape pipes, microfaults, oil shale breccias, and mass-transport deposits (Fig. 2.3).

### *2.4.2 Convolute Lamination*

#### 2.4.2.1 Description

Convolute lamination is developed mainly in the profundal, organic-poor parallel-laminated micrites of the Fossil Butte Member. Deformed intervals are 0.5–4.5 m thick, with gradational or sharp, but non-erosive lower and upper boundaries (Figs. 2.4A–D, 2.5A–E, 2.6A, B). Individual folds can be up to 80 cm in amplitude and 2–65 cm in width. Intensity of deformation shows a full spectrum, from gentle folding, with short-wavelength, low-amplitude alternating synclines and anticlines (Fig. 2.4A), through larger folds (Fig. 2.4C), into chaotically folded beds exhibiting asymmetrical, open to tight, overturned and recumbent folds (Fig. 2.5B, D). In beds containing these complex structures, disharmonic folds, as well as larger folds with superimposed smaller ones, are also present (Fig. 2.6A, B), and the axial planes are inclined at various angles and variably curved, and lack an overall preferential orientation. Internal detachment surfaces occur locally (Fig. 2.5B). Sediments above do not show thickness changes related to the morphology of underlying structures. Convolution occurs as the only deformation feature present in a disturbed interval, as one component of brittle–ductile structures, or in conjunction with sedimentary dikes; on a smaller scale, convolute lamination is frequently associated with fluid-escape cusps.

| Deformation Feature | Description | Lithology | |
|---|---|---|---|
| *Convolute Lamination* | complex folds without preferred orientation, with sharp or gradational boundaries, in intervals 0.5–4.5 m thick | in laminated organic-poor micrite | 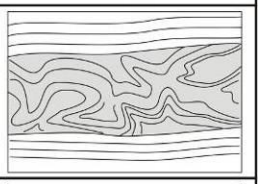 |
| *Load Structures* | irregular folds up to 1.6 m wide and 0.35 m in amplitude, with intervening cuspate features, and sedimentary dikes at their base | at the base of structureless dolomicrite beds | 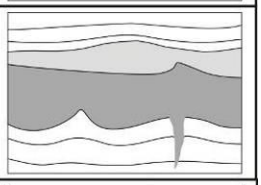 |
| *Brittle–Ductile Features* | complex association of mm- to cm-scale folds, fault-related folds, microfaults and breccia in 5–35 cm thick intervals | interlaminated organic-poor and organic-rich micrite | 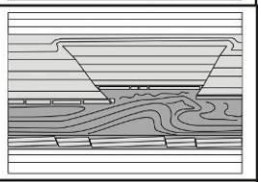 |
| *Sedimentary Dikes* | isolated downward- and/or upward-tapering dikes 1 cm–2 m long and 1–50 cm wide; linear in plan view; infill of carbonate mud, silt, breccia or composite | dominantly in laminated organic-rich micrite |  |
| *Fluid-Escape Cusps* | cm-scale cuspate features; crests filled with carbonate mud | in gently folded, laminated organic-poor micrite | 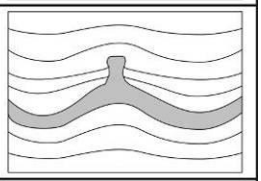 |
| *Fluid-Escape Pipes* | dm-scale, ovoid to lobate concretions with central conduit, oriented vertical to bedding | in laminated organic-poor micrite, with local folding | 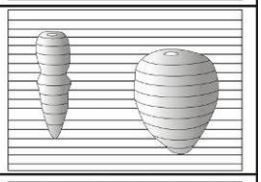 |
| *Microfaults* | single or grouped, mm- to cm-scale normal, reverse, and thrust faults with varying shapes in intervals 3 cm–4 m thick; dying out both upwards and downwards | in laminated organic-poor micrite | 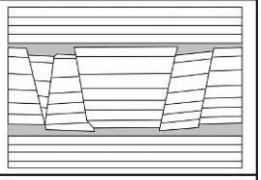 |
| *Oil Shale Breccias* | monomict breccia beds of aligned micrite clasts <5 cm in size, with organic-rich matrix, fault-related folds, microfaults, and sharp and planar boundaries | in organic-rich dolomicrite | 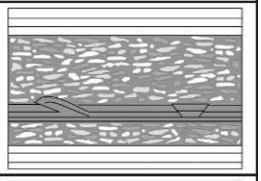 |
| *Mass-Transport Deposits* | breccia beds 5 cm–3 m thick, underlain by folded and/or faulted zone; fragments composed of shallow-water micrite and non-calcareous mudstone | dominantly in laminated organic-poor micrite | 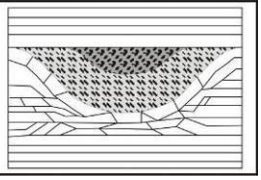 |

**Figure 2.3** Classification, description, lithological distribution, and simplified sketch of sedimentary deformation features observed in profundal deposits of Fossil Basin.

Most convoluted beds have limited lateral distribution. However, two convoluted intervals are traceable for at least 25 km without major change in deformation characteristics (Fig. 2.5A–E; see Correlation). At South Fork Twin Creek, the upper deformed interval (Fig. 2.6A, B) is overlain by ~ 2 m of laminated micrites with scattered large, thickly lined, branching burrows. This unit is sharply overlain by thoroughly bioturbated beds, representing an abrupt change in bioturbation index of 1–2 to 5–6 (Taylor and Goldring, 1993). This relationship with bioturbation can be traced laterally about 1 km.

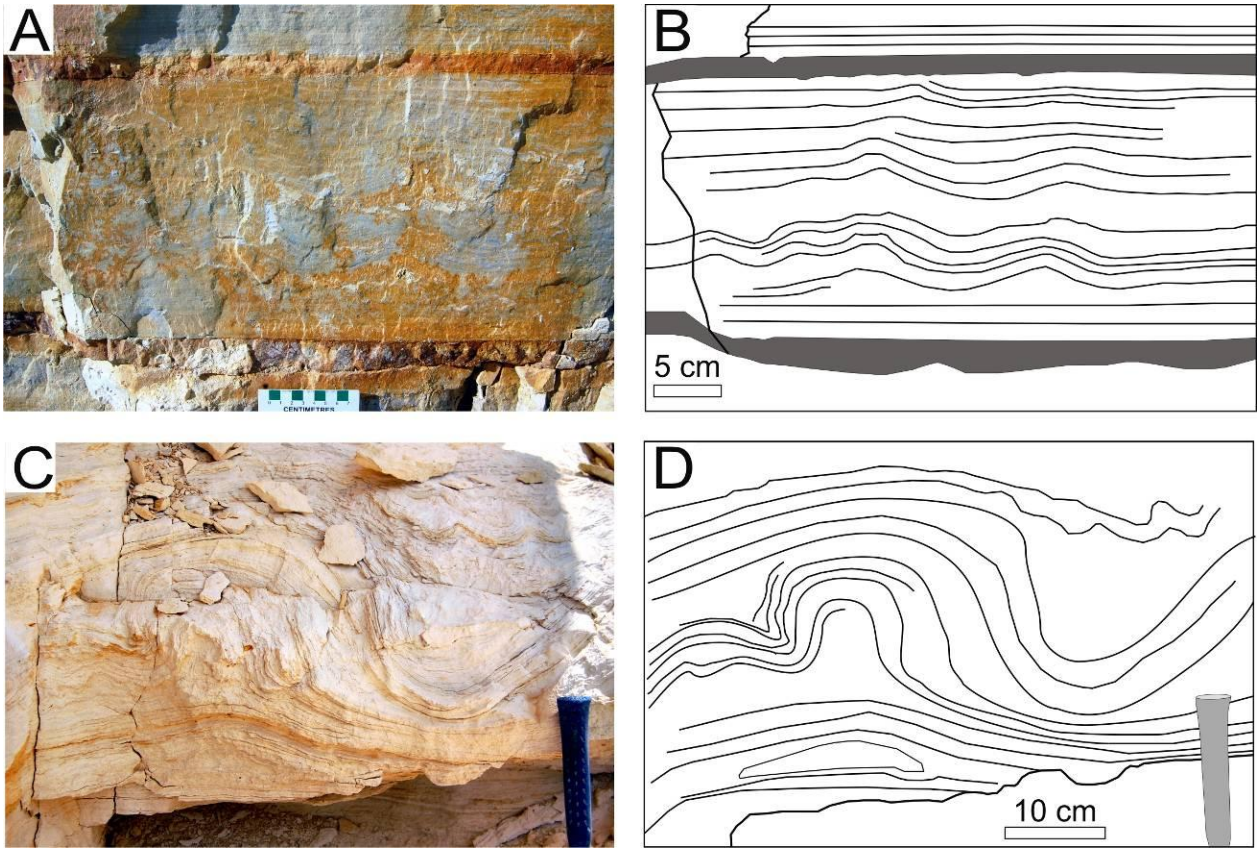


**Figure 2.4** Convolute lamination in laminated micrites. A) Undulating laminae forming low-amplitude folds, bounded by tuff beds (orange) (WQ). B) Tracing of A (tuff beds in dark-gray). C) Undulating laminae passing into high-amplitude folds (AR1). D) Tracing of Part C.

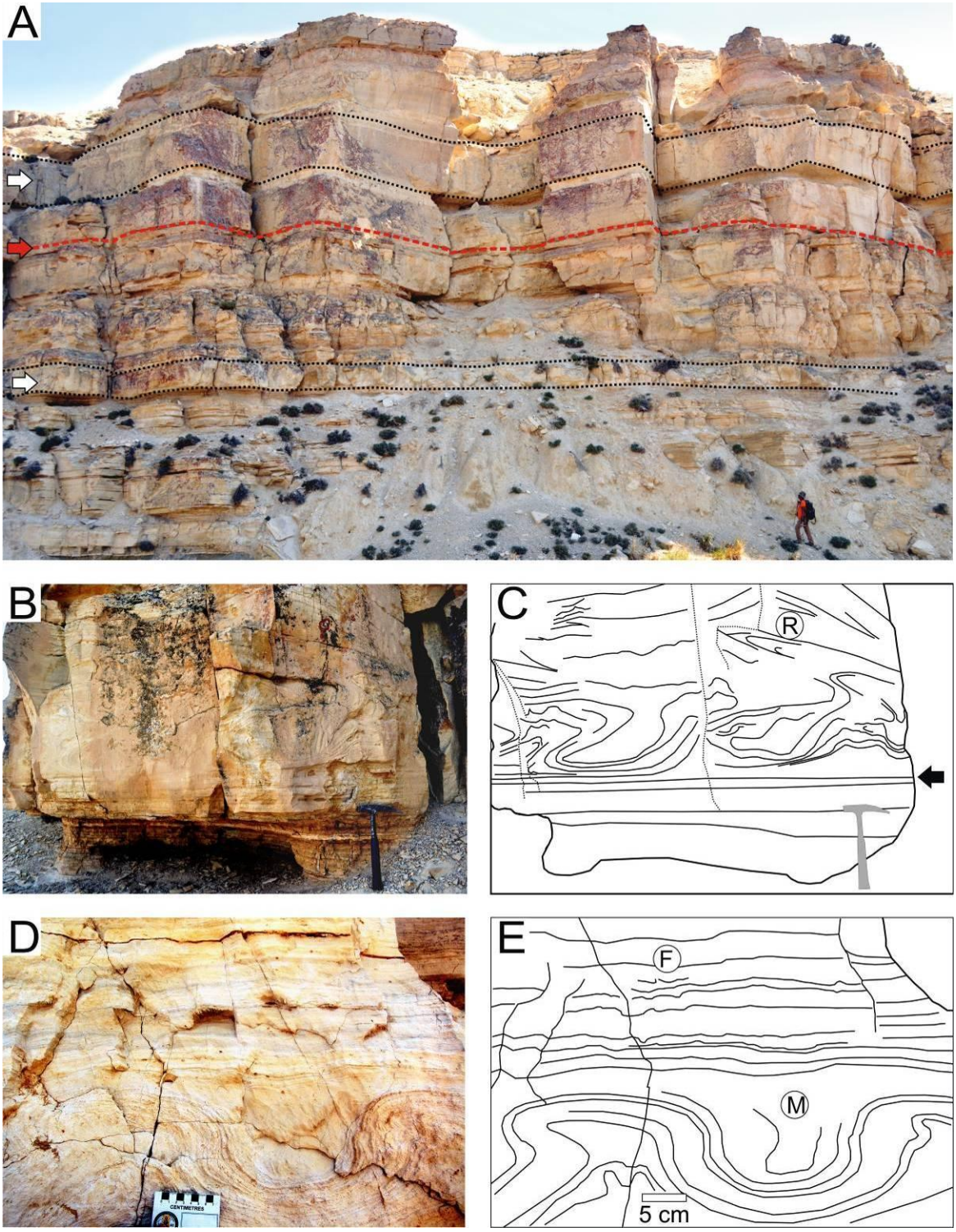


**Figure 2.5** Convolute lamination in laminated micrites. A) Cliff face showing two convoluted intervals (white arrow and black dashed lines) and the K-spar tuff (red arrow and dashed line) (LC). B) Close-up of lower convoluted interval. C) Tracing of Part B, with recumbent fold in upper right (R). D) Same convoluted interval ~ 20 km to the south (AR1). E) Tracing of Part D, with structureless carbonate mud in the core of the syncline (M) and small fluid-escape cusp in upper center (F).

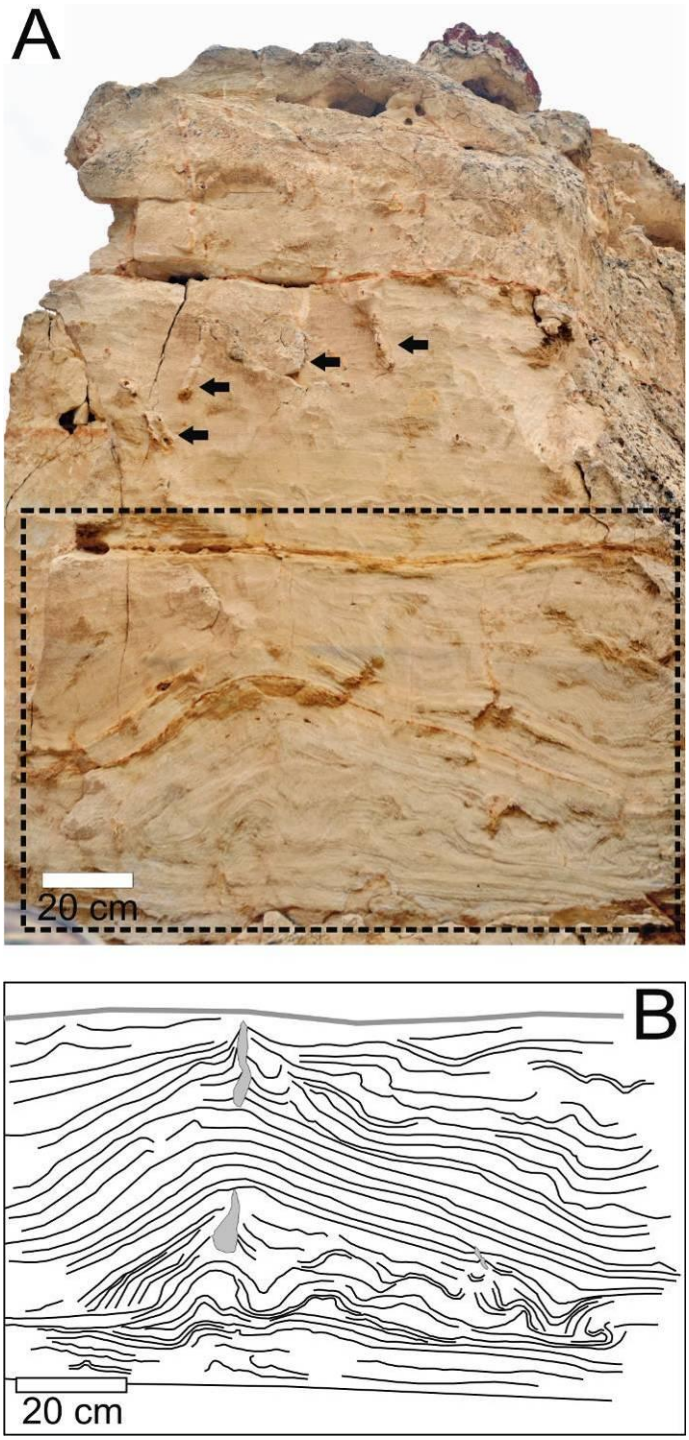


**Figure 2.6** Upper part of a 4.5 m thick convoluted interval in laminated micrites (SFTC2). A) Complexly folded laminae overlain by gently undulating bioturbated laminae, with subvertical, thick-walled, downward-bifurcating burrows (black arrows) (bioturbation index = 1–2), and capped by strongly bioturbated (bioturbation index = 5–6) bed. B) Tracing of area outlined in Part A, showing folds and fluid-escape cusps containing remobilized carbonate mud (gray).

2.4.2.2 Interpretation

Convolute lamination belongs to a diverse family of soft-sediment deformation structures and is frequently associated with ball-and-pillow and flame structures (e.g., Kuenen, 1953; Anketell et al., 1970; Allen, 1977; Visher and Cunningham, 1981; Mills, 1983). Encountered mostly in sandstones, it is considered to form by: (1) loss of shear strength through liquefaction (with or without fluidization); (2) shearing by currents on the sediment surface and frictional drag exerted by moving sediment flows; (3) rapid depositional events leading to unstable density gradients and loading; or (4) downslope slumping.

Slumping can be ruled out by the lack of uniform axial planes of the folds characteristic of downslope movement (e.g., Strachan, 2002; Alsop and Marco, 2011). Shearing by currents and sediment loading can be discarded because convoluted structures are not overlain by beds indicative of flow capable of creating shear, and rapid deposition and reverse density gradients are also precluded by facies attributes. Highly distorted fold geometries with variable sizes imply ductile response to chaotic stresses rather than gravitational collapse. The unaffected overlying sediments and the gradational boundaries point to in situ, intrastratal deformation through liquefaction or thixotropy. Variations in the rheological properties are responsible for the development of sharp versus gradational contacts, variable degrees of convolution vertically or laterally within the same interval, and detachment surfaces (Owen, 1996b). Fluid-escape cusps indicate localized fluidization.

The convoluted intervals are best explained by cyclic pore-pressure increase and stresses triggered by seismic shaking, and thus they are interpreted as seismites (see Trigger Mechanism). Comparable seismites occur widely in marine carbonates (e.g., Pratt, 1994; Pope et al., 1997; Bachmann and Aref, 2005) and lacustrine facies (e.g., Hempton and Dewey, 1983; Rossetti and Góes, 2000; Jones and Omoto, 2000; Bowman et al., 2004; Koç Taşgin et al., 2011; Berra and Felletti, 2011). Multiple convoluted intervals over a short stratigraphic thickness imply deformation from a single event or a series of events closely spaced in time.

### *2.4.3 Load Structures*

2.4.3.1 Description

Four distinctive massive dolomicrite beds, 15–145 cm thick, are unique to the Fossil Butte Member. They occur within intervals of laminated micrites and are white to light-yellow, are chalky textured, lack bioturbation and fossil fish, and serve as marker beds (Buchheim, 1994a). They display and undulating, non-gradational lower contact that forms laterally variable load structures (Fig. 2.7A–C). Laminae in the underlying beds are locally truncated (Fig. 2.7A), and overlying ones are folded, conforming to sharp, wavy upper contacts (Fig. 2.7B). Load structures may be present also along the interface between two amalgamated dolomicrite beds (Fig. 2.7C). Individual load structures are up to 1.6 m wide and 35 cm in amplitude, and generally show irregular shapes. Sedimentary dikes are commonly connected to these beds. Locally, where dolomicrite beds are interbedded with thin beds of laminated micrite or tuff, these layers show brecciation and mixing with the dolomicrite (Fig. 2.7B).

#### 2.4.3.2 Interpretation

Load structures are commonly reported from siliciclastic deposits where they form in sediments with low shear strength as a response to unstable density contrasts or uneven loading during rapid deposition (e.g., Owen, 2003). However, the dolomicritic beds are lithologically uniform and there is no evidence of density differences from the underlying, semi-cohesive laminated carbonate mud. Connected sedimentary dikes indicate that they were sourced from the dolomicrite beds themselves. Thus these dikes, the gently undulating lower and upper contacts, and the mixed interbedded sediments indicate an intrastratal origin of deformation, rather than sediment loading from rapid deposition. The low-energy depositional setting, laterally extensive intrastratal deformation, and associated sedimentary dikes point to an external, earthquake origin whereas other mechanisms can be ruled out (see Trigger Mechanism). The dolomicrites had a unique response to seismic shaking, in that liquidization and plastic deformation were coupled with downward injection.

**Figure 2.7** (on next page) Load structures in massive dolomicrites. A) Amalgamated dolomicrite interval (buff and white) showing large-scale thickness changes, with lowermost bed (white) foundered into laminated micrite (light-gray) (dashed line) (SHQ). B) Deformed bed showing tuff (orange) squeezed around irregular masses of dolomicrite (light-gray) (FB1). C) Folding along contact zones between three dolomicrite beds (light-gray and buff), with flame structure at base of lowest bed (black arrow), over- and underlain by laminated micrites (FB1).

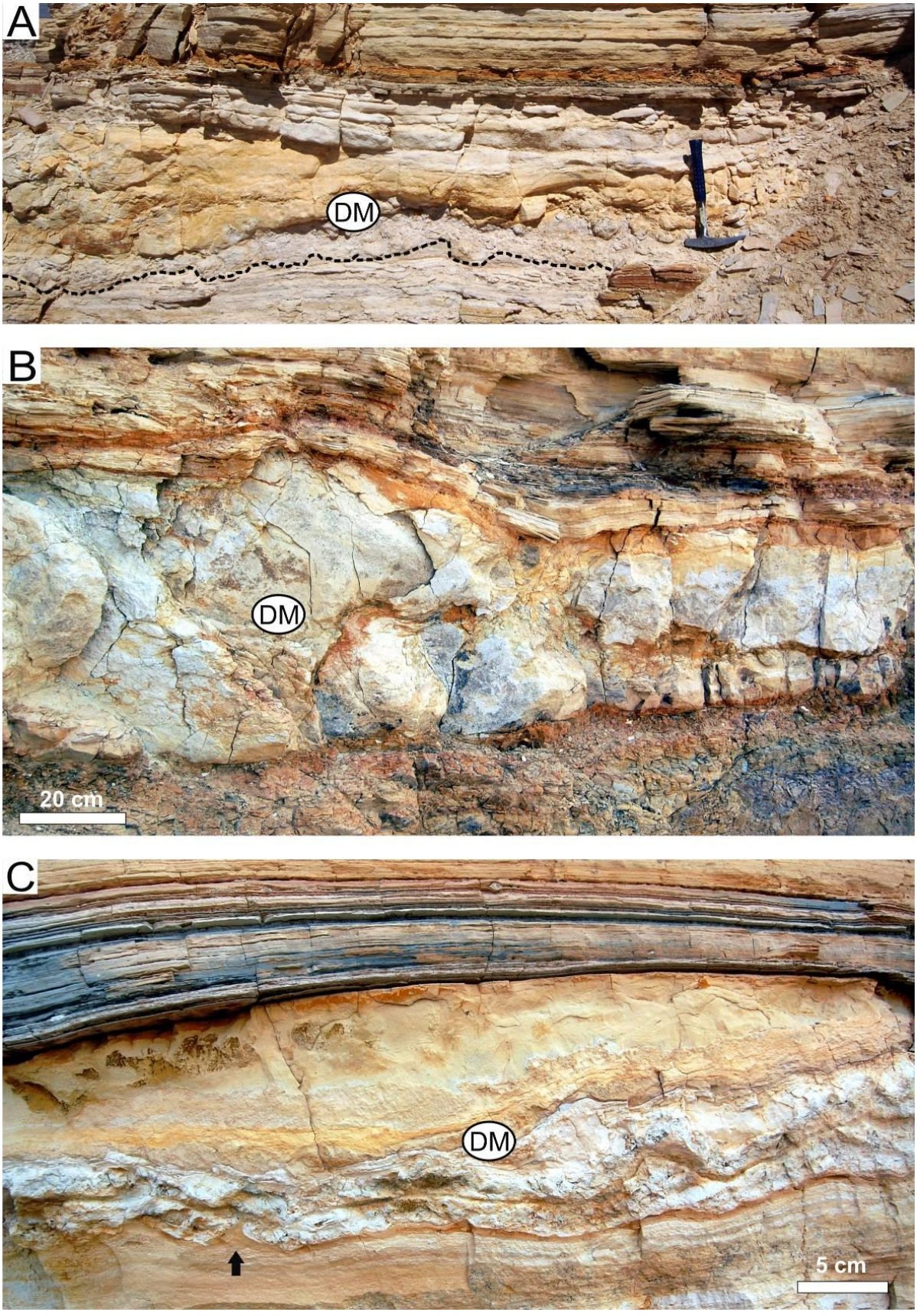
A
DM
B
DM
20 cm
C
DM
5 cm

Dolomicrites are sandwiched in between undeformed, laminated micrites, which indicates that after their deposition profundal sedimentation resumed. They were interpreted by Buchheim (1994a) as the result of episodes of precipitation in the water column and subsequent settling of dolomite mud during abrupt, short-lived hypersaline events. Alternatively, this anomalous facies may represent resuspension of shallow-water sediment by earthquakes or strong oscillatory waves (seiches) and redeposition in deeper areas, similar to "homogenites" documented elsewhere (Kastens and Cita, 1981; van Loon et al., 1995; Chapron et al., 1999).

### *2.4.4 Brittle–Ductile Features*

#### 2.4.4.1 Description

Complex structures developed in parallel-laminated sediments are characterized by coexisting plastic and brittle deformation features, where loading, complex folding, brecciation, microfaults, and fault-related folds occur in a single layer (Figs. 2.8A–H, 2.9A, B). Deformation is confined to intervals 5–35 cm thick, bounded by undisturbed layers of the same facies. Their lower and upper contacts can be sharp (Figs. 2.8A, G, 2.9A, B) or gradational (Fig. 2.8B, C, E). In both cases, the most intense deformation is towards the middle. Open to tight and recumbent folds exhibit variable amplitudes axial plane dip directions in organic-rich laminae, and individual folds can be disrupted by superimposed smaller kinks, microfaults, or fault-related folds (Fig. 2.8E, F). Laminae may show millimeter-sized, bead-like boudinage features (Figs. 2.8D, 2.9A, B). Brittle features in organic-poor laminae include small-scale normal, reverse and thrust faults, all with variable dips (Figs. 2.8A, B, 2.9B), as well as breccias.

Breccia bodies with irregular geometries occur at the front of folded and faulted structures (Fig. 2.8E, F) or as part of more complex features (Figs. 2.8G, H, 2.9B). These are centimeter to decimeter in scale, and they pass into undeformed carbonates either gradationally or abruptly. The clasts are platy, granule- to pebble-sized fragments with subangular to subrounded edges, and are identical to the adjacent laminated micrites. They typically float in a structureless muddy matrix (Fig. 2.8G, H), although in places the fragments are still partly attached to the host micrite layer (Fig. 2.9B). Towards the top of deformed beds fluid-escape features may be filled by structureless mud, and a variably thick rudstone consisting of intraclasts of the laminated micrite in a sandy matrix may also be present (Fig. 2.8G, H). Brittle–ductile features are locally associated with sedimentary dikes, mass-transport deposits, and oil shale breccias.

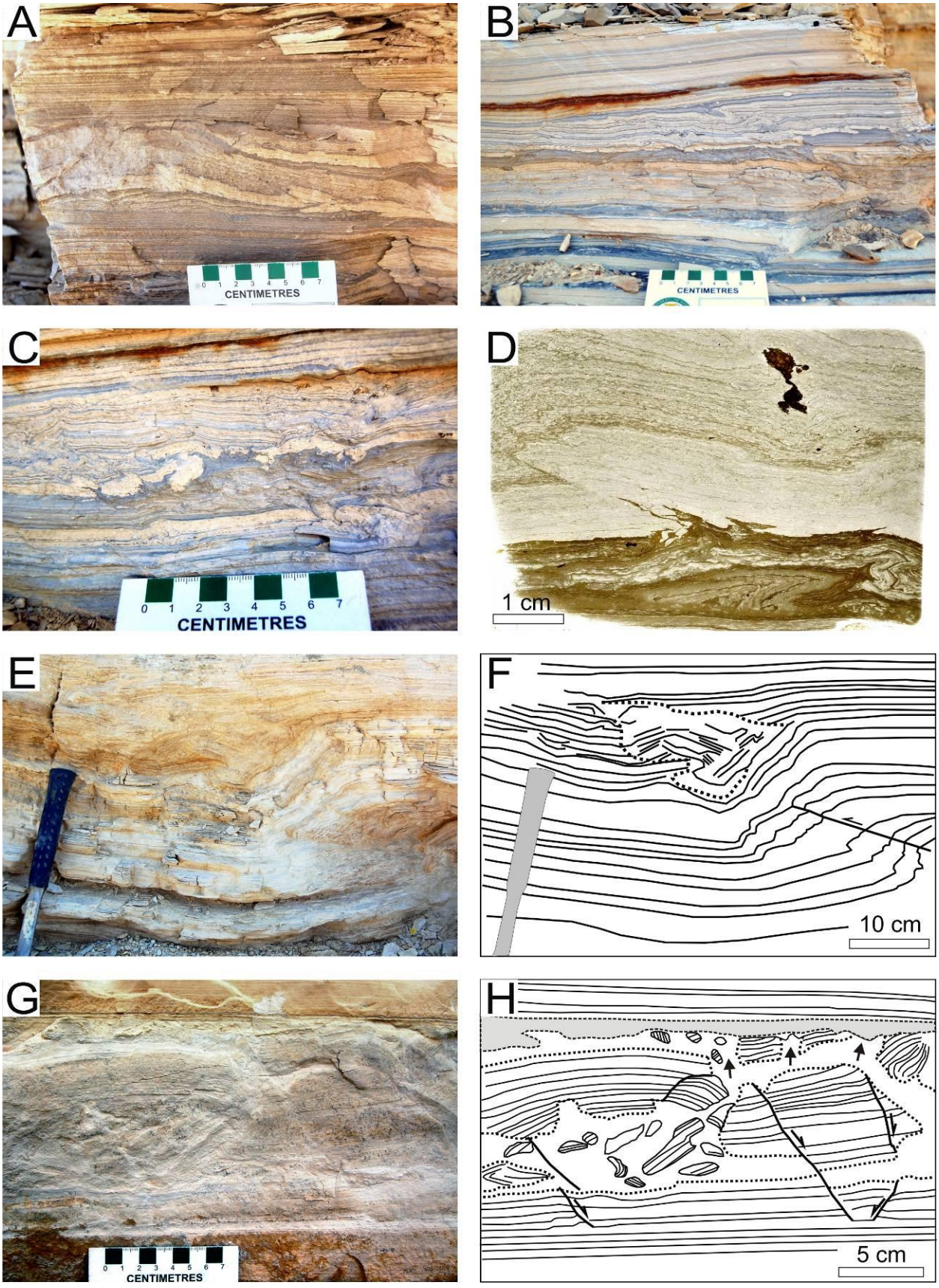
A
CENTIMETRES
B
CENTIMETRES
C
0 1 2 3 4 5 6 7
CENTIMETRES
D
1 cm
E
F
10 cm
G
CENTIMETRES
H
5 cm

**Figure 2.8** (on previous page) Brittle–ductile deformation structures in laminated micrites. A) Fragmentation and faulting (normal and reverse), with pop-up structures, in light-colored organic-poor intervals, with folding in darker, organic-rich interval below (CCQ). B) Complex deformation features in oil shales, showing folds, fault-related folds, and both extensional and compressional microfaults. Ductile deformation is more common in darker-colored organic-rich laminae, whereas brittle deformation is more common in light-colored organic-poor laminae (SHQ). C) Similar to Part B, with ruptured and squeezed light-colored organic-poor lamina (in middle) (SHQ). D) Thin section photomicrograph showing irregular and recumbent folding in organic-rich interval at base and small-scale reverse faults and related folding in overlying organic-poor interval, with variable dips of fault planes and axial planes of the folds and numerous parallel microfaults (right side) (CCQ). E) Reverse fault and fault-propagation fold (right side), with brecciated laminae at the nose (FB1). F) Tracing of Part E, with the brecciated zone outlined by dotted line. G) Faulted and disrupted oil shale, showing a brecciated zone with muddy matrix and, on top, an irregular layer of laminated micrite fragments in structureless silty matrix (SFTC1). H) Tracing of Part G, showing deformed zone outlined by dotted line, fluid-escape structures (black arrows), and brecciated layer on top (gray).

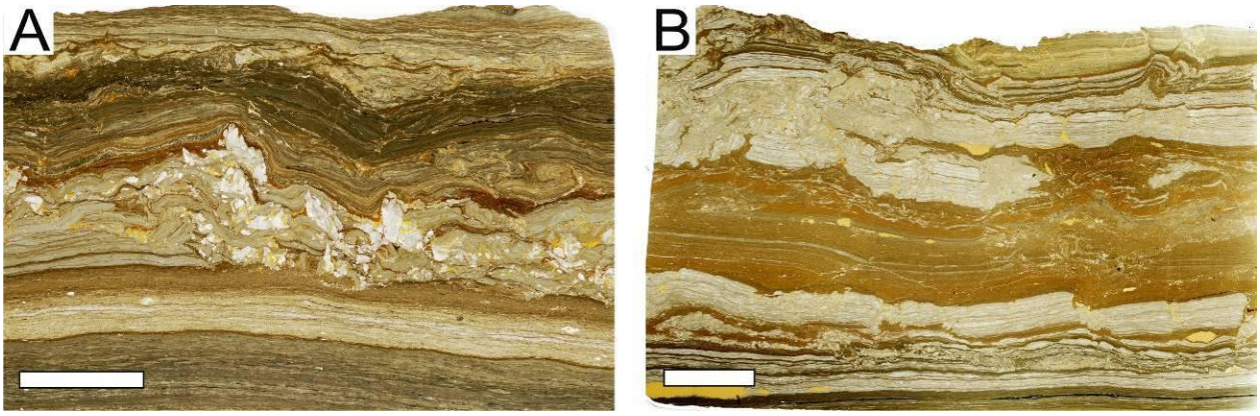


**Figure 2.9** Brittle–ductile deformation structures in laminated micrites consisting of dark-colored organic-rich laminae and light-colored organic-poor laminae. Thin section photomicrographs (SHQ). A) Irregular folding showing variably dipping axial planes, with recumbent fold (center right) and disruption of fragmented calcite pseudomorphs (white). B) Folding, microfaulting, and brecciation, with shingling of fragments. Scale bars are 1 cm.

#### 2.4.4.2 Interpretation

The coexistence of brittle and ductile features reflects a complex response of the semi-cohesive sediments to external stresses (e.g., Rodríguez-Pascua et al., 2000; El Taki and Pratt, 2012), controlled by variable rheological properties due to varying organic content. Thus, plastic behavior is more typical in organic-rich intervals, whereas organic-poor layers show microfaulting and brecciation. The structureless mud forming the core of fluid-escape features or the matrix of the breccias indicates that brecciation, obliteration of primary sedimentary

structures by fluidization, and sediment injection upward and sideways co-occurred (e.g., Davenport and Ringrose, 1987; Rossetti, 1999). The sharp or gradational boundaries and the uniform thickness of the overlying strata indicate intrastratal deformation. Confining sediments must have had a contrasting rheology, but small-scale deformation features, if present, were likely caused by the same triggering event.

Although brittle–ductile features are often identified as slumps with the implication that they formed on a slope (e.g., Moretti and Sabato, 2007), true slumps are characterized by imbricated compressional features, such as thrusts and asymmetrical fold geometries with unidirectional axial planes (e.g., Strachan, 2002; Alsop and Marco, 2011). However, features described here lack a preferred orientation where compressional features coexist with extensional ones, indicating that deformation is the result of chaotic shear stresses and not gravity-driven lateral displacement. These hybrid structures in a low-energy setting are best explained by the passage of shear waves and surface waves during seismic shaking (e.g., Pratt, 1998b, 1999, 2001; Rossetti 1999; Rodríguez-Pascua et al., 2000; Rossetti and Góes, 2000; Kahle, 2002; Montenat et al., 2007; Moretti and Sabato, 2007; Berra and Felletti, 2011; Martín-Chivelet et al., 2011; El Taki and Pratt, 2012) (see Trigger Mechanism). Fracturing and brecciation can result from either differential rheology or strain-hardening during shaking. Irregular rudstone deposits on the top of deformed layers reflect near-surface deformation and might represent redeposition of resuspended or elutriated sediment after liquefaction (Owen, 1987; Oliveira et al., 2009) or material remobilized by a seiche that may have been triggered by the same event (Alsop and Marco, 2012).

### *2.4.5 Sedimentary Dikes*

#### 2.4.5.1 Description

Sedimentary dikes (including crack fills and small dikes or “dikelets”) are common in laminated micrites with variable organic content and locally interbedded with detrital siliciclastic sediments (Figs. 2.10A–E, 2.11A–E, 2.12A–G, 2.13A–C, 2.14A–F, 2.15A–F). Most commonly, dikes are isolated, without a connection to a source bed (Figs. 2.10E, 2.11A, C–E, 2.12C, D, 2.14A–C). Occasionally, however, the feeder interval is seen to be a structureless dolomicrite bed capping downward-tapering dikes (Fig. 2.15A–F). In one case it is represented by just a discontinuity surface with dikes penetrating both upwards and downwards (Fig. 2.10A–D). On

the bedding plane, as observed at the Smith Hollow Quarry, dikes continue laterally for several tens of meters and are oriented approximately north–south (Fig. 2.11B). They are slightly curving, and narrower dikes splay from the larger dikes, forming a quasi-orthogonal pattern. The cells in these are ten or so meters across.

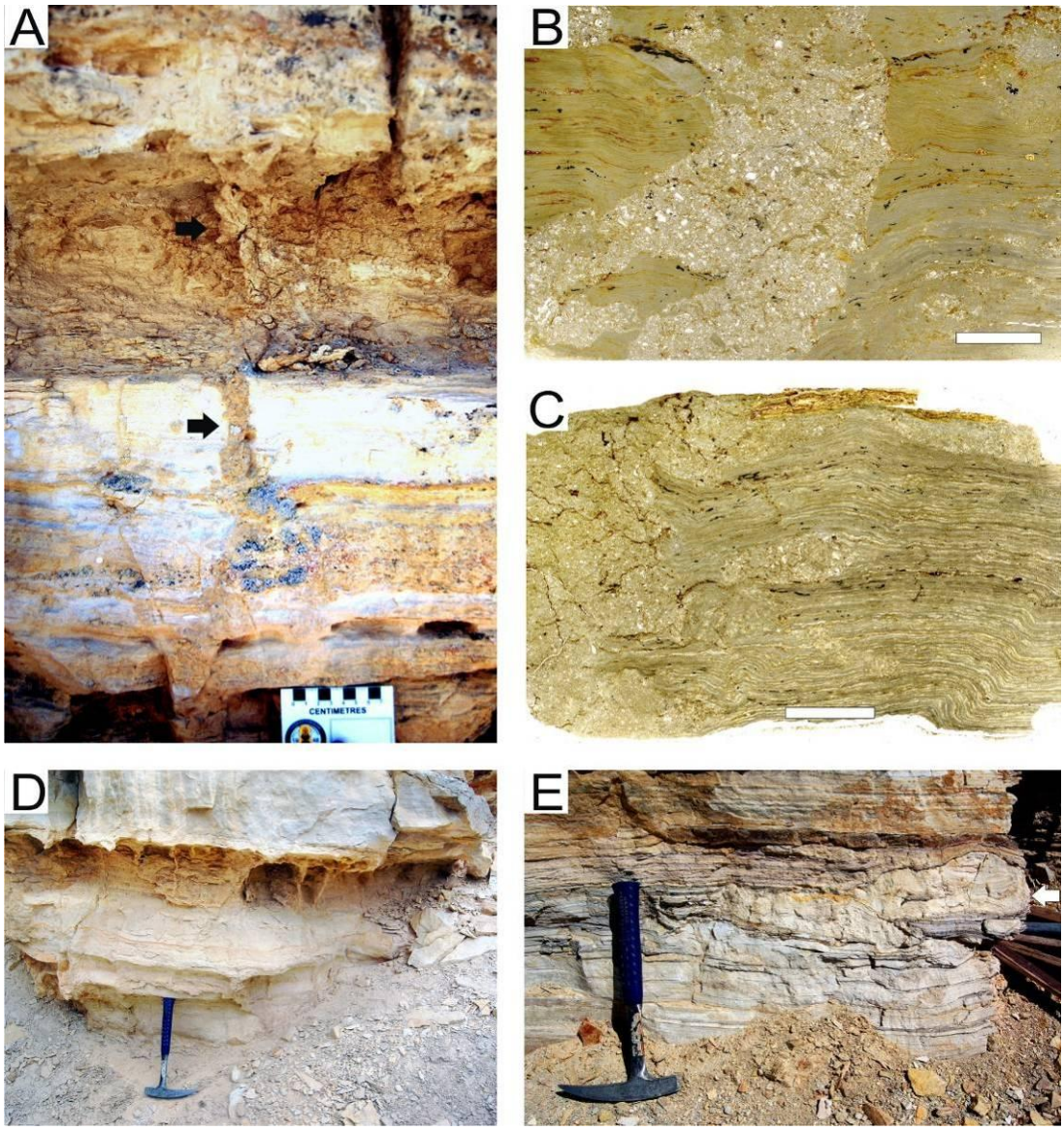


**Figure 2.10** Sedimentary dikes in laminated micrites: A) Downward-extending dike > 40 cm long (black arrows) (AR1). B) Thin section photomicrograph of variably folded and disrupted laminae cut by wide dike and smaller dikes (right side) filled with calcite sand, angular sand- and silt-sized micrite fragments, and carbonate mud (AR1). C) Thin section photomicrograph of variably folded and disrupted laminae with dike (left side) and sills (right side) (AR1). D) Dikes from same stratigraphic position as Parts A–C (standing in relief due to weathering of host) (SFTC1). E) Isolated, subhorizontal, bulb-shaped dike (white arrow) in oil shale filled with carbonate mud (SHQ).

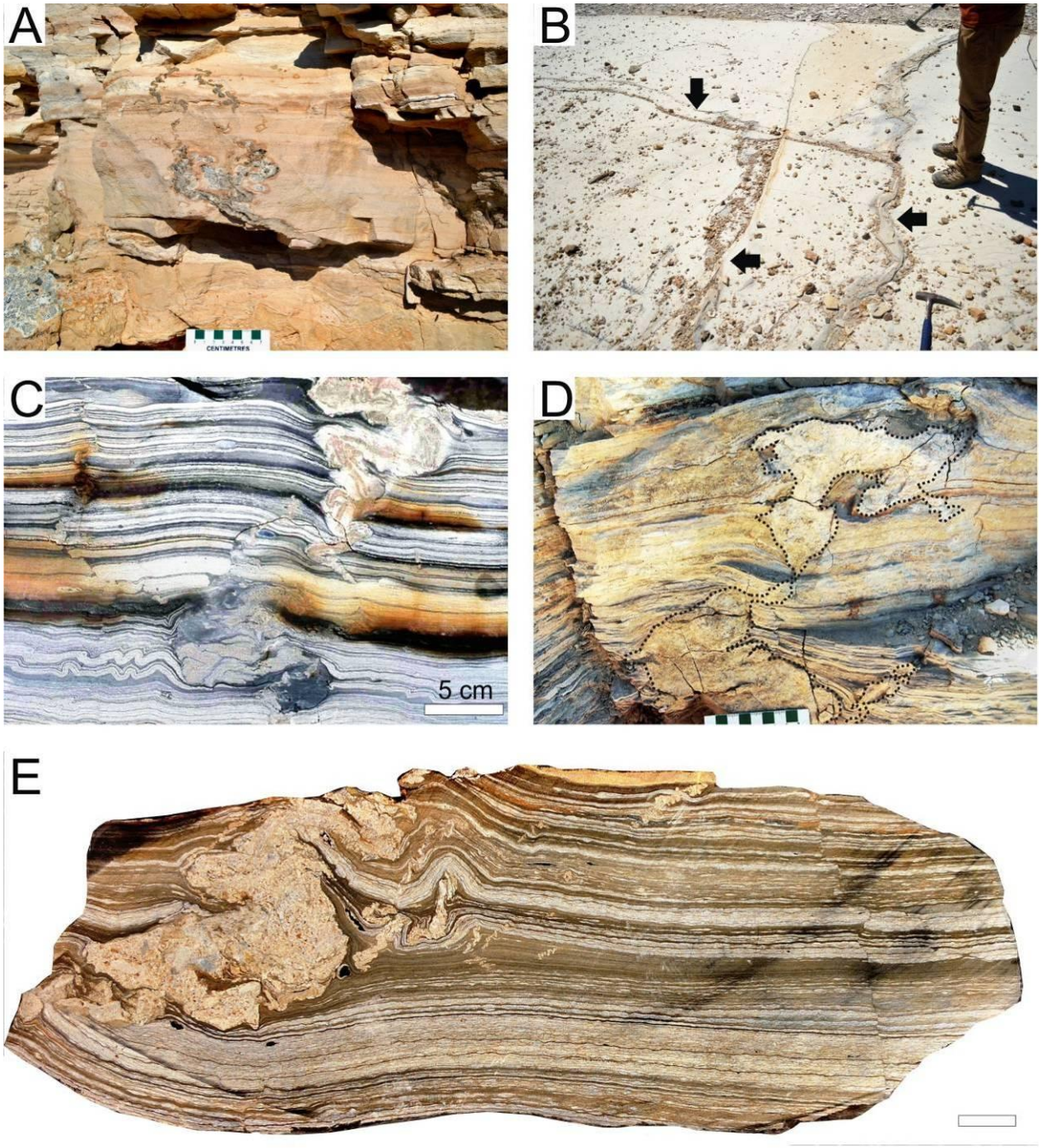


**Figure 2.11** Sedimentary dikes in laminated micrites. A) Isolated, ptygmatically folded sand-filled dikes, with convoluted bed underlying host bed (NFB2). B) Dikes (black arrows) forming quasi-orthogonal pattern on bedding plane (orientation ~ 005° and ~ 090°) (Figure 2.12A shows detail of dike by feet and hammer) (SHQ). C) Two interconnected dikes associated with folds and microfaults, showing multiple infilling events with brecciation (upper right) (SHQ). D) Two interconnected carbonate mud-filled dikes (outlined by dotted line) (SHQ). E) Slab showing portion of dike filled with carbonate mud- to sand-sized material having structureless internal fabric, with isolated, millimeter- to centimeter-sized folded dikes (center) and microfault (right side) (SHQ) (scale bar is 1 cm).

Dikes vary widely in cross section, from irregular to bulbous, and in size, from several millimeters up to 2 m in length and 0.5 m in width. They generally show moderate sinuosity and branching and commonly pass downwards or upwards into subtle cracks that are ptygmatically folded (Figs. 2.11A, C–E, 2.12A–D, 2.13C). Dikes often change thickness and/or orientation at lithological boundaries (Figs. 2.12A–D, 2.13C, 2.14E, F, 2.15A, B), with small projections along the lamination (Figs. 2.11D, E, 2.12B, 2.14E, F). Where dikes reach siltstone beds below, they bifurcate and laminated sediments are intruded into the siltstone (Fig. 2.15B, C). The lamination of the host sediment is usually disturbed and bent around the dikes, showing both down- and upwarping. The thickness of laminated intervals also show thickening towards the dikes (Figs. 2.11E, 2.12C, D). In many cases silicified dikes form the core of isolated concretions, where the surrounding lamination is bent and draped around them (Fig. 2.15E, F).

The infill is typically structureless carbonate. In cases where a dike connects to a dolomicrite source bed, the infill is the same. Fractured, shingled, or multiple fillings, with brecciated internal structures and vertical zonation, are also common (Figs. 2.11C, E, 2.12E–G, 2.13A). Dikes with brecciated infill usually occur in the same deformed horizon with those filled with uniform-sized sediment. Carbonate fragments in the infill are angular, up to 2 cm in size, and can be laminated or structureless. Some dikes show a thin (up to 2 mm) lining of laminated sediment along their margins; the thickness of the laminae in these linings is slightly greater than the thickness of the laminae of the host micrites (Figs. 2.12E-G, 2.13B). These marginal veneers terminate downwards or upwards, or pass into zones where they are dislodged fragments. They have sharp boundary with the host sediment and a straight or ragged border with the adjacent infill.

Dikes are frequently associated in the same interval with other deformation features such as small-scale simple or complex folding, breccias, and microfaults (Figs. 2.11C, E, 2.12C–G, 2.13C). Organic-poor laminae in the vicinity of the dikes often show fragmentation, buckling, and irregular thickening and thinning, forming boudinage-like structures (Figs. 2.11E, 2.12B, 2.13C).

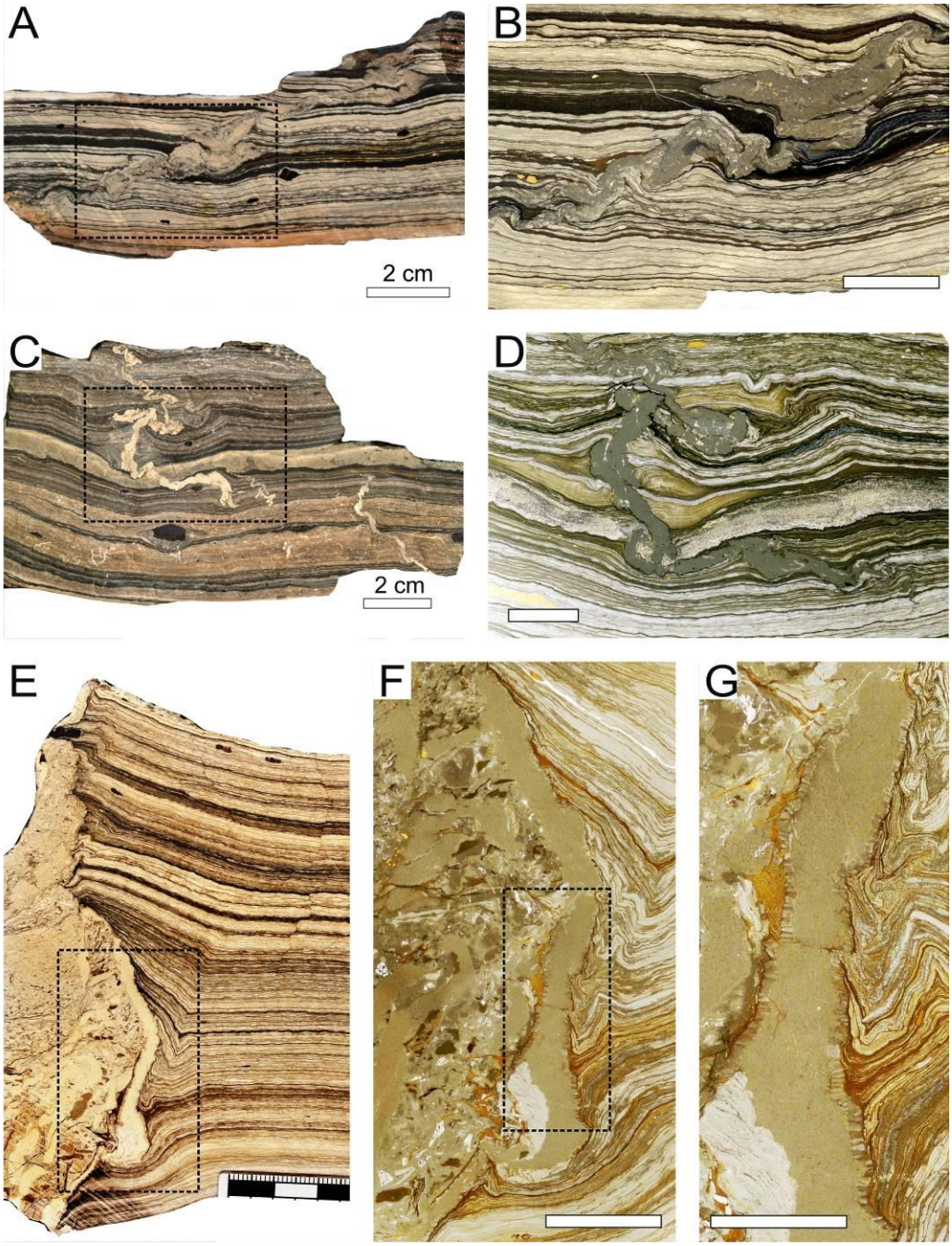


**Figure 2.12** Sedimentary dikes in laminated organic-rich micrites (SHQ). A) Slab showing oblique dike (sample taken from dike by feet and hammer in Figure 2.11B). B) Thin section photomicrograph of area outlined in Part A, showing dike filling of carbonate mud mixed with silt- and sand-sized angular fragments of host laminae; boudinaged structures are common in light-colored organic-poor laminae (scale bar is 1 cm). C) Slab showing centimeter-sized, isolated, squeezed and ptygmatically folded narrow dikes. The main dike cuts 1 cm thick, homogenized detrital silt layer (across middle); lamination around dikes is bent both upward and downward and also slightly offset (right side). D) Thin section photomicrograph of area outlined in Part C, showing dike filling of carbonate mud, fragmentation of the dikes, and thickening of organic-rich laminae adjacent to dike (scale bar is 1

cm). E) Slab showing two dike generations: the first-formed narrow carbonate mud-filled dike flanked (to left) by later large dike with multiple fillings; host laminae faulted and folded adjacent to dikes. F) Thin section photomicrograph of area outlined in Part E, showing filling of narrow dike with carbonate mud and large dike with carbonate mud, silt, and sand- to pebble-sized fragmented material, ~1 mm thick zone detached from host sediment that lines wall of dike on right and smaller vertical dike filled with carbonate mud (scale bar is 1 cm). G) Close-up of area outlined in Part F, showing carbonate mud infill of first-formed dike and narrow, < 1 mm thick veneer of laminated micrite adjacent to it which is locally disrupted (scale bar is 5 mm).

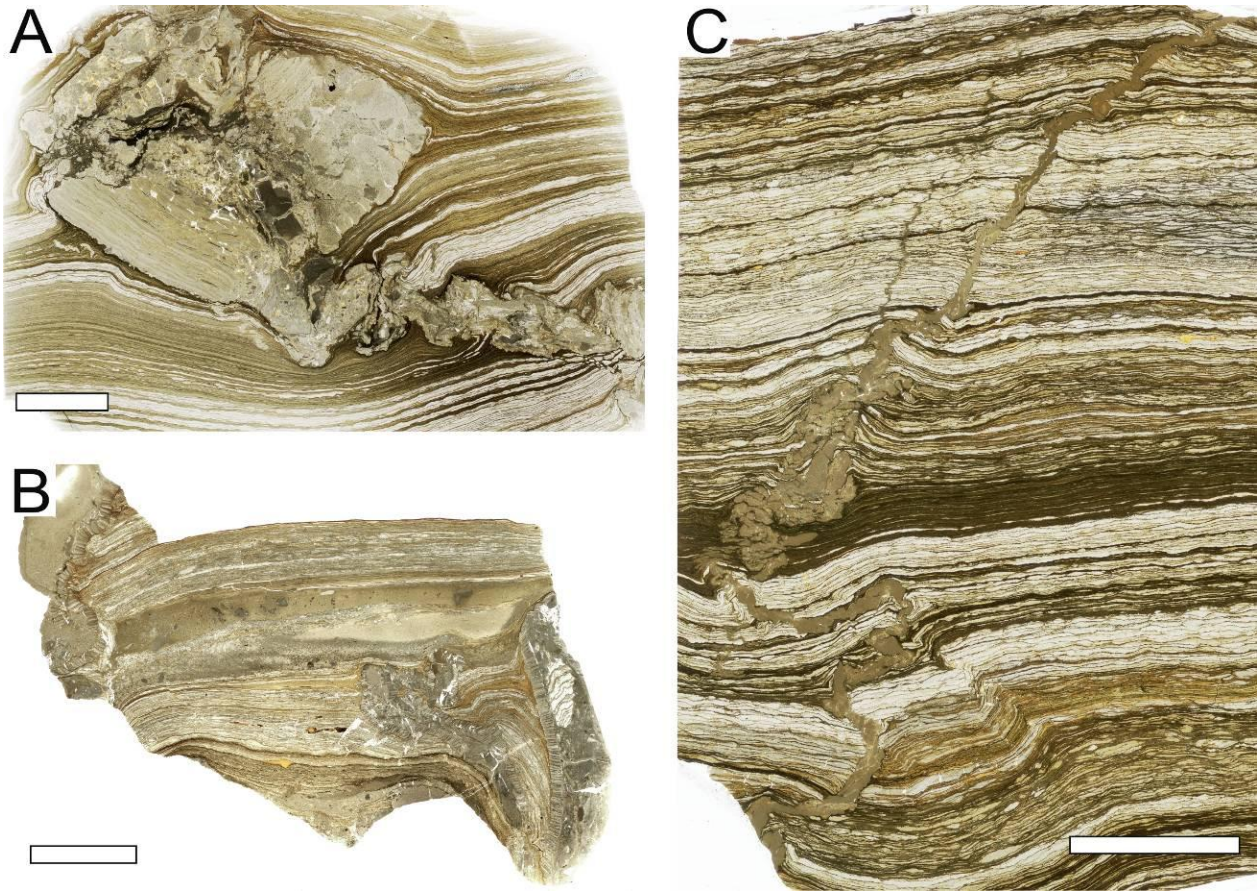


**Figure 2.13** Sedimentary dikes in laminated organic-rich micrites. Thin section photomicrographs (SHQ). A) Oblique dike filled with angular, fragmented carbonate material including laminated micrite clasts up to ~ 2 cm in length, and strongly compacted host laminae. Millimeter-sized ptygmatically folded dikes penetrating downward and upward from organic-poor laminae at left of large dike. B) Several dikes filled by carbonate mud (left), silt-sized material (middle), and sand-sized, angular, micrite, and laminated clasts (right). Dikes have 1–2 mm thick veneer of laminated micrite that has been disrupted and detached. C) Oblique dike that has been squeezed and ptygmatically folded, filled dominantly by carbonate mud; host laminae folded and faulted. Scale bars are 1 cm.

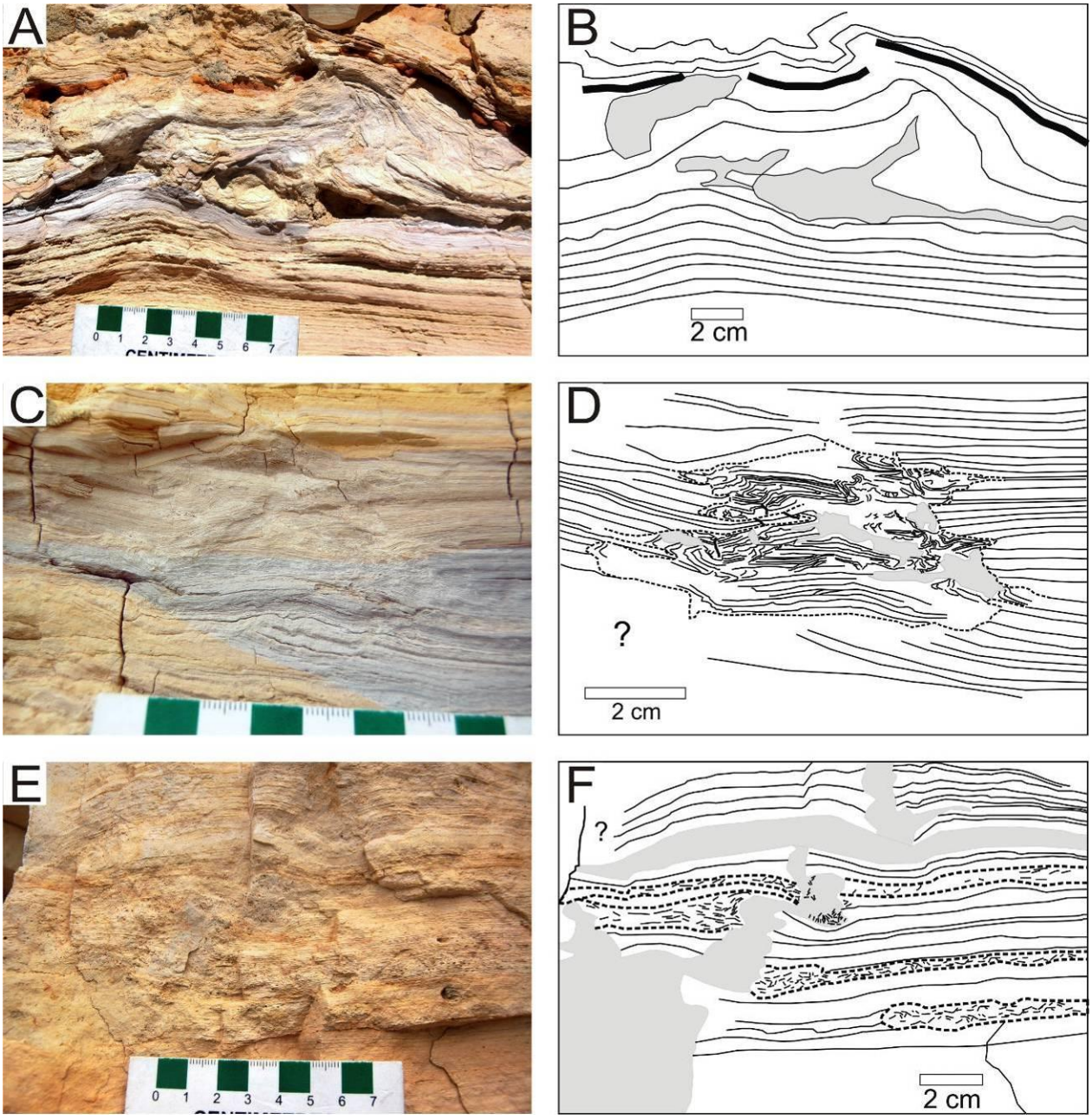


**Figure 2.14** Sedimentary dikes and associated deformation structures in laminated micrites. A) Folded organic-rich laminae around carbonate-mud-filled dikes (SHQ). B) Tracing of Part A, with dikes (gray) and a disrupted tuff layer above (thick black line). C) Localized deformation showing brecciated laminated sediment and dikes (NFB1). D) Tracing of Part C, with the sedimentary dikes (gray) and localized deformed zone outlined by dashed line. E) Dikes and sills(?) filled with carbonate mud, flanked by folded and brecciated laminated micrite, and cutting brecciated beds (NFB1). F) Tracing of Part E, with dikes (gray) and brecciated beds (outlined by dashed lines).

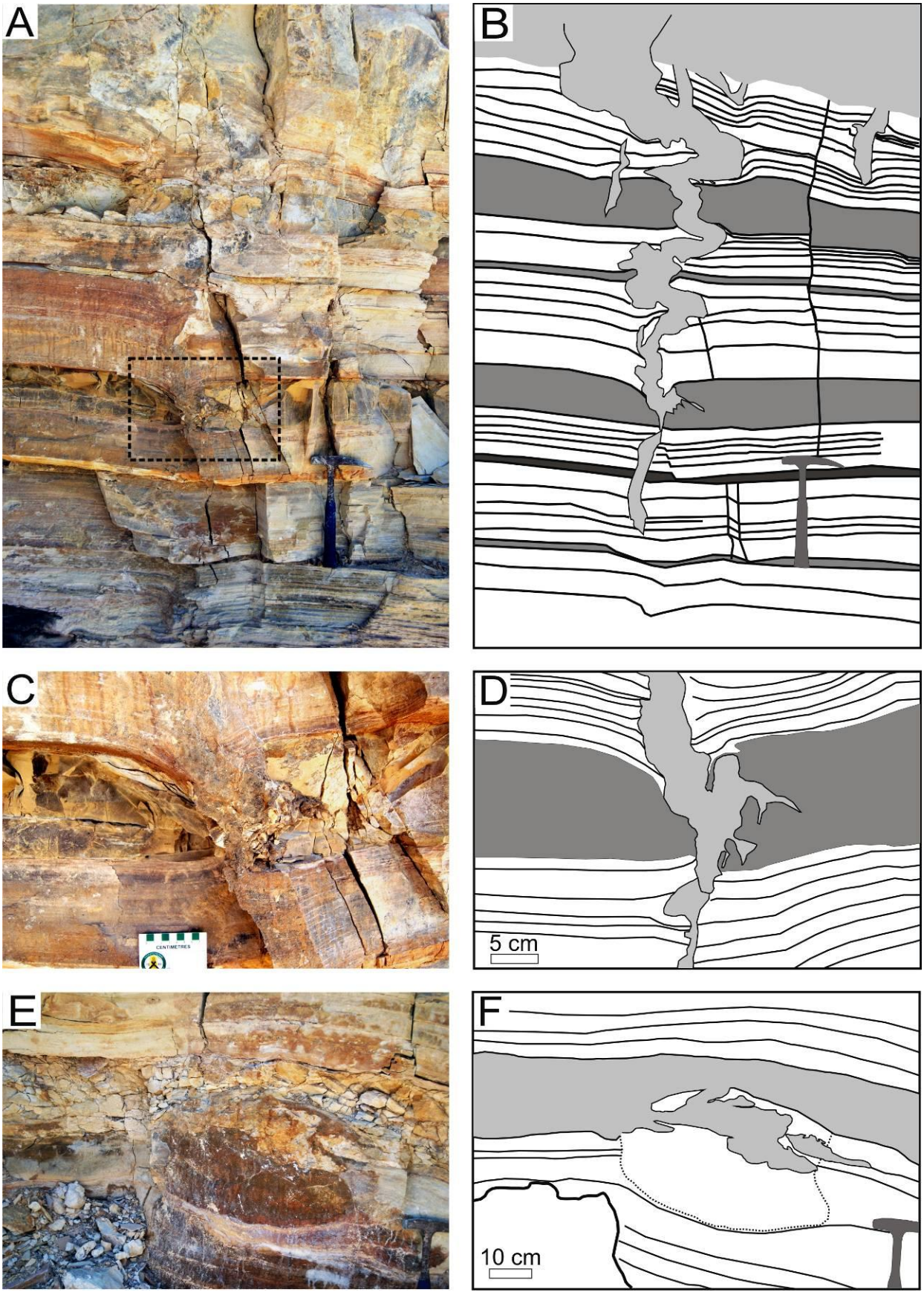
A
B
C
D
5 cm
E
F
10 cm

**Figure 2.15** (on previous page) Sedimentary dikes associated with structureless dolomicrites. A) Dikes sourced from dolomicrite bed at top and penetrating downward through laminated micrites (SHQ). Major dike in middle crosses two siliciclastic mudstone beds. B) Tracing of Part A (dolomicrite and dike in light-gray; siliciclastic mudstone in medium-gray; tuff in dark-gray; continuation of dike into dolomicrite bed marked by solid black line); outcrop fractures shown by vertical black lines. C) Area outlined in Part A, showing splaying of dike into siliciclastic mudstone. D) Tracing of Part C, with dike (light-gray) and siliciclastic mudstone (dark-gray). E) Small subhorizontal dikes sourced from dolomicrite bed (across center) and penetrating laminated micrite (forming core of a siliceous concretion) (CCQ). F) Tracing of Part E, with dolomicrite and dike (light-gray), and concretion (dotted line).

#### 2.4.5.2 Interpretation

Sedimentary dikes have been recorded from oil shales of the Green River Formation (Bradley, 1930; Picard and High, 1972; Smoot, 1983; Birgenheier and Vanden Berg, 2011; Tänavsuu-Milkeviciene and Sarg, 2012). In the Fossil Basin two groups of sedimentary dikes were identified: those which are isolated, and those with a well-defined feeder or source interval. Sharp contacts of the dikes with the host strata indicate a profound rheological contrast between the crack infills and the host sediment at the time of formation. Changes in the thickness, orientation and tilting of the dikes at lithological boundaries further point to the effect of rheological differences, involving post-emplacement deformation. Fracturing of siltstone interbeds and the splaying of the dikes within these beds indicate forceful injection of the remobilized material. The structureless nature of the sedimentary fill suggests fluidized sediments injected from the source beds (e.g., Daley, 1971; Owen, 1987).

The laminated veneers along the walls of some dikes represent host sediment that was preferentially cemented immediately adjacent to the dike. The greater thickness of the laminae compared to surrounding micrites indicates that cementation occurred before significant compaction. The host sediment separated from the veneer and dike margin during a later deformation and injection event. The role of sedimentary dikes as fluid-flow pathways during early diagenesis is further supported by compaction of the lamination in the host sediments away from the dikes as well as silicification and concretion formation.

Sedimentary dikes without a visible source bed indicate either that the bulk of the layer was remobilized and injected, or there was a lateral component to injection from a cryptic source bed (Rodríguez-Pascua et al., 2000), or the dike consists of material ejected from the host laminae (Pratt, 1998b). Where a source bed is preserved, however, the downward-tapering morphology

and the downward bending of the host laminae indicate downward injection. The obliteration of primary sedimentary features in dolomicrite source beds is evidence for loss of shear strength and mobilization (Surlyk et al., 2007).

Ptygmatic folding of the dikes and the bending of the lamination around them have been attributed to dewatering and distortion during the emplacement of the fluidized sediment (Pratt, 1998a, b, 1999) or subsequent compaction (e.g., Shelton, 1962; Tanner, 1998; Parize et al., 2007). Closely spaced cracks showing both straight and sinuous morphology in a single deformed bed of uniform lithology and multiple infilling indicate two or more generations of sediment mobilization and distortion (e.g., Pratt, 1998b, 1999; Surlyk et al., 2007).

Downward emplacement of dikes has been interpreted as the result of: (1) desiccation of clay-bearing sediment with cracks filled passively from above (e.g., Allen, 1986a, 1987); (2) tectonically mediated fissuring leading to Neptunian dikes (e.g., Montenat et al., 2007); (3) shrinkage and dewatering due to compaction (Picard and High, 1972; Tanner, 1998; Harazim et al., 2013) or earthquakes (Pratt, 1998a); or (4) sudden sediment loading and hydrofracturing (Parize and Friès, 2003; Parize et al., 2007).

Although similar dikes elsewhere in the Green River Formation were ascribed to desiccation by Bradley (1930) and Smoot (1983), the depositional setting, the lack of other pedogenic features, their geometrical attributes, and nature of the infilling material preclude a subaerial origin. Similarly, dike morphology and the nature of the infill do not support a Neptunian origin. The stratigraphic succession indicates that no depositional event involving sudden loading could have occurred. Mass-transport deposits may have been capable of loading, but dikes do not show a relationship with such units, and all the evidence points to intrastratal formation. Instead, these dikes formed by the development of elevated pore pressure causing dewatering and fluidization and injection of sediment (e.g., Hurst et al., 2003, 2011; Huuse et al., 2010). The formation of upward-propagating dikes was directed by the upward-decreasing pore-pressure gradient. Examples of downward-propagating dikes indicate dewatering of the laminated micrites and concomitant injection of fluidized sediment from the overlying source bed (Pratt, 1998a). Upward- and downward-propagating dikes in the same interval indicate pore-pressure gradients in both directions.

Due to the lack of other feasible mechanisms, these dikes are explained as injection features triggered by stresses generated by earthquakes, where fluidized and fragmented material filled

fissures generated by subaqueous intrastratal dewatering and shrinkage of the carbonate mud (Pratt, 1998a, b, 1999). This process resulted in the formation of laterally extensive, oriented sedimentary dikes confined to specific stratigraphic intervals. Segregation and remobilization of granular carbonate mud from carbonate-rich, organic-poor laminae is indicated by their irregular thickness. Carbonate-sand-filled dikes related to the discontinuity surface represent remobilized remnants of the layer. The association of other deformation features further support an earthquake trigger. The dikes have two prominent strike directions, likely governed by the paleostress field or the direction of propagating seismic waves (Pratt, 1998a, b, 2002a; Rodríguez-Pascua et al., 2000; Jolly and Lonergan, 2002). Small-scale ptygmatically folded cracks resemble those often referred to as "syneresis cracks" (Pratt, 1998a) and traditionally attributed to the effects of fluctuating salinity (e.g., Burst, 1965; Plummer and Gostin, 1981). These micrite-filled cracks are also similar to "molar-tooth structure", which is locally abundant in Proterozoic marine carbonate successions (Pratt, 1998b, 2011). Their close spatial relationship to larger dikes in Fossil Basin confirms a genetic link, and thus they are also interpreted as seismically induced, rather than passive chemical shrinkage.

### *2.4.6 Fluid-Escape Cusps*

#### 2.4.6.1 Description

Cusps occur in laminated micrites showing laterally extensive folding or convolute lamination. They form the crests of folds where the lamination is curved upwards and truncated. In cross section they are cuspate or triangular-shaped features up to 15 cm long and 4 cm wide, filled with structureless carbonate micrite (Figs. 2.6B, 2.16A).

#### 2.4.6.2 Interpretation

Similar cuspate features have been referred to as "water-escape structures", "flame structures", "pillars", "injection structures", "diapirs", "fluidization channels", "sand/mud volcanoes" or "sediment conduits". They have been reported from various depositional environments, such as lacustrine (Rodríguez-Pascua et al., 2000; Moretti and Sabato, 2007), fluvio-lacustrine (Dasgupta, 1998; Neuwerth et al., 2006), fluvial (Owen, 1995, 1996a; Obermeier, 1996), eolian (Moretti, 2000), tidal (Greb and Archer, 2007), marine (Lowe, 1975;

Alfaro et al., 2002; Hildebrandt and Egenhoff, 2007; Rodríguez-López et al., 2007; Oliveira et al., 2009), and glacial (Cheel and Rust, 1986), and various origins have been invoked. The formation of these features is driven by the vertical shear associated with fluid drag during fluidization, and they indicate localized water escape from the underlying sediments. (Lowe, 1975; Owen, 1987, 2003).

The infill of the cusps represents carbonate mud particles elutriated from below. Fluidization developed in the cores of the domal structures, which indicates that the location of fluid escape in these beds was governed by the morphology of the plastically deforming host sediment and superimposed on it. This indicates that they are genetically related and formed by elevated pore pressures and fluidization triggered by seismic activity (see Convolute Lamination and Trigger Mechanism).

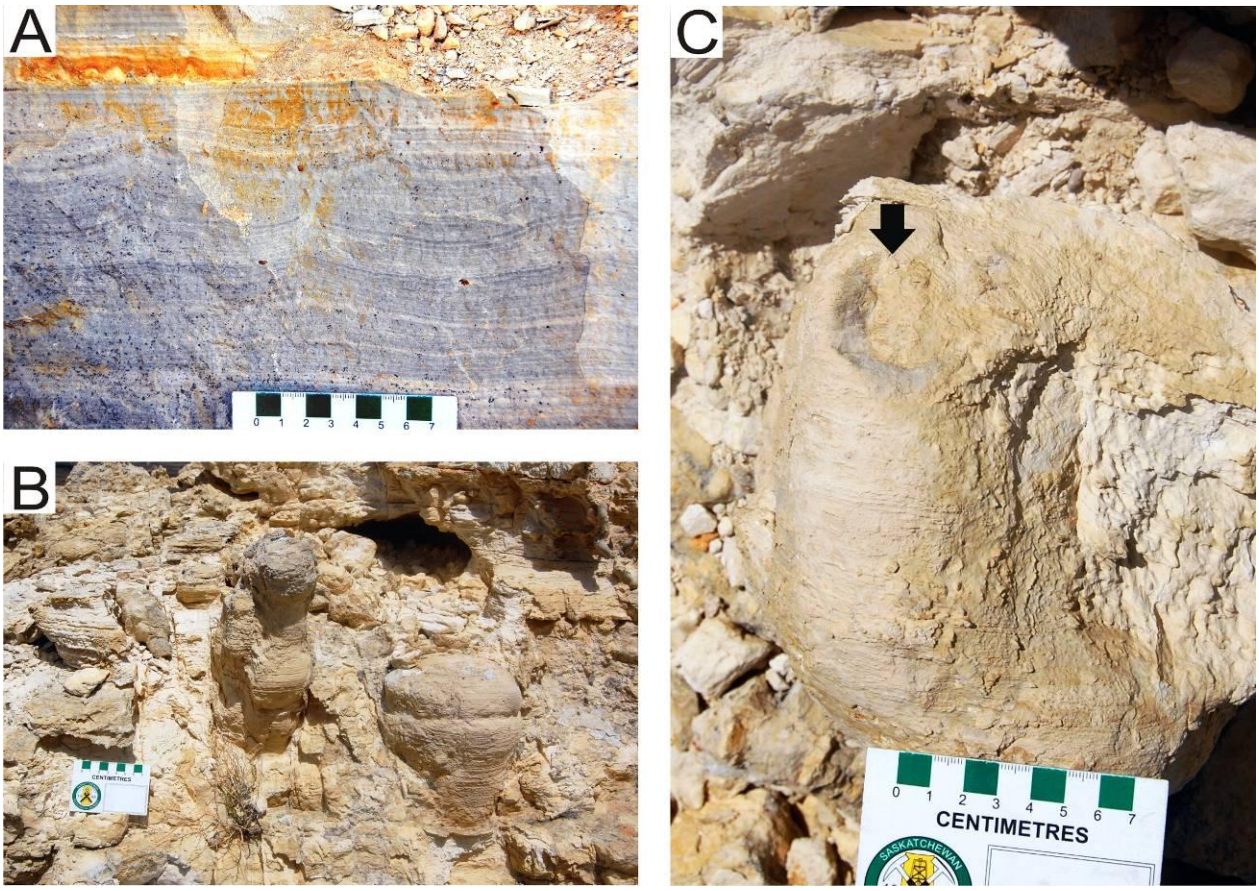


**Figure 2.16** Fluid-escape features in laminated micrites. A) Fluid-escape cusp (middle) filled with carbonate mud in gently undulating bed (WQ). B) Irregular cylindrical or ovoid fluid-escape pipes in partly bioturbated micrites (AR1). C) Close-up of Part B, showing vertical tube (black arrow) in core of concretion.

### *2.4.7 Fluid-Escape Pipes*

#### 2.4.7.1 Description

Isolated to clustered concretions with crudely ovoid, bulbous, cylindrical, lobate and rarely branching shapes are present in a single gently undulating, partly bioturbated micrite interval 1.5 m thick (Fig. 2.16B, C) at the same stratigraphic level in the Angelo Member at two sections 1.5 km apart (see Correlation). They range from 2 to 25 cm in diameter and from 5 to 35 cm in length. Most are oriented perpendicular to bedding but some are slightly tilted, and their external surfaces retain the imprint of the horizontal lamination of the host bed. Internally they are nonlaminated, and consist of equant angular fragments of micrite 25–50 μm across. They exhibit a central tube or fissure that is partially or completely filled with blocky calcite cement. The host micrite exhibits low-amplitude folding in places.

#### 2.4.7.2 Interpretation

These concretions bear no resemblance to smaller horizontal and vertical burrows with meniscus fillings (Buchheim et al. 2011). They are superficially similar to diagenetic concretions attributed to subaqueous springs (e.g., Massari et al., 2001). However, the laminated micrite likely had relatively low permeability, and because the concretions are confined to a single interval, there is no evidence of them having acted as conduits for groundwaters from an aquifer under the adjacent land surface. Larger cylindrical fluid-escape structures or fluidization pipes have been related to overpressure resulting from tectonic stresses (e.g., Draganits et al., 2003; Ledésert et al., 2003; Nyman et al., 2006, 2010). The lateral extent of the host interval and the folding of the lamination point to seismically induced deformation. Thus, these concretionary features are interpreted as fluid-escape pipes because of their nonlaminated nature and axial cavity. The branching morphology of some examples might be the result of overprinting by multiple fluid-escape events. Lamination on the sides of the concretions is most likely the result of concretion growth beyond the fluidized core and into the host muds.

### *2.4.8 Microfaults*

#### 2.4.8.1 Description

Small-scale faults occur in various facies (e.g., deltaic sandstone, non-bioturbated or partly bioturbated laminated micrite) throughout the studied interval (see Correlation) and can be classified into three, often co-occurring types: (1) high-angle normal faults, (2) listric normal faults, and (3) reverse and thrust faults (Fig. 2.17A–C). They are commonly associated with other complex deformation structures and locally with sedimentary dikes. Generally, within a single interval faults form subparallel arrays (Fig. 2.17A), but single or splaying faults also occur (Fig. 2.17B). In all cases, they gradually die out both upwards and downwards. Faults are mostly planar and straight, but some fault surfaces are wavy, ragged or segmented, with changing dip angles (Fig. 2.17A, B). Moreover, the dip of the fault planes may vary markedly within the same bed (Fig. 2.17C).

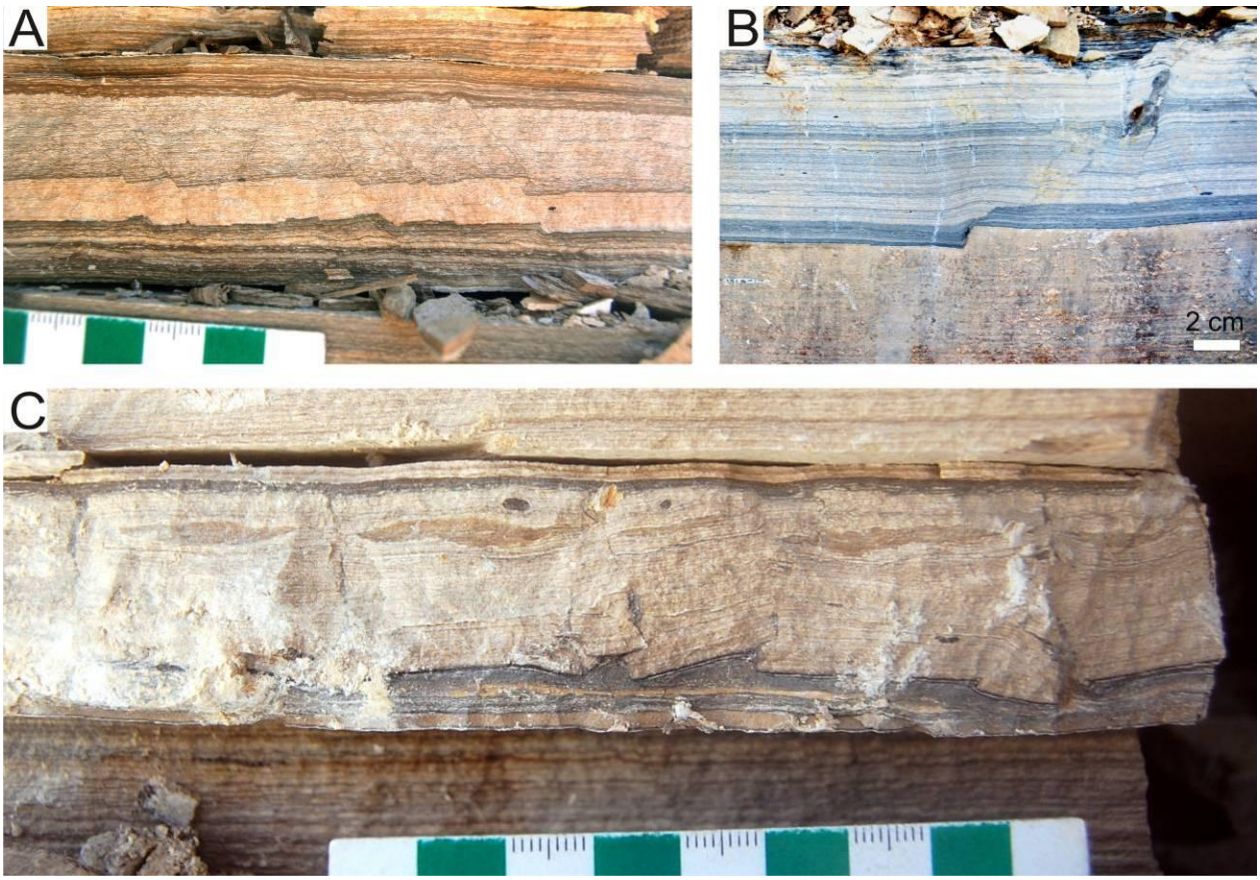


**Figure 2.17** Microfaults in laminated micrites. A) Array of normal microfaults ~ 1 cm apart confined to 3 cm thick, light-colored organic-poor interval bounded by dark-colored organic-rich laminae; small thrusts present in laminae below (CCQ). B) Normal microfault passing upward into cluster of faults in upper interval with variable amount of upward and downward displacement, which die out above and below (SHQ). C) Folding and disruption of organic-poor laminae, with fault planes filled by organic-rich mud from above and below (CCQ).

Thickness of deformed intervals ranges from 3 cm up to 4 m. Fault planes, where they form groups, are spaced about 5 mm to several tens of centimeters apart. The throw of faults ranges from few millimeters up to 75 cm and may vary within a single interval or along a single fault plane. In many cases the faults affect only specific intervals of light-colored, organic-poor sediment, and these discrete horizons are bounded by dark-colored folded, structureless, or laminated organic-rich sediments (Figs. 2.8A, 2.17A, C). The host is generally tilted, and often dislocated into larger blocks (Fig. 2.17C) whose laminae can be further disrupted by folds, fractures or smaller microfaults (Figs. 2.8D, 2.17A). Large, angular fragments of the faulted sediment may be present as 'floating' clasts within a structureless matrix (Fig. 2.8G). In some places voids between the ruptured strata and dilated fault planes are filled with dark-colored organic-rich mud (Fig. 2.17C). In others the normal faults developed graben or half-graben features. Subsequent passive sediment infill of the deformed relief or local fault-related changes in the thickness of the deposits was not observed.

#### 2.4.8.2 Interpretation

Faulting points to strain increase that exceeded the yield strength of the sediments layer, causing brittle failure of the relatively stiff material that may have been rendered cohesive by partial lithification (Owen, 1987). Variability in fault geometry, fault planes, and dip can be related to rheological heterogeneities (Price, 1966; Davison, 1987; Ferrill and Morris, 2003). Contrasting properties were likely governed in part by variable organic content (e.g., Grimm and Orange, 1997). This led to brittle deformation mainly in the rheologically susceptible organic-poor deposits, while organic-rich intervals behaved plastically (e.g., Rossetti and Góes, 2000). In other cases, the coexistence of brittle deformation and plastic behavior within the same organic-poor interval suggests that deformation occurred in the ductile–brittle field transition within semi-cohesive sediments.

The downward and upward disappearance of the microfaults and their close association with other stratally bounded deformation features indicate that they formed at shallow burial depths, rather than at the sediment–water interface (Pratt, 1994; Pope et al., 1997; Kahle, 2002). Faults contemporaneous with sedimentation can be related to rapid sediment influx and loading or slope failure in such areas as deltas or submarine slopes and canyons (e.g., Rider, 1978; Prior et al., 1982). Such mechanisms are discarded here based on the depositional setting and the

morphological characteristics of the faults. Microfaults have been attributed also to differential compaction (e.g., Guiraud and Séguret, 1987). However, compaction would most often generate vertical or subvertical normal faults, rather than a combination of compressional and extensional features of widely varying geometries. Furthermore, in Fossil Basin microfaults occur in lithologically uniform successions where stresses from differential compaction were unlikely.

Most examples of synsedimentary microfaults are ascribed to seismic activity (e.g., Seilacher, 1969; El-Isa and Mustafa, 1986; Davenport and Ringrose, 1987; Pratt, 1994; Mohindra and Bagati, 1996; Grimm and Orange, 1997; Bhattacharya and Bandyopadhyay, 1998; Kahle, 2002; Mörner, 2005; Fortuin and Dabrio, 2008; Koç Taşgin et al., 2011; El Taki and Pratt, 2012). The close association of intrastratal compression and dilation indicates that they occurred in the same deformation event and the ultimately disorganized nature of shaking led to variably oriented shear stresses (e.g., Plaziat et al., 1990; Pratt, 1994; Grimm and Orange, 1997; Matsuda, 2000; Rodríguez-Pascua et al., 2000; Kahle, 2002). The infill of the voids between ruptured and tilted blocks of laminated micrite indicates fluid migration and remobilization of organic-rich carbonate mud derived from the adjacent layers or within the deformed interval through fluidization during shaking (e.g., Grimm and Orange, 1997).

### *2.4.9 Oil Shale Breccias*

#### 2.4.9.1 Description

The two ~ 0.5–1 m thick intervals of organic-rich dolomicrite (i.e., oil shale) at the base of the Angelo Member show contorted lamination and brecciation right across the study area. These laterally extensive, monomict brecciated beds are characterized by non-graded, tilted, folded, and faulted laminated platy intraclasts, < 5 cm in length, that are aligned parallel to the bedding plane (Fig. 2.18). In most cases the original lamination of these beds is obscured. The clasts are surrounded by a structureless matrix of mudstone with high organic content. The lower and upper boundaries of the beds are generally planar, and are over- and underlain by undeformed, laminated micrites. Occasionally they are over- or underlain by mass-transport deposits and deformed with the surrounding beds.

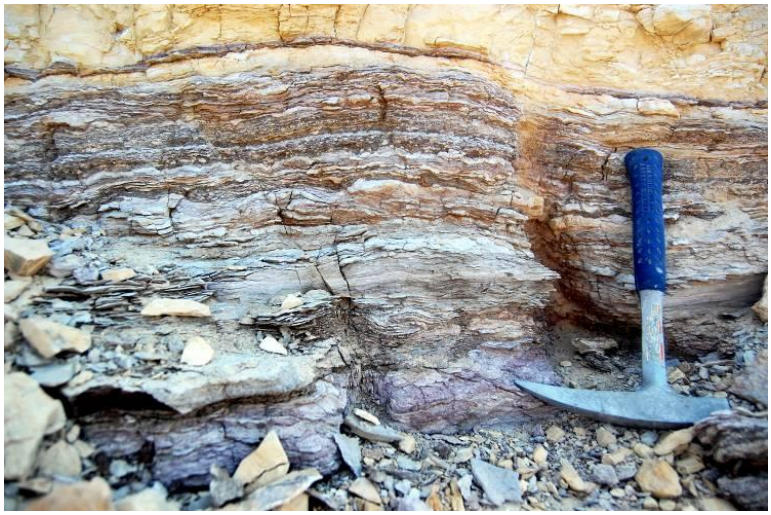

**Figure 2.18** Oil shale breccia, showing folded and faulted platy intraclasts (FB1).

#### 2.4.9.2 Interpretation

Brecciated oil shale beds are present in all the subbasins of the Green River Formation, and they have been interpreted as the result of desiccation (Bradley, 1931, 1973; Eugster and Hardie, 1975) or various kinds of mass-transport deposits such as slumps, slides, debris flows, or high-energy turbidity currents, with no trigger specified (e.g., Dyni and Hawkins, 1981; Birgenheier and Vanden Berg, 2011; Tänavsuu-Milkeviciene and Sarg, 2012). In Fossil Basin these beds differ from those interpreted as mass-transport deposits in other subbasins in that: (1) their lower boundary does not show scouring; (2) the clasts are composed predominantly of fragments of laminated profundal deposits, i.e., mainly the host sediment instead of transported shallow-water carbonates; (3) the clasts are not graded; and (4) there is an absence of indicators of large-scale lateral transport of cohesive material. In addition to brittle failure, shearing is evident by the aligned platy clasts, and folded laminae record plastic behavior. The monomict nature and the uniformity of deformation style indicate that the clasts formed by in situ intrastratal disruption with minimal lateral translation. The interpretation that these beds are turbidites (e.g., Dyni and Hawkins, 1981) can therefore be rejected here.

Their laterally extensive nature, their internal fabric, the absence of appreciable depositional slope, and their close association with mass-transport deposits points to a tectonic origin (see Trigger Mechanism). Organic-rich muds had an initial cohesive state and high shear strength (e.g., Smoot, 1983; Grimm and Orange, 1997) and may have behaved in a thixotropic

fashion (Picard and High, 1972; Brenchley and Newall, 1977; Grimm and Orange, 1997), whereas the organic-poor layers were stiffer. This led to in situ disruption, shearing and sliding of variably cohesive sediments during shaking (Pope et al., 1997; Stollhofen, 1998; Pratt, 2001).

### *2.4.10 Mass-Transport Deposits*

#### 2.4.10.1 Description

Parallel-laminated micrites are commonly interbedded with brecciated units 5 cm to up to 3 m thick (Figs. 2.19A–D, 2.20A–C). These beds are generally matrix-supported, monomict to oligomict, and occur as single or amalgamated beds (Fig. 2.19A), some of which are coarsening-upward (Fig. 2.19B). The matrix is carbonate silt or mud. The clasts are tabular, angular to subrounded, 0.5–20 cm in diameter, and composed of deformed (folded, faulted, or tilted) laminated or structureless micrite, chert, tuff, and locally siliciclastic siltstone and mudstone (Fig. 2.19B, C). Common are curvilinear stringers of clasts that are, in three dimensions, concave-up surfaces. In general the deformed layers are over- and underlain by laminated deposits (Figs. 2.19A, 2.20A). The upper boundaries of the beds are normally planar, while the lower are undulating and erosional, and the underlying succession commonly shows plastic and brittle deformation features (Figs. 2.19D, 2.20B, C). Where the mass-transport beds are amalgamated, scours occur at the base of each bed. Decimeter-scale injection features at the base, and fracturing and mixing of the sediments at the top, are also common. Most beds can be traced laterally for several tens of meters or can be correlated between two or more studied locations (see Correlation).

At Smith Hollow Quarry a lenticular, concave-up and planar-topped feature, 18 m wide and 4 m deep, is filled with contorted and mottled green siliciclastic mudstone and brecciated laminated micrite (Fig. 2.20A–C). This channel-like feature is overlain by undisturbed laminated sediments, and underlain by a zone of brecciated oil shale breccia, parallel-laminated micrite and tuff layers, which show mixing, thrusting and folding (Fig. 2.20B, C). This deformed zone gradually passes laterally into undeformed beds.

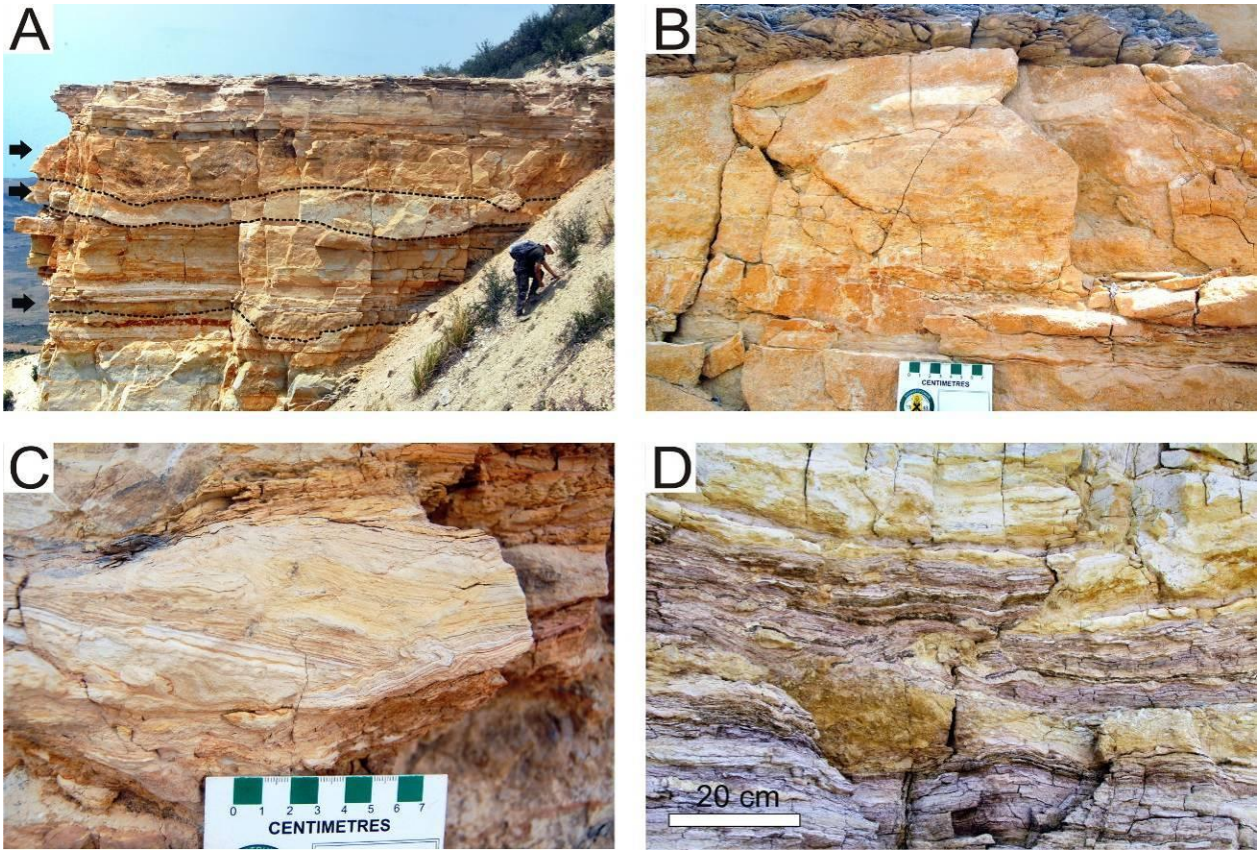


**Figure 2.19** Mass-transport deposits in laminated micrites. A) Outcrop showing several beds of mass-transport deposits (black arrows), each with irregular, erosional base (dashed lines) (NFB1). B) Reverse-graded bed, with structureless (shallow-water) clasts, sharply overlain by oil shale breccia (NFB1). C) Organic-rich laminated micrite clast showing folding, within a mass-transport deposit (FB1). D) Mass-transport deposit sourcing dikes and sill in underlying oil shale breccia (FB2).

#### 2.4.10.2 Interpretation

These beds are interpreted as mass-transport deposits consisting of slumps and debrites, which are typical deposits of subaqueous mass-flows (e.g., Nemec, 1990; Mulder and Cochonat, 1996; Mulder and Alexander, 2001). The channel-like feature is considered a chute, and its green siliciclastic mudstone infill as well as the clasts in other brecciated beds suggest that the material was transported from shallower areas. The source beds were well lithified, and after fragmentation and transportation the pore spaces between the clasts were filled by mixed carbonate mud, silt and occasionally tuffaceous material. Clasts with the same lithology and parallel lamination as the over- and underlying succession became incorporated during transportation and, in many cases, deformed plastically.

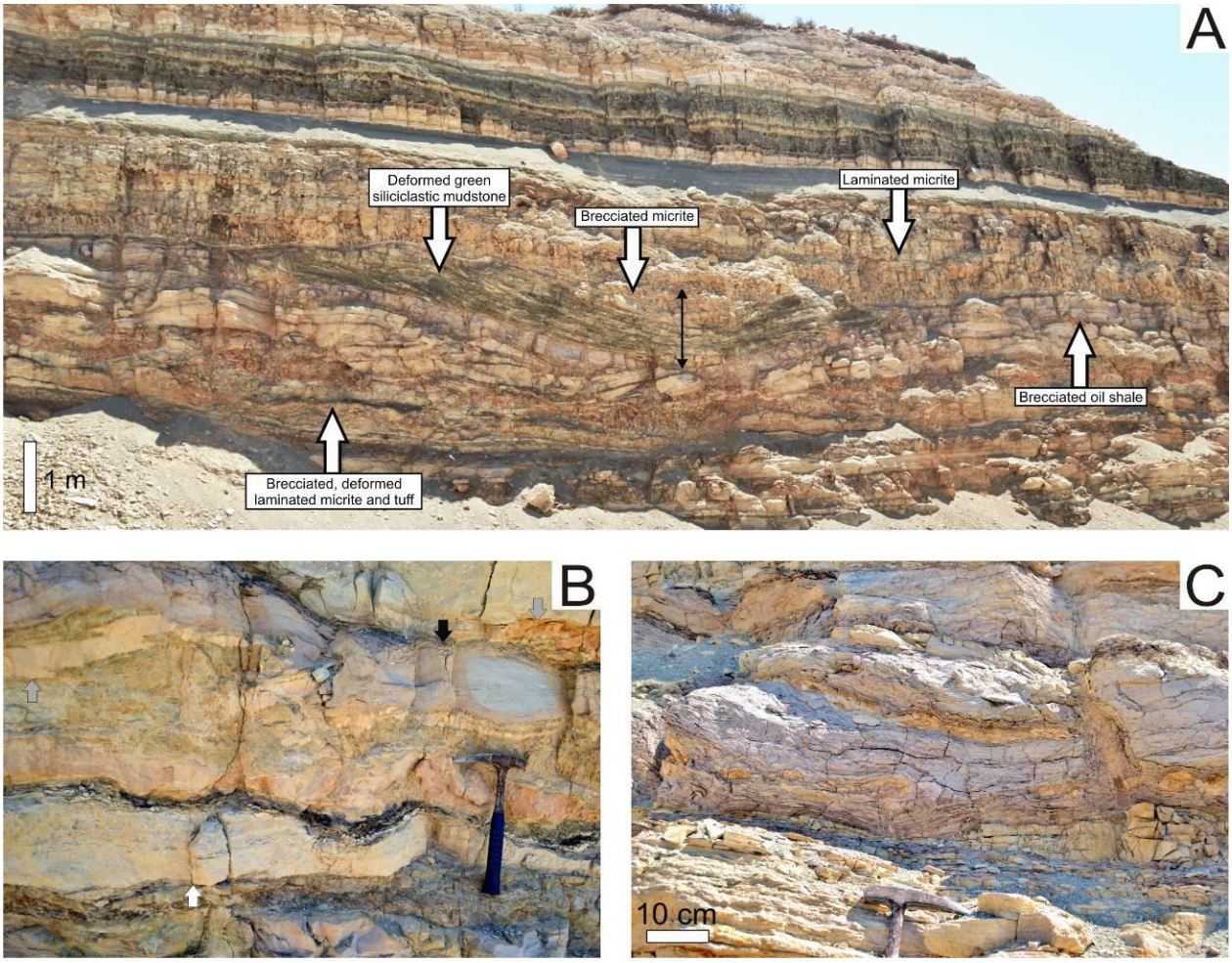


**Figure 2.20** Mass-transport deposit and associated deformation structures (SHQ). A) Chute filled by sheared green siliciclastic mudstone overlain by brecciated micrite. Chute is underlain by oil shale breccia passing downward into sheared zone, and overlain by undeformed laminated micrites. B) Brittle–ductile deformation within 2 m thick zone below chute in oil shale (black arrow), laminated micrite (white arrow) and tuff (gray arrow), showing thrusts, folds, and disrupted beds. C) Folded oil shale breccia with dikes and sills filled with fragmented material.

Mass-transport deposits generally occur in lacustrine basins with a sharp shelf–slope break (e.g., Bøe et al., 2004; Schnellmann et al., 2007; Sauerbrey et al., 2013). Instability and failure of the slope can be triggered by processes intrinsic to the sedimentary environment itself, i.e., autogenic, or by external – allogenic – processes (e.g., G. Owen et al., 2011; Mastrogiacomo et al., 2012). These include oversteepening or sedimentary overloading (e.g., Lewis, 1971; Postma, 1983; Stromberg and Bluck, 1997; Owen and Moretti, 2008), water-level changes (e.g., Rothwell et al., 2000), tides (Wells et al., 1980), storm waves (e.g., Osleger et al., 2009), or earthquakes

(e.g., Field et al., 1982; Rossetti and Santos, 2003; Monecke et al., 2006; Carrillo et al., 2006; Schnellmann et al., 2007; Waldmann et al., 2010; Alsop and Marco, 2011, 2012).

The occurrence of mass-transport deposits in beds deposited below storm wave base rule out most autogenic mechanisms (see Trigger Mechanism). The most widely accepted threshold for spontaneous slumping is about 2° in siliciclastic settings (Lowe, 1975). This threshold might be even higher in carbonate-dominated settings if there is early cementation. However, seismically triggered slumping may occur on very gentle (< 1° or 17 m/km) slopes (Field et al., 1982; García-Tortosa et al., 2011). A seismic origin may be justified if: (1) a steeper slope (> 1°) was present but the size of the deposit is larger than other, more frequent mass-wasting deposits generated by 'background' processes; or (2) sedimentation and deformation occurred in a more or less flat area. In the central area of Fossil Basin the depositional slope was negligible (Buchheim, 1994a). Consequently, formation of brecciated intervals is most probably due to earthquakes, which induced disruption, liquefaction, and slumping of the semi-lithified, low-permeability deposits. In cases where the basal layer is an organic-rich interval, thixotropic properties could have facilitated detachment (e.g., García-Tortosa et al., 2011).

### 2.5 Correlation

The style of sediment deformation in general is controlled mainly by the driving forces and the rheological properties of the host sediment. Consequently, variation in the style, size, morphology, thickness, or areal extent of the deformation features can be expected which may coincide with lateral facies variations (e.g., Rodríguez-López et al., 2007).

Brecciation and mass transport of disrupted sediments are more common in the northern and eastern parts of the study area, near the shoreline of the former lake, where non-laminated carbonate sediments with low organic content were more competent and had more homogeneous mechanical properties (Fig. 2.21A, B). Farther offshore, organic-poor micrites are laminated and interbedded with organic-rich layers, and thus exhibit more ductile features, with convolute bedding and infrequent brittle–ductile features and sediment injection. On the other hand, sedimentary dikes and brittle–ductile deformation dominate in heterogeneous laminated micrites, with higher organic content, towards the depocenter of the lake. Here the sediment may have had higher viscosity, largely due to its organic content, and the style of deformation indicates a plastic or hybrid brittle–ductile response, shrinkage, and possibly thixotropic behavior.

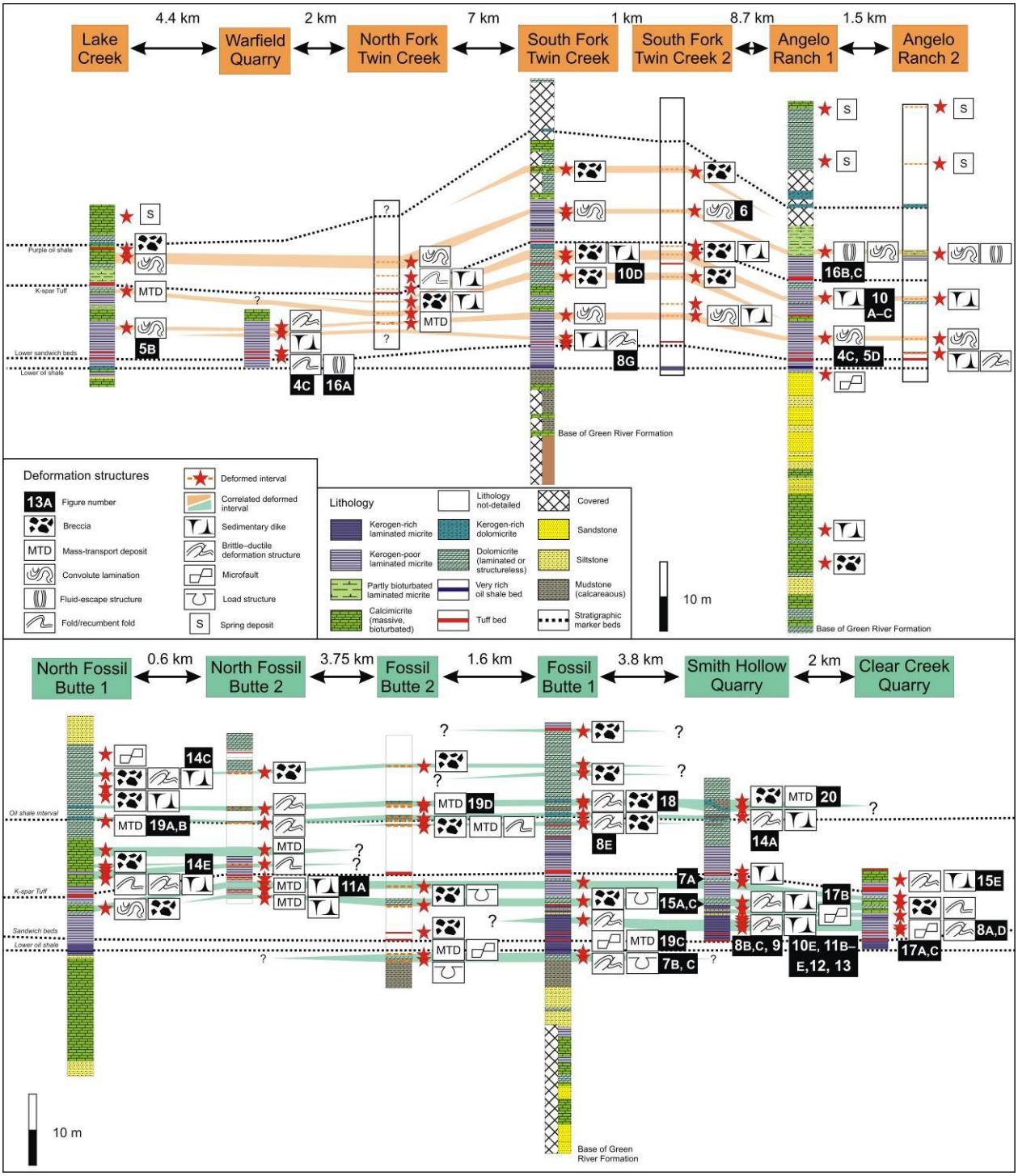


**Figure 2.21** Correlation of deformed horizons between measured sections in Fossil Basin (Fig. 2.1C). A) Along eastern side. B) Down basin axis. Stratigraphic positions of photographed outcrops (Figs. 2.4–20) are shown by black labels with white lettering. Stratigraphic sections at North Fossil Butte, Fossil Butte, Angelo Ranch, and Lake Creek are modified from logs in Buchheim and Eugster (1998) and Buchheim et al. (2011).

Distinctive laterally extensive intervals that are relatively uniform in deformation style include: (1) the two convoluted zones; (2) the deformed structureless dolomicrite beds; (3) some of the intervals containing mixed brittle–ductile deformation structures; (4) the organic-rich deposits hosting sedimentary dikes; and (5) the oil shale breccias and some of the mass-transport deposits in their stratigraphic context (Fig. 2.21A, B). Mass-transport deposits show subtle lateral changes in the style and degree of deformation or in the associated structures such as presence or absence of sedimentary dikes.

In other cases, beds with laterally changing deformation style can correlated based on the general characteristics of the deformed beds and/or the stratigraphic position. For example, microfaulted and complexly deformed beds showing brittle–ductile features at the Clear Creek Quarry are correlated to beds with sedimentary dikes in oil shales at the Smith Hollow Quarry. The stratigraphic interval containing the "sandwich beds" also hosts various deformation features across the study area (Fig. 2.21A, B). However, these features change laterally in terms of style of deformation or disappear. Other deformed horizons pinch out laterally and occur only at one or adjacent locations within ~ 2 km of each other. For example, some of the mass-transport deposits at North Fossil Butte, Fossil Butte, and South Fork Twin Creek sections, which are above the oil shale interval, are localized. These point to rheologically controlled deformation affecting only specific facies.

## 2.6 Discussion

### *2.6.1 Trigger Mechanism*

The formation of sedimentary deformation structures requires at least four critical preconditions: (1) the presence of rheologically susceptible sediment; (2) a deformation mechanism (e.g., liquefaction, fluidization, thixotropy, cracking, shrinkage); (3) a driving force (e.g., gravitational body force, shear stresses); and (4) a trigger agent (Allen, 1982, 1986b; Owen, 1987; Jones and Omoto, 2000; Moretti, 2000; G. Owen et al., 2011). Earthquakes are the most commonly cited trigger (e.g., Seilacher, 1969, 1984; Plaziat et al., 1990; Pratt, 1994, 1998a,b, 1999; Pope et al., 1997; Rodríguez-Pascua et al., 2000; Moretti, 2000; Rossetti, 1999; Rossetti and Santos, 2003; Neuwerth et al., 2006; Moretti and Sabato, 2007; Montenat et al., 2007; Spalluto et al., 2007; El Taki and Pratt, 2012). Other, non-seismic trigger agents that have been invoked include drag by subaqueous currents (e.g., Greb and Archer, 2007), rapid sediment

deposition and overloading (e.g., Lewis, 1971; Postma, 1983; Stromberg and Bluck, 1997; Moretti et al., 2001; Owen and Moretti, 2008), differential sediment loading (Needham, 1978; Dasgupta, 1998), wave-induced cyclical stresses (Molina et al., 1998; Alfaro et al., 2002), sudden changes in groundwater level (Owen, 1996a; Massari et al., 2001), ice movement and cryoturbation (Obermeier, 1996; Chunga et al., 2007), bioturbation (e.g., Klappa, 1980; Owen et al., 2008; Buatois and Mángano, 2011), or gravity failure of slopes (Kleist, 1974; Oliveira et al., 2009), including cases where oversteepening is caused by erosion (Alexander, 1987). As alternatives to seismic shaking, deformation represented by brittle failure has been attributed to other intrinsic processes like evaporite dissolution, wave action, or fluid flow under pressure (e.g., Warren, 1983; Cowan and James, 1992; Friedman, 1997).

Distinguishing between seismically and non-seismically induced deformation structures is complicated by the fact that the morphology of deformation structures is controlled mainly by the initial rheological properties of the sediment and the applied stresses (i.e., the driving forces), which are ostensibly independent of the trigger mechanism (Owen, 1987). Consequently, several trigger mechanisms can potentially cause the same kind of deformation structure, and diagnostic criteria to identify the real trigger agent may appear obscure (e.g., Ricci Lucchi, 1995). However, consideration of crosscutting relationships and morphology, the rheologies and forces required to generate the deformation features, and the depositional setting will usually point to the most feasible source (e.g., Sims, 1975; Pratt, 1998a, b; Jones and Omoto, 2000; G. Owen et al., 2011; El Taki and Pratt, 2012).

The paleogeographic position of Fossil Basin and the prevailing climate (Roehler, 1993; Wilf, 2000; Zachos et al., 2008) preclude the possibility of ice-induced deformation. Biogenic structures in the form of burrows show typically more regular patterns and morphology and are clearly distinguishable from deformation structures. All the deformation features in Fossil Basin occur in facies deposited below the storm wave base (Buchheim, 1994b; Buchheim and Eugster, 1998). Moreover, using the slope gradient estimated by Buchheim (1994a) and the facies map of Buchheim and Eugster (1998) (Fig. 2.2B), water depth of Fossil Basin was probably on the order of 6–8 m in its central part, with an effective wave base of < 2 m, indicating insignificant wave action. This, along with the host facies, precludes the role of cyclic stress or current drag caused by the action of storm waves and bottom currents. Resonant oscillatory waves (seiches), including those formed by earthquakes (e.g., Kastens and Cita, 1981; Chapron et al., 1999;

Carrillo et al., 2006) may have been responsible for depositing the structureless dolomicrite beds, but otherwise there is no evidence for significant bottom scour associated with the deformed intervals.

Shear stresses related to overriding mass transport can be discarded for most features because the overlying units are in gradational contact or marked by a small truncation, with no evidence of large bedding-parallel detachment surfaces. Overloading by rapid deposition is not viable in Fossil Basin for causing folding, dewatering, and sediment injection, because the overlying sediments are typically composed of finely laminated micrites of profundal origin indicative of slow rates of sedimentation. Gradational upper contacts or minor intrastratal truncations indicate deformation in a confined stratigraphic interval, sealed by beds with contrasting lithology and consequently rheology.

Structures attributed to small-scale translation and mass-transport deposits represent instability at the sediment–water interface. In a lake basin characterized by a virtually flat depositional surface and low-energy environment, this instability was most probably induced by seismic shaking rather than by other processes, such as overloading, oversteepening, or undercutting due to erosion. The morphological characteristics of the deformation features in Fossil Basin are not typical of down-slope movement, which usually results in dislocation surfaces and more or less uniformly oriented slump folds, whether they were triggered by seismic activity or not (e.g., Strachan, 2002; Alsop and Marco, 2012). Moreover, sediments with high organic content have unique physical properties, because their high water content, high initial shear strength, and high sensitivity makes them particularly susceptible to failure upon abrupt disturbance (e.g., Grimm and Orange, 1997). Disturbance of organic-rich carbonate mud precursors of oil shales by seismic shaking and possibly thixotropic failure might have contributed to the formation of mass-transport deposits (García-Tortosa et al., 2011) and in situ oil shale breccia intervals (Buchheim, 1982) rather than slope failure and long-distance transport as turbidites (Dyni and Hawkins, 1981). As the deformation of organic-rich thixotropic muds on a flat surface requires stresses to exceed a threshold, this adds support for earthquake-induced shaking as the trigger.

In Fossil Basin, most deformed intervals are laterally continuous for up to 25 km, and deformed layers are bounded above and below by undeformed beds of similar facies, with horizontal bedding planes remaining intact. These attributes imply recurring, short-lived

deformation events that affected only sediments with a susceptible rheological state at the time. Furthermore, they indicate that either: (1) the deformed intervals were at, or close to the sediment–water interface when deformation happened; or (2) the deformation occurred intrastratally, i.e., in shallowly buried intervals confined by the overlying sediments. However, the general absence of passive sediment collecting in topographic lows on the upper surfaces of disturbed beds points to the second explanation. The low-energy regime and the presence of the undeformed beds of the same lithology above and below deformed intervals mean that 'autokinetic' (*sensu* Leeder, 1987; Owen and Moretti, 2011) trigger mechanisms, such as internal and normal sedimentary and/or erosional processes can be rejected. Consequently, deformation structures in Fossil Basin are best explained as seismically induced, i.e. seismites, that formed by increased pore pressure, loss of shear strength, and horizontal and vertical stresses related to seismic shaking. The tectonically active setting of Fossil Basin during deposition (e.g., Coogan, 1992) supports this interpretation. A comparable range of structures has been inferred to be seismites in other marine and lacustrine units (e.g., van Loon and Wiggers, 1976; Brenchley and Newall, 1977; Grimm and Orange, 1997; Jones and Omoto, 2000; Rodríguez-Pascua et al., 2000; McLaughlin and Brett, 2004; El Taki and Pratt, 2012). The absence of other types of seismites, such as vein arrays (e.g., Ohsumi and Ogawa, 2008) is due to lack of sediments with the appropriate rheological properties.

The generally accepted threshold in magnitude sufficient to cause liquefaction of surface or shallow subsurface sediment is $M_w \geq 5$ (e.g., Allen, 1986b; Leeder, 1987; Ambraseys, 1988; Galli, 2000; Mörner, 2005; Castilla and Audemard, 2007). However, little is known from modern examples about the response of a variety of buried sediments in subaqueous settings. Nevertheless, we assume that earthquake shaking intensity of a minimum of MMI ≥ VI was necessary to induce failure of subaqueous sediments under shallow burial (e.g., Hibsch et al., 1997; Rodríguez-Pascua et al., 2003; Berra and Felletti, 2011) as well as instability generating mass-transport deposits (e.g., Keefer, 1984; Monecke et al., 2004, 2006; St-Onge et al., 2012).

### *2.6.2 Tectonic Activity and Lake Evolution*

Fossil Basin is located in the Sevier Fold and Thrust Belt, with the seismite-bearing outcrops lying ~ 3 km above and ~ 10–30 km from the front of the Absaroka and Hogsback thrusts and related fault systems (Fig. 2.1A). Early Eocene activity of these structures has been

documented based on the presence of rockslides, debris flows, mudflows, conglomerates, offsets, fault-propagation folds, and steeply inclined beds in the vicinity of the Fossil Basin and also along the front of the thrust belt (e.g., Dorr and Gingerich, 1980; Coogan, 1992; DeCelles, 1994). Deformation caused by recent thrust-related earthquakes (e.g., Galli, 2000; Castilla and Audemard, 2007; McCalpin, 2009) suggests that the Eocene structures could have produced analogous events of strong magnitude. The observed deformation features are therefore the direct sedimentary record of strong earthquakes through the time interval studied.

Movements of these structures must have contributed to the evolution of lacustrine sedimentation at both long- and short-term scales. For example, the gradual northward shift of the depocenter shown by the thickness changes across the basin (Buchheim et al., 2011) point to warping of the underlying crust (Oriel and Tracey, 1970) or uplift of the margins and the southern areas (Coogan, 1992). Similarly, this tectonic activity was largely responsible for the progressive isolation of the basin, during which subsidence and accommodation gradually exceeded basin-filling processes, as shown by the changeover of lake types (Buchheim et al., 2011).

There are also two deformed intervals that mark short-term changes. Organic-rich micrites constituting the basal part of the Fossil Butte Member indicate rapid expansion of the lake (Buchheim et al., 2011). This could have been caused by climatic changes that led to increased precipitation. However, there is no concomitant increased input of siliciclastic sediment which would be expected. Instead, abundant sedimentary dikes and mixed brittle–ductile features (Fig. 2.21A, B) suggest that lake expansion was due more likely to structural movements that caused regional tilting. The upper convoluted zone at most locations separates laminated micrites below and structureless or poorly bedded micrites above, with a sudden increase in the amount of bioturbation locally, and marks the boundary of the Fossil Butte and the Angelo members (Buchheim and Eugster, 1998; Buchheim et al., 2011). Thus this deformed zone indicates instantaneous changes in bathymetry, facies, and lake type, from balanced-fill to underfilled, likely caused by final isolation and the diversion of the drainage pattern around Fossil Basin.

Spring deposits are common in the Angelo Member and are also present in the Fossil Butte and Road Hollow members (Buchheim and Eugster, 1998; Buchheim et al., 2011) (Fig. 2.21A). Hence, syndepositional tectonism could also have caused short hypersaline events and the consequent precipitation of dolomicrites. It could even have influenced water chemistry over the long term because of increased subaqueous spring activity (cf. Lee et al., 2013). These

observations suggest that tectonics controlled not only the potential accommodation but also the amount or quality of water input. Independent, paleobotanical evidence for synchronous climate change is equivocal, but no major changes are apparent (Wilf, 2000; Pietras and Carroll, 2006). Consequently, in Fossil Basin tectonics rather than climate exerted the primary control over lake character.

Synchronous tectonic events are also documented in the neighboring Lake Gosiute in the greater Green River Basin (Fig. 2.1A, B). Major changes in facies, paleohydrology, and lake type at the boundary between the Tipton Shale and Wilkins Peak members have been attributed to tectonic activity along the Wind River Range and subsequent drainage diversion (Pietras et al., 2003; Pietras and Carroll, 2006; Törő et al., 2015). Clustering of these events at ~ 52–51 Ma records a tectonically active phase of both the Sevier Fold and Thrust Belt and the Laramide orogeny, which clearly had a fundamental influence on the Green River paleo-lake system.

## 2.7 Conclusions

Detailed field observations of the lacustrine Green River Formation (early Eocene) in Fossil Basin of southwestern Wyoming have revealed the hitherto unappreciated abundance of laterally extensive deformation structures of various types. The Fossil Butte and Angelo members host at least 11 well-defined deformed horizons, which can be correlated for up to 25 km in the northern part of the former lake basin. Eight main types of sediment deformation structures were categorized: (1) convolute lamination, (2) load structures, (3) brittle–ductile features, (4) sedimentary dikes, (5) fluid-escape structures (cusps and pipes), (6) microfaults, (7) oil shale breccias, and (8) mass-transport deposits. Deformation is recorded mainly in profundal laminated micrites, and, less commonly, in partly bioturbated sublittoral micrites, all of which were deposited in a low-energy environment. This setting was characterized by a negligible depositional slope, low and uniform sedimentation rates, and an absence of storm waves, subaqueous currents, and frequent gravity-related signatures including slumps and turbidites. Crack arrays that resemble desiccation cracks are, rather, small-scale sedimentary dikes.

The deformed layers are typically confined above and below by undeformed beds of the same facies, which implies sporadic, short-lived, syndepositional events that affected only near-surface sediments under shallow burial. These sediments were susceptible to deformation before their rheology changed as lithification advanced. The resulting structures are interpreted to record

in situ loss of shear strength, liquidization, plastic deformation, sediment mobilization, or brittle failure. In turn, these processes were caused by increased pore pressure and stresses induced by earthquake shaking of the subaqueous sediment pile. This conclusion is based on: (1) the tectonically active setting of the lacustrine basin and proximity to fault systems known to have been active during the time of the deposition; (2) the sedimentary environment and attributes of the successions; (3) the lateral extent of the deformed intervals; and (4) the recurrence of deformation features at different stratigraphic levels. Mass-transport deposits and oil shale breccias formed due to seismicity affecting a virtually flat to imperceptibly dipping lake bottom, which led to disruption and translation. These deformation structures are similar to many other examples from low-energy lacustrine and marine successions that have been interpreted seismites.

Late-Laramide movements along the Absaroka and Hogsback thrusts and related faults in the Sevier Fold and Thrust Belt ~ 52–51 million years ago is considered to have been the source of earthquakes that affected Fossil Basin and the greater Green River Basin as well. The stratigraphic distribution of deformed intervals indicates that tectonic activity had an important impact on the evolution of the lake by inducing changes in the location of depocenter and paleohydrology of the area. Consequently, the identification and integration of similar, laterally extensive deformation features in other subbasins of the Green River Formation could provide a previously unexploited means to track syndepositional structural movements and their effects on lake character. The occurrence of such features in an otherwise low-energy lacustrine environment is critical for the interpretation of the sedimentological record not only of the Green River Formation in Wyoming but also of other lacustrine or marine deposits elsewhere.

### 2.8 Relationship of manuscript to thesis

The manuscript represents the first detailed study on sedimentary deformation features in the well-studied Green River Formation. The Fossil Basin was an ideal candidate to carry out such analysis because it represents a microcosm of the other larger Green River lakes and provides outcrops that are better exposed and more accessible than those of Lake Gosiute and Lake Uinta, which made tracing of individual features easier.

The manuscript discusses the process of origin of individual deformation structures, the rheological properties and burial state of the sediments at the time of deformation, and proposes a

seismic trigger based on the characteristics of the structures, as well as the sedimentological context. Furthermore, the manuscript also considers and discusses the possible effects of tectonic movements in the Sevier Fold and Thrust Belt on the evolution of the basin. This aspect provides ground for understanding some of the observed changes not only in the Fossil Basin, but also in the neighboring greater Green River Basin (discussed in detail in Chapter 3).

The described deformation features differ significantly differ from ‘conventional’ structures described in the literature as they occur in laminated carbonate mudstones with variable organic content. They represent an unusual suite of structures, and their characteristics add to our understanding of the behaviour of carbonate mudstones upon seismic disturbance. Thus, the manuscript will serve as a valuable reference for future studies involving the Green River Formation (Chapter 3 and 4), and other studies on paleoseismic deformation in marine or lacustrine carbonates in general.

# CHAPTER 3

# TECTONICALLY INDUCED CHANGE IN LAKE EVOLUTION RECORDED BY SEISMITES IN THE EOCENE GREEN RIVER FORMATION, WYOMING

Törő, B., Pratt, B.R., and Renaut, R.W., 2015, Tectonically induced change in lake evolution recorded by seismites in the Eocene Green River Formation, Wyoming: Terra Nova, v. 27, p. 218–224.

## 3.1 Abstract

Seismogenic sedimentary structures—seismites—provide an opportunity to understand the effects of syndepositional tectonics on lacustrine sedimentation. The lowermost Wilkins Peak Member (Eocene Green River Formation, Wyoming, USA) contains laterally extensive intervals displaying folds, load structures, mixed brittle–ductile deformation, microfaults, breccias and sedimentary dykes which formed intrastratally in a low-energy, sublittoral lacustrine environment. They developed in situ by liquefaction and plastic or brittle behaviour of semi-lithified sediment, or by remobilization and injection of granular material. Their morphological attributes and lateral extent, zonation in deformation intensity, and the depositional setting all imply deformation triggered by earthquake-induced stresses in shallow-buried sediment. Their stratigraphic distribution coincides with a shift in hydrological conditions from a balanced-filled to an underfilled lake type independent of climate change. This study is the first to ascribe seismites to a pulse of tectonic activity that caused a synchronous change in lacustrine evolution.

## 3.2 Introduction

Although lakes are relatively short-lived sedimentary basins, their isolation and dominantly low-energy setting mean they can be high-resolution archives of paleoenvironmental changes, such as climate, geomorphology, hydrology, and their tectonic milieu (Cohen, 2003; Renaut and Gierlowski-Kordesch, 2010). The conceptual subdivision whereby variations in facies and their stacking patterns define three major categories: overfilled, balanced-filled, and underfilled, reflects primarily the relative contributions of climate and accommodation in lake evolution (Carroll and Bohacs, 1999; Bohacs et al., 2000, 2003).

Lacustrine deposits may have susceptible rheologies ideal for recording large-magnitude seismic events (e.g., Sims, 1975; Ricci Lucchi, 1995). Earthquake-induced sedimentary structures ('seismites') may provide a powerful tool to better understand the contribution and significance of tectonic events in the evolution of lacustrine systems, especially those in tectonically active regions. Although seismites have been reported extensively (e.g., Moretti and Sabato, 2007; Beck, 2011), direct linkage with syntectonic changes of lake-basin type has not yet been attempted.

The Green River Formation (Eocene) is one of the best-studied ancient lacustrine deposits (e.g., Smith et al., 2008). It accumulated in a tectonically active region where synchronous faulting has been inferred (e.g., Pietras et al., 2003). However, in situ sedimentary deformation features have not been recorded and integrated with the regional-scale evolution of the lacustrine system. Using seismites preserved in the Green River Formation of southwestern Wyoming, this study documents for the first time the sedimentary record of syndepositional tectonic activity that also induced changes in the hydrological balance of a lake basin.

### 3.3 Geological Setting

The Greater Green River Basin is flanked by the Sevier Fold and Thrust Belt to the west, and Precambrian-cored uplifts on its northern, eastern and southern margins, and is subdivided by intrabasinal arches, all of which were periodically active during the waning stages of the Laramide Orogeny (e.g., Dickinson et al., 1988; DeCelles, 1994) (Fig. 3.1A). Their movements modified the regional drainage, geomorphology, gradients around the paleolakes and locations of depocentres (Roehler, 1992, 1993; Pietras et al., 2003; Carroll et al., 2006, 2008).

Lake Gosiute occupied the Greater Green River Basin and passed through hydrologically open to closed and back to open conditions during its history (Roehler, 1993). These stages are recorded by distinct facies associations: the fluvial-lacustrine (overfilled) and fluctuating profundal (balanced-filled) Tipton and Laney members, and the evaporitic (underfilled) Wilkins Peak Member (Carroll and Bohacs, 1999) (Fig. 3.1B). These changes reflect the longer term interplay between climatic and tectonic controls under an overall warm climate that led to variable sediment supply, accommodation and water influx (e.g., Smith et al., 2008).

This study focuses on the transition between the Rife Bed of the Tipton Member and the overlying Wilkins Peak Member in southeastern Bridger Basin (Fig. 3.1A, B). It is recorded by a

rapid facies change over 2–3 m, from organic-rich oil shale to organic-poor calcareous mudstone and siltstone, marking a shift to more saline and alkaline lake chemistry (e.g., Pietras and Carroll, 2006).

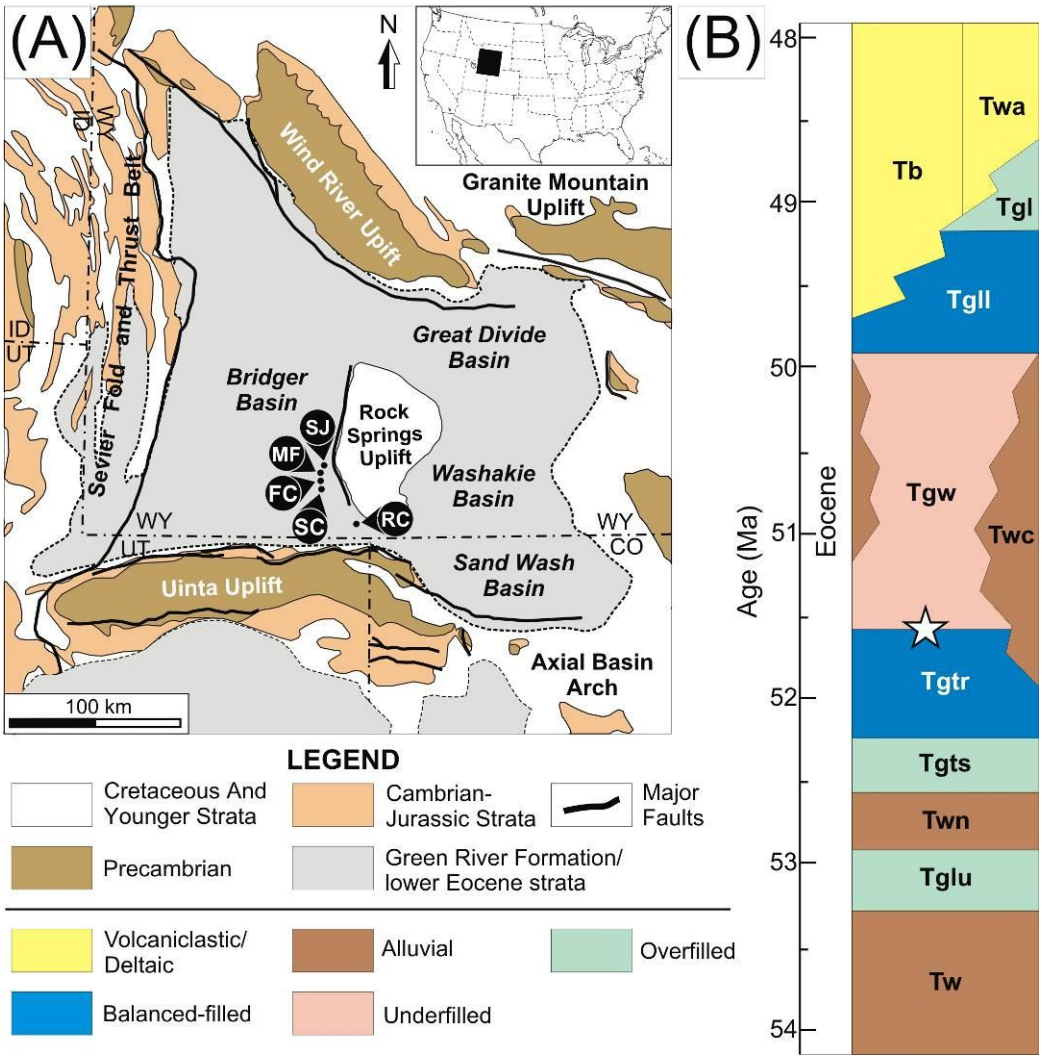


**Figure 3.1** A) Regional geological map of the greater Green River Basin, southwestern Wyoming (modified after Smith et al., 2008). Studied locations: SJ – Slippery Jim Canyon; MF – Middle Firehole Canyon; FC – Firehole Canyon; SC – Sage Creek; RC – Red Creek. B) Simplified stratigraphy, study interval (white star) and lake type stages of the Green River Formation (modified after Smith et al., 2008, 2010). Tw – Wasatch Formation (main body), Twn – Niland Tongue; Twc – Cathedral Bluffs Tongue, Tg – Green River Formation, Tglu – Luman Member, Tgts – Scheggs Bed, Tipton Member, Tgtr – Rife Bed, Tipton Member, Tgw – Wilkins Peak Member, Tgll – lower LaClede Bed, Laney Member, Tgl – upper LaClede Bed, Laney Member, Tb – Bridger Formation, Twa – Washakie Formation.

### 3.4 Sedimentary Facies

In five outcrops near the contemporary depocentre (Fig. 3.1A) the lowermost Wilkins Peak Member is organized into repetitive 3–5 m thick packages ("cycles" of Pietras and Carroll, 2006). These are dominated by parallel-laminated carbonate mudstone, with upward-increasing intercalation of wavy- or lenticular-laminated calcareous siltstone; oil shale is present at the base and calcareous sandstone at the top. Sandstones display wave-ripple cross-lamination and, less commonly, combined-flow ripple cross-lamination. There is a southward-coarsening trend, marked by increased intercalation of very fine- to medium-grained sandstone.

These sediments were deposited in the shallow profundal to sublittoral zones of Lake Gosiute, below storm wave base (parallel-laminated carbonate mud with variable organic content) or between fair-weather wave base and storm wave base (carbonate mud, silt and sand) (Roehler, 1990) (Fig. 3.2). Sedimentary deformation features are abundant only in the lowest two cycles (Fig. 3.3A). The studied interval lacks indicators of a playa-lake setting, such as evaporite mineral casts, polygonal desiccation cracks or pedogenic modifications, all of which are common higher in Wilkins Peak Member (e.g., Pietras and Carroll, 2006).

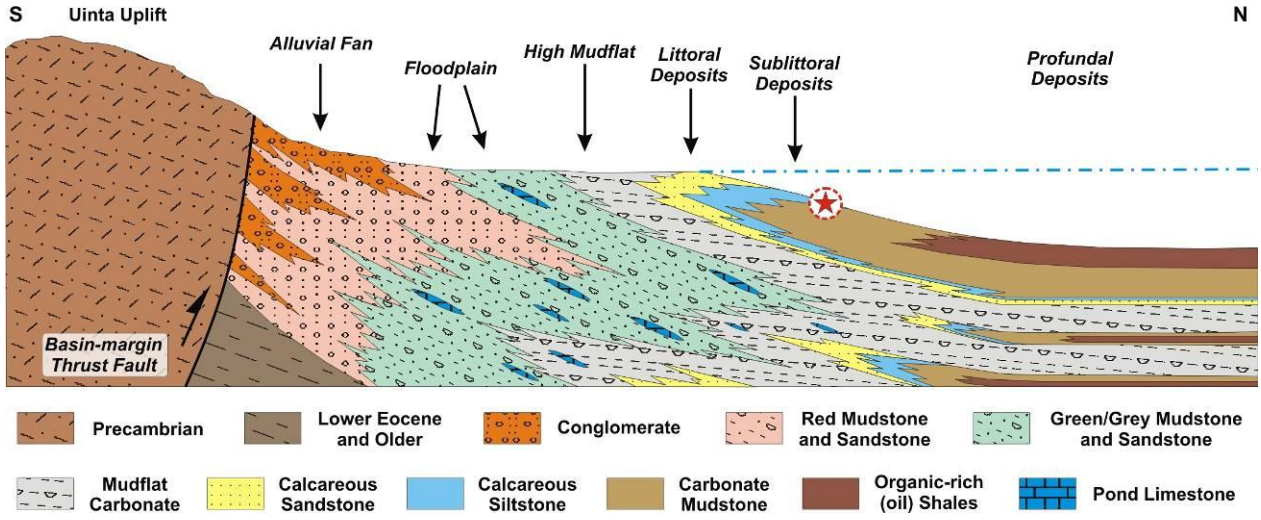


**Figure 3.2** Schematic depositional model for the southern Greater Green River Basin (modified after Roehler, 1993; Renaut and Gierlowski-Kordesch, 2010) (not to scale). Seismites described here occur in sublittoral calcareous siltstone deposits (star). Slope gradient was on the order of 0.02–0.5° (Surdam and Wolfbauer, 1975; Roehler, 1990). The diagram is vertically exaggerated to show facies relationships.

### 3.5 Deformation Features

Deformation is present in five or six horizons, separated from each other by undeformed strata with either sharp or gradual boundaries. The style of deformation is fairly uniform in the northern area, shown by millimetre- to centimetre-scale, composite brittle and ductile features that form crumpled horizons in intercalated siltstone and mudstone (Fig. 3.3B). Individual deformed intervals up to 80 cm thick can be traced laterally for > 20 km and include folds, load structures, microfaults, breccias and sedimentary dykes. In general, breccias and dykes are more common in the southern locations.

Folds are irregularly spaced < 25 cm apart, up to 15 cm high and 10 cm wide, and exhibit variable geometry, with open to tight and recumbent shapes (Fig. 3.3B, D). Successive beds within a single deformed interval commonly show different fold geometry, orientation and wavelength.

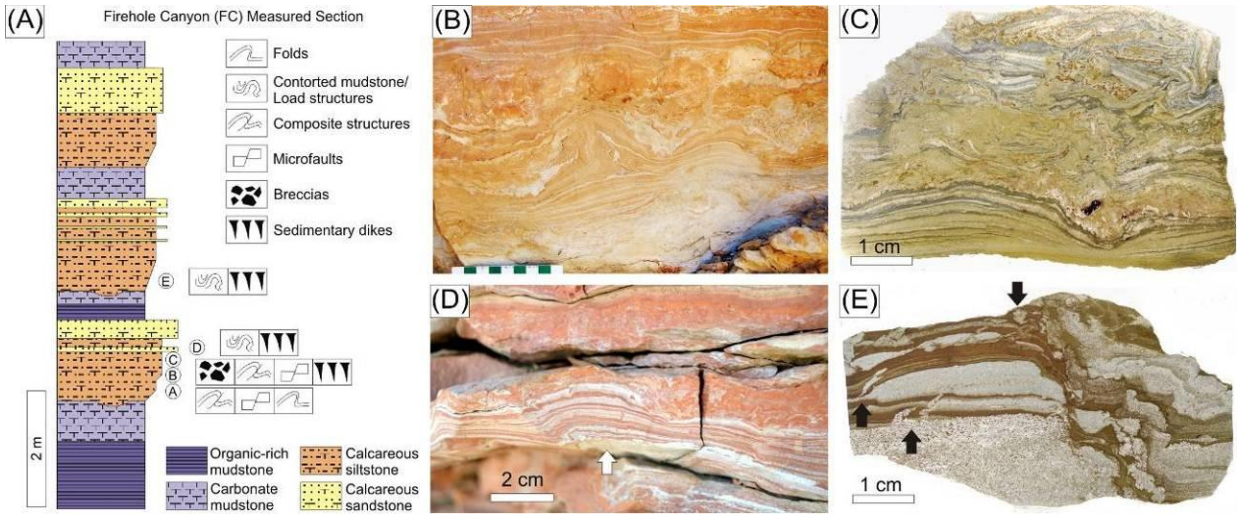


**Figure 3.3** A) Stratigraphic section at FC with five deformed intervals (A–E). B) Composite deformation feature with irregular folding and brecciation, sandwiched between less deformed and microfaulted intervals (interval C; MF). C) Thin section photomicrograph showing load structure filled with brecciated laminated mudstone (interval A; SJ). D) Load structure composed of disrupted and churned mudstone with folds, microfaults, and millimetre-scale dykes below (arrow) (interval B; SJ). E) Thin section photomicrograph showing normal microfault in intercalated siltstone and sandstone with isolated and upward-protruding dykes (arrows) (interval E; MF).

Mudstone interbeds have irregular thickness and are typically highly contorted or disrupted and churned. Millimetre- to centimetre-scale load structures are common at their bases penetrating the underlying folded and faulted siltstone (Figs. 3.3C, D, 3.4A). These structures are

up to 5 cm in diameter, filled by fragmented material with a mud-rich matrix, and irregularly spaced 1–10 cm apart.

Sets of laminated siltstone and sandstone are commonly offset by microfaults with high-angle normal, reverse and thrust geometries. Different types of faults, with variably dipping fault planes and various lengths and throws, may co-exist in a single bed (Figs. 3.3D, E, 3.4B). Displacement ranges from a few millimetres to 5 cm, and microfaults die out both upwards and downwards. They occur in intervals 1–40 cm thick which are overlain by contorted mudstone beds (Fig. 3.3B, D).

Breccias in siltstone and sandstone, interbedded with mudstone, form irregular bodies up to 1 m in size, whose boundaries with undeformed laminae are either sharp or gradational (Fig. 3.4C, D). A single interval hosts several breccia bodies and other deformation features, and can be traced laterally at least 50–100 m. The top and base of the host interval typically pass sharply into undeformed beds. The breccias consist of randomly oriented clasts up to 10 cm long, with angular to subangular edges, that are locally folded and faulted. The clasts commonly 'float' in a structureless mixed muddy matrix. In places, breccia bodies have an obliquely oriented, crudely curvilinear shape, resembling sedimentary dykes (Fig. 3.4C, D).

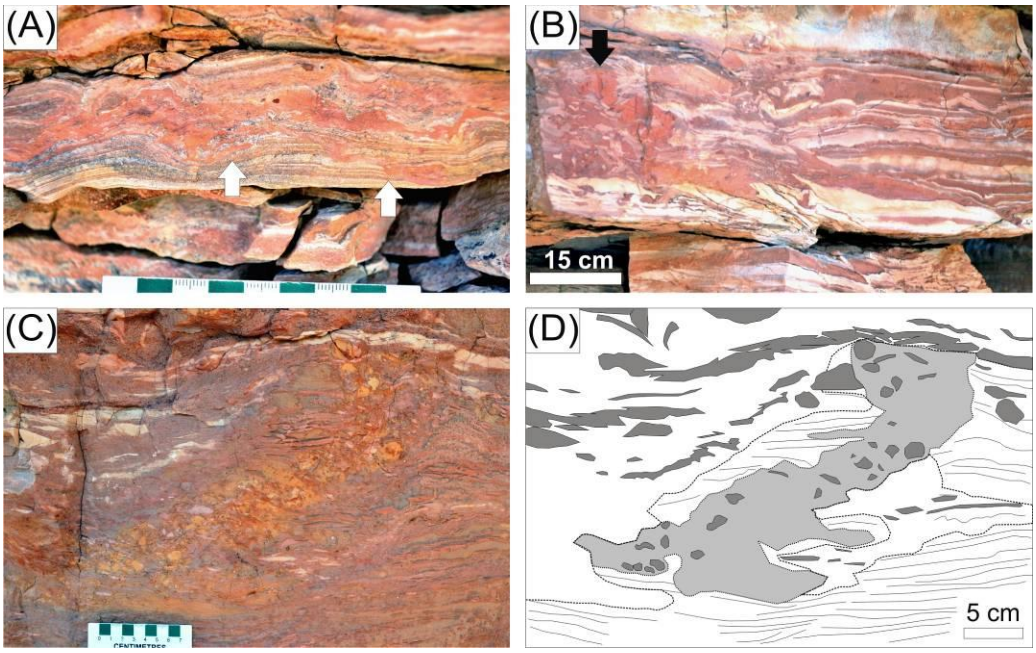


**Figure 3.4** A) Load structure associated with dykes (arrows) (interval B; SJ). B) Intercalated siltstone and mudstone showing array of reverse microfaults with a mud-filled dyke (black arrow) and brecciation (left side) (interval C;

FC). C) Oblique breccia body within disrupted siltstone (interval C; SC). D) Tracing of C, showing the breccia body (light grey), surrounded by disrupted laminae (dashed lines), and 'floating' clasts (dark grey).

Sedimentary dykes are abundant as intrusions up to 3 m long and 5 cm wide (Fig. 3.5A) filled with homogenized lime mud, silt or a mixture with sand- and pebble-sized mudstone clasts (Fig. 3.5B). Dykes display ragged, folded and bifurcating linear paths with sharp boundaries in both cross-section and plan view. At distinct lithologic boundaries they commonly show step-like offsets. At Red Creek, they have two prominent orientations (~005° and ~120°). At Middle Firehole Canyon, many of them follow normal microfault planes and penetrate downwards through several, locally folded, siltstone interbeds (Fig. 3.5C). The upper termination of most dykes is against parallel- or wavy-laminated siltstone or sandstone, or, in some places, mudstone. The overlying bed locally shows folding, irregular thickness or brecciation. Where visible, dykes taper downwards, indicating that they were sourced from above.

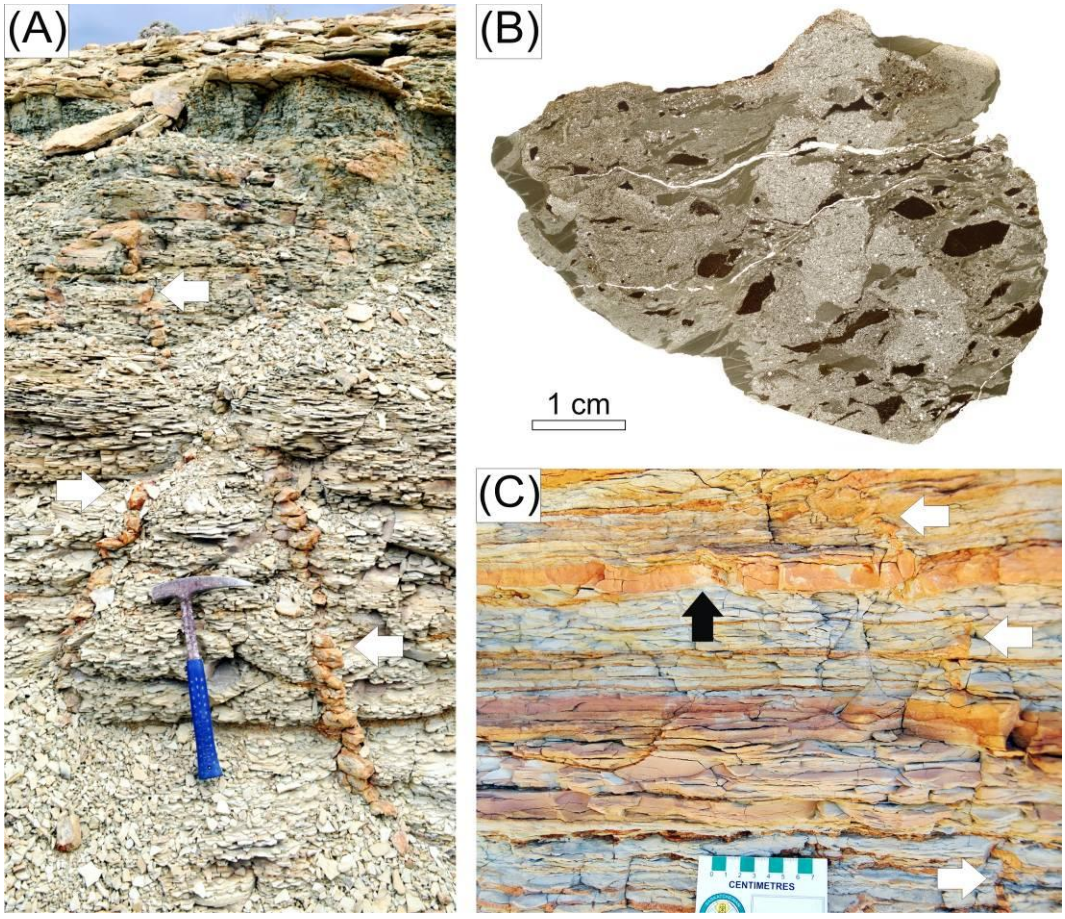

**Figure 3.5** (on previous page) A) Two cross-cutting sets of metre-scale dykes (arrows) in laminated carbonate mudstone (interval E; RC). B) Thin section photomicrograph showing a breccia-filled dyke penetrated in turn by folded silt -rich dyke (middle) (interval E; RC). C) Intercalated mudstone and siltstone with gently folded siltstone bed (black arrow) cut by a dyke (white arrow) following a normal fault plane (interval E; MF).

## 3.6 Discussion

### *3.6.1 Deformation Mechanism and Rheology*

Soft-sediment deformation features are mostly related to loss of shear strength in unconsolidated to semi-consolidated deposits through liquefaction and/or fluidization driven by internal and external forces including density contrast, elevated pore pressure and physical stress (e.g., Owen, 1987). The style of deformation, in turn, is controlled by the rheological properties of the host sediment and the magnitude of the force exerted on it (e.g., Pratt, 1998a; Spalluto et al., 2007).

All the deformation features in the studied interval are interpreted to have formed intrastratally at shallow burial depth, as shown by the lack of truncation by erosive lake floor processes and the common gradual transition into undeformed beds both upwards and downwards. Because nearly the full spectrum of deformation styles are seen in the same bed and the structures pass laterally into each other, a common genesis is implied. Comparable structures have been widely reported from marine and lacustrine units (e.g., Rodríguez-Pascua et al., 2000; Bachmann and Aref, 2005; Berra and Felletti, 2011; El Taki and Pratt, 2012).

The ductile features (folds and load structures) formed by liquefaction and squeezing of semi-cohesive sediments, whereas brittle features (microfaults, breccias) formed in more cohesive sediments. The lithological heterogeneity resulted in different mechanical properties, variable responses to the same event, and formation of composite structures. Disrupted muddy layers indicate a lower resistance to liquefaction. Intercalated silt- and sand-rich beds commonly show abundant microfaults and are overlain by plastically deformed beds, suggesting a more consolidated state of underlying layers and simultaneous brittle and plastic deformation.

The irregular geometry of the breccias, the flat and non-erosive bed tops, and the transitional boundaries to undeformed host sediment all indicate that brecciation resulted by partial liquidization of the carbonate mud interbeds and brittle failure of the cohesive, coarser grained layers without significant transportation (Kahle, 2002; El Taki and Pratt, 2012). Where

breccias fill sedimentary dykes, a genetic sequence of temporally closely spaced events can be inferred, including (1) liquefaction, (2) brecciation and homogenization, and (3) remobilization through injection.

The intrastratal formation of sharp-walled sedimentary dykes indicates shrinkage and brittle failure of semi-lithified sediments with concomitant injection of granular material in directions defined by the stress field (Pratt, 1998a; Jolly and Lonergan, 2002). Thus these dykes are not neptunian dykes formed by the passive infilling of pre-existing fissures. Although downward emplacement is dominant, lateral or upward injection may have occurred in some instances (e.g., Rodríguez-Pascua et al., 2000).

### *3.6.2 Trigger Mechanism*

A number of natural trigger mechanisms have been invoked to generate comparable deformation structures, including the wave action, sediment loading, drag by currents, ice-induced stresses or earthquakes. Consequently, positive identification of the most likely origin is often perceived to be elusive (G. Owen et al., 2011).

The mid-latitude paleogeographic location and the warm paleoclimate (e.g., Roehler, 1993; Wilf, 2000) exclude glaciotectonics. The tranquil depositional setting and lack of mass-transport or channel deposits rule out overloading and drag by bottom currents. Shear stresses associated with tidal currents (e.g., Greb and Archer, 2007) are unlikely in lakes. The facies evidence, combined with an inferred low slope gradient (~0.02–0.5°; Surdam and Wolfbauer, 1975; Roehler, 1990), preclude deformation from breaking or pounding waves (Dalrymple, 1979; Nataraja and Gill, 1983; Alfaro et al., 2002), or gravitational instability. Moreover, most such triggers would generate only localized features and cannot explain a lateral extent in some cases > 20 km.

A desiccation origin for the sedimentary dykes is rejected based on the depositional context, the overall sheet-like geometry and oriented nature of the dykes, the lack of evidence of subaerial exposure, and the absence of fabrics that would be expected if the cracks were open and filled passively from above by subaerial or fluvial processes (e.g., Neal et al., 1968; Eugster and Hardie, 1975; Harris, 2004).

The observed associations and morphologies of deformation structures are best explained as the result of liquefaction, fluidization, and shear stresses induced by shaking during syndepositional earthquakes. The cyclic and chaotic stresses related to the repeated passage of seismic waves during sporadic events explain the: (1) unoriented and contorted nature of the folded and faulted structures; (2) recurrence of deformed intervals bound stratally by undeformed beds; (3) superposition of brittle and ductile structures in rheologically heterogeneous sediment; and (4) large lateral extent. The southward increase in the relative proportion of breccias and sedimentary dykes might be related to changes in facies and rheology, or higher deformation intensity and, in turn, proximity to source of the earthquakes.

### *3.6.3 Implications*

Three nearby fault zones were active during deposition of the lowermost Wilkins Peak Member at ~51.5 Ma: the Sevier Fold and Thrust Belt, 110–140 km to the west (Coogan, 1992); the Laramide Wind River Thrust system, 95–130 km to the north (Pietras et al., 2003); and the Uinta Thrust system, 15–50 km to the south (Roehler, 1993; Bradley, 1995) (Fig. 3.1A). Considering modern and ancient analogues, and empirical relationships between magnitude and epicentral distance for liquefaction (e.g., Galli, 2000; Monecke et al., 2004; Castilla and Audemard, 2007; Berra and Felletti, 2011), seismites identified here were most likely triggered by earthquakes with a magnitude $\geq 5$ and epicentral intensity $\geq$ VI, sourced at the northern front of the Uinta Uplift (Figs. 3.1A, 3.2). The lateral zonation of deformed beds further supports this interpretation.

The shift from a balanced-filled to an underfilled state that occurred at the boundary of the Tipton and the Wilkins Peak members has been ascribed to increasing aridity (e.g., Bradley and Eugster, 1969; Roehler, 1993) or tectonic isolation of the lake basin (Pietras et al., 2003). The sedimentary deformation features, as the stratigraphic archive of syndepositional earthquakes, imply that, rather than climatically forced, the change in paleohydrological conditions of Lake Gosiute was indeed tectonically induced through the diversion of the regional drainage system.

## 3.7 Conclusions

Lacustrine deposits of the Eocene Green River Formation of southwestern Wyoming exhibit laterally extensive sedimentary deformation structures in the boundary interval between the Tipton and Wilkins Peak members. These are interpreted as seismites formed in situ by selective liquefaction processes and elevated shear stresses in rheologically heterogeneous, sublittoral deposits under shallow burial. Their morphological characteristics, the depositional setting, and the zonation of deformation intensity imply that deformation was triggered by earthquakes with a magnitude of $\geq 5$, related to the activity of basin-bounding faults of the Uinta Uplift to the south. For the first time, such seismites have been linked directly to a syntectonic change in lake-basin type, in this case, from balanced-filled to underfilled.

Syndepositional tectonism potentially influences the hydrology, hydrogeology, watershed geology, spring activity and local climate. Thus, it ultimately affects lake chemistry and sedimentation, especially in regions of active tectonics, such as rift systems or orogenic belts (e.g., R.B. Owen et al., 2011; Lee et al., 2013; Cohen et al., 2015). This study demonstrates that seismites should be more widely utilized to assess the contribution of tectonics in lake evolution, not only in other sub-basins of the Green River Formation, but also in other modern or ancient lake deposits, where lacustrine conditions changed in a tectonically active setting.

## 3.8 Relationship of manuscript to thesis

The manuscript reports on the morphological characteristics and origin of exceptionally preserved and laterally extensive brittle–ductile deformation features in the transitional interval between the balanced-filled Tipton Member and the underfilled Wilkins Peak Member in the southeastern Bridger Basin, Wyoming. Based on their morphological characteristics, lateral extent and zonation, and the depositional context, the study shows that these features can be related to tectonic movements along the nearby Uinta Uplift. These were, in part, synchronous with the structural movements inferred for the Fossil Basin (Chapter 2), indicating a regional tectonic event that affected both areas. The stratigraphic position of the deformed horizons demonstrates that tectonism influenced the hydrologic balance of paleolake Gosiute and induced instantaneous changes in lake-basin type at ~51.5 Ma. The manuscript is the first to focus on sedimentary deformation features in the Bridger Basin, and also the first to ascribe seismites to change in lake character.

# CHAPTER 4

# CHARACTERISTICS AND IMPLICATIONS OF SEDIMENTARY DEFORMATION FEATURES IN THE GREEN RIVER FORMATION IN UTAH AND COLORADO

Törő, B., and Pratt, B.R., in press, Characteristics and implications of sedimentary deformation features in the Green River Formation (Eocene) in Utah and Colorado, in Birgenheier, L., Vanden Berg, M., and Ressetar, R., editors, The Uinta Basin and Uinta Mountains: Utah Geological Association Guidebook.

## 4.1 Abstract

The Eocene Green River Formation and associated fluvial strata hosts a large variety of widely distributed and laterally extensive synsedimentary to early post-depositional deformation features. Although mostly overlooked in past studies, these structures provide insight into the rheology of the sediments and hydrodynamic conditions at the time of deformation, and they have implications about basin configuration and bottom topography, and the structural history of the region.

In the Uinta and Piceance Creek basins of Utah and Colorado, deformed intervals are present in littoral (sand-dominated) to profundal (oil shale) lacustrine deposits, as well as fluvial facies. Deformation structures exhibit a wide range of morphology, size, and style, ranging from ductile (convolution, folding, load and pinch-and-swell structures) to brittle (microfaults, breccias), to sedimentary injection into fissures and cracks forming dikes, to various mass-transport deposits. In most cases, these layers are bound above and below by undisturbed beds of similar facies with horizontal bedding planes, which implies short-lived but recurring events that affected only sediments with a susceptible rheological state. Deformation typically occurred intrastratally, i.e. under shallow burial. The variations in deformation style, size, morphology, and areal extent are related to differences in grain size and type, water content, cementation, organic content, thickness of susceptible material, lateral facies variation, and the nature of the driving force. Some of the sedimentary injection features overprint each other, indicating multiple events affecting a single interval.

We interpret most of these features as seismically induced (‘seismites ‘) based on: (1) the tectonic setting of the basin; (2) the sedimentary environment and sedimentological characteristics of the host succession; (3) the lateral extent of deformation structures; (4) their recurrence at different stratigraphic levels; and (5) their similarity to those ascribed to seismically induced deformation elsewhere and reproduced experimentally. They developed as a result of increased pore pressure and a complex combination of extensional, compressive and shear stresses acting in many directions caused by shaking during strong earthquakes. Mass-transport deposits indicate in situ disruption and failure of the imperceptibly dipping lake floor. Other potential trigger mechanisms, such as wave-induced cyclical pore pressure increase, current-generated shear stresses, changes in groundwater level, desiccation, and bioturbation, or overloading, oversteepening, and collapse caused by increased sedimentation rate, however, in most cases can be discarded based on the morphological characteristics of the deformation features and the depositional setting of host facies. These ‘seismites’ represent the direct sedimentary record of syndepositional tectonic activity in the Uinta Basin.

## 4.2 Introduction

The Eocene Green River Formation represents one of the best documented ancient lake systems globally (e.g., Smith et al., 2008). Carbonate-rich sediments were deposited in large, intermittently connected lakes with siliciclastic alluvial strata around their margin during the early and middle Eocene, and deposition roughly coincided with late phases of shortening in the surrounding Sevier belt and Laramide uplifts (e.g., Love, 1970; Steidtmann et al., 1983; Dickinson et al., 1988; DeCelles, 1994). These rocks have been subjected to detailed paleobotanical (e.g., Wing and Greenwood, 1993; Wilf, 2000), geochemical (e.g., Rhodes et al., 2002; Carroll et al., 2008; Davis et al., 2008, 2009; Doebbert et al., 2010, 2014; Frantz et al., 2014), chronostratigraphic (e.g., Machlus et al., 2008; Cumming et al., 2012; Aswasereelert et al., 2013; Smith et al., 2014b), chemostratigraphic (Keighley, 2013) and paleogeographic study (Smith et al., 2014a), along with pioneering sedimentological analysis (e.g., Bradley, 1931, 1964; Eugster and Surdam, 1973; Carroll and Bohacs, 1999). Consequently, the Green River Formation is an unparalleled archive of paleoenvironmental conditions in the continental interior of western North America for this time.

Despite these comprehensive studies and the well-documented tectonic setting, sedimentary deformation features have been mostly overlooked. Our field observations showed that in fact these turn out to be abundant throughout the Green River Formation (Törő and Pratt, in press; Törő et al., 2015). In the Uinta and Piceance Creek basins, they revealed a diverse suite of structures in various lithologies from profundal laminated carbonate mudstones to cross-bedded shoreline sandstones to fluvial deposits. The purpose of this study, therefore, is to provide for the first time detailed description of these features mainly in the Uinta Basin in order to understand the deformation processes and the rheological state of the sediments at the time of deformation, and to evaluate these in regard to the evolution of the depositional environment and the tectonic setting of the lake basin.

### 4.3 Synsedimentary Deformation

Synsedimentary deformation can occur in unconsolidated to consolidated sediments during or shortly after deposition (e.g., Maltman, 1984; Owen et al., 2011). As rheology is the primary control over deformation style, it includes a wide range of in situ features that demonstrate plastic, brittle–ductile, and brittle responses, depending on sediment cohesiveness. Ductile deformation is the most commonly recognized syndepositional deformation because it dominates in siliciclastic facies, especially in sandy deposits (e.g., Owen, 1987). Syndepositional brittle and hybrid brittle–ductile deformation is common in carbonate successions because of the greater range of rheology that potentially can be present as the sediments undergo early diagenetic alteration (e.g., Plaziat et al., 1990; Pratt, 1994, 1998b; Kahle, 2002). Nevertheless, there are cases where carbonates have the mechanical behavior of fine-grained granular sediments and behave plastically (e.g., Bachmann and Aref, 2005; El Taki and Pratt, 2012; Törő and Pratt, in press; Törő et al., 2015).

Sedimentary deformation features generally form as a result of drastic decrease in yield strength of unconsolidated to weakly lithified sediment. The temporary change into a liquid-like and plastic state is reached through liquefaction or fluidization (Allen, 1982; Owen, 1987; Maltman and Bolton, 2003). Thus, convolute bedding, load structures, and sedimentary dikes are the most commonly identified deformation features in sandstones. The responses of carbonates, evaporites, and fine-grained siliciclastics are typically different from those found in silts and sands, resulting in the formation of unique hybrid brittle–ductile and brittle deformation

structures including folds, microfaults, cracks, vein arrays, and breccias (e.g., Pratt, 1998a, b, 2001; Jones and Omoto, 2000; Rossetti and Góes, 2000; Kahle, 2002; McLaughlin and Brett, 2004; Bachmann and Aref, 2005).

There are several natural processes that can induce, or trigger, deformation. However, as the nature of the response depends on more general factors such as sediment type, driving mechanisms, and areal extent and thickness of rheologically susceptible sediments (Owen, 2003), the determination of the actual trigger mechanism can be difficult (Jones and Omoto, 2000; Montenat et al., 2007; Owen et al., 2011). Nevertheless, the study of sedimentary deformation features is an integral part of the depositional history because they are evidence for syn- to early post-depositional physical processes, and thus they provide insight into hydrodynamic conditions of the sedimentary environment, the paleoslope in the basin, or the presence of syndepositional tectonic activity in the case of seismically induced structures (Mills, 1983; van Loon and Brodzikowski, 1987; van Loon, 1992).

Earthquake-induced deformation features (‘seismites’ sensu Seilacher, 1969, 1984), are widely used to track the sedimentary record of syndepositional tectonic events in recent and ancient lacustrine deposits (e.g., Sims, 1973, 1975; Ricci Lucchi, 1995; Moretti and Sabato, 2007; Beck, 2011), thanks to their highly susceptible rheological properties and deposition under low-energy conditions (Renaut and Gierlowski-Kordesch, 2010). A wide range of features has been considered seismites, including in situ brittle or ductile deformation structures as well as those formed by sub-aqueous sediment failure (e.g., Marco and Agnon, 1995; Chapron et al., 1999; Becker et al., 2005; Carrillo et al., 2006; Montenat et al., 2007).

## 4.4 Geological Setting

### *4.4.1 Regional Geology of the Green River Formation*

The Green River Formation (GRF) of the Uinta Basin was deposited in the large, mostly internally drained Lake Uinta between ~54 and 43 Ma (Picard, 1955; Fouch, 1975; Ryder et al., 1976; Castle, 1990; Fouch et al., 1994; Smith et al., 2008; Davis et al., 2009). The Uinta Basin was periodically connected to the Piceance Creek and other basins across the Douglas Creek Arch (Pitman, 1982; Young, 1995; Smith et al., 2008) (Fig. 4.1). This paleotopographic sill, in combination with temporal fluctuations in lake level, sediment supply, and changes in drainage

pattern, as controlled by tectonics and climate (Carroll and Bohacs, 1999), had a profound impact on lake chemistry, lake evolution, and the preserved facies (Smith et al., 2008; Davis et al., 2009). After an initial episode of freshwater conditions, the lake eventually evolved from a brackish into a hypersaline system (Smith et al., 2008; Davis et al., 2009).

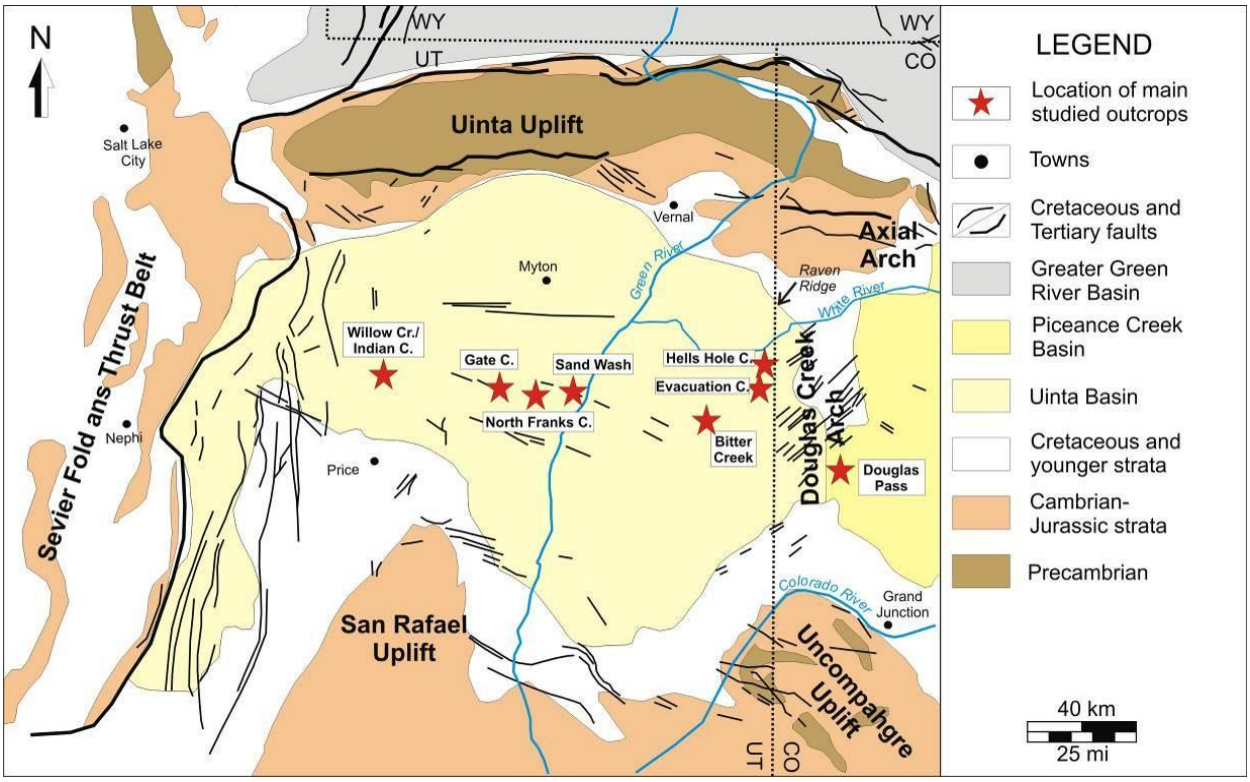


**Figure 4.1** Simplified geological map of northeastern Utah and neighboring Wyoming and Colorado (modified after Smith et al., 2008; Johnson et al., 2010a).

The lacustrine infill of the Uinta Basin is asymmetrical and over 4 km thick at the depocenter to the north, which was proximal to the rapidly uplifting Uinta Mountains (Franczyk et al., 1992). The Uinta Basin today is an erosional remnant of this gentle asymmetrical syncline, and only deposits of the southern side of the basin are preserved in outcrop. A detailed stratigraphic framework has yet to be established, and the subdivisions of the GRF are only locally applicable (e.g., Weiss et al., 1990; Remy, 1992; Ruble and Philip, 1998; Keighley et al., 2003; Birgenheier and Vanden Berg, 2011; Burton et al., 2014) (Fig. 4.2). Marker beds can be recognized only here and there, due to variable exposure, limited subsurface dataset, and basin-wide variation in the lithofacies. Only the Mahogany Oil Shale Zone (MOSZ) can be used a

reliable regional marker beds across the basin (e.g., Bradley, 1931; Cashion and Donnell, 1972, 1974).

Numerous studies revealed details of the sedimentology of the GRF in the Uinta and adjacent Piceance Creek basins (e.g., Picard and High, 1968, 1972; Weiss, 1969; Williamson and Picard, 1974; Fouch, 1975; Ryder et al., 1976; Dyni and Hawkins, 1981; Pitman et al., 1982; Castle, 1990; Franczyk et al., 1991, 1992; Fouch et al., 1992; Remy, 1992; Morris and Richmond, 1992; Ruble and Philip, 1998; Keighley et al., 2002, 2003; Schomacker et al., 2010; Birgenheier and Vanden Berg, 2011; Tänavsuu-Milkeviciene and Sarg, 2012; Sarg et al., 2013; Burton et al., 2014). Although sedimentary deformation structures have been reported (e.g., Bradley, 1931; Cashion, 1967; Picard and High, 1972; Cole and Picard, 1975; Remy, 1992; Keighley et al., 2002; Birgenheier and Vanden Berg, 2011; Tänavsuu-Milkeviciene and Sarg, 2012), they were mainly neglected or overlooked and no attempts have been made to determine their origin and significance. Outcrop locations for this study were chosen based on these previous studies in order to integrate our observations with a well-documented stratigraphic context.

### *4.4.2 Lithofacies and Depositional Environment*

In general, lacustrine strata comprise gray-to-black and green mudstones and shales formed in open lacustrine areas and in sheltered embayments where wave action and fluvial influence were minimal (Ryder et al., 1976; Remy, 1992). Shales and carbonates that accumulated in deeper parts of the system are characterized by very fine lamination and high organic content. The southern margin of Lake Uinta, along with the area of the Douglas Creek Arch and a much narrower zone at the northern part, was dominated by carbonate-rich shoreline facies where other types of carbonates (e.g., calcareous siltstone and sandstone, ooid and ostracode grainstone, and microbial carbonates) are intercalated with thickly bedded or massive mudstones. Microbial carbonates (stromatolites and thrombolites) formed in wave-agitated littoral settings are usually intercalated with various kinds of grainstones, while those related to low-energy sublittoral settings are encased in laminated carbonate siltstones or mudstones (e.g., Sarg et al., 2013). Siliciclastic sediments were delivered from the actively uplifting Uinta Mountains to the north, and from highlands of the Uncompahgre Uplift and the San Rafael Swell to the south (Fouch, 1975; Pitman et al., 1982; Keighley et al., 2003; Davis et al., 2009). As a result of different

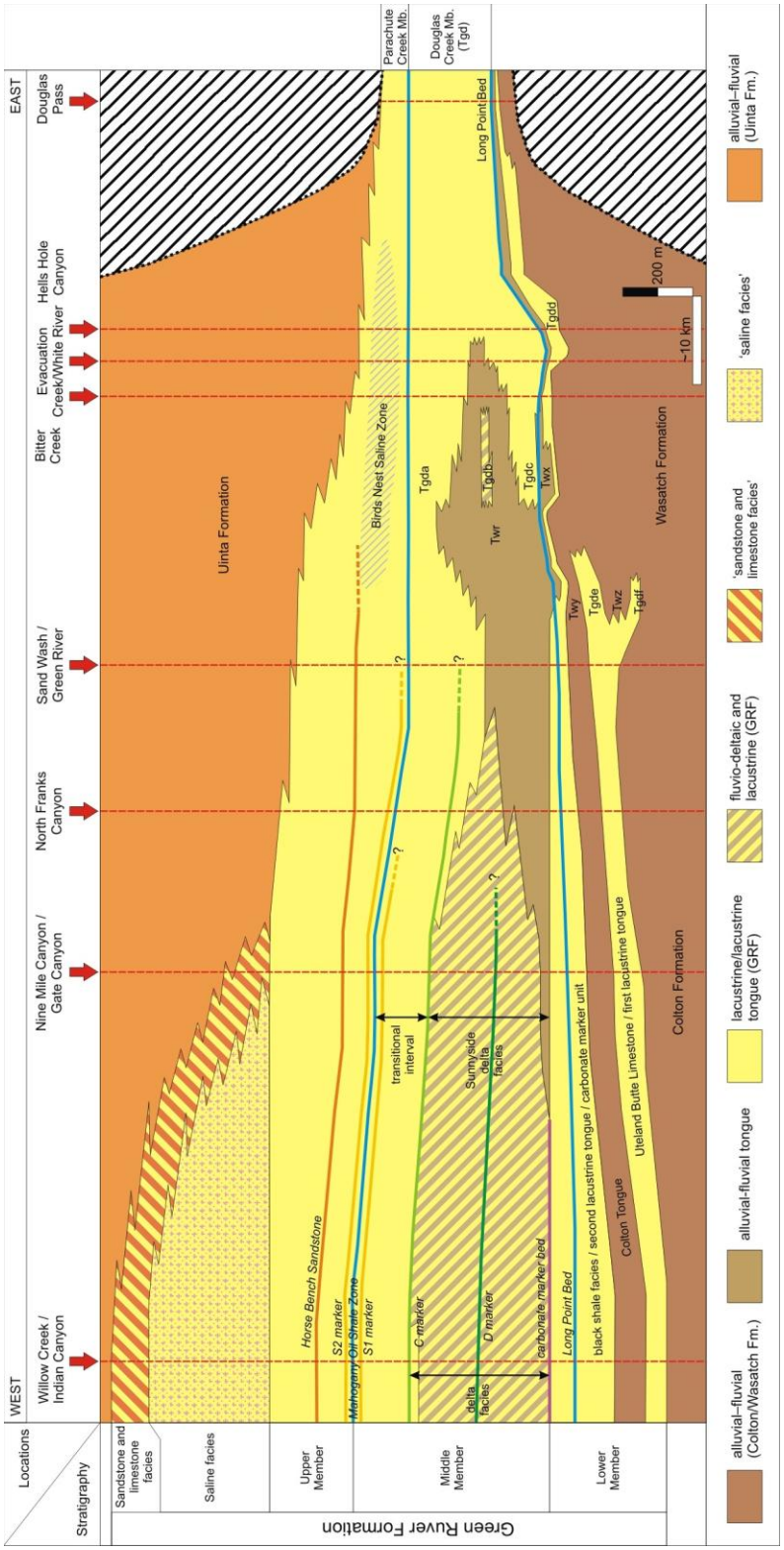


**Figure 4.2** Stratigraphic cross-section of the Green River Formation from Willow Creek/Indian Canyon (Utah) to Douglas Pass (Colorado) (modified after Cashion, 1967; Johnson et al., 1988; Morgan et al., 2003, Tänavsuu-Milkeviciene and Sarg, 2011).

topographic gradients, lake sediments pass laterally to sandstones and green, gray and red mudstones of deltaic or fluvial-floodplain origin along the gently dipping southern shoreline, and sandstones and conglomerates of alluvial-fan origin at the steeper northern margin (Picard and High 1972; Ryder et al., 1976; Castle, 1990; Borer and McPherson, 1998; Keighley et al., 2003; Schomacker et al., 2010).

Terminology of depositional environments follows Cohen (2003) and Renaut and Gierlowski-Kordesch (2010), where the littoral zone is above fair-weather wave base, the sublittoral zone is between fair-weather wave base and storm wave base, and the profundal zone is below storm wave base.

## 4.5 Sedimentary Deformation Structures

Observations of outcrops, polished surfaces, and thin section are used to characterize the deformation structures, determine deformation mechanism, gauge the timing of formation in relation to shallow burial, and ascertain the rheological attributes of the sediments during deformation. We focus on features found in the deposits of the Uinta Basin in northeastern Utah, with few examples from the adjacent Piceance Creek Basin in northwestern Colorado (Appendix 1). The terminology used in this study is based on the classification of Owen (1987, 2003), Rossetti (1999), Rodríguez-Pascua et al. (2000), and Montenat et al. (2007).

### *4.5.1 Load Structures*

#### 4.5.1.1 Description

Load structures are characterized by folding of an interface between two sediment layers, and include load casts, pseudonodules, and ball-and-pillow structures (Allen, 1982; Owen, 1987, 2003). Here, these structures are defined by roughly regularly spaced, broad and rounded, decimeter-sized synforms separated narrow, cuspate antiforms sometimes called diapirs or flame structures. The internal lamination in the load structures is not disrupted and generally remains parallel to the folded interface and thus appears concentric.

Centimeter-scale load structures, occasionally associated with flame structures, are abundant in marginal lacustrine and deltaic deposits of the middle GRF at Willow Creek (Fig. 4.3A). At Gate Canyon, where deformation is usually overlain by wave-ripple cross-laminated

sandstone, attached pseudonodules occur in a sandstone unit that can be traced for more than 30 m along the outcrop (Fig. 4.3B). At Sand Wash the Horse Bench Sandstone (Fig. 4.3C, D) and the S1 marker (Fig. 4.3E, F) hosts pseudonodules and ball-and-pillow structures in the upper part of hummocky and tabular cross-bedded medium-grained sandstone. These extend laterally for up to 150 m along the outcrop and cross stratification is preserved in the least deformed parts of the bed. Comparable features are also present at the uppermost part of the GRF in wave- and current rippled shallow-lacustrine sandstones near White River (Fig. 4.3G). In all cases, no lithological contrast across their interface was observed and load structures do not show consistent vergence.

At Douglas Pass, load structures are common at the base of deltaic sandstone beds (Fig. 4.4A) and at the base of microbial and bioclastic carbonate layers (Fig. 4.4B–D). The deltaic deposits show loading into laminated carbonate mudstones that are capped by planar bedded grainstones and stromatolites. Internally the load structures show loading and folding. The sandstone overlying the load structures is massive or folded and thins laterally or is missing at seemingly irregular intervals.

Load structures at the base of carbonate beds are filled with breccia, composed of a mixture of broken fragments of grainstone, mudstone, and microbial carbonates, up to 40 cm long, within a massive matrix of carbonate mud, silt and sand (Fig. 4.4B–D). These features penetrate into underlying massive to faintly laminated carbonate mudstone. Stromatolite clasts in the deformed layer are folded close to the contact between the underlying mudstone and the breccia's infill. They are usually flanked by diapirs of the underlying mudstone bed and overlain by grainstone, microbialite, or carbonate mudstone beds. Overlying laminated mudstone beds frequently fold around the upward protruding clasts (Fig. 4.4D).

Load structures are also common at the base of tuff layers intercalated with silty carbonate mudstones (Fig. 4.4E, F). They show irregular (Fig. 4.4E) to somewhat regular patterns (Fig. 4.4F) and in few cases are associated with small-scale sedimentary dikes (see 'Sedimentary Dikes' below). Although some tuff layers may show normal grading, they are usually massive or contorted.

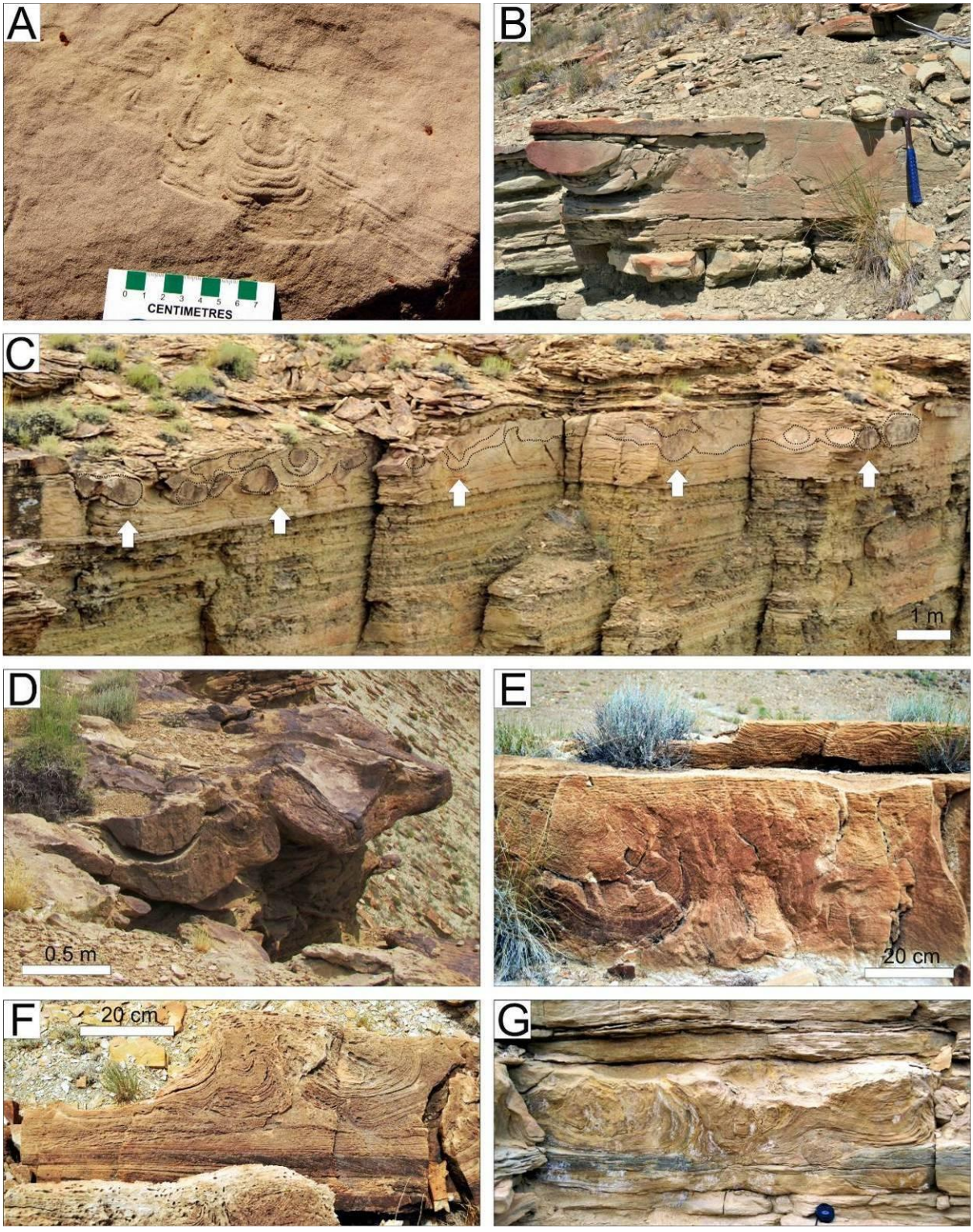


**Figure 4.3** A. Localized load structures up to 15 cm wide in cross-stratified uniform, medium-grain deltaic mouth-bar sandstone (delta facies, Willow Creek, UT); B. Symmetrical load structures 15–25 cm wide and up to 20 cm thick, with massive internal structure in cross-laminated fine- to very fine-grained lacustrine sandstone (upper member, Gate Canyon, UT); C, D. Load structures in the upper part of hummocky cross-stratified lacustrine

shoreline sandstone (Horse Bench Sandstone, Sand Wash, UT) in cross section outlined with dotted lines and marked by arrows (C) and plan view (D) forming broad basins and curvilinear domes or ridges; E, F. Load structures on the top of cross-stratified shoreline sandstone, up to 0.7 m wide and 0.4 m thick, with concentric lamination that is locally folded overlain by combined-ripple cross-laminated sandstone (S1 marker bed, Sand Wash, UT); G. Load structures on the top of current-ripple cross-laminated shoreline sandstone bed (upper member, White River, UT).

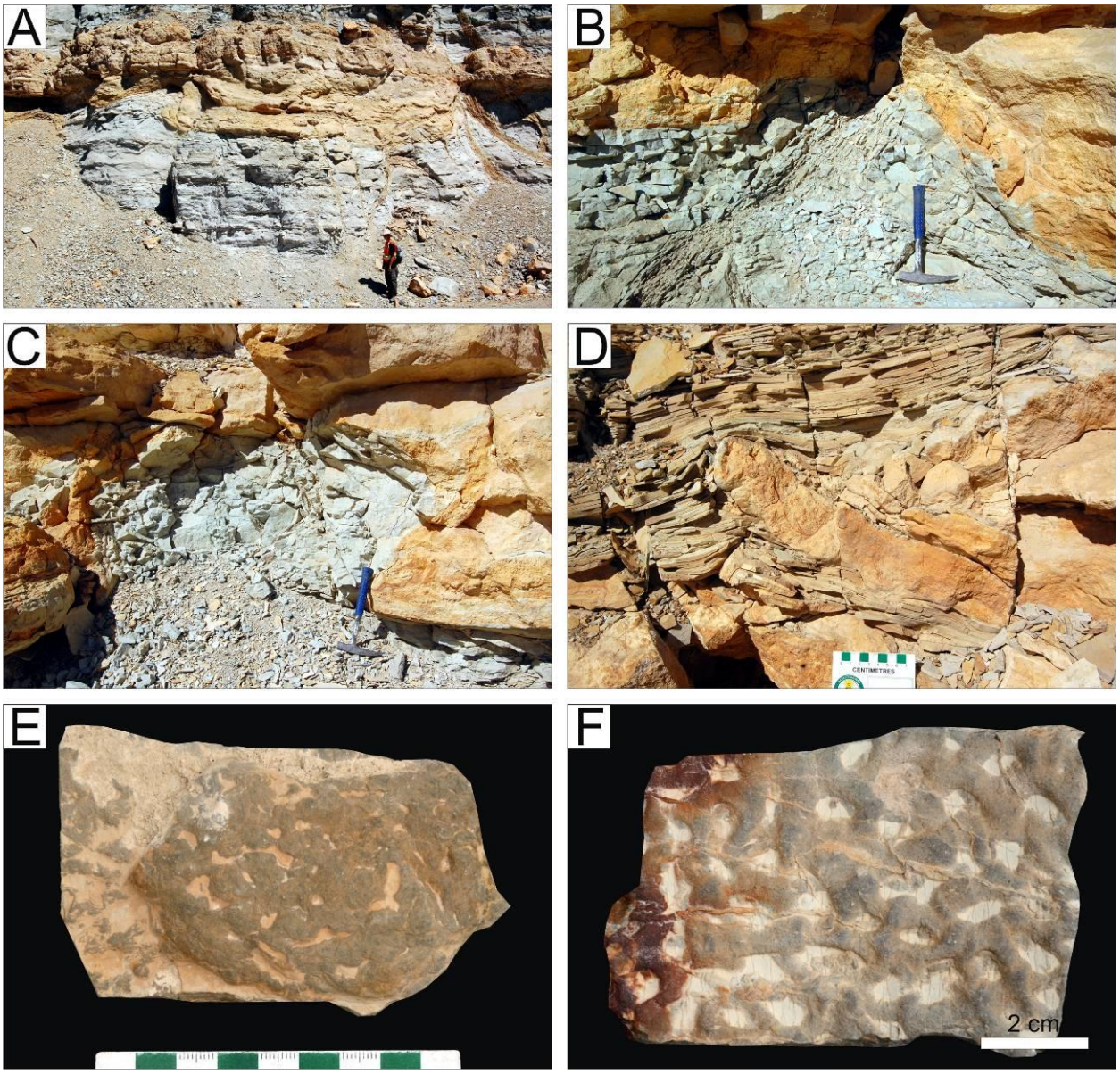


**Figure 4.4** A. Large-scale load structure at the base of deltaic mouth-bar/distributary channel sandstone, overlain by microbial and shoal carbonates (L1 zone, Douglas Pass, CO); B–D. Load structures, with variable dimensions, locally reaching up to 1 m in height and more than 2 m in width, filled with brecciated carbonates, overlain by ooid grainstone and microbial carbonate (B, C) or laminated mudstone (D) (L5 zone, Douglas Pass, CO); E, F. Load structures at the base of 1 cm thick tuff layers (upper member, Nine Mile Canyon, UT).

#### 4.5.1.2 Deformation Mechanism

Load structures are related to liquefaction and a drastic reduction in shear strength of the unlithified sediments where the plastic deformation of an interface is usually driven by an unstable density gradient or uneven loading (Anketell et al., 1970; Owen, 1987; Moretti et al., 1999). Although the complexity or extent of deformation structures is controlled by the ratio of kinematic viscosity between sediment layers, and magnitude and duration of the driving force (Anketell et al., 1970; Mills, 1983), load structures may form in the absence of lithological contrasts (Owen, 2003).

Localized load structures in deltaic deposits at Willow Creek are interpreted as the result of localized increased pore-pressures at interfaces within trough cross-bedded sandstone before the deposition of the overlying sand. The morphology of load structures at Gate Canyon, Sand Wash, and White River indicates selective liquefaction of the upper intervals of cross-stratified sands post-depositionally and the loading of the material in one or more events, rather than 'passive' loading of the migrating subaqueous dunes into the underlying material. In these cases, major lithologic contrast in not apparent and selective liquefaction is then related to variable rheological properties of the sediment due to changing packing and porosity. As noted by Remy (1989), meter-scale hummocky cross-stratification within these intervals is the result of longer term combined flows in shallow lacustrine setting, rather than short-lived storm events (Morsilli and Pomar, 2012).

The sand-filled load structures at Douglas Pass were previously interpreted as deltaic distributary channel deposits (Tänavsuu-Milkeviciene and Sarg, 2012). However, distributary channel deposits do not show soft-sediment deformation stratigraphically higher in the section. Moreover, the irregular thickness and the deformed appearance of the sand layer outside the load structure indicate that downslope slumping as a deformation mechanism also can be ruled out because deformation is not confined to the channel. Rather, deformation is related to the liquefaction of the underlying mudstone and the deltaic sandstone that occurred after deposition and intrastratally after further burial.

Load structures filled with brecciated carbonate or tuff material indicate loading driven in part by reverse-density gradients. It is important to note, however, that the density contrast between two layers is not solely sufficient to cause deformation, as evidenced by the undeformed intervals showing similar differences in grain-size or composition. Thus, the interface between

the two units with different bulk densities was deformed through the liquefaction of the underlying carbonate mudstone post-depositionally. Alternatively, the development of load structures at the base of tuff layers is related to deposition and instantaneous loading of tuff material over a soft 'soupy' substrate. The brecciated infill of the load structures at Douglas Pass indicates a significant erosional event before their formation, and the infill can be interpreted as subaqueous mass-transport deposition of early-lithified materials. Mudstone diapirs between the load structures indicate plastic deformation and intrusion of the underlying carbonate mud where the mudstone fragments of the infill also originated from. The overlying microbial carbonates and grainstones indicate that deformation was taking place in a wave-agitated shallow-lacustrine environment.

### *4.5.2 Convolution*

#### 4.5.2.1 Description

Convolution partly overlaps in morphology with load and flame structures, but generally they are characterized by more diverse and irregular geometries. At Nine Mile Canyon convolution occurs in the middle and upper portion of fluvial channel sandstone (Fig. 4.5A, B), where the deformed interval is truncated by a sharp planar surface on the top, and overlain by heterogeneously convoluted cross-laminated sandstone. The whole unit is overlain by undeformed mudstone interbedded with sandstone. The folding is irregular and exhibits no particular vergence. At other locations examined, channelized sandstones with similar lithofacies and similar stratigraphic occurrence do not show convolution. Comparable structures are also present in the fluvial deposits at Evacuation Creek (Fig. 4.5C). Convoluted sandstones, sand volcanoes, and "slumps" from the Nine Mile Canyon area were noted by Keighley et al. (2002) and Schomacker et al. (2010).

At Gate Canyon convolution is present in the littoral deposits of the S1 marker bed showing meter-scale tabular cross-bedding (Fig. 4.5D) (cf. Remy, 1992). The style of deformation changes laterally with changing facies, and convolution can be traced into load structures at the top of the same interval (Fig. 4.5E). The deformation gradually dies out as the sand bed gets thinner. The interval has a flat and sharp upper surface which is overlain by planar bedded sandstone, interbedded with laminated mudstone and siltstone. Folds within the interval showed no particular orientation.

Large-scale convolution is present in a thick fluvial channel sandstone bed of the Uinta Formation, approximately 20 km south of Myton (Fig. 4.5F, G). The convolution affects the whole exposure that is more than 100 m wide. Deformation occurs only in the lower half of the channel fill, which is cut into greenish-grey floodplain mudstones and overlain by tabular, trough cross-bedded sandstone. The thickness of the convoluted interval is variable and contorted zones pass laterally into slightly folded or undeformed sandstone over short distances. Undulation of the upper surface of the deformed interval is caused by the upward-protruding flame structures.

#### 4.5.2.2 Deformation Mechanism

Convolution has been mainly described from siliciclastic deposits without the presence of a density contrast, where its origin has been ascribed to elevated pore pressures, partial liquefaction, and loss of shear strength in unconsolidated sediment (e.g. Kuenen, 1958; Anketell et al., 1970, Lowe, 1975; Allen, 1977; Visher and Cunningham, 1981; Mills, 1983; Owen, 1987, 2003; Guiraud and Plaziat, 1993; Moretti et al., 2001).

The sharp upper surface of the deformed intervals at Nine Mile Canyon, Gate Canyon, and Evacuation Creek indicates that either: (1) deformation occurred before the deposition of the overlying sediments and the abrupt contact formed by erosion of the sediment after liquefaction; or (2) intrastratal liquefaction occurred in a confined interval. By contrast, the deformation in the Uinta Formation has a gradual upper boundary indicating that liquefaction happened intrastratally after shallow burial and the intensity of deformation dissipated upwards.

**Figure 4.5** (on next page) A–B. Convolute bedding in 1.5 m thick and 25 m wide medium-grained cross-stratified fluvial channel sandstone overlain by current-ripple cross-laminated sandstone, where the lowermost part is undeformed, while the convoluted interval is truncated by a sharp planar surface that is overlain by a 25 cm thick heterogeneously convoluted, current- and wave-rippled sandstone bed (Sunnyside delta, Nine Mile Canyon, UT); C. Convolute bedding in fluvial channel sandstone ~2 m thick and ~5 m wide (R4 zone, Evacuation Creek, UT); D, E. Convolute bedding (D) passing laterally into load structures (E) in tabular cross-bedded shoreline sandstone (S1 marker bed, Gate Canyon, UT); F, G. Convolute bedding in tabular and trough cross-bedded fluvial channel sandstone (B member, Uinta Formation, south of Myton, UT).

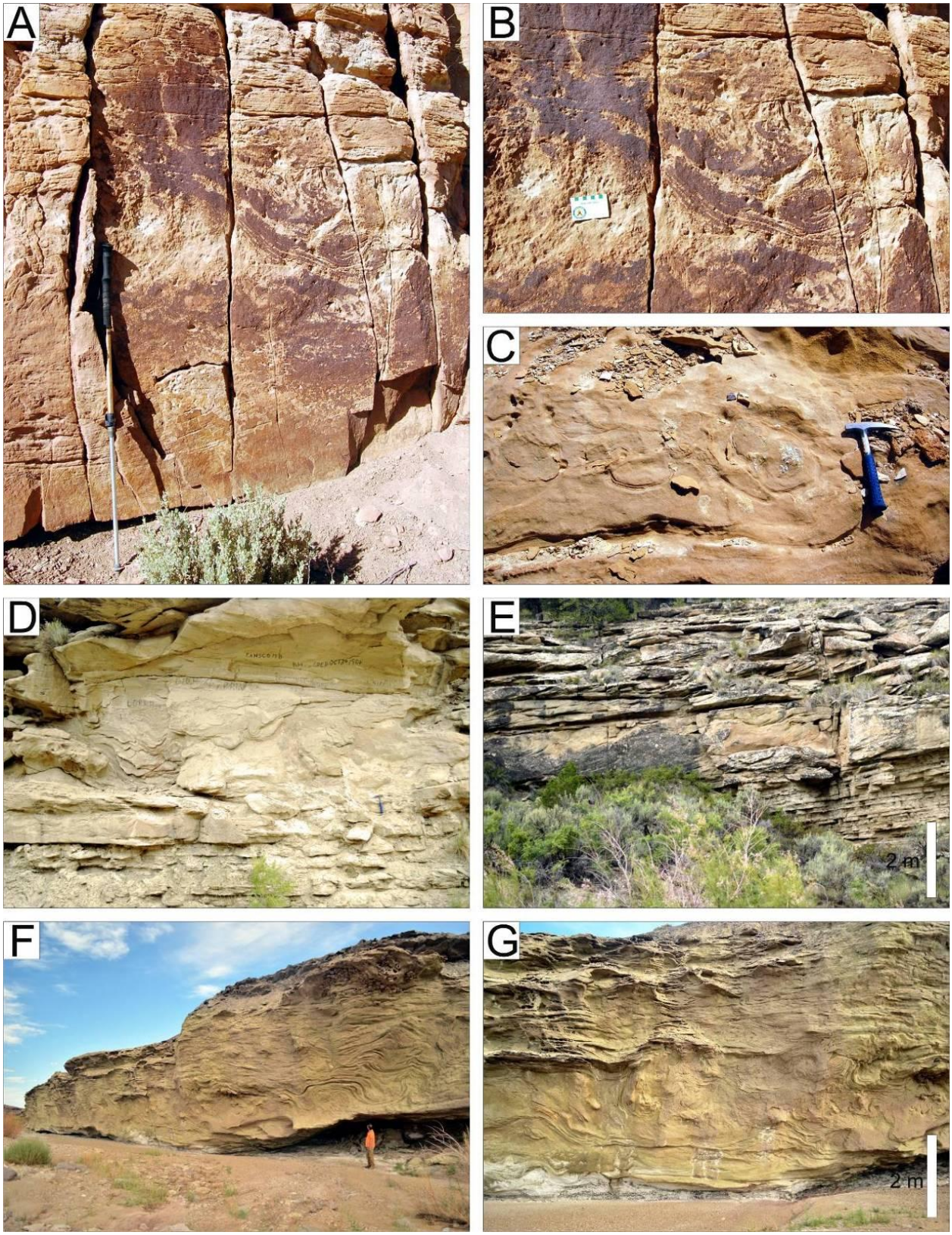
A
B
C
D
E
2 m
F
G
2 m

### *4.5.3 Folding*

#### 4.5.3.1 Description

Although folding, with variable morphology, is involved in other deformation features such as load structures and convolution, it also occurs independently, both in littoral cross-bedded sandstones, microbial carbonates, and laminated carbonate mudstones deposited from profundal environment.

Folding is present in the upper member of the GRF at Gate Canyon (Fig. 4.6A) and in the Horse Bench Sandstone at Sand Wash (Fig. 4.6B) in littoral cross-bedded sandstone intervals. Here the deformation is characterized by gentle, low-amplitude folds with local, cuspate features resembling flame structures. At Gate Canyon the deformation affects two sandstone beds, overlain by carbonate mudstone and interbedded tabular-cross-bedded sandstone. In the Horse Bench Sandstone deformation is overlain by mudstone with interbedded cross-laminated sandstone.

Folded stromatolite layers occurring at Indian Canyon (Fig. 4.6C) and at Evacuation Creek (Fig. 4.6D), are intercalated in sublittoral parallel laminated carbonate mudstone and can be traced laterally for tens of meters. These centimetre-scale folds show tight and recumbent geometries. At Evacuation Creek these deposits also show fluid-escape features with the disruption of the stromatolites and the mudstone interbeds (Fig. 4.6D).

Recumbent and kink folds, up to tens of centimeters in size, are common in profundal laminated organic-rich oil shale deposits (Fig. 4.6E–H). Recumbent folds are usually complex and characterized by sharp hinges, straight limbs, and broad parabolic forms. Within individual intervals the axial planes show no overall preferred orientation. In most cases the under- and overlying deposits are undeformed laminated oil shale. In other places, they are bounded by oil shale deposits showing other kinds of deformation, such as pinch-and-swell structures and microfaults. Recumbent-folded intervals commonly show gradual transition into brecciated beds (see ‘Oil shale breccias’ below).

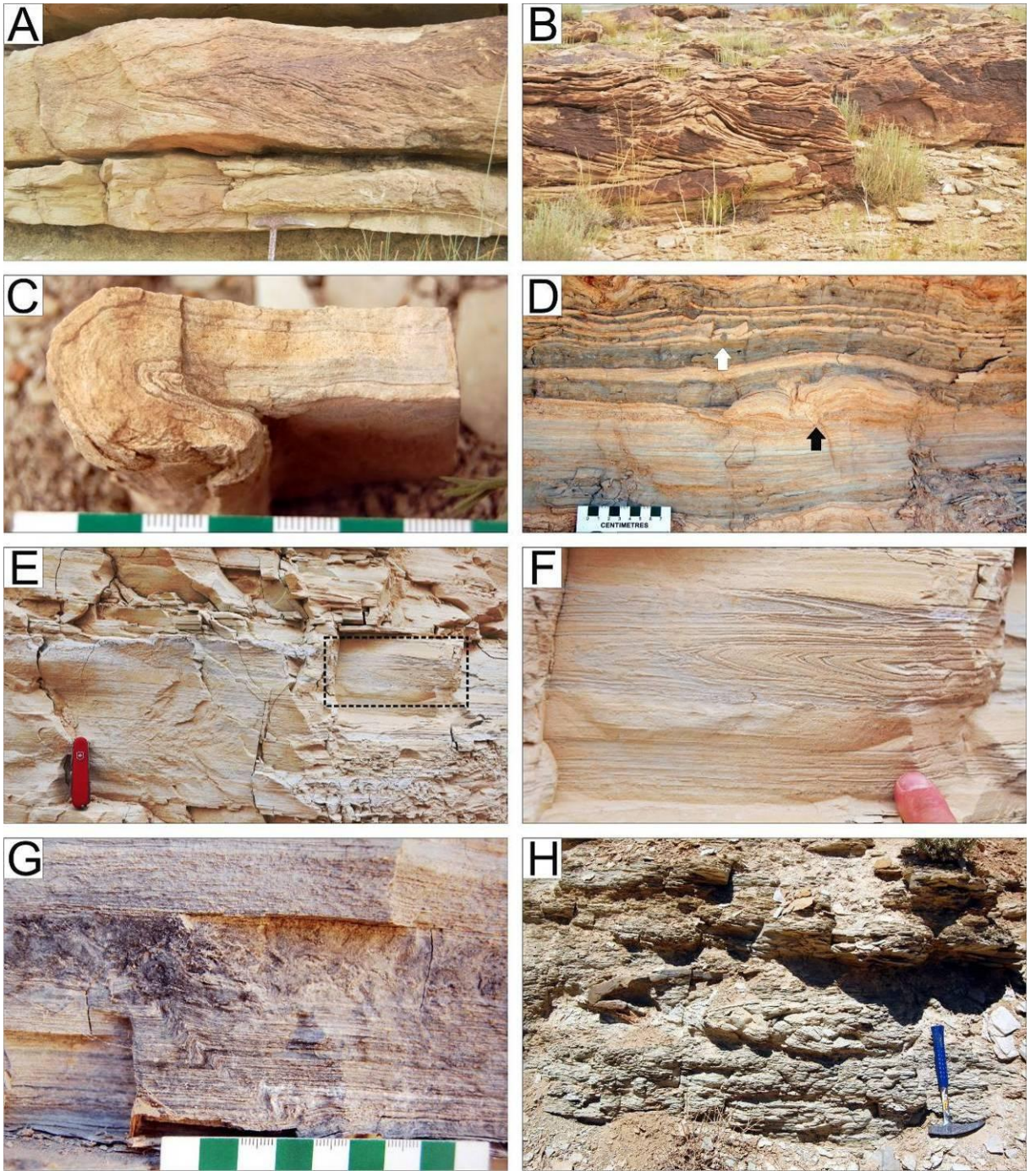


**Figure 4.6** A. Folded tabular cross-bedded shoreline sandstone overlain by combined- and wave-ripple cross-laminated sandstone (upper member, Gate Canyon, UT); B. Folded cross-stratified sandstone in 25–50 cm thick sandstone beds with load structures (Horse Bench Sandstone, Sand Wash, UT); C. Recumbent-folded microbial carbonate (upper member, Indian Canyon, UT); D. Folded low-relief stromatolites (black arrow) overlain by interbedded gray mudstone and disrupted laminated carbonate mudstone (white arrow) (R3 zone, Evacuation Creek, UT); E, F. Recumbent-folded oil shale (MOSZ, Hells Hole Canyon, UT); G. Kink fold in oil shale (MOSZ, Hells Hole Canyon, UT); H. Recumbent-folded oil shale and tuff layer (MOSZ, White River, UT).

#### 4.5.3.2 Deformation Mechanism

Plastic deformation, in general, indicates that the sediment was still soft or semi-cohesive during deformation. Although the mechanism of deformation might be similar, there are significant rheological differences between siliciclastic, microbial, and organic-rich sediments. Folding in cross-bedded sands may represent an early initial state of loading or convolution and, thus, it is usually attributed to the loss of shear strength through liquefaction (e.g., Allen and Banks, 1972; Allen, 1977; Guiraud and Plaziat, 1993; Wells et al., 1993; Røe and Hermansen, 2006).

Plastic deformation in microbial carbonates must have happened at the sediment–water interface or at very shallow burial depth due to the likelihood of early diagenetic cementation (e.g., Sumner, 1997). Millimeter- to decameter-scale folds, 'roll-up' structures, and convolution have been reported in microbialites from both shallow- and deeper-marine settings (Demicco, 1985; Pratt, 1994; Schieber, 1999; Simonson and Carney, 1999; Kahle, 2002; Schieber et al., 2007; Pruss et al., 2010; Martín-Chivelet et al., 2011). Here, folded stromatolites are intercalated within fine-grained, sublittoral carbonates, indicating an overall low-energy setting. Where folding is associated with fluid-escape and disruption indicating increased pore pressure, deformation must have occurred intrastratally.

The flat-lying axial planes of the recumbent folds in the oil shale deposits indicate no vertical displacements, and thus, the deforming shear forces acted only tangentially, i.e., parallel with the base and top of the deformed interval. In general, organic-rich sediments have a high initial water content and high shear strength and stability, but also elevated sensitivity, and, thus, they behave thixotropically upon disturbance (Grimm and Orange, 1997). As a result, recumbent-folded intervals indicate plastic deformation in semi-cohesive organic-rich muds that occurred when external forces exceeded a certain threshold to cause failure of the sediments. Undisturbed laminated oil shale above and below suggests quiet -water lacustrine deposition. In general, sharp and flat upper and lower boundaries of recumbent folded layers imply deformation within confined intervals. Folded oil shale deposits in the GRF have been previously reported by Bradley (1931) and Picard and High (1972) from the Uinta Basin, and by Grabowski and Pevear (1985) and Tänavsuu-Milkeviciene and Sarg (2012) from the Piceance Creek Basin, and they were usually attributed to slumping. It is possible that the plastic nature of organic-rich muds

upon deposition or under shallow burial allows hydroplastic deformation (sliding, gliding, or laminar flow) of the sediments in the absence of liquefied state.

### *4.5.4 Pinch-and-Swell Structures*

#### 4.5.4.1 Description

Pinch-and-swell structures (‘loop bedding’) are abundant locally in organic-rich oil shale (Fig. 4.7A–D), and usually they alternate with units that lack deformation. They are characterized by irregular thickening and thinning bundles of laminae with or without disruption and loss of the lateral continuity. As a result, the morphology is similar to loops or links of a chain (thus ‘loop bedding’ of Calvo et al., 1998). The thickness of individual bundles ranges from a few millimeters to centimeters, the length of each structure is up to few decimeters, and the overall thickness of the deformed layer is up to 2 m. Small-scale folds and microfaults, mainly listric to dipping ~45°, are frequently associated (Fig. 4.7C, D), or occur in under- and overlying beds. Similar structures were observed in the GRF by Bradley (1930, 1931), Cole and Picard (1975), Dyni (1981), and Grabowski and Pevear (1985).

#### 4.5.4.2 Deformation Mechanism

Thinning and thickening of the laminae indicate ductile deformation in semi-cohesive sediment, while the associated microfaults reflect concomitant brittle behavior. The morphological variability of these structures reflects the composition-dependent deformational behavior of the laminae and the variable rheology of the sediment. In oil shale muds deformation was controlled mainly by the variable organic content of the laminae which resulted in contrasting rheological properties. Simple forms indicate purely ductile deformation and stretching of alternating laminae where the competence contrast was less pronounced, similar to how classic boudinage forms during metamorphism. Complex structures, showing significant contortion, rupture of laminae, and dislocation along internal discontinuity surfaces, indicate deformation at the boundary of the brittle–ductile deformational fields.

Taken together, simple to complex structures represent a continuum of responses, due to the interplay between progressive lithification and the extensional stresses affecting the sediment package. Because thick oil shale successions in the GRF lack pinch-and-swell structures, or they

are only present sporadically, this implies rheological control or variation in the timing and intensity of the deformation mechanism. The abundance of these features in oil shales with high organic content and relatively few organic-poor (carbonate-dominant) intercalations indicates that the rheological properties of these sediments were more conducive to this type of behavior.

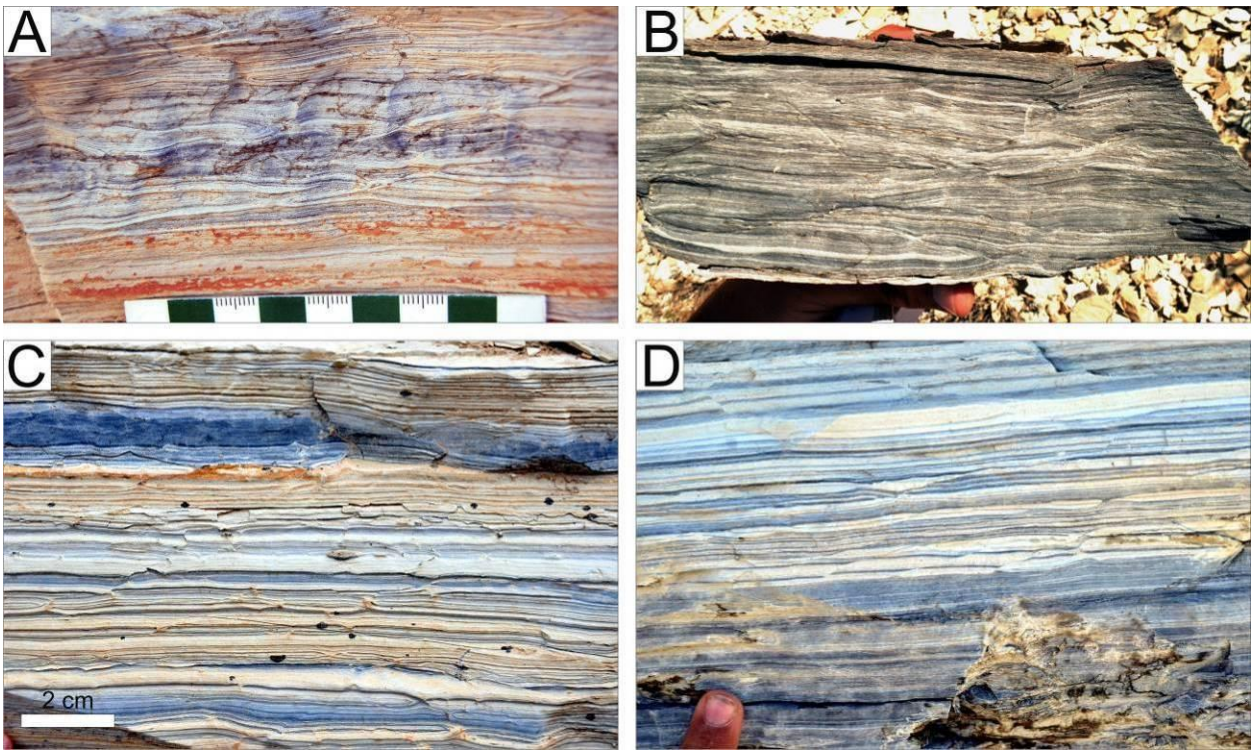


**Figure 4.7** Pinch-and-swell structures in laminated oil shale showing various stages of development (MOSZ, Hells Hole Canyon, UT); A. Small boudins; B. Large-scale boudins and major discontinuity surfaces; C, D. Small boudins and microfaults.

### *4.5.5 Shear Structures*

#### 4.5.5.1 Description

Shear structures are most common in the MOSZ at Gate Canyon and Evacuation Creek. They usually form distinct intervals, with sharp and flat lower and upper boundaries, over- and underlain by undeformed oil shale laminae (Fig. 4.8A, C, E). Their thickness, however, can change significantly over short distances (Fig. 4.8C, D). Deformed horizons typically host composite deformation features, showing irregular folds with variable geometries, fault-related folds, microfaults dominated by thrust and reverse forms, slickensides, and sinusoidal duplexes

and en-echelon fabrics (Figs. 4.8A, B, E, 4.9A–F). These features usually have a well-defined vergence that is consistent at the outcrop scale. The indicated direction of shearing is towards the north (~015°) at Gate Canyon and towards the southwest (~230°) at Evacuation Creek.

At Gate Canyon deformation occurred in four distinct intervals up to 110 cm thick, showing similar vergence and these are separated by undeformed, laminated deposits (Fig. 4.8A). At Evacuation Creek the MOSZ hosts two deformed horizons (Figs. 4.8C, D, 4.9A–F). Although in most cases horizontal displacement along these structures cannot be determined, within the lower interval it is on the order of tens of centimeters. Two of the undeformed beds between them vary laterally in thickness (Fig. 4.8C) and exhibit planar to low-angle lamination.

#### 4.5.5.2 Deformation Mechanism

Synchronous folding and faulting implies that sediment was in a semi-cohesive state when combined brittle–ductile deformation occurred. Deformation is focused within distinct intervals which indicate that shearing was concentrated at these horizons (Fig. 4.10). Similarly to recumbent folds, the formation of shear structures requires increased tangential stresses that are parallel or slightly oblique to the bedding surfaces. The thickness change between the two deformed horizons at Evacuation Creek can be attributed to the development of lake-floor undulations after the formation of the lower horizon. Thus, the two horizons imply two distinct events.

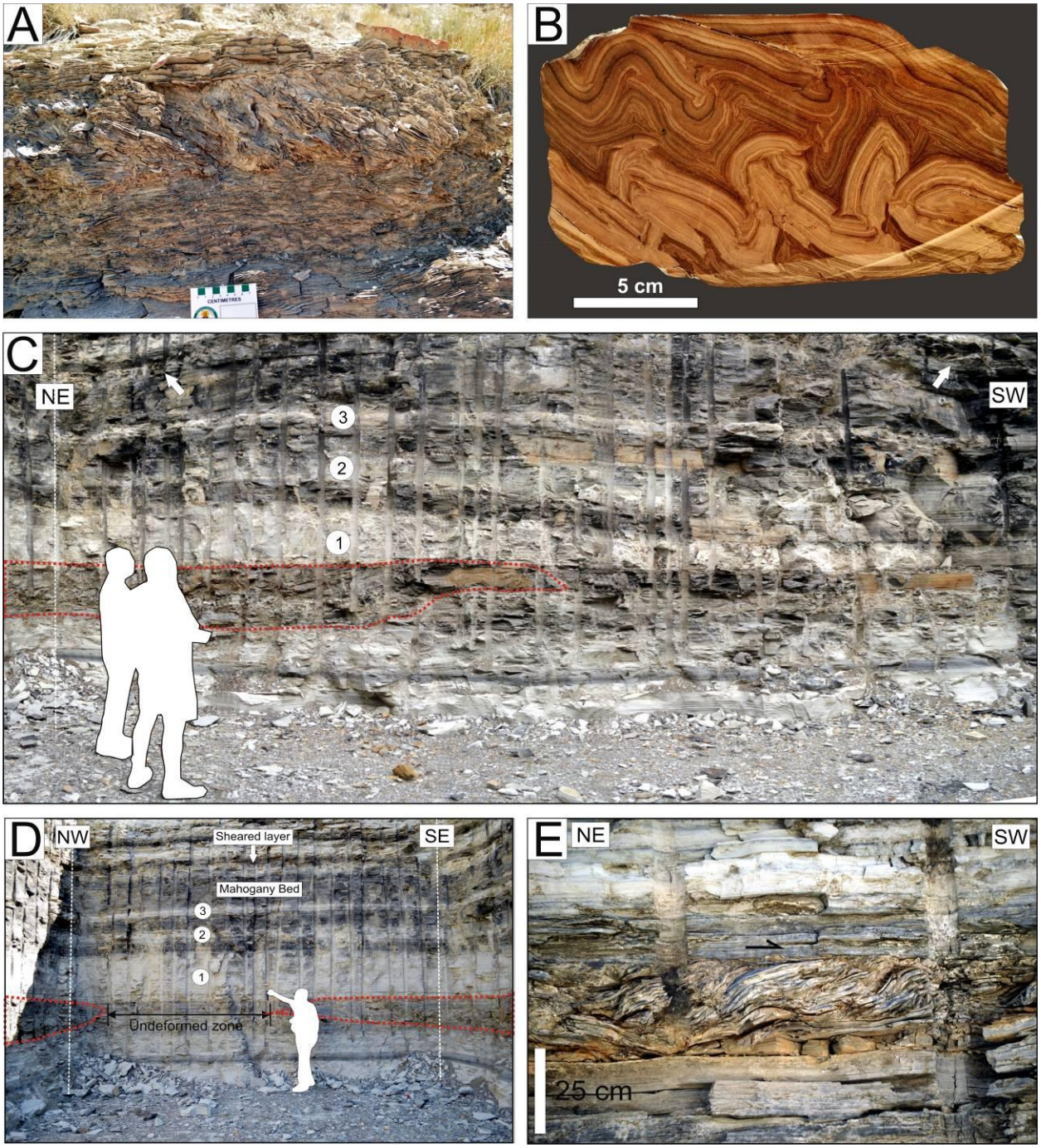


**Figure 4.8** A. Shear structures in a ~20 cm thick interval of oil shale showing imbrications, duplexes and folding, indicating top-to-left shear (MOSZ, Gate Canyon, UT); B. Oil shale showing imbrication, folding, and faulting (White River Mine, UT); C, D. Two sheared intervals in oil shale (MOSZ, Enefit Box Cut, Evacuation Creek, UT). The lower interval is up to 70 cm thick (marked by red dotted line), laterally restricted, and gradually dies out towards the southwest. The upper horizon is laterally persistent and ~25 cm thick (marked by arrows). The oil shale beds (numbered) between the two intervals show significant thickness changes over a distance of 5–10 m; E. Detail of the upper sheared interval, with complex folding and duplexes, indicating top-to-right shear.

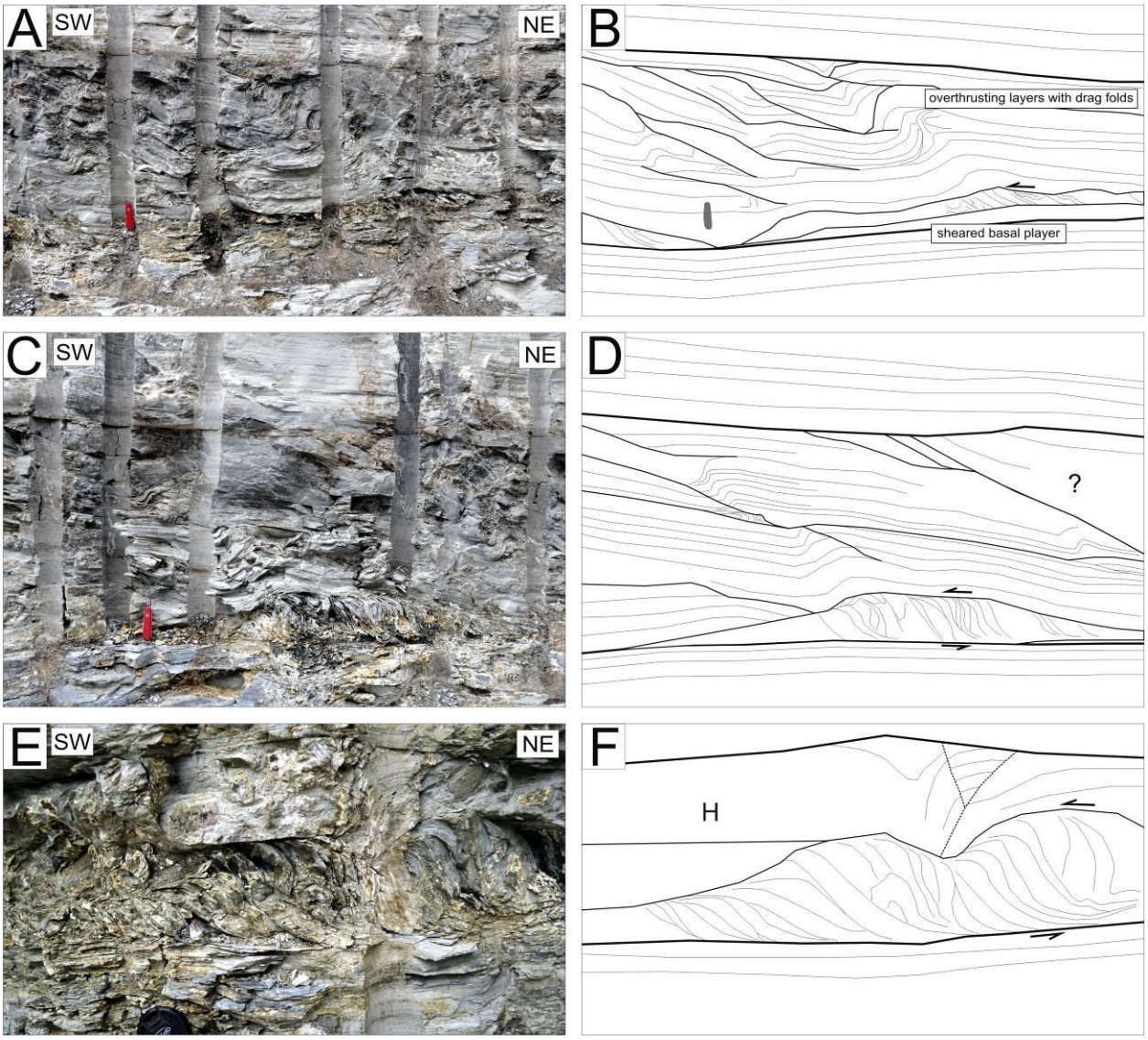


**Figure 4.9** Details of the lower sheared interval (MOSZ, Enefit Box Cut, Evacuation Creek, UT). A, B. Shear structure with microfaults, fault-related folds, and a basal interval with duplexes; C, D. Shear structure underlain by irregular basal interval showing duplexes; E, F. Close-up duplexes and folding above basal décollement surface. 'H' indicates outward facing hinge.

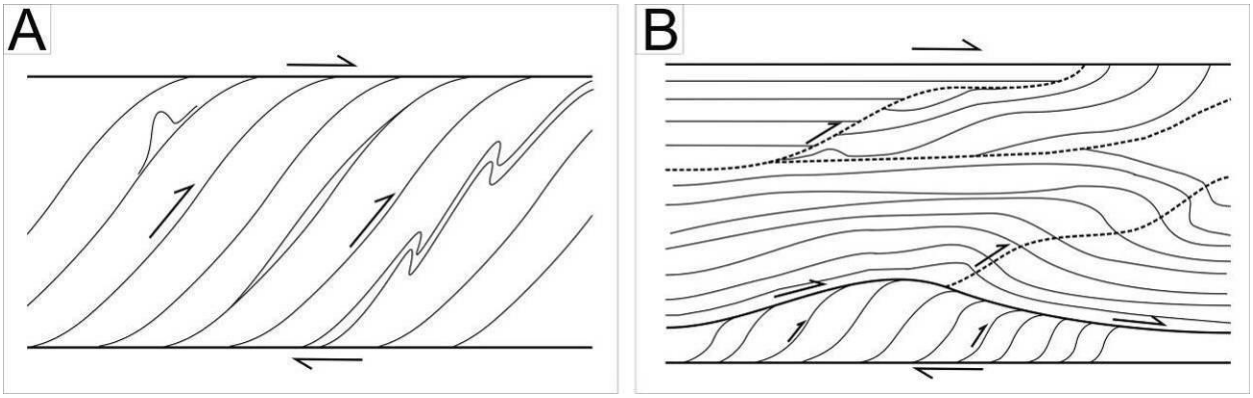


**Figure 4.10** Schematic diagrams of shear structures in laminated oil shale. A. Simple geometry; B. Complex geometry (not to scale).

### *4.5.6 Mass Transport Deposits*

#### 4.5.6.1 Description

At Douglas Pass deltaic, littoral, and sublittoral deposits are cut by a sharp erosional surface, forming a concave channel-like feature or chute ~8 m deep and ~20 m wide (Fig. 4.11A). The chute is filled with intact to intensely deformed sandstone, siltstone, and mudstone fragments up to 40 cm floating in a mud-rich matrix (Fig. 4.11B–F). Sediments below the surface are distinctly bedded without deformation. Generally, the contact towards the margin of the chute is marked by an orange-weathering breccia layer bed (Fig. 4.11D). The interval is overlain by a laterally extensive microbial carbonate layer that can be traced laterally beyond the boundaries of the chute (Fig. 4.11A).

Laterally extensive volcaniclastic debris flow deposits, somewhat similar to mass-transport deposits at Douglas Pass, occur in the Upper GRF in the eastern Uinta Basin (Vanden Berg et al., 2013). A laterally extensive chaotic interval is also present within the MOSZ at Sand Wash (Keighley and Vanden Berg, 2013; Törő et al., 2014; Keighley et al., this volume). This interval is up to 10 m thick and hosts deformed sublittoral to profundal deposits showing large-scale recumbent folds and extensive breccia bodies, with meter-scale clasts and tilted rafts of oil shale on its top.

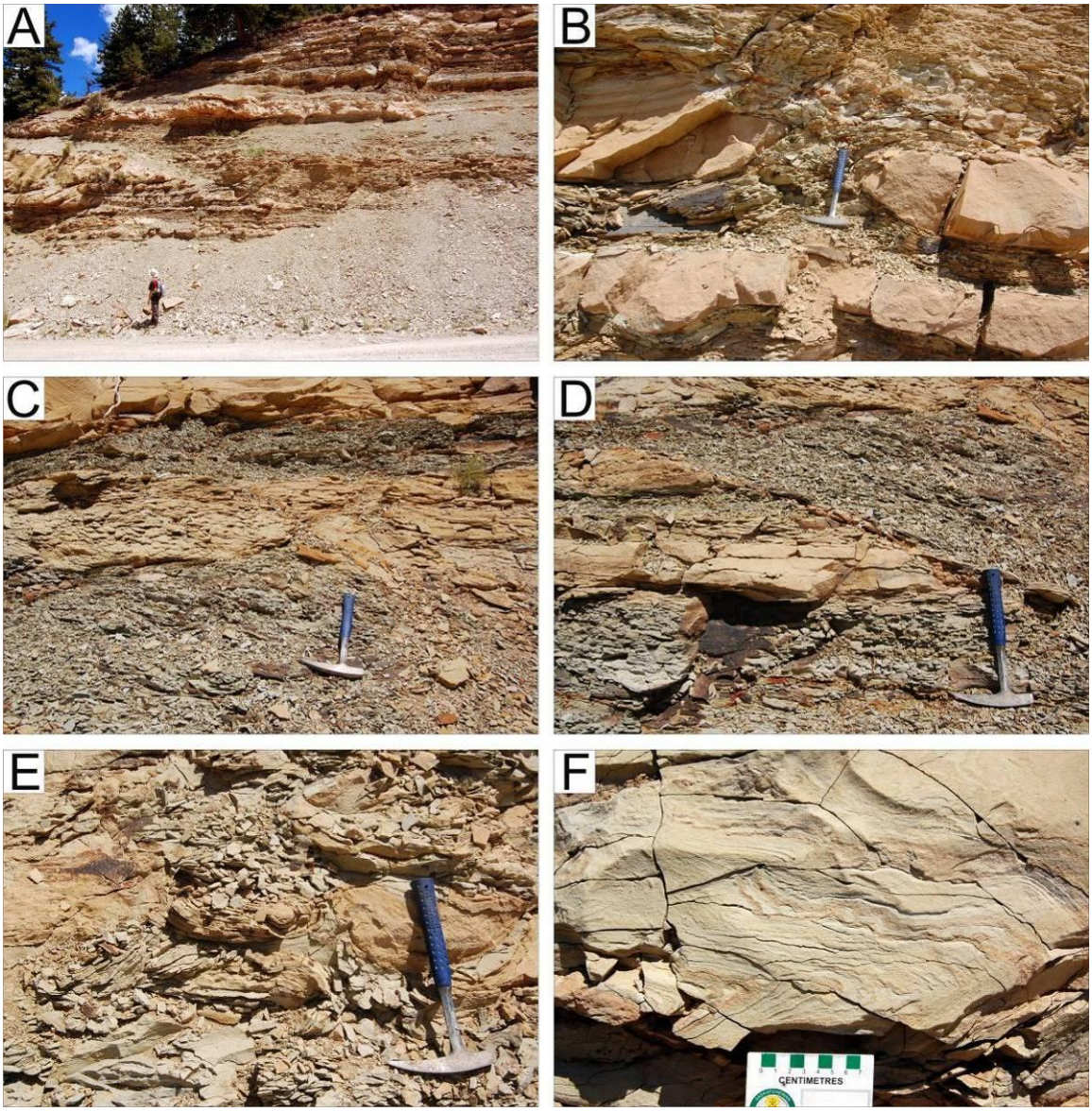


**Figure 4.11** Mass-transport deposit at Douglas Pass (CO). A. Interbedded distributary channel sandstone and lacustrine mudstone cut by sharp erosion surface, overlain by structureless silty mudstone containing sandstone and mudstone blocks The lower ~3 m of the chute is a chaotic mixture of pebble- and boulder-sized sandstone, siltstone and carbonate mudstone clasts with mud-rich matrix. This interval is overlain by ~5 m thick interbedded undeformed massive or laminated mudstone and siltstone showing gentle folding and thinning towards the margins (left); B. Close-up of erosion surface in A showing gently folded sandstone bed overlain by silty mudstone with sandstone block ~40 cm in size (right) and truncated bed (left); mudstone fills the fissures formed between the intact bed and the detached block and the muddy matrix is plastically deformed and bent around the clasts; C. Large sandstone block showing internal folding; D. Interbedded massive mudstone and sandstone cut by a sharp planar erosion surface overlain by massive mudstone containing sandstone blocks. The surface is underlain by a discontinuous layer of orange-colored breccia, containing mudstone and sandstone fragments; E. Ball-and-pillow structures in sandstone blocks within a mud-rich matrix; F. Sandy mudstone block with internal folding.

4.5.6.2 Deformation Mechanism

Mass-transport deposits are formed by transitional mass-flow processes, including slumps, slides, debris flows, grain flows, and turbidites (Nemec, 1990; Mulder and Cochonat, 1996; Mulder and Alexander, 2001). These deposits are generally characterized by a sharp, erosive base, chaotic infill, and deformation structures at their base or internally, showing both plastic and brittle behaviour.

At Douglas Pass the lower surface of the chute points to a high-energy erosional event. Based on their lithology, the clasts originated from the erosion of the underlying deposits. Soft-sediment deformation of the clasts in the basal, brecciated part of the infill indicates disruption and liquefaction of the semi-cohesive clasts. Other clasts deformed plastically, or remained intact during transportation. The poor sorting and the present of pebble- and boulder-sized deformed clasts, the brecciated infill is interpreted as a subaqueous debris flow deposit, while the laminated carbonate mudstone and siltstone deposits are interpreted as sublittoral deposits, representing subsequent infill of the chute. Thus, the subaqueous channel was formed in a setting with relatively low sedimentation rate.

*4.5.7 Brecciated Oil Shale*

4.5.7.1 Description

Oil shale breccias ("blebby and streaked" oil shales; Bradley, 1931; Dyni and Hawkins, 1981) forming laterally extensive deformed intervals occur in all the subbasins of the GRF, and they are especially common in the Piceance Creek Basin. These intervals are up to 2 m thick and characterized by disrupted, tilted, folded, overturned, and brecciated layers (Fig. 4.12A–F). Fold axes are sub-parallel to stratification (Fig. 4.12E). Folded layers may pass into breccias over distances of a few tens of meters. Breccias consist of pebble-sized intraclasts floating in a massive, organic-rich matrix, which gives them a distinctive appearance on weathered surfaces (Fig. 4.12A–C). Evaporite crystals, their pseudomorphs, or siliciclastic material can be incorporated (Fig. 4.12F). The clasts are aligned parallel to the bounding surfaces of the breccia layers, or randomly distributed. Grading is not apparent. Some intraclasts show plastic or brittle deformation such as irregular folds and microfaults (Fig. 4.12D). The brecciated layers are over- and underlain by undeformed oil shale. Their base is usually sharp and along the bedding surface.

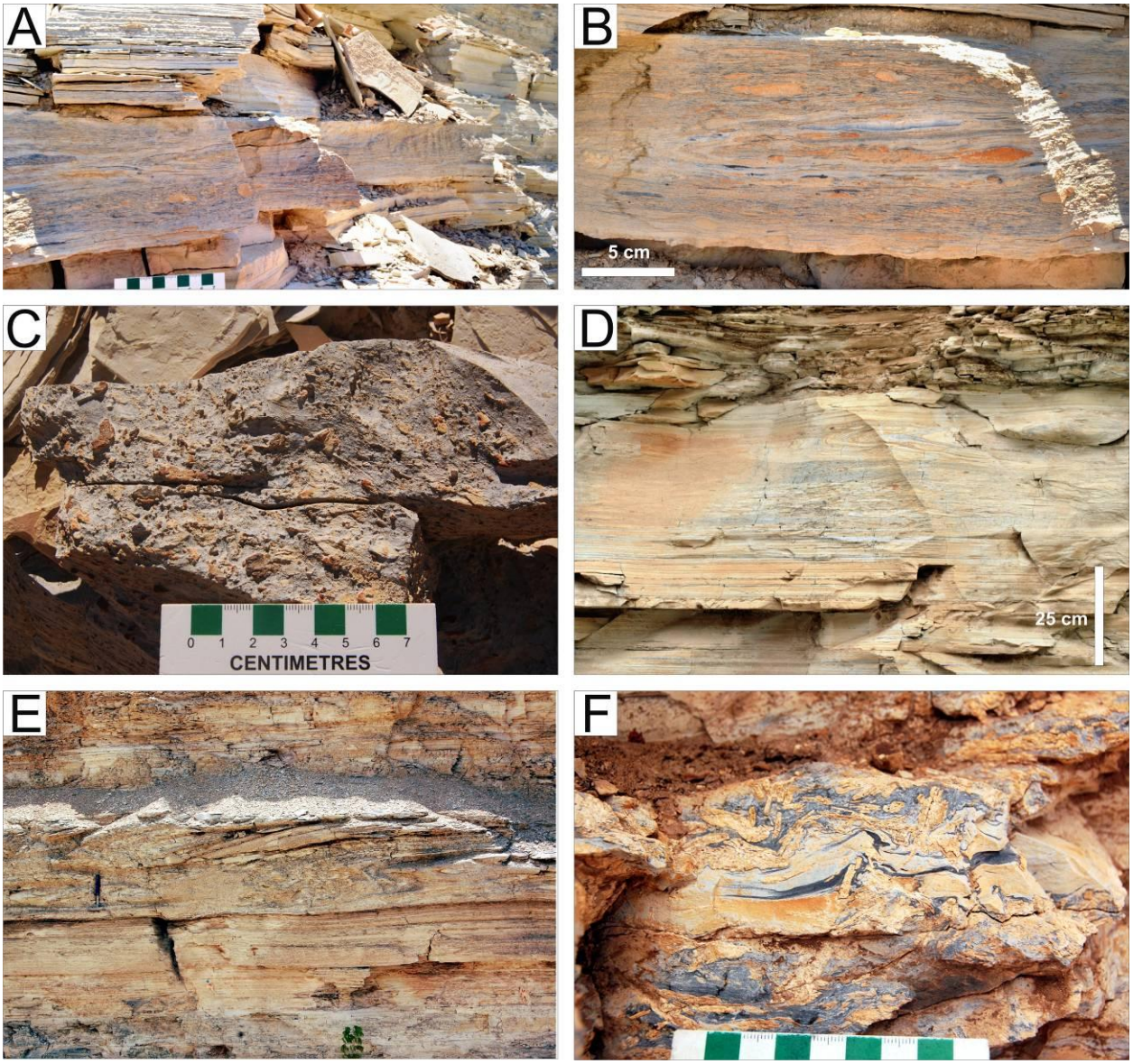


**Figure 4.12** A–D. Brecciated oil shale (MOSZ, Hells Hole Canyon, UT). A. Tabular breccia bed; B. Breccia bed with recumbent-folded middle part; C. Weathered surface showing carbonate mudstone clasts; D. Breccia bed with a recumbent-folded intraclast at top; E. Recumbent-folded oil shale (MOSZ, Piceance Creek Basin, CO) (hammer for scale); F. Folded oil shale with evaporite pseudomorphs (R8 zone, Piceance Creek Basin, CO).

#### 4.5.7.2 Deformation Mechanism

Folding and brecciation in oil shale intervals have been previously noted in the Uinta and Piceance Creek basins by Bradley (1931), Picard and High (1972), Dyni and Hawkins (1981), Johnson (1981), Grabowski and Pevear (1985), Borer and McPherson (1998), Johnson et al. (2010b), Birgenheier and Vanden Berg (2011), and Tänavsuu-Milkeviciene and Sarg (2012).

Most commonly they were interpreted as the result of mass-transport deposits of gel-like organic ooze. Alternatively, the monomict nature of most oil shale breccias and the uniformity of style of deformation may indicate that the intraclasts formed by the disruption of quasi-in situ material, with little if any lateral translation (Törő and Pratt, in press). Carbonate-rich intraclasts floating in a massive matrix indicate that disruption took place in rheologically heterogeneous sediment, where the behavior of individual layers was primarily controlled by organic content. After disruption, the intraclasts of stiffer, partly cemented, organic-poor carbonate were incorporated into an organic-rich matrix.

Organic-rich deposits are thought to have high initial stability (Smoot, 1983; Grimm and Orange, 1997), where high carbonate content and early diagenetic processes increase their cohesiveness. As a result, intraclastic breccias in oil shale deposits indicate the breakage, shearing and sliding of thixotropic sediments due to stresses that exceeded a certain threshold. The flat base of the deformed intervals implies that disruption and transportation happened along well-defined surfaces that most likely marked rheological boundaries. In situ disruption and short distance transport could also explain the gradational boundaries of some these units (cf. Tänavsuu-Milkeviciene and Sarg, 2012).

### *4.5.8 Sedimentary Dikes*

The term ‘sedimentary dike’ is used here to describe centimeter- to meter-scale cracks or fissures filled with sediment that differs in lithology from their host, irrespective of the infilling sediment and its source, or the process of formation. Similar features have been called clastic or sandstone dikes or dikelets, although they may be filled with clay, silt, or carbonate mud (e.g., Montenat et al., 2007). The term ‘mudcrack’ has been used extensively to describe not only polygonal cracks exhibiting a wide variety in size, morphology, and infill, but also linear or spindle-shaped cracks formed in littoral to profundal deposits of the GRF (e.g., Bradley, 1930, 1931, 1964; Picard, 1966; Surdam and Stanley, 1979; Smoot, 1983). Although mudcracks are generally taken as evidence of subaerial exposure, the host facies, morphology, mode of preservation (positive epirelief, positive hyporelief, or negative epirelief), and the characteristics of their infill suggest other processes of origin. Sedimentary dikes or cracks are one of the most common deformation features in the GRF, in various lithologies deposited in littoral to profundal settings.

4.5.8.1 Type 1 – Spindle-shaped, sinuous, and linear cracks

**Description:** Short (<5 cm) downward- or upward-tapering dikes are common in intervals of laminated or thinly bedded siltstone and sandstone (Figs. 4.13A–H, 4.14A–H), and may occur on bedding planes in groups, radiating from a single point (Fig. 4.13A, C, G) or singly, in large numbers (Figs. 4.13B, D–F, H, 4.14G). Most commonly they form 0.1–1 cm high ridges preserved in positive hyporelief at the base of the beds, or, less commonly, in positive epirelief on bed tops. In plan view, they show a wide variety of morphologies, including straight, curved, sigmoidal, and sinusoidal lenses or lines. Locally their orientation appears related to primary sedimentary structures such as ripples (Figs. 4.13D, 4.14B). There are also many cases where dikes are grouped into two or three distinct populations based on their size or morphology on a single surface. Despite the large variety, patterns are fairly uniform on individual surfaces.

Where visible, in cross-sectional view the dikes are up to 1 cm long, 0.5 cm wide, and either parallel-sided, lenticular, V-shaped, bulbous, or a combination of these (Fig. 4.14E, F, H). Arrays of them are often highly contorted by folding, shingling, tilting, and smearing (Fig. 4.14E, F, H), and within a single interval dikes may show various morphologies and degrees or direction of distortion. Dikes are usually connected either above or below to silt- or sand-rich layers and penetrate into the intercalated finer-grained layers (Fig. 4.14A, C, D, E, F), and some follow planes of microfaults (Fig. 4.14H). Occasionally, on two-dimensional surfaces the dikes are detached from coarser-grained layers or lenses, and ‘float’ in a muddy matrix (Fig. 4.14F, H). Sometimes they enter into the under- or overlying layers with similar composition without a visible mud layer between them. Thus, when dikes are preserved on bedding surfaces, dikes originated either from the host bed or the overlying bed.

The infill of the dikes is usually structureless or internally churned showing mixing of the sediment and lacking vertical or horizontal lamination. Host sediments commonly show folding, loading, microfaults, or homogenization with obliterated original lamination (Fig. 4.14E, F, H) and the thickness of the source intervals is irregular (Fig. 4.14E, H). At any given stratigraphic interval the dikes are pervasive and can be found at the base or top of each laminae or bed (Fig. 4.14A, C). By contrast, dike-bearing layers alternate with those lacking dikes.

Type 1 sedimentary dikes are common across the basin in all thin-bedded lithologies, but they are particularly abundant in: (1) sublittoral lenticular- or wavy-laminated calcareous siltstone, in the MOSZ at Willow Creek, Gate Canyon, North Franks Canyon, in the upper

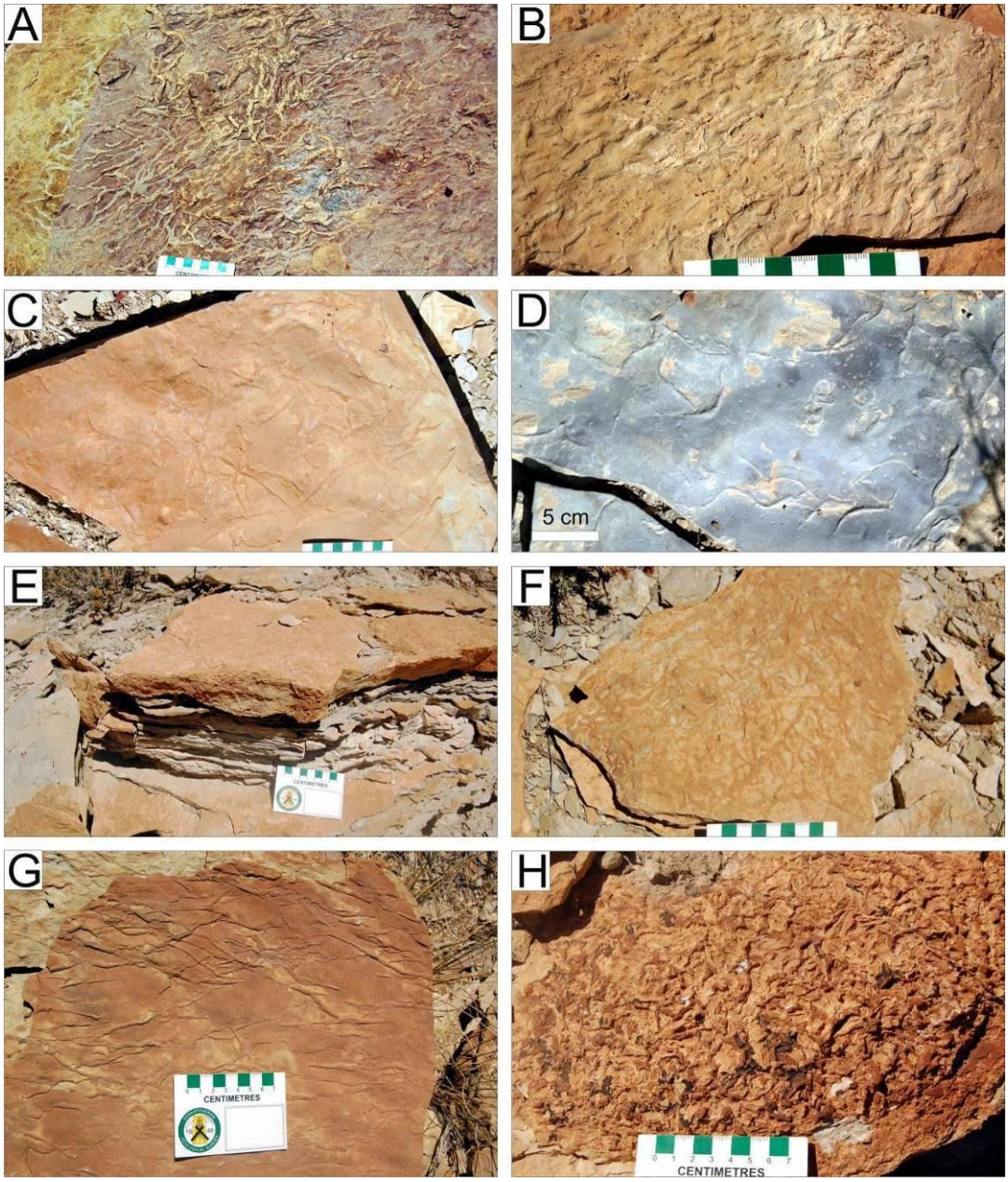


**Figure 4.13** Type 1 sedimentary dikes. A. Oriented, partly connected spindle-shaped cracks on base of wave-ripple cross-laminated deltaic sandstone forming incomplete rectangular or polygonal patterns (lower member, Willow Creek, UT); B. Dense population of crudely oriented, isolated spindle-shaped cracks on base of sandstone bed (Horse Bench Sandstone, Nine Mile Canyon, UT); C. Party interconnected, straight to curvilinear and radial cracks on top of bed (Horse Bench Sandstone, Nine Mile Canyon, UT); D. Base of siltstone bed with impressions of curvilinear cracks in ripple troughs in underlying sandstone; this pattern resembles the pseudofossil *Manchuriophycus* (upper member, Gate Canyon, UT); E, F. Densely cracked silty carbonate mudstone bed in cross section (E) and in plan view on base of bed (F) (Horse Bench Sandstone, Nine Mile Canyon, UT); G. Party interconnected, oriented linear cracks on top of sandstone bed (Horse Bench Sandstone, Nine Mile Canyon, UT); H. Dense population of non-oriented cracks on top of carbonate mudstone bed (Horse Bench Sandstone, Nine Mile Canyon, UT).

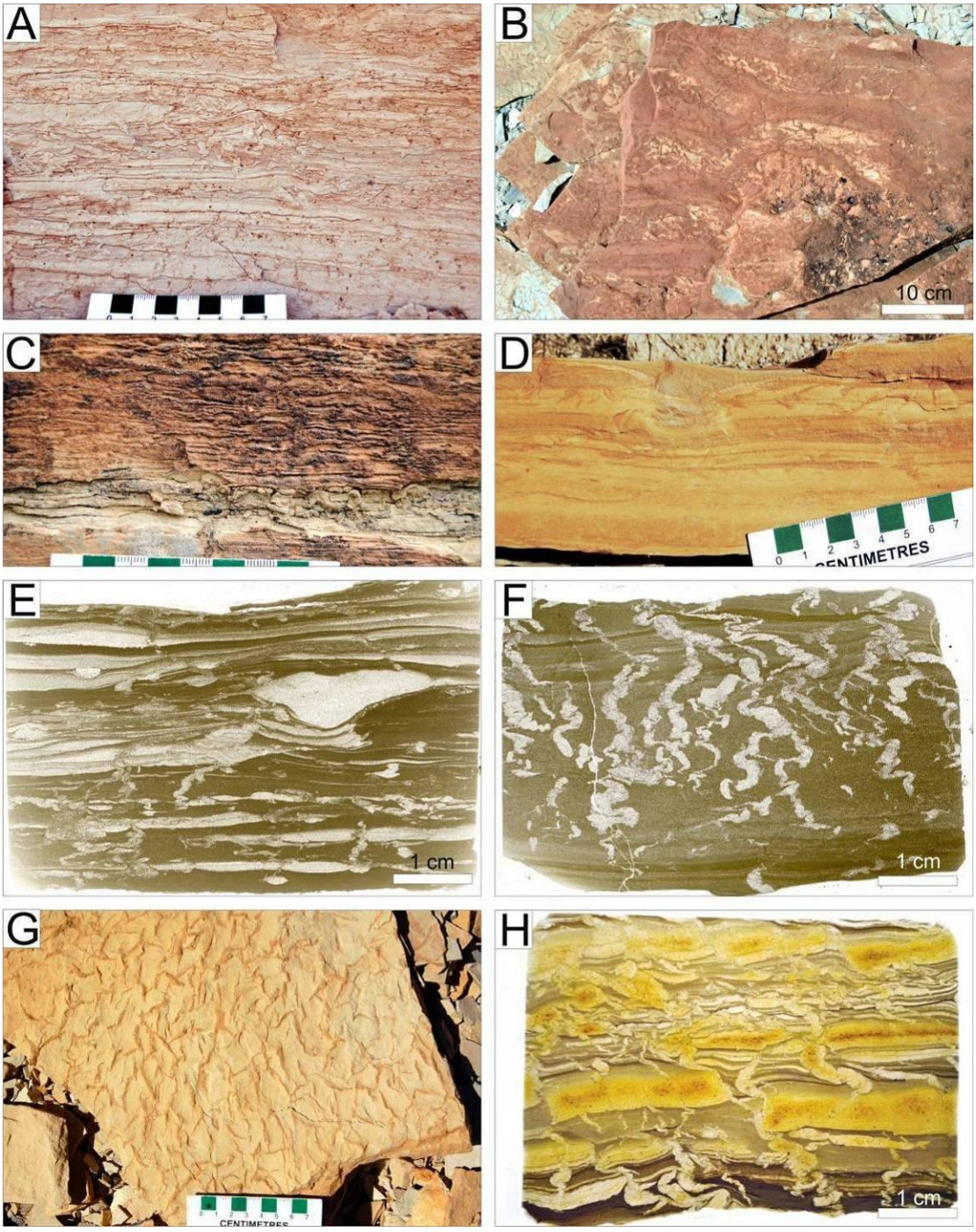


**Figure 4.14** Type 1 sedimentary dikes. A. Abundant dikes in wavy- and lenticular-laminated calcareous sandstone (MOSZ, Gate Canyon, UT); B. Oriented cracks in carbonate mudstone drapes in wave-ripple troughs of cross-laminated sandstone (S2 marker, North Franks Canyon, UT); C. Abundant dikes in wavy- and lenticular-laminated calcareous siltstone (middle member, North Franks Canyon, UT); D. Load structure (top) in lenticular-laminated siltstone containing sparse sedimentary dikes (upper member, Nine Mile Canyon, UT); E. Dikes filled with silt and fine sand in lenticular laminated carbonate mudstone (upper member, Nine Mile Canyon, UT); F. Dikes filled with carbonate silt, 'floating' in structureless carbonate mudstone penetrating numerous laminae (Piceance Creek Basin,

CO). G, H. Top of calcareous siltstone bed (G) showing oriented, partly interconnected, spindle-shaped cracks forming locally a triradiate pattern, which are abundant sedimentary dikes tilted in opposing directions in cross-section (H) showing lateral projections forming sills, with microfaulted laminae (R5 zone, Douglas Pass, CO). E, F and H are thin section views cut perpendicular to bedding.

member at the Nine Mile Canyon area, and at Douglas Pass (cf. Remy, 1992; Keighley, 2013); (2) carbonate grainstone deposits (middle member, Nine Mile Canyon area); (3) cross-laminated or cross-bedded shoreline deposits of the upper member especially the Horse Bench Sandstone in the Nine Mile Canyon area (cf. Remy, 1992) and in delta mouthbar sandstones at Willow Creek.

Similar features have been previously reported from the GRF as: (1) "mudcracks" (Bradley, 1930; Smoot, 1983); (2) "shrinkage cracks" (Picard, 1966); (3) "synaeresis cracks" (Remy, 1992); and (4) "dewatering structures" (Tänavsuu-Milkeviciene and Sarg, 2012). Type 1 sedimentary dikes also have similar geometries to the ones formed at the base of tuff layers (see 'Type 5 sedimentary dikes' below).

**Deformation mechanism:** The deformed and structureless infill, along with the isolated cracks, indicates that dike fills resulted from the remobilization and injection of liquidized granular material. In the case of dikes that occur in sublittoral deposits, upward emplacement, if present, together with the lack of scouring features by erosive lake-floor processes, indicate an intrastratal origin, which requires elevated pressure (e.g., Hempton and Dewey, 1983; Scott and Price, 1988; Obermeier, 1996; Alfaro et al., 1997; Pratt, 1998a, b; Rodríguez-Pascua et al., 2000; Berra and Felletti, 2011). In addition, the plastic or brittle deformation of the host interval, the complete disruption or homogenization of the lamination, and the dikes penetrating microfaults further indicate liquefaction and elevated stresses within the sediment layers. These features show that cracking and dike formation along multiple horizons happened simultaneously in these cases, rather than during the deposition of individual laminae or beds.

#### 4.5.8.2 Type 2 – Downward tapering dikes with massive or brecciated infill

**Description:** Type 2 sedimentary dikes are 0.1–2 m long and up to 25 cm wide with an overall parallel-sided or V-shaped geometry. In general, the infilling lithology of the dikes depends on the depositional setting of the host strata. Sand-filled dikes present at the base of structureless or cross-bedded medium-grained sandstone units at Willow Creek which may be

delta mouthbar deposits (Fig. 4.15B). These dikes are spaced 20–40 cm apart within a single interval and the infill is massive, without any horizontal or vertical bedding.

Sublittoral intercalated carbonate mudstone and calcareous siltstone units of the MOSZ host sedimentary dikes filled with structureless silt and sand and angular mudstone clasts (Fig. 4.15C–G). These dikes occur in the middle to upper interval of a coarsening- (and shallowing) upward unit. In cross-sectional view the dikes are vertical to sub-vertical features and penetrate downwards from multiple horizons of structureless silt intervals with rip-up clasts of laminated or massive mudstones. The dikes show irregular widening and narrowing (Fig. 4.15D, E), and individual dikes may break up into multiple swarms forming a dense network, with the brecciation of the host strata (Fig. 4.15C, D, E, F). Towards their top, mudstone laminae show folding and fragmentation, with laminae projecting upwards (Fig. 4.15D). In plan view, dikes are linear and oriented, showing ragged and bifurcating paths (Fig. 4.15G). Both in cross-section and plan view, the dikes have a prominent, sharp and even boundary towards the host sediment. Based on their infill and source interval, multiple dyke generations can be identified within a single interval.

Dikes in sublittoral to profundal laminated mudstone deposits with variable organic content are filled either with calcareous fine-sand and silt (Figs. 4.15A, 4.17A), grainstone (Fig. 4.16A–E), or carbonate mud with variable amount of silt (Figs. 4.16E, 4.17A–D). When a source interval can be ascertained, dikes taper downwards from a coarse-grained interbed with irregular thickness and they cut into underlying deposits (Figs. 4.16A–E, 4.18B). Otherwise, the dikes are isolated and either parallel-sided (Fig. 4.17A–D) or bulbous (Fig. 4.18A). In both cases, they are commonly tilted and folded (Figs. 4.15A, 4.16A–D, 4.17B–D, 4.18A, B, F, H), with lateral projections locally (Fig. 4.18B, C). Dikes within a single interval show a different degree and direction of folding and tilting (Fig. 4.16D, C). Where visible, they form linear or anastomosing patterns in plan view (Fig. 4.18C, G). The infill of the dikes is massive.

Sedimentary dikes at the base of ostracode, ooid, and intraclastic grainstone beds, commonly underlying stromatolites, are filled with material from above, but the infill is generally finer grained or has a muddy matrix (Fig. 4.16A–E). Mud-filled dikes in oil shale are commonly isolated (Fig. 4.18A, B) and commonly pass downwards and sideways into subtle narrow cracks (Fig. 4.18B–D). The original lamination of the host rock is frequently disrupted and folded in the vicinity of these dikes (Fig. 4.18B, E).

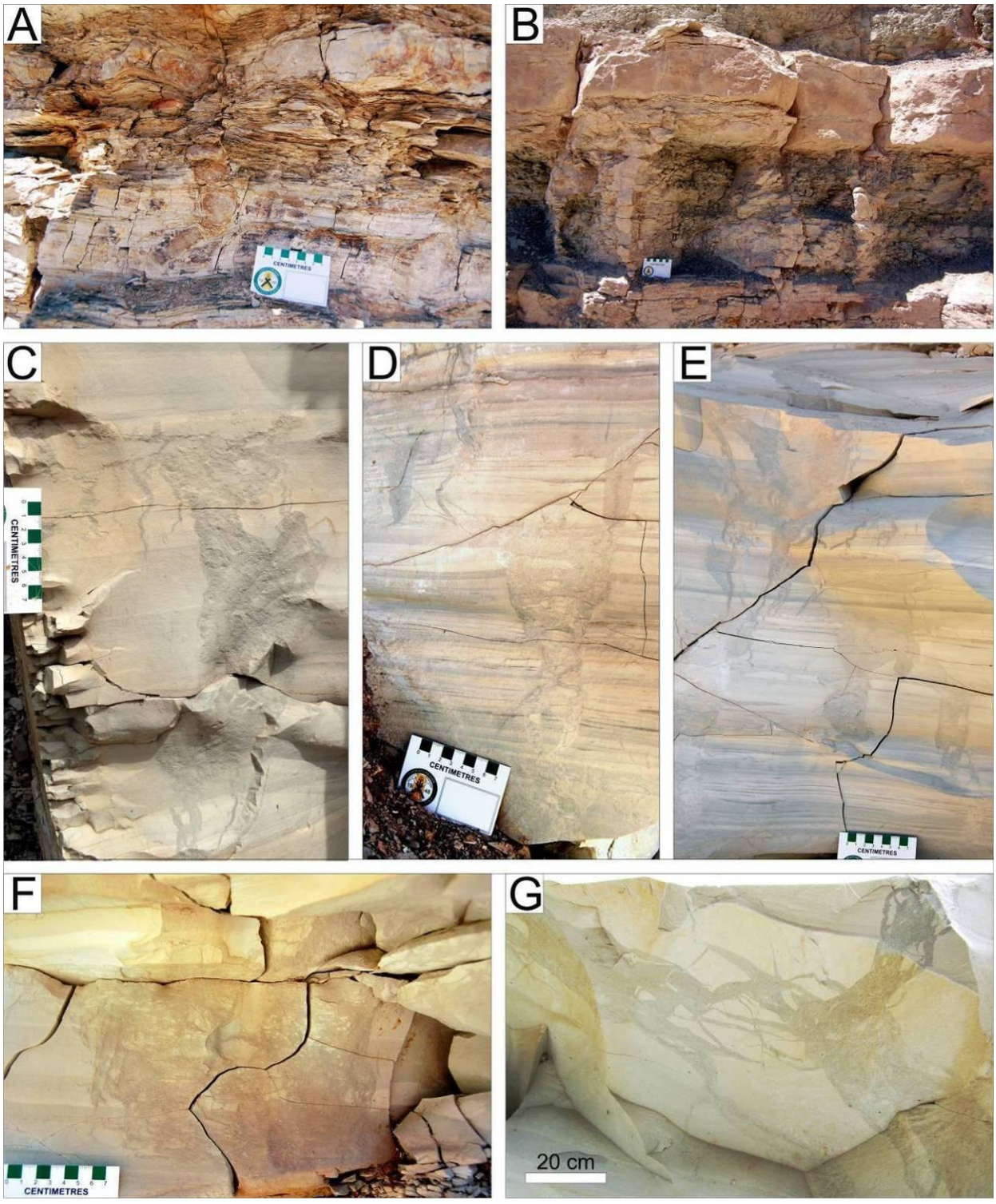


**Figure 4.15** Type 2 Sedimentary dikes (Willow Creek, UT). A. Sand-filled dike in organic-rich mudstone (lower member); B. Straight sand-filled dikes with sharp walls at base of structureless deltaic sandstone penetrating into massive or laminated green calcareous mudstone (delta facies); C–G. Downward-tapering silt- and breccia-filled dikes in wavy- to lenticular-laminated silty carbonate mudstone (MOSZ). C–F are views perpendicular to bedding, and G is surface developed parallel to bedding.

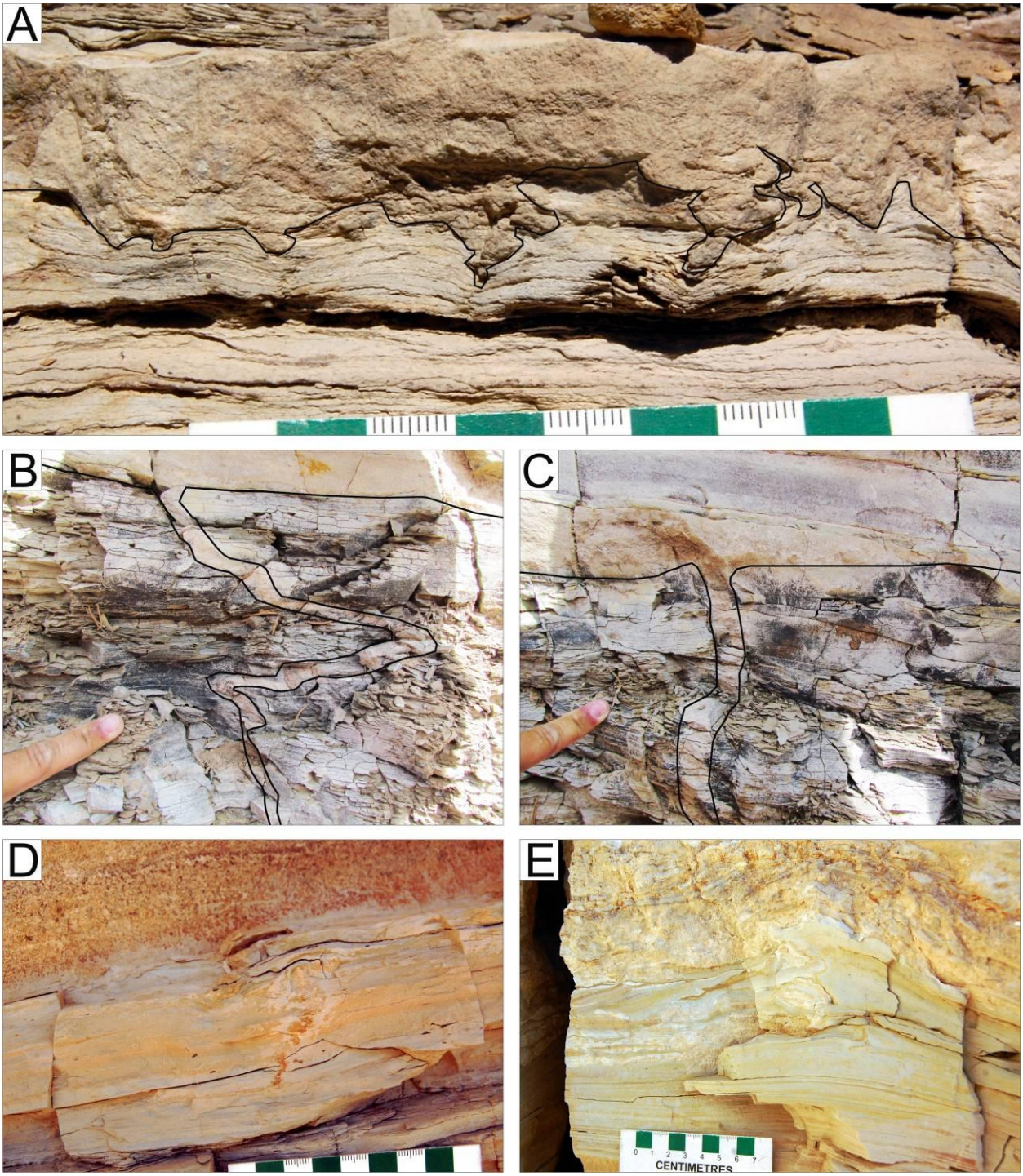


**Figure 4.16** Type 2 sedimentary dikes. A. Folded dikes (outlined by black line) filled with ostracode grainstone (lower member, Willow Creek, UT); B, C. Folded (B) and straight (C) dikes (outlined by black line) at base of ooid–ostracode grainstone bed in organic-rich mudstone (first lacustrine tongue, Nine Mile Canyon, UT); D. Folded dikes filled with ostracode grainstone in laminated carbonate mudstone (R4 zone, Evacuation Creek, UT); E. Folded dike filled with silty carbonate mud at base of intraclastic conglomerate bed underlain by laminated carbonate mudstone and capped by microbial carbonate (R5 zone, Douglas Pass, CO).

Dikes, similar to the ones described here, were previously identified in the GRF by Törő and Pratt (in press) in the Fossil Basin, and as "dewatering structures" by Birgenheier and Vanden Berg (2011) in the Uinta Basin and by Tänavsuu-Milkeviciene and Sarg (2012) in the Piceance Creek Basin. Remy (1992) described up to 4 cm wide and 10 cm long sedimentary dikes filled with ostracode grainstone as "mudcracks" in the carbonate marker unit. Large-scale sand-filled dikes are also common features in the oil shales of the upper Parachute Creek Member in the Piceance Creek Basin, and have been ascribed to liquefaction by Gulliver (2006).

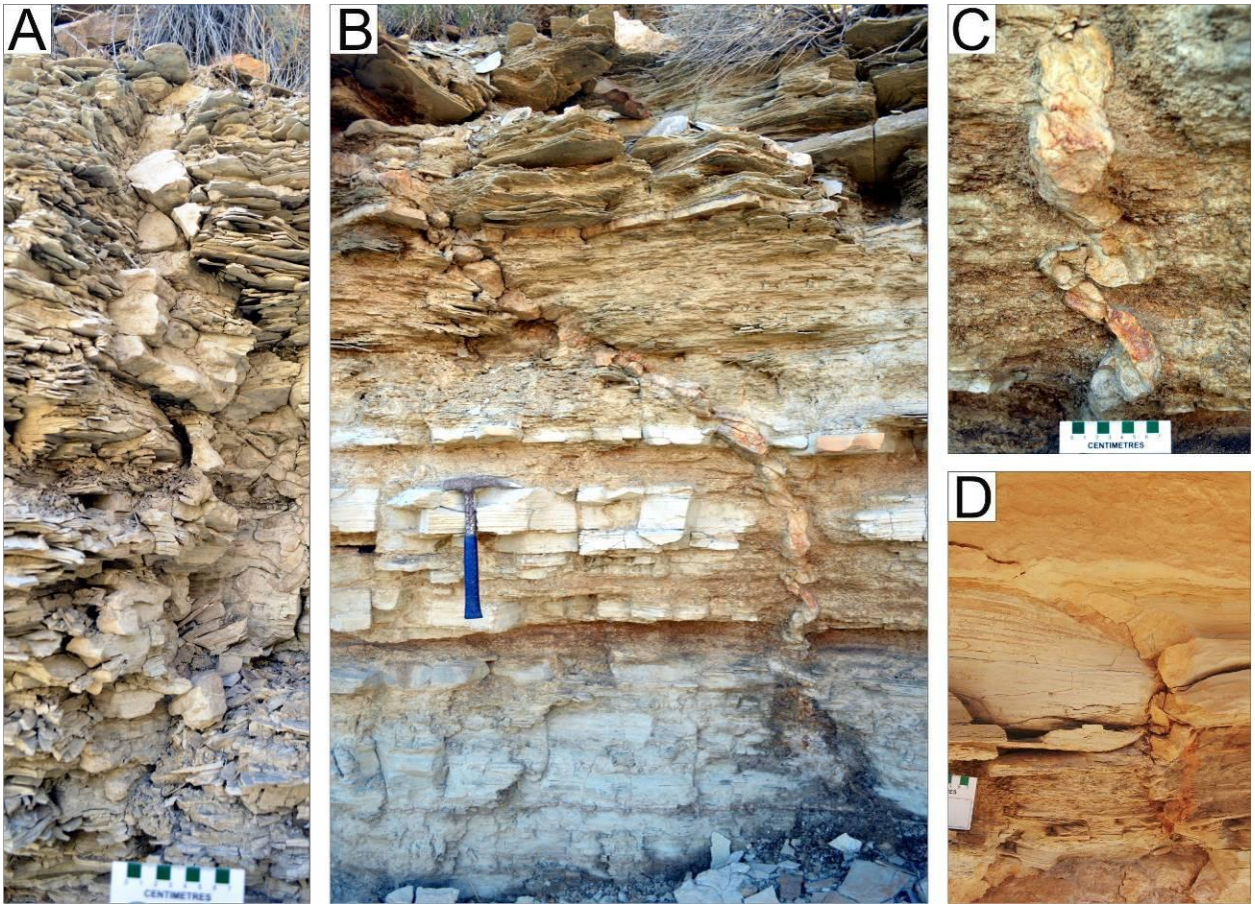


**Figure 4.17** Type 2 sedimentary dikes. A. Sand-filled dike in laminated carbonate mudstone (MOSZ, Gate Canyon, UT). B, C. Silty mud-filled dike in laminated carbonate mudstone (Birds Nest Zone, Bitter Creek, UT); D. Carbonate mud-filled dike in laminated carbonate mudstone (R4 zone, Evacuation Creek, UT).

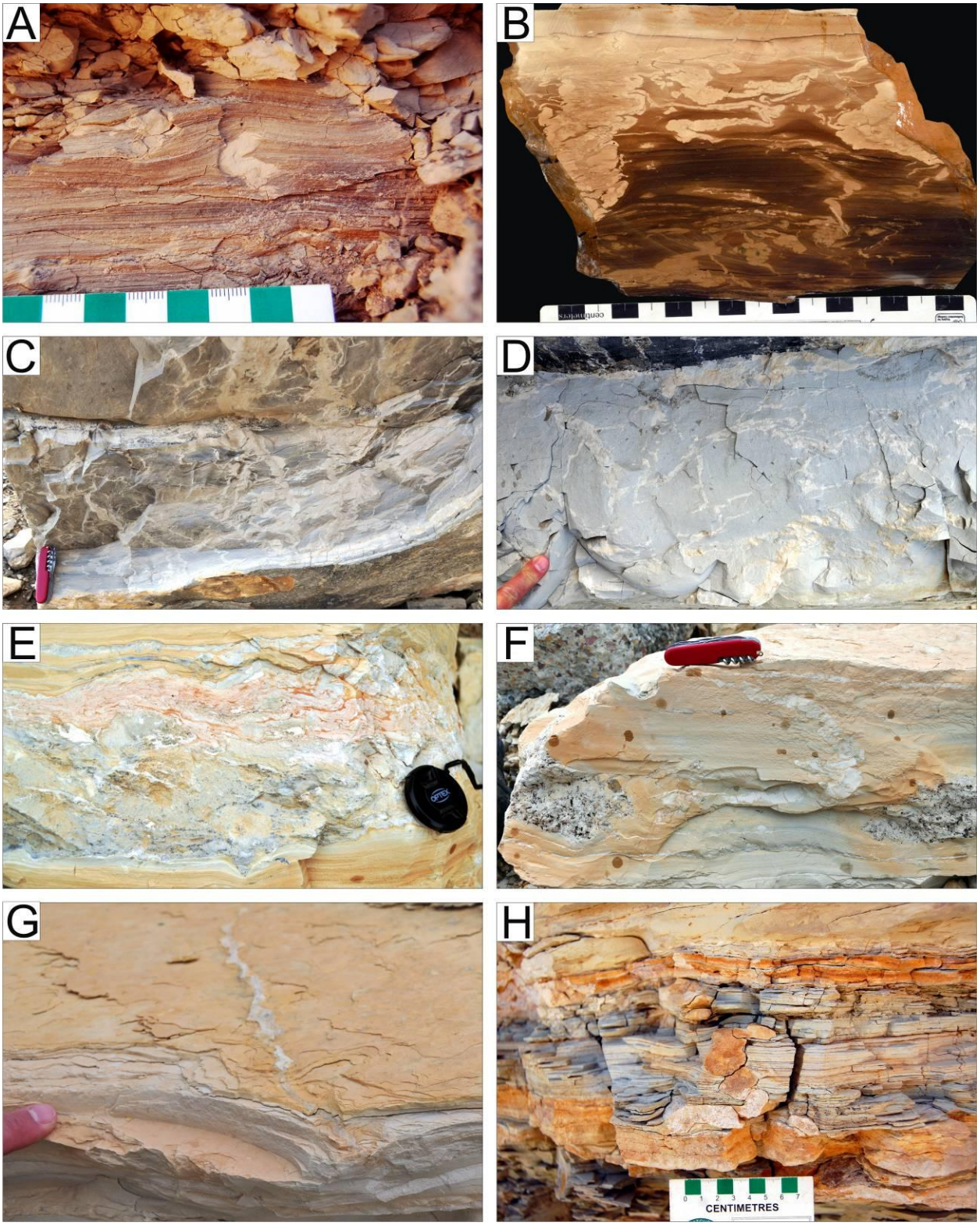


**Figure 4.18** Type 2 sedimentary dikes. A, B. Bulbous carbonate mud-filled dikes in oil shale in outcrop (A) and slabbed surface (B) showing narrow sinuous or zigzag patterns (MOSZ, Willow Creek Canyon, UT); C, D. Oriented, partly interconnected carbonate mud-filled dikes in oil shale viewed oblique (C) and perpendicular (D) to bedding

(black shale facies, Willow Creek, UT); E–G. Carbonate mud-filled dikes in oil shale (Birds Nest Zone, Evacuation Creek, UT). E. Dense population of dikes within disrupted zone; F. Folded and brecciated carbonate mud-filled dike adjacent to evaporite (nahcolite) pseudomorphs; G. Oblique view of carbonate mud-filled dike showing linear orientation in plan view; H. Folded carbonate mud-filled dike in laminated silty carbonate mudstone (R5 zone, Douglas Pass, CO).

**Deformation mechanism:** Sedimentary dikes and sills generally form by dewatering, fluidization and injection of granular material at elevated pore pressure leading to the formation of *upward*-propagating dikes (e.g., Obermeier, 1996; Hurst et al., 2003, 2011). Dike arrays in the GRF, however, are usually downward-tapering features, indicating *downward* propagation. Although the infill and the morphology of the dikes can vary, and the dikes can be either attached to a source layer or isolated, they show several common characteristics. Lamination of the host sediments usually is not, or only slightly, deformed, which indicates significant rheological contrast between the host rock and the infill at the time of deformation. The formation of sharp walls also indicates brittle failure and fracturing of the semi-cohesive or cohesive host sediment. The rheological difference is further indicated by changes in the thickness, orientation, and tilting of the dikes at rheological heterogeneities related to different grain size, organic content, and diagenetic state within the host interval.

The dense network of dikes and associated brecciation of the host deposits, the common sideway protrusions (sills), and the structureless nature of the sedimentary fill together indicate short-lived elevated stresses and forceful injection of the remobilized sediments into fractures (e.g., Daley, 1971; Owen, 1987). Multiple dike generations indicate multiple, closely spaced events of dike formation, while at other locations single horizons hosting sedimentary dikes indicate single events. Coarser-grained source layers can be interpreted as either thin lacustrine turbidites or thin carbonate shoal deposits (Tänavsuu-Milkeviciene and Sarg, 2012). When dikes are sourced from structureless mudstone intervals within laminated oil shales, those can indicate either an interval of shallow-water deposition, rapid precipitation events of carbonate mud (Buchheim and Eugster, 1998), or seiche deposits (Kastens and Cita, 1981; Chapron et al., 1999). Folding of the dikes and the bending of the lamination around them can be related to post-emplacement compaction during burial (e.g., Shelton, 1962; Tanner, 1998; Parize et al., 2007) or loss of volume of the host sediment and distortion during the emplacement of the fluidized

sediment (Pratt, 1998a, b, 1999). As neighboring dikes show various morphologies and folding in different directions, both factors might have contributed to their final morphology.

Where dikes are hosted by sublittoral to profundal deposits, the lack of erosional features related to lake-floor processes and the massive appearance and irregular thickness of the overlying source layers indicate liquefaction of the source interval and injection at shallow burial depth. These sedimentary dikes formed by cracking and intrastratal shrinkage of the host strata and concomitant injection into fissures formed by fracturing (Pratt, 1998a; Jolly and Lonergan, 2002). This resulted in the formation of oriented sedimentary dikes filled with structureless sediment and confined to specific intervals. Isolated dikes filled with carbonate mud might have related to the remobilization and segregation of lime mud from the surrounding sediment in the same manner as molar-tooth structure (Pratt, 1998b, 1999, 2011). In cases, where a source layer is not present, dikes may have formed by lateral flow (Rodríguez-Pascua et al., 2000) or the whole source layer was remobilized and injected. In littoral sediments that might have been affected by subaerial exposure, dikes need to be distinguished from passively infilled cracks formed by desiccation (cf. Allen, 1987; see Trigger Mechanism).

#### 4.5.8.3 Type 3 – Dikes filled with evaporites

**Description:** Fractures filled with evaporites or their calcite pseudomorphs are present at the Bitter Creek, Evacuation Creek, and Hells Hole Canyon areas and they are abundant in the Birds Nest Zone within the R8 zone of the upper Parachute Creek Member (Fig. 4.19A–D) (Birgenheier and Vanden Berg, 2011; Vanden Berg et al., 2013). These dikes are hosted within organic-rich massive or laminated carbonate mudstone. Locally they are associated with small, disseminated evaporite crystals or nodules of various sizes. They either form pervasive polygonal networks (Fig. 4.19A, B) or smaller scale dikes on the bedding surfaces (Fig. 4.19C, D). The dikes are usually quasi-vertical or slightly tilted, with tabular or V-shaped geometry in cross section. Some of the dikes resemble Type 1 or Type 2 sedimentary dikes both in plan view and cross-section, but the infill is represented by coarse sand-sized calcite pseudomorphs, shortite, or nahcolite.

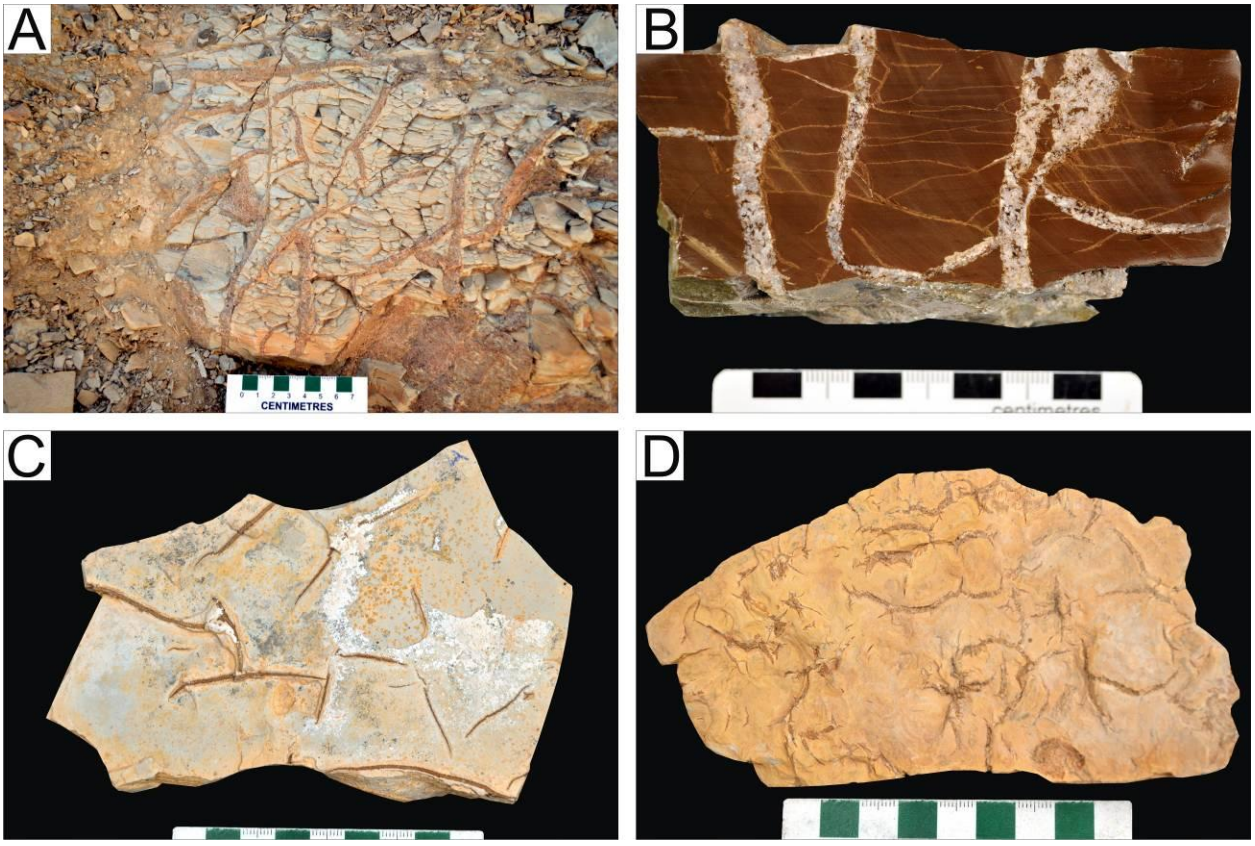


**Figure 4.19** Type 3 sedimentary dikes with sharp and straight or slightly sinuous margins in laminated carbonate mudstone, filled with calcite pseudomorphs after shortite. A, B. Bed top (A) and slabbed surface (B) showing partly interconnected linear cracks/dikes up to 2 cm wide and 50 cm long with sideway projections both in cross-section and plan view (Birds Nest Zone, Bitter, Creek, UT); C, D. Bed tops showing linear to curvilinear spindle-shaped or radiating partly interconnected cracks composed of two or more segments (Birds Nest Zone, Evacuation Creek, UT).

**Deformation mechanism:** Similar, shortite-, trona- and natron-filled fractures have been described from the Wilkins Peak Member of the Bridger Basin (Deardorff and Mannion, 1971; Birnbaum and Radlick, 1982; Leigh, 1991; Dyni et al., 1995; Wiig et al., 1995; Dyni, 1996; Pietras and Carroll, 2006; Jagniecki et al., 2013). Some of these studies attributed the formation of the dikes to overpressure of the pore fluids and hydrofracturing that developed some time after burial, but, in most cases, their origin was not explored in detail.

In the GRF, nahcolite is believed to have been precipitated from saturated brines in unlithified sediments at the lake bottom, forming isolated crystals or radiating crystal aggregates that are now preserved as cavities or nodules partly filled by calcite or nahcolite (Cashion, 1967; Dyni, 1981, 1996). Shortite, on the other hand, was formed post-depositionally in centimeter- to

meter-scale fractured zones within the nahcolite-bearing interval, and later got replaced completely or partly by calcite (e.g., Bradley and Eugster, 1969; Jagniecki et al., 2013). As shortite records lateral migration of Na–$CO_3$-rich brines during burial, the formation of the fractures must be synchronous with this migration. Moreover, precipitation and groundwater movement must have been accompanied by shrinkage of the host strata by dewatering and hydrofracturing to create adequate space for crystal growth.

#### 4.5.8.4 Type 4 – Tuff-filled sedimentary dikes

**Description:** Centimetre-scale dikes are commonly associated with tuff layers interbedded with the fine-grained profundal to sublittoral lacustrine carbonates (Fig. 4.20A–H, 4.21A–F). In plan view, smaller (<1 cm long) downward tapering dikes generally form irregular to slightly oriented networks of single or multiple segmented spindle-shaped dikes, similar to the Type 1 sedimentary dikes (Fig. 4.20A, B, D). The longer (>1 cm) cracks, however, usually show linear and bifurcating paths and characteristic downward tapering with sharp boundaries and sinuosity in cross-section (Figs. 4.20E–H, 4.21F). In other cases the dikes are tilted in variable degrees within a single interval (Fig. 4.20F, H). Some dikes crosscut the lower, coarser-grained part of normal-graded tuff layers, and larger crystals got incorporated into the infill and mixed with finer material (Fig. 4.20H). Upward-protruding dikes at the top of tuff layers are either small, a few millimeters high, forming incomplete polygonal patterns (Fig. 4.20B) or several centimeters long and folded, as well as forming sills within the overlying laminated deposits (Fig. 4.21A, C). The dikes are filled with structureless tuffaceous material from below or above, with variable amounts of carbonate mud and silt (Figs. 4.20E–H, 4.21C, D). Laminae of the host strata are generally disrupted and folded around the dikes. These originate from the upper massive or brecciated part of the source layer.

The undulatory base of many tuff layers resembles load structures (Figs. 4.20C, 4.21C). Tuff layers may also show disruption and brecciation, with centimeter-sized fragments of lacustrine deposits (Fig. 4.20A, E). Cracked tuff layers are usually altered, at least partly, into analcime, while non-altered tuffs do not show dikes at their base or top. In a single succession, however, not all the altered tuffs have dikes at their base or top.

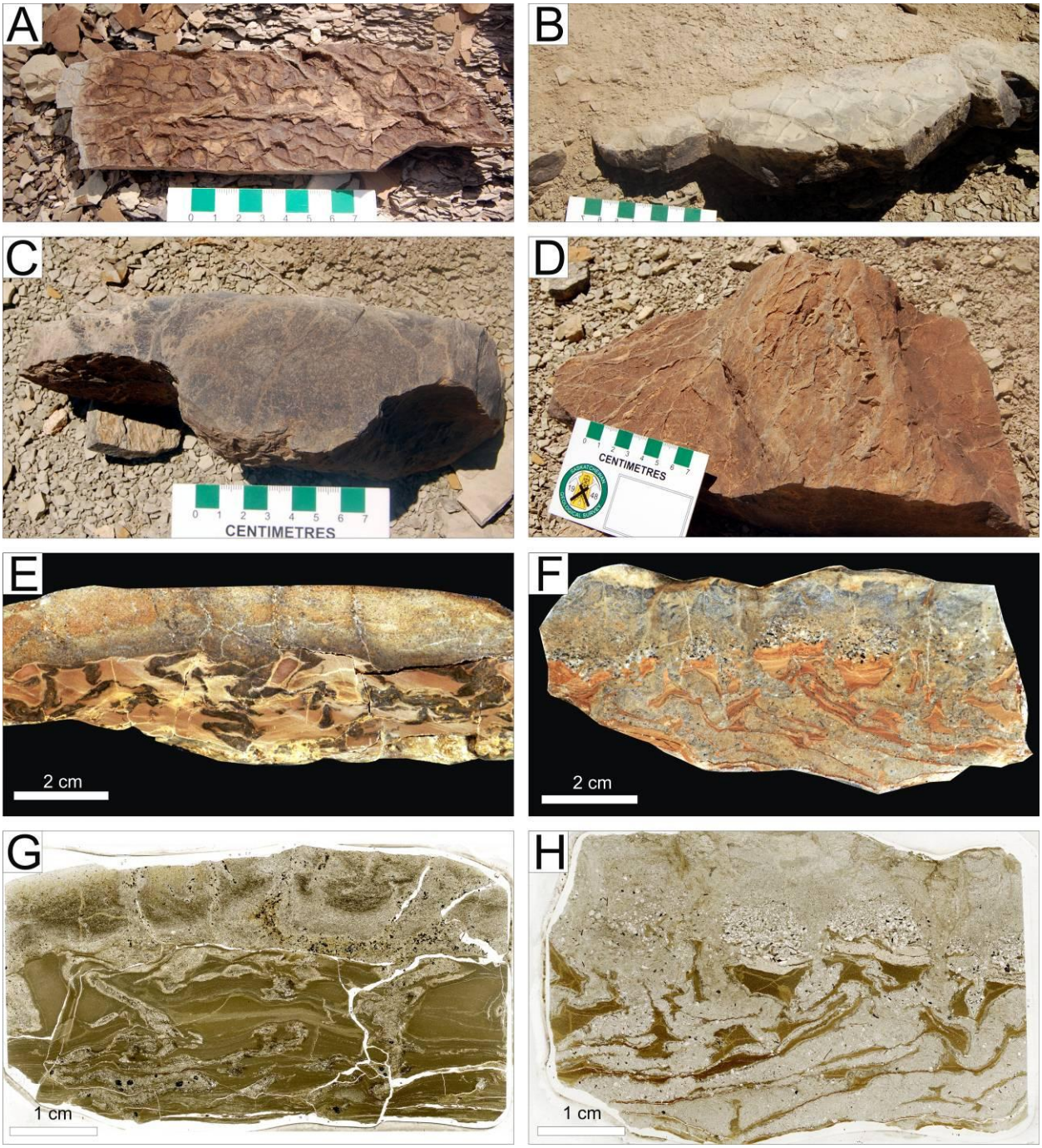


**Figure 4.20** Type 4 sedimentary dikes in tuff layers in laminated carbonate mudstone (upper member, Nine Mile Canyon, UT). A. Interconnected cracks at base of tuff layer; B. Interconnected cracks on top of tuff layer; C, D. Base of a tuff layer showing cross-section of a load structure (C) and bottom of bed (D) showing oriented, partly interconnected spindle-shaped cracks; E, G. Slabbed surface (E) and thin section (G) of cracked tuff layer showing downward tapering, folded dikes up to 4 cm long; F, H. Slabbed surface (F) and thin section (H) of normal-graded tuff layer showing dense network of tilted, folded, and downward-tapering dikes up to 5 cm long sourced from the upper part of the layer.

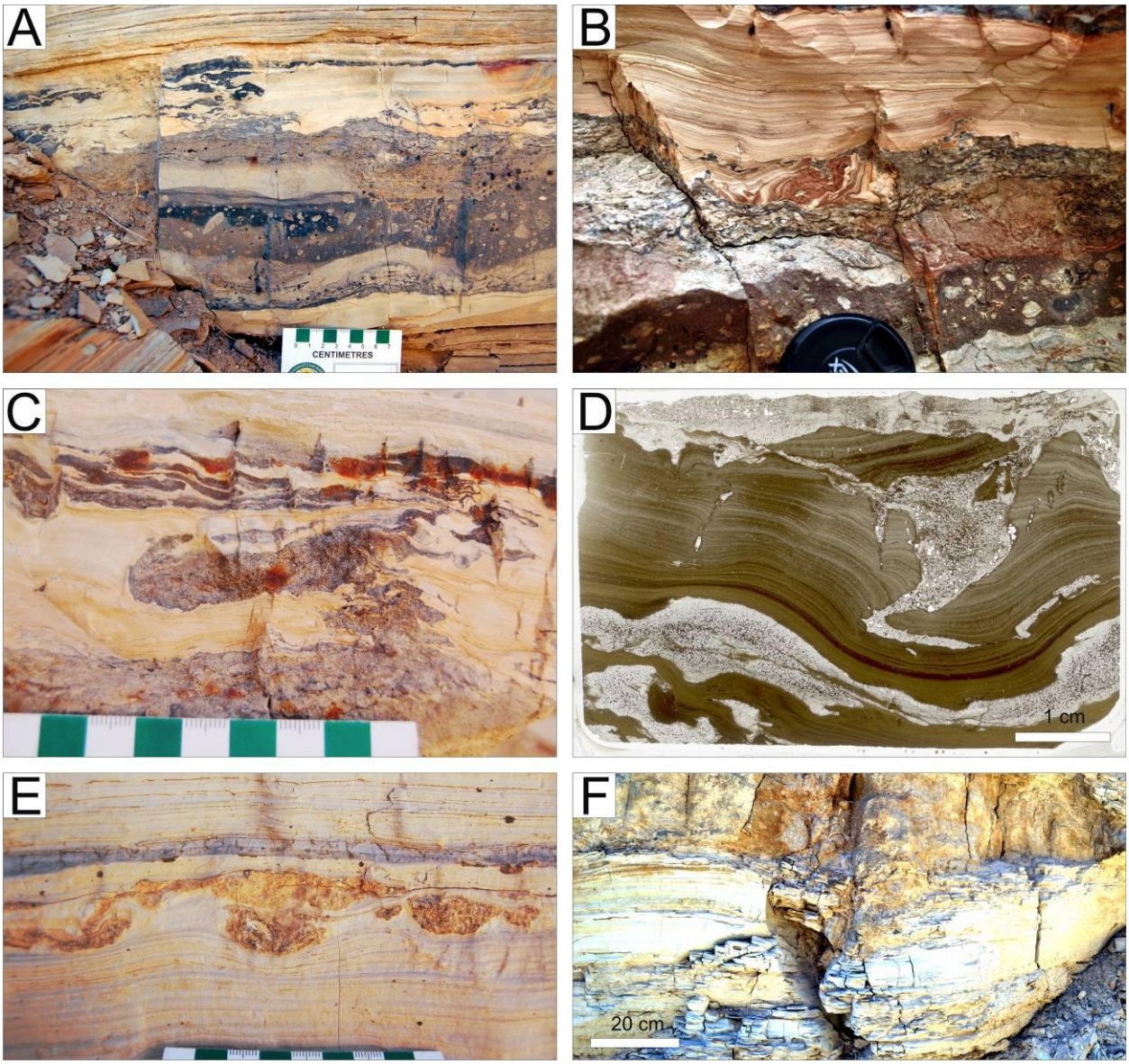


**Figure 4.21** Type 4 sedimentary dikes and related features in tuff layers in oil shale (MOSZ, Hells Hole Canyon, UT). A–C. Thick tuff layer with middle part containing lithic fragments (A), carbonate mudstone intraclasts (B), and dikes and sill at top (C); D. Thin section showing dike and folds; E. Tuff layer showing load structures and dike; F. Dike at base of 25 cm thick tuff layer.

**Deformation mechanism:** Tuff-associated dikes are common features in all the sub-basins of the GRF. Despite their frequent occurrence and the numerous studies on their early diagenetic alteration (Goodwin and Surdam, 1967; Iijima and Hay, 1968; Roehler, 1972; Tank, 1972; Goodwin, 1973; Ratterman and Surdam, 1981), only a few mention these dikes in passing (Cashion, 1967; Griggs, 1968; Surdam and Stanley, 1979; Grabowski and Pevear, 1985). Cashion

(1967) and Griggs (1968) noted injection features related to tuff layers and ascribed them remobilization of a colloidal gel, formed within the tuff during diagenesis (also see Type 5 sedimentary dikes below). Surdam and Stanley (1979) noted "mud cracks" in the Laney Member of the Washakie Basin, Wyoming, where wind-transported ash is thought to have filled desiccation cracks. The massive and distorted appearance of many of the tuff layers in the Piceance Creek and Uinta basins have been previously noted, and generally considered as the result of surface or subsurface remobilization and "plastic flowage" of the tuffaceous material (e.g., Bradley, 1931; Cashion, 1967; Remy, 1992).

The laterally uniform thickness and the normal grading of many of the tuff layers indicate gravitational settling of the tuff material in the water column. Other tuff layers are variable in thickness, with loading or scour features at their base, implying reworking and remobilization by bottom currents, frequently into lenses. The flow structures, the internal deformation within the tuff layers, and the dikes with incorporated phenocrysts indicate that the tuff material originated from the middle to upper portions of the tuff layers and got remobilized as a granular material. Small-scale dikes at the top of some of the tuff layers and the massive appearance of the tuff layers indicate that dikes formed through fluidization of the granular material caused by elevated pore water pressures at shallow burial depths. Thus, injection as a gel can be discounted. The sharp boundaries of these features indicate the brittle failure of the underlying carbonates that had greater rigidity. The variable style of folding and tilting of the dikes indicate that distortion is attributed to the combination of deformation during emplacement and differential compaction afterwards.

Elevated pore pressure in the subsurface has been attributed to active tectonic stress, disequilibrium compaction, hydrocarbon generation, or excess fluids sourced from dewatering caused by chemical or diagenetic alteration in the presence of a sealing lithology (e.g., Maltman and Bolton, 2003; Huuse et al., 2010; Hurst et al., 2011). The tuff layers, as granular and permeable beds, may have retained enough water to produce overpressure as the result of deep burial and disequilibrium compaction. This process, however, would result in the formation of solely upward protruding dikes, and would not explain the dominance of downward-tapering dikes.

Alternatively, as dikes are always related to altered tuff layers, volume changes of the tuff beds along with subaqueous shrinkage and dewatering of the underlying mud may have related to

the alteration of the tuff material during early diagenetic processes. Direct alteration of the vitric glass into analcime in saline, alkaline groundwater is associated with hydration of the volcanic glass and water removal from the surrounding sediment (Surdam and Parker, 1972; Mason, 1983). Thus, volume increase within the tuff layers and the dewatering and shrinkage of the host strata could have resulted in the remobilization of the tuff material into shrinkage cracks underneath. However, as noted by Iiyima and Hay (1968), analcime most likely formed by the alteration of intermediate zeolite phases, which, in turn, is a process associated with dehydration.

In the studied samples analcime crystals show relatively homogeneous distribution throughout, with no evidence of movement, shearing or fragmentation of individual crystals. This indicates that the tuffs were altered after the dikes were injected (Cashion, 1967; Griggs, 1968). Consequently, elevated pressures must have developed during the alteration of volcanic glass into alkali-rich zeolites, before the formation of analcime, which caused volume increase of the tuff bed, shrinkage of the underlying sediment and liquidization and remobilization of the tuffaceous material afterwards. Other deformation features, such as folding and brecciation of the tuff material with centimeter-sized clasts of folded laminated host strata, indicate that the tuff layers have been undergone significant intrastratal disruption after their deposition, which might be related to the same process.

#### 4.5.8.5 Type 5 – Volcanosedimentary dikes

**Description:** Four sedimentary dikes filled with tuffaceous material form widely spaced ridges on the surface in Nine Mile Canyon, between North Franks Canyon and Sand Wash (Fig. 4.22A–D). They cut at least 35–40 m of laminated profundal to sublittoral carbonates of the upper member of the GRF, in a stratigraphic sequence that extends approximately 50 m above the Horse Bench Sandstone (Fig. 4.22A, B). Individual dikes can be traced for several tens to hundreds of meters. The dikes are straight and parallel-sided both in plan view and cross-section. They form a widely spaced orthogonal pattern, with predominant strike directions of ~140° and ~220° and dips between 80° and 90°.

Internally the dikes have a massive texture, with phenocrysts and fragments of feldspar and small amounts of amphibole and biotite, similar to those in a probably correlative stratigraphic interval in the eastern Uinta Basin described as “tuffaceous dikes” composed of “altered rhyolite tuff” (Cashion 1967). Locally they contain black, rounded clasts of pyritic mudstone. The contact

between the dikes and the host strata is sharp, and the lamination within the host strata is generally undisturbed, but microfaults are locally present in beds adjacent to them. All dikes terminate upsection at the same stratigraphic position marked by a bioturbated tuffaceous sandstone which forms a conspicuous, resistant bench (Fig. 4.22A, B). The thickness of the sandstone bed is proportional to the thickness of the dikes and gradually thins with the thinning dikes. Locally, a stromatolite is present at the base of this bed. At the intersection of the dike and the sandstone bed, the sand shows a churned texture with dark grey mottling (Fig. 4.22D). The lower termination of the dikes was covered at all locations.

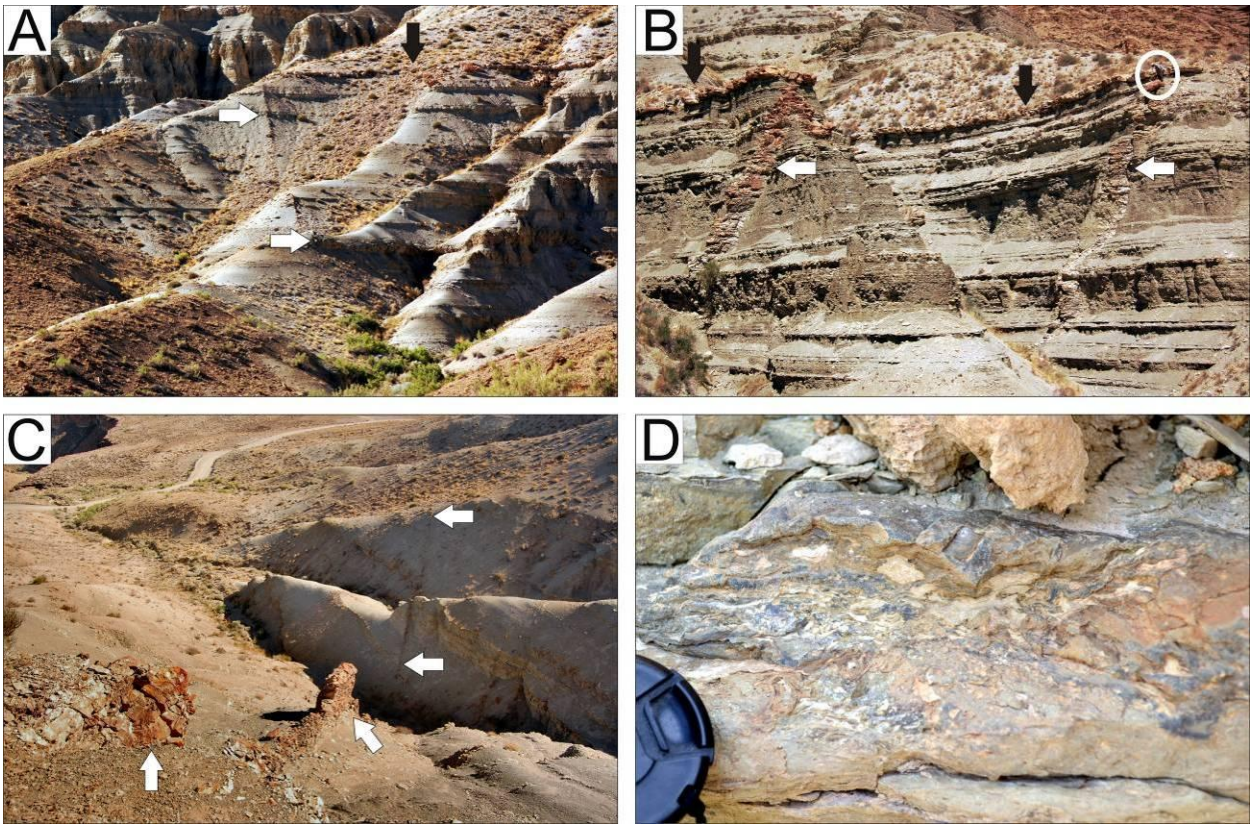


**Figure 4.22** Type 5 sedimentary dikes containing volcanosedimentary infill (upper member, Nine Mile Canyon, UT). A–C. Outcrop of 30 m thick interval of gray to light-green carbonate mudstone and siltstone cut by scattered, resistant-weathering dikes 3–50 cm thick (white arrows). Dikes terminate against sandstone bed 25–85 cm thick (black arrow). The thickness of the dikes changes significantly within few meters (C); D. Base of sandstone where dikes terminate showing fragmented material.

**Deformation mechanism:** Sharp boundaries of the dikes and microfaults indicate a greater degree of lithification and brittle failure of the host strata at the time of their formation. Their variable width was likely controlled by either variable pore pressures or slight variation in the rheological properties of the strata into which the dike was emplaced. The disrupted lower part of the sandstone bed at the upper termination of the dikes is the result of mixing of the tuffaceous material with the lacustrine sediments during emplacement at the lake-floor. This genetic relationship is further implied by the proportional thickness of the sandstone bed with the thickness of the dikes.

The dikes described by Cashion (1967) and those noted by Grabowski and Pevear (1985) as "injection" features were explained by intrusion of gel-like, water-saturated ash after burial, caused by overcompaction or diagenetic alteration of the tuff material. However, the dikes in Nine Mile Canyon show no distinctive alteration and internal plastic deformation is absent. Thus, they are interpreted as dikes that originated from the liquefaction and remobilization of a buried tuff bed. The Wavy and Curly tuffs ~100–130m below are potential source intervals.

#### 4.5.8.6 Type 6 – Décollement-related dikes

**Description:** Meter-scale sedimentary dikes filled with non-calcareous mudstone are present in the MOSZ at North Franks Canyon (Fig. 4.23A–B). The dikes form several sub-horizontal sills and oblique upward-protruding dikes with variable thickness, 0–3 m below the Mahogany Bed (Remy, 1992). The dikes are exposed on cliff faces and thus their aspect in plan view is uncertain. Individual dikes or sills show buckling as well as small offshoots (Fig. 4.23A). Locally, the dikes form small duplexes indicating top to the south shear, while shear structures within the host strata implied northward displacement. The upper termination of the dikes is marked by gradual decrease in their width in tandem with a slight facies change within the host strata (Fig. 4.23B) from parallel laminated carbonate mudstone into wavy and lenticular-laminated carbonate mudstones and calcareous siltstones, with N–S oriented Type 1 sedimentary dikes. The outcrop also displayed N–S oriented pervasive jointing. Mudstone intervals, with similar lithologies to the infill, are not exposed.

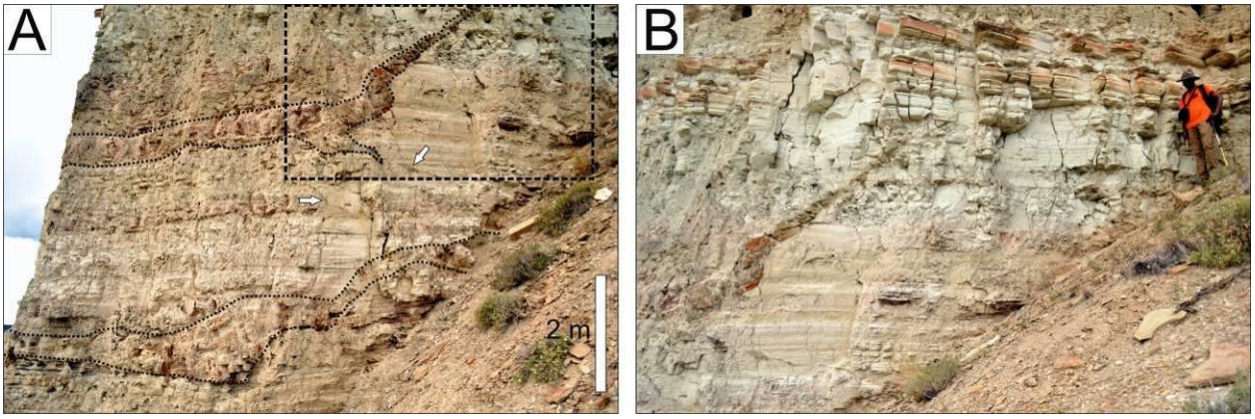


**Figure 4.23** Type 6 sedimentary dikes filled with non-calcareous mudstone (MOSZ, North Franks Canyon, UT). Their width ranges between 1 and 85 cm, with abrupt changes within short distances. A. Two sub-horizontal sills passing (to the right) into obliquely oriented dikes towards the left (outlined by dotted line), with small offshoots (arrows); B. Close-up of rectangular area outlined by dashed line in A, showing gradual, upward narrowing of obliquely oriented dike below silty carbonate mudstone (orange-colored).

**Deformation mechanism:** In the absence of associated beds with a similar composition to their infill, the oblique dikes and sub-horizontal sills are considered as allochthonous in a sense. Based on the occurrence of shear-related structures here and elsewhere within the MOSZ (e.g., shear structures at Gate Canyon and Evacuation Creek) the dikes are interpreted as remobilized non-calcareous or silicified mudstones that formed at multiple detachment surfaces. The sediment was most likely injected from a décollement surface into the extensional joints that formed under transpressional shear stresses during en-masse block movement of the strata above.

### *4.5.9 Microfaults*

#### 4.5.9.1 Description

Microfaults occur in laminated profundal to sublittoral deposits, affecting sporadic intervals up to 1 m thick. These structures can be classified into three groups: low-angle or listric normal faults (Fig. 4.24A), high-angle normal faults (Fig. 4.24B), and reverse faults (Fig. 4.24C, D), all of which may be present together in the same interval. They occur as individual features or associated with other deformation features such as fault-related folds (Fig. 4.24C), pinch-and-swell structures (Fig. 4.7C, D), shear structures (Fig. 4.9A–F), and sedimentary dikes (Types 1 and 5; Fig. 4.14H). Microfaults are often organized into an array of sub-parallel lineaments each

with miner offset, and they gradually die out both upwards and downwards. The offset of individual faults ranges from few millimeters up to tens of centimeters. Occasionally intervals show a gradual upward transition from fault-related folds into a thin disrupted layer containing fragments of the laminated host strata with an irregular upper boundary (Fig. 4.24C). In rare cases microfaults are associated with fluid-escape (flame) structures (Fig. 4.24D), where small domal structures are filled with structureless carbonate mud originating from below.

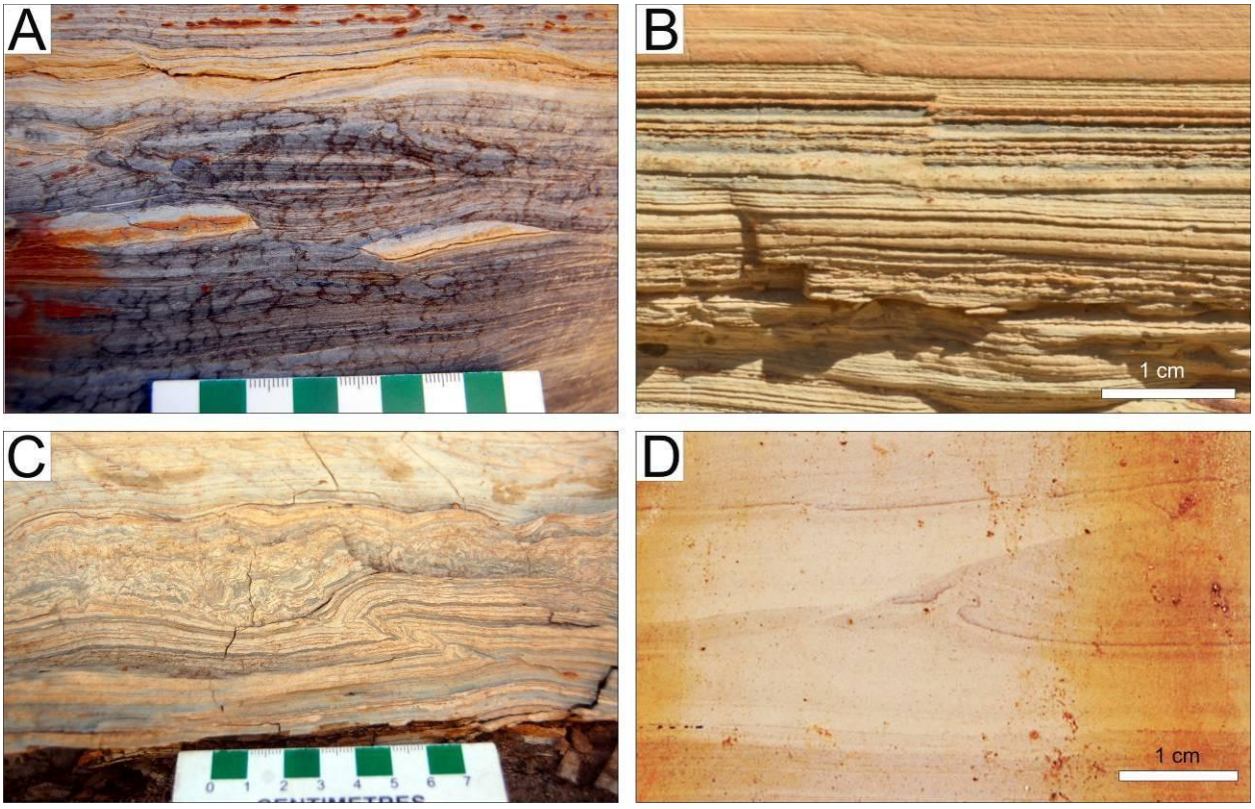


**Figure 4.24** A. Low-angle normal microfaults in oil shale (MOSZ, Hells Hole Canyon, UT); B. High-angle normal microfaults in oil shale (MOSZ, Hells Hole Canyon, UT); C. Fault-related fold overlain by breccia layer in oil shale (R8 zone, Piceance Creek Basin, CO); D. Reverse fault in carbonate mudstone, with small flame structure at the top of the footwall interval (R8 zone, Piceance Creek Basin, CO).

#### 4.5.9.2 Deformation Mechanism

In general, microfaults imply a strain increase that exceeds the yield strength of the sediment resulting in brittle failure (Owen, 1987). The associated folds indicate that deformation sometimes occurred in the brittle–ductile field transition within semi-cohesive sediment. Rare

flame structures imply that faulting was associated with localized fluidization of host carbonate mud. Gradual disappearance of the microfaults upwards and downwards indicate that they formed intrastratally, and not at the sediment–water interface (Pratt 1994; Pope et al. 1997; Kahle 2002; El Taki and Pratt, 2012). Grabowski and Pevear (1985) described microfaults in the MOSZ in Colorado and also considered them to have formed intrastratally. Dyni (1981) called them "fractures" and ascribed their carbonate mud infill to water-escape during burial.

Faulted and folded intervals overlain by brecciated layer resemble 'mixed-layers' described by Marco and Agnon (1995). They most likely formed by the disruption and suspension of the cohesionless and semi-cohesive lake sediment close to the sediment–water interface during syndepositional faulting. Underlying deposits were more cohesive and behaved in a brittle manner, indicated by the faults and fault-related folds. After the faulting event, normal sedimentation continued and carbonate mud draped the deformed interval.

### *4.5.10 Carbonate Breccias*

#### 4.5.10.1 Description

Carbonate breccias and intraclastic conglomerates: (1) occur over- and underlain by deltaic to littoral deposits (Fig. 4.25A–D); (2) form the core of stromatolites (Fig. 4.25F, G); (3) are interbedded with fine-grained, laminated littoral to profundal carbonate mudstones (Figs. 4.25E, H I, 4.26A–D); and (4) appear as mass-transport deposits (see 'Load Structures' and 'Mass-Transport Deposits' above).

At Willow Creek two resistant, orange weathering breccia layers form the base and the top of a 5 m thick interval that consist of stacked, laterally accreting sandstone beds, where each bed is up to 90 cm thick (Fig. 4.25A). These breccias are composed of a mixture of sand to pebble-sized angular fragments of gastropod shells, microbial carbonates, and massive or laminated carbonate mudstone, floating in a sandy matrix (Fig. 4.25B). The upper layer is finer grained and hydrocarbon-saturated. The laterally accreting units become thinner and finer grained towards the east-northeast along the ~25 m long outcrop. The whole succession is overlain by interbedded gray and green mudstone, siltstone and sandstone.

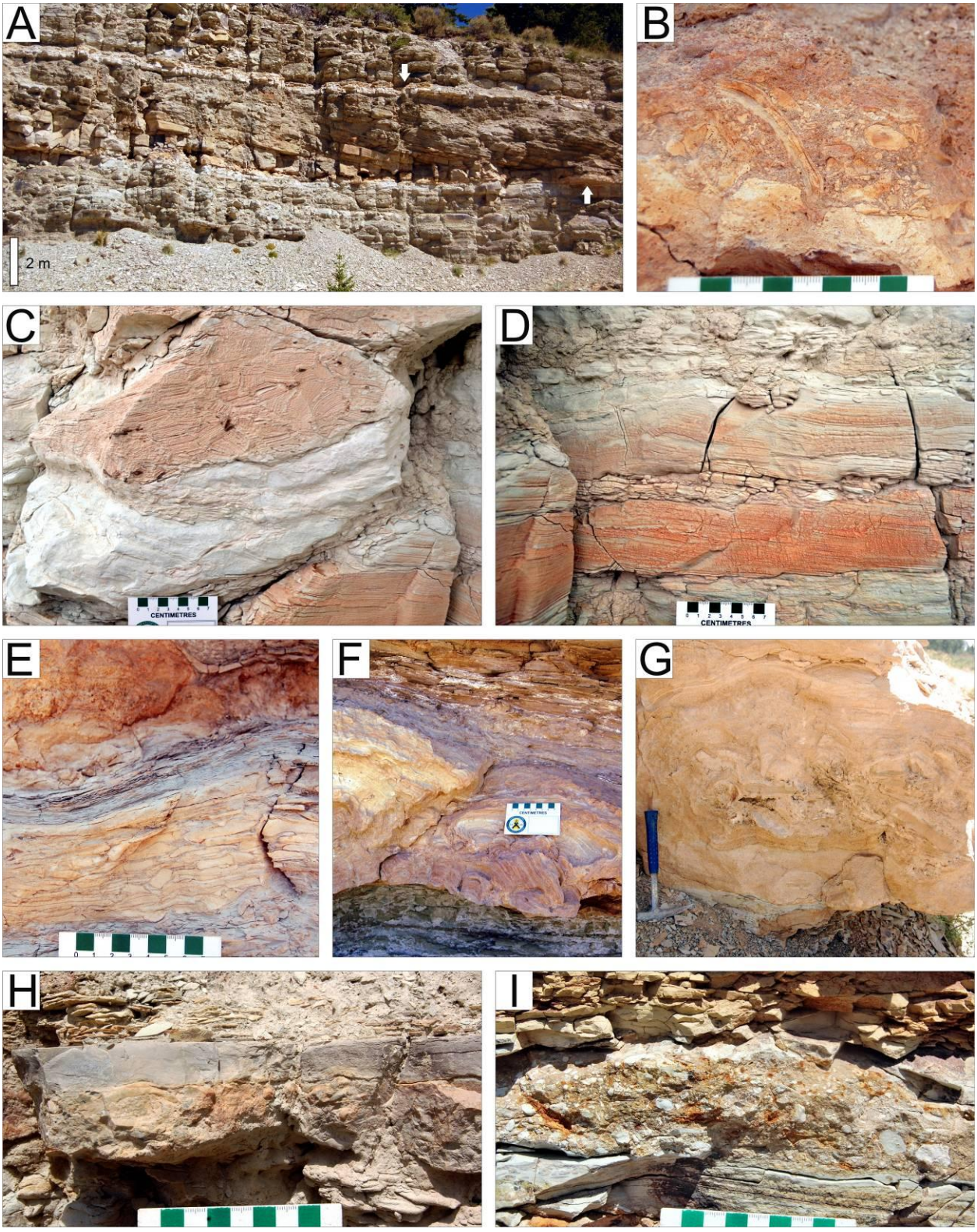


**Figure 4.25** A. Laterally accreting sandstone interval (Gilbert delta) showing thinning and fining to the ENE (right), with two laterally extensive brecciated intervals (arrows) immediately below and above the delta (S1 marker, Willow Creek, UT); B. Close-up of the lower breccia layer in A, showing carbonate mudstone and microbial carbonate

intraclasts is a sandy matrix; C, D. Brecciated laminated carbonate mudstone (middle member, North Franks Canyon, UT); E. Intraclastic conglomerate bed capped by laminated carbonate mudstone and microbial carbonate (R4 zone, Evacuation Creek, UT); F. Domal stromatolites overgrowing angular microbial carbonate fragments, under-and overlain by laminated carbonate mudstone (L3 zone, Evacuation Creek, UT); G. Toppled domal stromatolite overgrowing fragmented core mixed with ooid grainstone (L4 zone, Douglas Pass, CO); H, I. Intraclastic conglomerate layer interbedded with siltstone (R3 zone, Douglas Pass, CO).

At North Franks Canyon a breccia layer with centimeter-sized angular fragments comprises the upper part of a 1 m thick interval of laminated carbonate mudstone that can be traced laterally for at least 20 m (Fig. 4.25C). The fragments are composed of the same material as the host, and the bed has an irregular lower and a flat upper boundary. The host strata under the breccia show microfaulting and upward-increasing brecciation (Fig. 4.25D). The breccia is sharply overlain by a 4 m thick coarsening-upward succession of littoral to sublittoral carbonate mudstone, siltstone, and fine-grained sandstone (the S1 marker bed; Remy, 1992).

Breccias composed of fragmented carbonate mudstone and stromatolite clasts with a grainstone matrix often form the base or the core of domal stromatolites or thrombolites at Evacuation Creek and Douglas Pass (Fig. 4.25F, G). The clasts are angular to sub-angular and up to 25 cm in size. Massive littoral carbonate mudstones and ooid grainstones underlying the domal stromatolites also include decameter-scale fragmented stromatolite clasts. Occasionally fragments are coated by a second generation of stromatolites.

Intraclastic conglomerate layers within littoral to sublittoral siliciclastic and carbonate intervals are composed of platy, sub-angular to sub-rounded clasts of laminated and massive carbonate mudstone, siltstone, and stromatolites (Fig. 4.25E, H, I).

At one location at Douglas Pass silicified carbonate mudstone fragments form a laterally extensive 5–20 cm thick layer that is locally overlain by stromatolites up to 30 cm in diameter, and can be traced laterally for more than 70 m (Fig. 4.26A–D). The platy clasts are up to 10 cm long and they locally form small tepee-like structures (Fig. 4.26C, D). This interval is underlain by laminated carbonate mudstone and silty oil shale, and overlain by laminated sublittoral silty carbonate mudstone.

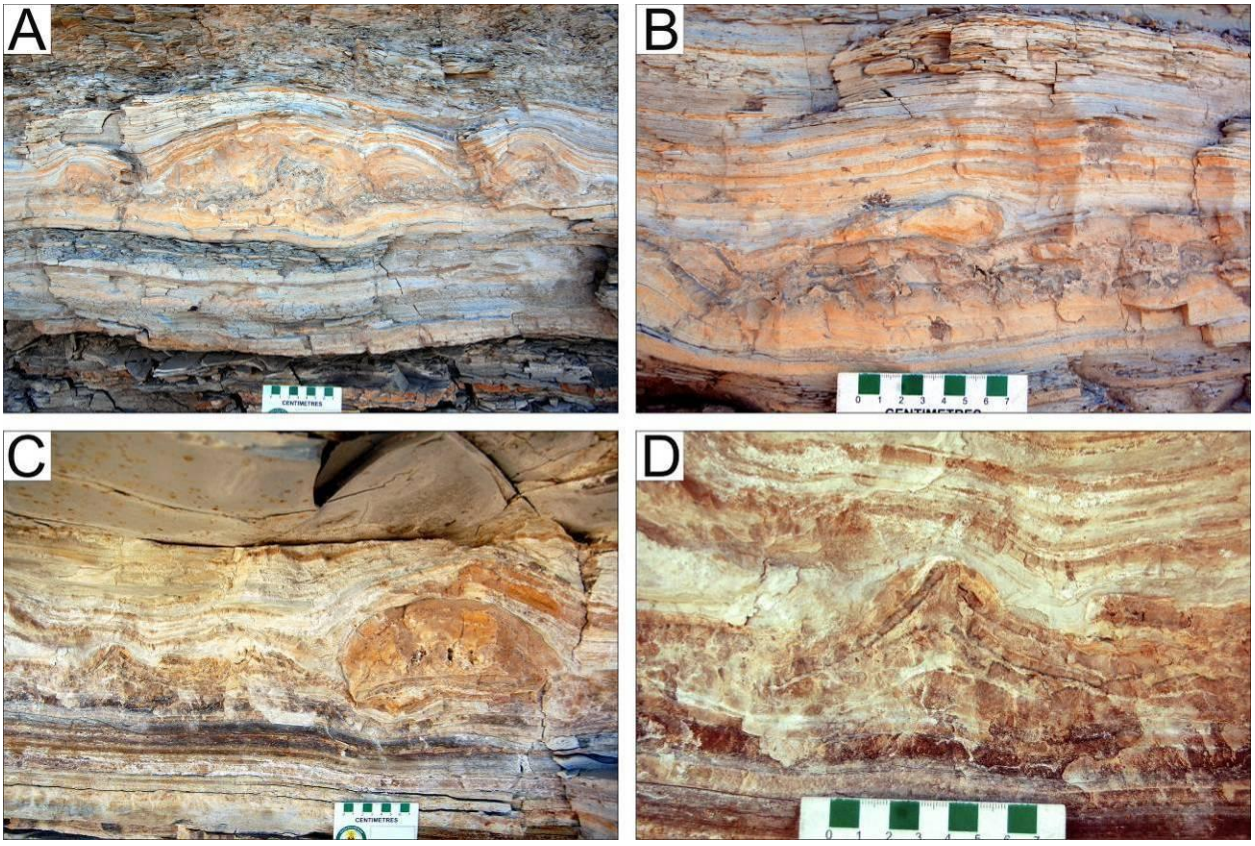


**Figure 4.26** Breccia locally overgrown by microbial carbonate (R1 zone, Douglas Pass, CO). A. Stromatolites covering silicified mudstone and microbial intraclasts; B. Carbonate mudstone grading upward into partly silicified breccia layer; C. Partly silicified carbonate mudstone overlain by intraclastic conglomerate which is overgrown by stromatolite (right side) and overlain by carbonate mudstone; D. Close-up of left side of C, showing tepee-like structure of brecciated silicified carbonate mudstone laminae.

#### 4.5.10.2 Deformation Mechanism

Similarly to microfaults, breccias indicate brittle failure when external forces exceeded the tensile strength of semi-lithified to lithified material. They are confined to carbonate-rich sediment because of preferential early cementation, which is especially typical of microbial carbonates (e.g., Sumner, 1997; Last et al., 2010). In some beds transportation is indicated by the rounded nature of the clasts.

Brecciation of littoral or sublittoral carbonates and microbial carbonates have been reported from both shallow- or deep-marine settings (e.g., Hiscott and James, 1985; Pratt, 1994, 2002b; Pope et al., 1997; Kahle, 2002; Milroy and Wright, 2002; Schroeder et al., 2009; McGlue et al., 2010). Fragmented intervals are commonly interpreted in the GRF as indicators of regression and

subsequent transgression, and deposition in subaerial or very shallow conditions with storm action that marks sequence boundaries or flooding surfaces (e.g., Tänavsuu-Milkeviciene and Sarg, 2012; Sarg et al., 2013). Tepee structures in both lacustrine and marine strata are commonly considered as indicators of deposition under subaerial or very shallow conditions, typically on a strandplain or tidal flat with fluctuating saturation and salinity (Handford et al., 1984; Kendall and Warren, 1987; Last et al., 2010). Those at Douglas Pass were interpreted previously as marking a sequence boundary that resulted from very short-lived subaerial exposure (Tänavsuu-Milkeviciene et al., 2012). This interpretation is plausible if the deformed intervals are associated with other indicators of a shallow-water environment where the action of waves or currents (littoral sandstones or grainstones) or subaerial exposure (root traces, polygonal desiccation cracks, and other pedogenic modifications) can be envisaged. Other breccias are intercalated within laminated sublittoral deposits, indicating a submerged lower energy environments (e.g., Sarg et al., 2013) and, thus, these are similar to autoclastic breccias (e.g., Pratt, 2002b; Montenat et al., 2007).

## 4.6 Discussion

### *4.6.1 Rheological Control on Deformation*

The morphology and size of the deformed structure depends primarily on the rheological properties of the sediment, the driving forces acting on the sediment during deformation (e.g., density contrast, unequal loading), and the areal extent and thickness of the rheologically susceptible sediment, and not solely on the trigger mechanism (e.g., Mills, 1983; Owen, 1987; Pratt, 1998a; Spalluto et al., 2007; Moretti and Ronchi, 2011; Owen and Moretti, 2011). Deformation occurs only if the applied force exceeds the yield strength of the deposit. Thus, the mechanical behavior of the sediment and the morphology and lateral extent of deformation are controlled by lithological properties, such as degree of cementation, permeability and porosity due to grain size and packing, and presence of clay and organic matter.

Rheology in the deposits of the GRF was governed by the depositional setting. In general, plastic deformation, in the form of load structures and convolution, occurred in non-cohesive or semi-cohesive coarse-grained sediments deposited in fluvial, deltaic and littoral environments. Organic-rich deposits in profundal environments are thought to have exhibited gel-like properties with high initial shear strength in their early diagenetic stage (e.g., Bradley, 1931, 1970; Smoot,

1983). These were also prone to plastic deformation, as evidenced by complex fold structures at various scales, inhomogeneous disruption demonstrated by the oil shale breccias, and also to intrastratal shrinkage, as shown by the sedimentary dikes. Deformation in lithologically heterogeneous intervals, with variable mechanical properties resulted in the formation of brittle–ductile features such as microfaults, fault-related folds, shear structures, and sedimentary dikes. In sublittoral and littoral carbonates brittle failure dominated and led to brecciation.

### *4.6.2 Trigger Mechanism*

Those trigger agents that are related to normal, 'background' sedimentary and/or erosional processes are often called 'autogenic' (or 'autokinetic'), whereas those of external origin are called 'allogenic' (or 'allokinetic') (e.g., Leeder, 1987; Owen and Moretti, 2008). Most common autogenic triggers include breaking and pounding waves, shear stresses and turbulence related to subaqueous currents, rapid sediment loading, glaciotectonics, groundwater seepage, pressure fluctuations during burial, and biogenic processes (e.g., Owen, 1987, 1996a, b; Owen and Moretti, 2011) (Table 1). Allogenic triggers include earthquakes and extra-terrestrial impacts. Deformation features formed by autogenic triggers should show an intimate relationship with the sedimentary facies. Such a linkage, however, should be less pronounced or non-existent in the case of external triggers (Owen et al., 2011).

| Depositional Environment | Groundwater | Overloading | Wave action | Currents | Slope instability | Earthquakes |
|---|---|---|---|---|---|---|
| Fluvial | **X** | **X** | | **X** | | **X** |
| Deltaic | **X** | **X** | **X** | **X** | **X** | **X** |
| Nearshore | **X** | | **X** | **X** | | **X** |
| Sublittoral | | | | **X** | | **X** |
| Profundal | | | | | **X** | **X** |

**Table 4.1.** The range of possible triggers that have been most commonly invoked to explain the origin of synsedimentary deformation.

There are certain criteria that are used to assess the likelihood of a seismic origin for ancient features: (1) deformation is laterally extensive in recurrent horizons; (2) deformation structures are comparable to modern examples; (3) they occur in a tectonically active setting; and

(4) they show zonation in intensity, complexity, or abundance (Sims, 1975; Obermeier, 1996; Rossetti, 1999; Ettensohn et al., 2002; Greb and Dever, 2002; McLaughlin and Brett, 2004; Montenat et al., 2007). However, the trigger is only one factor and deformation features showing similar morphologies may be caused by different mechanisms (e.g., Owen and Moretti, 2011; Owen et al., 2011). Moreover, seismically deformed beds can change in morphology and deformation style or even disappear laterally as result of thickness changes or lateral facies variations and (Rodríguez-López et al., 2007; Alfaro et al., 2010), or with increasing distance from the epicentre. Accordingly, recognition of the trigger mechanism can be problematical, and many commonly used criteria are unreliable or non-diagnostic (Leeder, 1987; Ringrose, 1989; Li et al., 1996; Pope et al., 1997; Jones and Omoto, 2000; Montenat et al., 2007; Owen et al., 2011) (Table 2). Nevertheless, these criteria, combined with the analysis of the sedimentological and paleoenvironmental context, may support earthquakes as the most likely trigger.

| Criteria Supporting Seismic Origin | Problem |
|---|---|
| Deformation is laterally continuous in recurring intervals separated by undeformed beds | Other recurring triggers could also affect a wide area |
| Deformation structures are similar to other features known to have been seismically induced | Different triggers can produce similar structures |
| Tectonically active sedimentary setting | Does not exclude other triggers |

**Table 4.2.** Commonly used criteria for the recognition of sedimentary deformation related to a seismic trigger and their shortcomings (after Owen et al., 2011).

In the case of the Uinta Basin, glaciotectonics can be excluded due to its mid-latitude paleogeographic position and the warm climate of the early to middle Eocene (e.g., Wilf, 2000; Zachos et al., 2001; Smith et al., 2008). Biological disturbance can also be discarded as bioturbation structures have different morphologies and size (e.g., Klappa, 1980; Owen et al., 2008; Buatois and Mángano, 2011). Deformation related to concentrated vertical fluid movement (water or gas) and artesian springs (e.g., Deynoux et al., 1990; Guhman and Pederson, 1992; Holzer and Clark, 1993; Li et al., 1996; Owen, 1996a; Massari et al., 2001; Ledésert et al., 2003; Deville et al., 2010; Huuse et al., 2010) is also unlikely to induce deformation, because the volcanic centers were relatively distant (e.g., Carroll et al., 2008; Davis et al., 2009). Also,

breccias and other deformation features do not follow vertical paths, except those formed by fluidization and upward injection (e.g., Type 5 sedimentary dikes).

#### 4.6.2.1 Deformation in Fine-Grained Deposits

Where deformation structures are encased in fine-grained deposits formed either in sheltered littoral or deeper-water sublittoral to profundal settings away from coarser-grained sediment input, rapid depositional events, overloading, strong wave action, undercutting due to erosion, or drag by subaqueous currents are unlikely as the sedimentary record lacks indicators of such events. Additionally, deformed intervals are usually confined stratigraphically by undeformed deposits of the same facies. This indicates that deformation is related to short-lived events, affecting only rheologically susceptible deposits, after which the relatively slow sedimentation in a low-energy setting resumed.

Organic-rich thixotropic muds had high initial shear strength (Smoot, 1983; Grimm and Orange, 1997), and their disturbance required stresses to exceed a given threshold. Thus, mass-transport deposits, together with laterally extensive soft-sediment deformed and brecciated oil shales, represent exceptional catastrophic events in the history of Lake Uinta that caused in situ disruption, translation and local transportation. The widely accepted threshold for typical gravity-induced slumping is 2° in siliciclastic deposits (Lowe, 1975), and this threshold might be even higher in carbonate-dominated settings due to early cementation. Seismically triggered slumping, on the other hand, may occur on slopes with dips as little as 0.25° (Field et al., 1982). Selecting seismic activity as the most likely cause of slumping is commonly regarded as difficult to substantiate because there are a number of sedimentary processes can be involved in the formation of mass wasting (e.g., Allen, 1982; Ricci Lucchi, 1995). Nevertheless, a seismic origin is favored if: (1) the slope is relatively steep (>1°), but the size of the mass-movement deposit is larger than co-occurring, stratigraphically more frequent mass-wasting events generated by autogenic processes; or (2) if mass movement occurred on a more or less flat depositional surface. Lake Uinta had a slope along its southern margin and the Douglas Creek Arch estimated to be ~0.01–0.03° and decreasing towards the profundal area (e.g., Bradley, 1931; Lundell and Surdam, 1975; Moncure and Surdam, 1980; Dyni, 1981). Thus, spontaneous slumping can be ruled out. Moreover, apart from shear structures, deformation features show no clear vergence or

unidirectional axial planes that are characteristic of downslope movement (e.g., Strachan 2002; Alsop and Marco 2012).

Sedimentary dikes within sublittoral to profundal deposits are best explained as the result of elevated pore pressure, hydrofracturing or dewatering and shrinkage of the host sediment, and synchronous liquidization of coarser-grained layers due to seismic shaking (Plaziat et al., 1990; Pratt, 1998a, b; Törő and Pratt, in press). Pinch-and-swell structures have been attributed to extensional forces during compaction (Dyni, 1981; Grabowski and Pevear, 1985). However, intercalation within thick oil shale successions lacking deformation eliminates progressive burial as it would have affected the sedimentary succession uniformly (cf. Hesselbo and Trewin, 1984; Calvo et al., 1998; Rodríguez-Pascua et al., 2000). Microfaults with uniform geometries within a single interval could conceivably be generated by differential compaction (e.g., Dyni, 1981; Grabowski and Pevear, 1985; Guiraud and Séguret, 1987). However, most cases show variable orientations in lithologically uniform successions, and a seismic origin is preferred (e.g., Seilacher, 1969; Davenport and Ringrose, 1987; Plaziat et al., 1990; Pratt, 1994; Grimm and Orange, 1997; Bhattacharya and Bandyopadhyay, 1998; Mörner, 2005; Fortuin and Dabrio, 2008; Koç Taşgın et al., 2011; El Taki and Pratt 2012).

Furthermore, deformed beds are overlain by undeformed units with a gradual or sharp but non-erosive boundary, implying that deformation occurred either at the sediment–water interface or under shallow burial depth. Because most autogenic processes can be discounted, in situ deformation structures (e.g., folds, pinch-and-swell structures, shear structures, sedimentary dikes, and certain microfaults) must be ascribed to allogenic processes that occurred repetitively. Earthquakes provide the only reasonable trigger mechanism, and consequently, the suite of synsedimentary deformation features are interpreted as seismites (Seilacher, 1969, 1984) (Appendix 2).

#### 4.6.2.2 Deformation in Coarse-Grained Deposits

Where in situ deformation features occur in a littoral setting, subaqueous currents, wave action, oversteepening, and the affects of base-level changes are potential triggers besides earthquakes. On the other hand, mass-transport deposits may occur on relatively steep (>2°) slopes, where slope failure can be initiated by oversteepening or sedimentary overloading (e.g., Lewis, 1971; Postma, 1983; Stromberg and Bluck, 1997), water-level changes (e.g., Rothwell et

al., 2000), tides (Wells et al., 1980), storms (e.g. Osleger et al., 2009), or earthquakes (e.g., Field et al., 1982; Pope et al., 1997; Bhattacharya and Bandyopadhyay, 1998; Rossetti and Santos, 2003; García-Tortosa et al., 2011; Mastrogiacomo et al., 2012).

Deformation related to shear stresses generated by tidal currents (e.g., Greb and Archer, 2007) is unlikely in lakes (e.g., Talbot and Allen, 1996; Renaut and Gierlowski-Kordesch, 2010). Breaking or pounding waves are capable of inducing liquefaction as shown by modern geotechnical studies (Seed and Lee, 1966; Sangrey et al., 1969; Seed and Rahman, 1977; Dalrymple, 1979, 1980), and this process has been invoked for several ancient examples (e.g., Kerr and Eyles, 1991; Martel and Gibling, 1993; Molina et al., 1998; Bouchette et al., 2001; Chen et al., 2009; Chen and Lee, 2013). Wave height of at least 4 m is estimated to be required to induce liquefaction (e.g., Nataraja and Gill, 1983; Alfaro et al., 2002). Lake Uinta had a fetch of approximately 100–130 km or more, considering northerly winds (Bradley, 1931; Ryder et al., 1976; Franczyk et al., 1992). In the modern Great Salt Lake, with a smaller fetch of ~65 km, waves generated by storm winds are on the order of 0.6–0.9 m and occasionally reach 1.2 m (Woodhall, 1980). In the Wyoming part of the Green River lake system, which had similar physiographic properties to Lake Uinta, Roehler (1990) estimated an average wave height of 1.5 m. Nevertheless, large storm waves >5 m high have been reported from the Great Lakes (e.g., Nataraja and Gill, 1983). Consequently, in Lake Uinta exceptional storm events, if they occurred, might have produced large waves capable of inducing liquefaction in littoral deposits.

Ripple cross-lamination in beds overlying hummocky or tabular cross-stratified sandstones exhibiting convolution, folds, and load structures indicates that intensity of wave action was low by the time deformation occurred, implying an external trigger (e.g., Hempton and Dewey, 1983; Bowman et al., 2004; Samaila et al., 2006; Alfaro et al., 2010; Koç Taşgın et al., 2011). Similarly, reverse density gradient systems may have formed in the littoral setting by the intercalation of sand, silt, and mud, but deformation through liquefaction still required an external trigger.

Early cementation of littoral carbonate sediment would have lowered their susceptibility to deformation by gravitational instability or storm waves. Externally triggered mass-transport deposits, in turn, could have generated load structures, such as those at Douglas Pass.

The gently dipping floor of Lake Uinta might have been steeper near the locations of deltaic input or along the tectonically active northern margin, possibly reaching 1–2° (Dyni,

1981). Oversteepening, as well as overloading by rapid depositional events related to turbidites or slumps, could have occurred near delta fronts (e.g., Owen and Moretti, 2008), although such features were not encountered in the study area. Additionally, closed basins are prone to frequent base-level fluctuations (e.g., Carroll and Bohacs, 1999; Keighley et al., 2003). Thus, lake-level falls might have caused incision and reworking and undercutting. Surfaces ascribed to this process, however, are low-relief features overlain by undeformed fluvial–deltaic sediments (Keighley et al., 2003; Tänavsuu-Milkeviciene and Sarg, 2012). The amplitude of these fluctuations is also disputed (Schomacker et al., 2010). The channel feature at Douglas Pass is filled by poorly sorted conglomerate and sublittoral deposits lacking evidence for subaerial exposure. This points to a time of slope instability and mass transport in an overall low-energy and low-gradient subaqueous setting (e.g., Lundell and Surdam, 1975) rather than incision during lake-level fall.

The origin of Type 1 sedimentary dikes that occur in littoral or deltaic deposits might conceivably be related to microbial mats (e.g., Parizot et al., 2005; Eriksson et al., 2007a, b; Lan and Chen, 2012, 2013), salinity fluctuations (e.g., Van Houten, 1964; Donovan and Foster, 1972; Plummer and Gostin, 1981), compaction (Kidder, 1990; Tanner, 1998; Harazim et al., 2013), gravitational forces (Picard, 1966), desiccation (Astin and Rogers, 1991), or earthquakes (Pratt, 1998a). Subaqueous shrinkage or cracking of thin microbial mats is unlikely, as the morphology of the dikes is markedly different, they preserved in positive epirelief on bedding surfaces rather than negative epirelief, and no other structures indicating the formation of microbial mats have been found. Triggering by gradual compaction and dewatering can be ruled out because seepage of pore fluids cannot account for sediment mobilization. Also, the dikes are not associated with structures indicating subaerial exposure. Syneresis due to salinity fluctuations is unlikely in shallow-water carbonates due to the lack of adequate amount of swelling clays (cf. Burst, 1965; Demicco and Hardie, 1994). Moreover, they typically occur intermittently in well-defined intervals, indicating that their formation is not related to specific depositional processes or paleoenvironmental conditions at the sediment–water interface.

Type 2 sedimentary dikes in littoral settings could be mistaken for desiccation cracks (Allen, 1986a, 1987; Harris, 2004). However, features indicating pedogenesis are absent, the dikes are not polygonal, and the infills show no layering as would be expected if the cracks were open and filled subaerially (cf. Neal et al., 1968; Allen, 1987). Even if they were polygonal, such

patterns are not unique to subaerial features (e.g., Eyles and Clark, 1985; Pratt, 1998a; Tanner, 1998).

Convoluted strata in fluvial deposits are overlain by mudstone-dominated intervals, which indicates that pressure fluctuations due to sedimentation were insufficient to liquefy underlying strata, and thus a seismic origin is indicated (e.g., Allen, 1977; Guiraud and Plaziat, 1993; Koç Taşgın et al., 2011; Moretti and Ronchi, 2011).

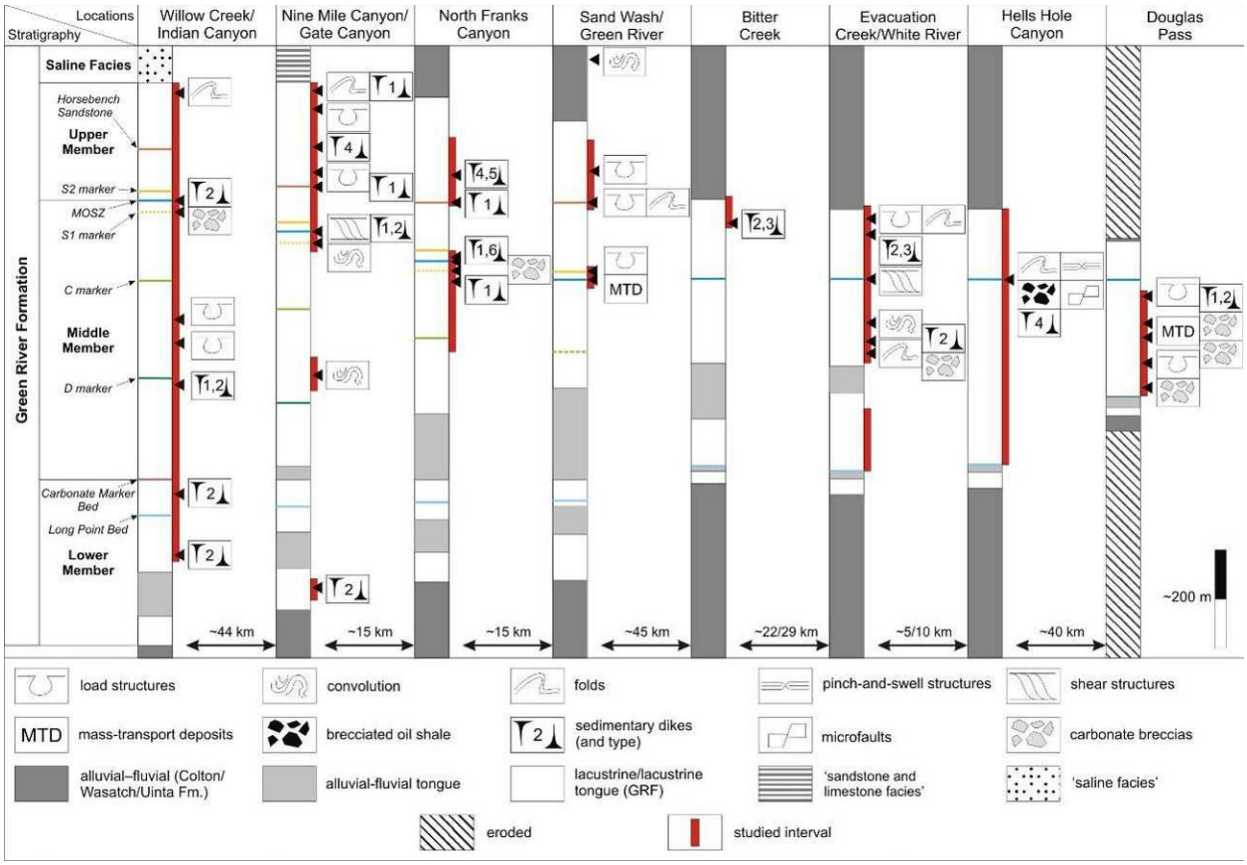


**Figure 4.27** Distribution of sedimentary deformation features in the Green River Formation of the Uinta Basin. Position of marker intervals is based on Cashion (1967), Johnson et al. (1988), Morgan et al. (2003), and Tänavsuu-Milkeviciene and Sarg (2011).

Because precise lithostratigraphic correlation between outcrops has yet to be achieved for the Uinta Basin and adjacent Piceance Creek Basin, the stratigraphic relationships of the deformed intervals can only be approximated (Fig. 4.27). Nevertheless, there are certain intervals that show pervasive deformation at a number of locations. Such an interval is the MOSZ, where deformation is represented by sedimentary dikes (Type 1, 2, 4, 6), shear structures, and mass-

transport deposits right across the basin. The S1 marker bed and adjacent strata host convolution, load structures, and carbonate breccias at Gate Canyon and North Franks Canyon. The S2 marker bed contains load structures and convolution at North Franks Canyon and Sand Wash. Similarly, the Horse Bench Sandstone displays sedimentary dikes (Type 1) and load structures over a wide area along Nine Mile Canyon, from Gate Canyon to Sand Wash. The lateral persistence of these features supports a seismic trigger. Vice versa, the localized nature of most deformation features does not rule out a seismic origin, because of subtle lateral variation in facies and thus rheological properties.

### *4.6.3 Implications*

#### 4.6.3.1 Sedimentary Implications

These sedimentary deformation features are relevant for the understanding of the depositional environment and basin configuration. For example, sedimentary dikes of various morphologies, infill composition, and host lithologies have been previously interpreted as desiccation cracks. As with other sedimentary successions where these had been viewed as diagnostic of subaerial exposure (e.g., Pratt, 1998a, b; Whitmore and Strom, 2010), this explanation profoundly influenced the interpretation of the depositional history of the GRF. "Mudcracks" have been taken as evidence for the development of a frequently exposed mudflat (e.g., Bradley, 1931; Eugster and Surdam, 1973; Eugster and Hardie, 1975; Smoot, 1983; Remy, 1992). In turn, based on periodic desiccation other fundamental aspects of the lake system were determined, such as the origin and depositional setting of oil shales (Bradley, 1930, 1970), the origin of carbonate particles (Smoot, 1978), or the lack of varves (Eugster and Hardie, 1975). However, the analysis of the morphological characteristics of such dikes and their sedimentary context may indicate subaqueous or intrastratal origin. Consequently, these deformation features are critical evidence for the bathymetry, paleolimnology, paleoclimate, and the overall evolution of the lake system.

Other features, such as mass-transport deposits and shear structures, provide information on lake-floor topography. For example, shear structures at Evacuation Creek indicate that emplacement took place towards the south, which is opposite to the general slope direction assumed for the Uinta Basin (e.g., Ryder et al., 1976; Franczyk et al., 1992). Either the tectonic forces that induced failure overwhelmed gravitational forces, or seismically induced movement

was downslope into localized shallow depressions, indicating that the overall slope was not uniform after all.

Although oil shales have usually been considered to have formed laterally continuous blankets of consistent thickness, at Evacuation Creek thickness changes over short distances suggest that a gently undulating lake-floor topography developed. The close association of shear structures suggests that seismic action may have played a role in generating these irregularities, possibly by inducing a seiche.

#### 4.6.3.2 Tectonic Implications

Lacustrine deposition in the Uinta Basin coincides with the late-stage tectonic events of the Sevier Fold and Thrust Belt and the Laramide Orogeny (e.g., Dickinson et al., 1988; DeCelles, 1994). There are several fault zones that were active during this time, including the Uinta Uplift (Bradley, 1995), the Douglas Creek Arch (Johnson and Finn, 1986; Bader, 2009), the Sand Wash, Jacks Canyon, and Duchesne fault zones (Osmond, 1992; Groeger and Bruhn, 2001; Morgan et al., 2003), and numerous other fault zones within the subsurface (Fouch et al., 1992; Osmond, 1992). Thus, seismically induced features can be used as direct evidence to track the sedimentary record of tectonic movements along these structures.

The magnitudes of paleoearthquakes can be estimated by considering modern analogs (e.g., Keefer, 1984; Obermeier, 1996; McCalpin, 2009), empirical relationships between magnitude and maximum epicentral distance of liquefied sites (e.g., Ambraseys, 1988; Galli, 2000; Castilla and Audemard, 2007), and corresponding studies on sedimentary deformation features in recent and ancient deposits (Hibsch and others, 1997; Rodríguez-Pascua and others, 2000, 2003; Monecke and others, 2004, 2006; St-Onge and others, 2004; Berra and Felletti, 2011). Based on these studies, in-situ deformation structures and mass-transport deposits described here must have been generated by earthquakes with a magnitude $\geq 5$. Apart from in situ features, earthquake-induced mass-transport deposits are widely used as paleoseismic archives in modern marine and lacustrine basins (Atwater, 1987; Chapron et al., 1999; Schnellmann et al., 2007; Waldmann et al., 2011; Strasser et al., 2013). This study shows that these should be more widely utilized in the lacustrine deposits of the Green River Formation.

In the evolution of lacustrine basins climate and tectonics are equally important controlling factors, although the latter is less frequently emphasized (Carroll and Bohacs, 1999). Tectonic movements in and around the Uinta Basin potentially induced differential tilting or sagging, or raised or lowered the adjacent sills. These events would have been superimposed on regional Laramide subsidence trends and ultimately influenced base-level, and are recorded in the preserved stratal packaging (cf. Keighley et al., 2003). Additionally, syndepositional tectonism might have influenced regional hydrology and drainage patterns (Rhodes et al., 2002; Pietras et al., 2006; Carroll et al., 2008; Törő et al., 2015), geomorphology (Carroll et al., 2006), and spring activity (Lee et al., 2013), all of which are capable of inducing changes in lake chemistry and sedimentation either in short- or long-term time frames.

Seismites described here demonstrate that tectonic movements occurred repeatedly and influenced sedimentation within the basin throughout its history. For example, the MOSZ and its stratigraphic vicinity represent a transitional interval from balanced-fill to evaporative underfilled lake conditions in the Uinta Basin (Smith et al., 2008; Birgenheier and Vanden Berg, 2011). Tectonic events recorded by seismites in this interval indicate that the change in the long-term balance of subsidence, sediment input, and water fill within the basin was, at least partially, tectonically mediated. However, systematic mapping and correlation of deformed intervals within a uniform stratigraphic framework, both in cores and outcrops, are yet to be achieved in order to identify co-genetic structures in littoral versus profundal areas and to utilize the full potential of seismites in understanding the interplay of tectonics and lake evolution.

## 4.7 Conclusions

Outcrop investigation of sedimentary deformation features in the Green River Formation of the Uinta Basin, Utah, provides a new window on Eocene depositional events and paleoenvironmental conditions. Lacustrine to fluvial–deltaic deposits display a wide range of previously overlooked exceptional syn- to early post-depositional sedimentary deformation features, including load structures, convolution, folds, pinch-and-swell structures, shear structures, oil shale breccias, various sedimentary dikes, microfaults, carbonate breccias, and mass-transport deposits. Apart from the last, most deformation was intrastratal and took place under shallow burial. The style of deformation was primarily controlled by the rheological properties of the sediments at the time when stresses were applied. Based on their morphological

characteristics, plastic deformation features are interpreted as the result of episodic liquefaction, fluidization, or folding of unlithified to semi-cohesive sediment. Brittle features in the form of microfaults and breccias formed when external forces exceeded the tensile strength of the sediment. Sedimentary dikes demonstrate a variety of processes, including a combination of shrinkage or hydrofracturing and sediment remobilization and injection under elevated pore pressures. The resulting fissures acted as fluid conduits. Mass-transport deposits represent instability of the low-relief lake floor and exceptional erosional events. In the studied interval there is no evidence for episodes of subaerial exposure, and features previously described as "mudcracks" are reinterpreted as subaqueous and intrastratal sedimentary dikes.

The morphological attributes of the sedimentary deformation features, their lateral extent, their widespread and episodic occurrence, the depositional setting of the host strata, plus the active tectonic setting, combined indicate that deformation was triggered by syndepositional earthquakes related to nearby structural elements. In turn, these seismically induced structures—seismites—provide insight on the rheological properties of the sediments upon deposition and during early diagenesis, hydrodynamic conditions of their depositional environment, configuration of the basin floor, and syndepositional tectonic activity.

Our study confirms that the information potential of sedimentary deformation features is considerable. They are largely untapped archives of key aspects of lacustrine processes, paleoenvironmental conditions, deformation processes, and the effects of tectonics on lake evolution as a whole.

### 4.8 Relationship of manuscript to thesis

Study of sedimentary deformation features in the Green River Formation is an unexplored aspect of the local geology of the Uinta Basin, and the manuscript represents the first study concentrating on structures preserved in fluvial to profundal lacustrine deposits. The manuscript provides detailed description of synsedimentary to early post-depositional features, discussion on their deformation mechanism, the controlling factors of deformation, and criteria to distinguish between seismic and non-seismic triggers. Controls on variations in lateral extent and morphology are also discussed, and attributed to changing facies and rheological properties. Most of the described features are ascribed to seismic shaking due to earthquakes that were related to movements along nearby structures. The manuscript places emphasis on the use of deformation

features to better understand the depositional setting and the implications of earthquake-induced features (seismites) to reconstruct the paleotectonic history of the basin. The stratigraphic position of deformed intervals, especially those within the Mahogany Oil Shale Zone, provides further implications for the evolution of the basin. A part of this study, which focuses on a mass-transport complex in the south-central part of the basin, was published as a separate manuscript (Keighley et al., 2015) that is not included here.

# CHAPTER 5
# SUMMARY

Detailed sedimentological field work across a large area in Wyoming, Colorado and Utah revealed an unparalleled suite of sedimentary deformation features in lacustrine deposits of the Green River Formation (Eocene) and associated fluvial strata. Despite being the most-studied ancient lacustrine system worldwide, most of these deformation features have never been studied before and some have been mentioned only by passing. Thus, the main chapters in this thesis provide the first detailed analysis of these features, with special emphasis on the governing factors and processes of deformation responsible for their origin.

Deformation features have been found in a variety of sediments, from sandstones to organic-poor or organic-rich carbonate mudstones that were deposited in fluvial to profundal environments (Fig. 5.1). Deformation in these deposits is represented by brittle and plastic behavior, as well as sediment injection. The deformed layers are confined by undeformed beds with similar facies to the deformed ones, indicating intrastratal deformation in most cases. As the style of deformation was principally governed by the rheological properties of the sediment, there is a relationship between the sedimentary facies and the type of deformation structures. For example, sand-rich deposits show almost exclusively load structures, folds, convolution with a lack of brittle structures, such as breccias, due to their high plasticity upon liquefaction. Fine-grained carbonates, however, show a wider range of behavior with ductile, brittle, and hybrid brittle-ductile feature, the latter found exclusively in finely laminated carbonate mudstones. This variety of structures implies the variability of sediment rheology upon disturbance.

Although folds, convolution, and load structures found in sand-rich fluvial and littoral deposits are frequently reported globally, complex folds, brittle-ductile features, and sedimentary dikes filled with carbonate mud that occur in sublittoral to profundal carbonates represent a unique set a features that have been rarely, if ever, described in the literature.

In general the deformation structures presented here can be attributed to elevated shear stresses and selective liquefaction and fluidization processes. Based on the morphological characteristics of the structures, as well as the sedimentological and tectonic setting of the lake basins, deformation was triggered by syndepositional earthquakes. Additionally, many of these features could be correlated along the outcrops for > 25 km, further suggesting a seismic origin.

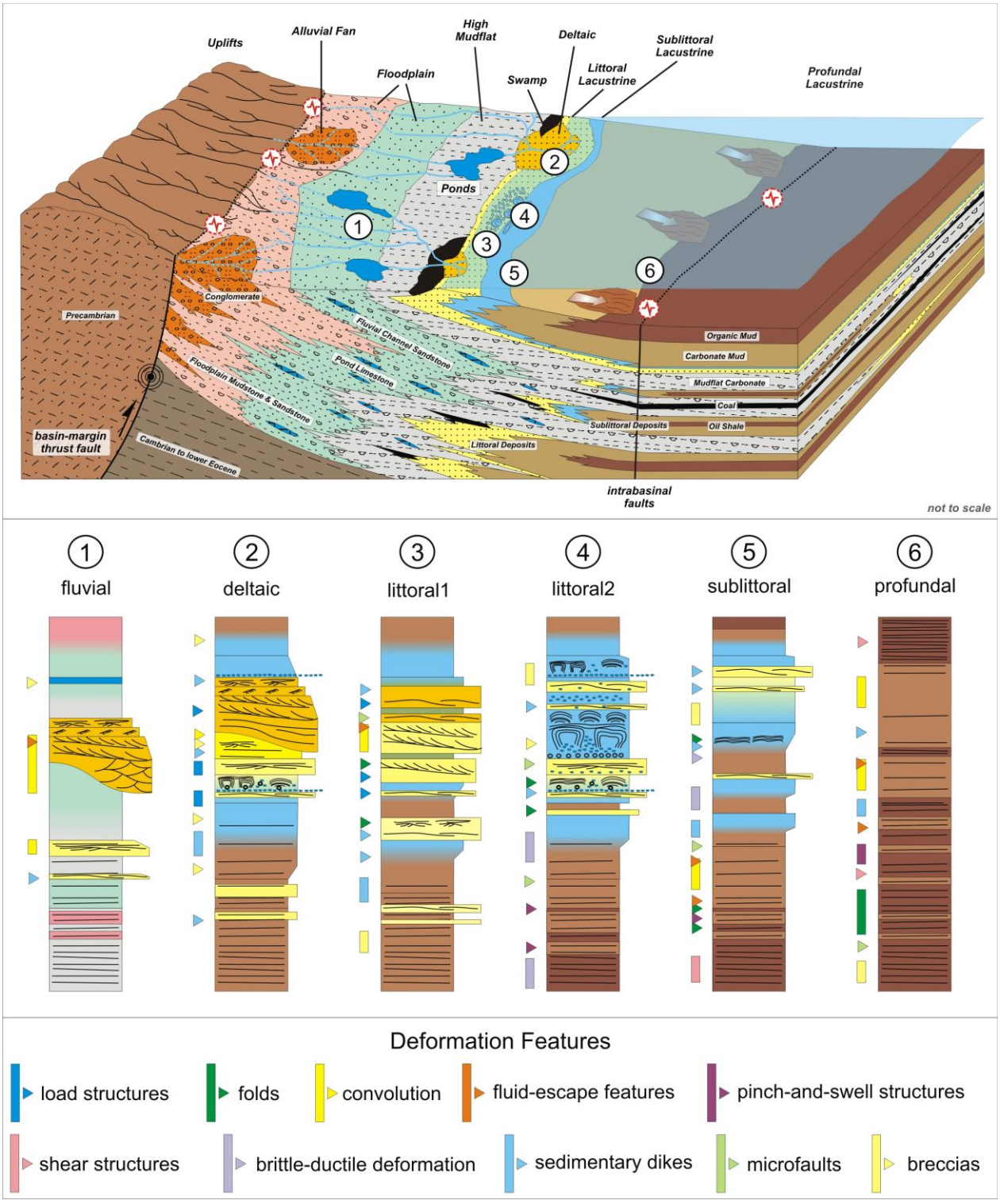


**Figure 4.27** Schematic depositional model for the Green River Formation (modified after Roehler, 1993; Renaut and Gierlowski-Kordesch, 2010) (not to scale), and representative stratigraphic sections for key depositional settings with the distribution of sedimentary deformation features (colored rectangles and triangles).

Small-scale deformation features in carbonate mudstones, previously described as ‘mudcracks’ and taken as evidence for subaerial desiccation, are reinterpreted here as sedimentary dikes triggered by earthquakes subaqueously. This implies that in many cases the magnitude of lake-level changes in the Green River system was not as large as previously thought and the oil shales might have deposited in a more submerged setting.

These seismically induced deformation features (“seismites”), as evidences for syndepositional earthquakes, also indicate that the lake basins of the Green River Formation were frequently affected by tectonic movements along the Sevier Fold and Thrust Belt and the uplifts of the Laramide Orogeny. Moreover, many deformed intervals coincide with regional changes in the depocenter, relative lake level or an abrupt change in lithology. This indicates that syndepositional tectonic events, rather than climate, had a major impact on the Green River system and induced changes in the regional depositional setting and lake character. Although seismites have been widely reported from lacustrine settings, these studies represent the first attempt to integrate deformed horizons with the depositional history of an area in order to understand how syndepositional tectonism might have affected sedimentation and lake chemistry.

These studies show that the detailed analysis of synsedimentary deformation structures can be an integral part of understanding the depositional and tectonic history of a basin, an aspect that is rarely exploited in sedimentological studies. Similarly, earthquake-induced structures (seismites) are hitherto unrecognized archives of tectonic events that should be more widely used to understand the contribution of tectonics on basin evolution, both lacustrine and marine settings.

LIST OF REFERENCES

Alexander, J., 1987, Syn-sedimentary and burial related deformation in the Middle Jurassic non-marine formations of the Yorkshire Basin, *in* Jones, M.E., and Preston, R.M.F., editors, Deformation of Sediments and Sedimentary Rocks: Geological Society of London, Special Publication 29, p. 315–324.

Alfaro, P., Moretti, M., and Soria, J.M., 1997, Soft-sediment deformation structures induced by earthquakes (seismites) in Pliocene lacustrine deposits (Guadix Baza Basin, Central Betic Cordillera): Eclogae Geologicae Helvetiae, v. 90, p. 531–540.

Alfaro, P., Delgado, J., Estévez, A., Molina, J.M., Moretti, M., and Soria, J.M., 2002, Liquefaction and fluidization structures in Messinian storm deposits (Bajo Segura Basin, Betic Cordillera, southern Spain): International Journal of Earth Sciences (Geologische Rundschau), v. 91, p. 505–513.

Alfaro, P., Gibert, L., Moretti, M., García-Tortosa, F.J., Sanz de Galdeano, C., Galindo-Zaldívar, J., and López-Garrido, A.C., 2010, The significance of giant seismites in the Plio-Pleistocene Baza palaeo-lake (S. Spain): Terra Nova, v. 22, p. 172–179.

Allen, J.R.L., 1977, The possible mechanics of convolute lamination in graded sand beds: of the Geological Society of London, Journal, v. 134, p. 19–31.

Allen, J.R.L., 1982, Sedimentary structures: Their character and physical basis, Volume II.: Amsterdam, Elsevier, Developments in Sedimentology, v. 30, 663 p.

Allen, J.R.L., 1986a, On the curl of desiccation polygons: Sedimentary Geology, v. 46, p. 23–31.

Allen, J.R.L., 1986b, Earthquake magnitude-frequency, epicentral distance, and soft-sediment deformation in sedimentary basins: Sedimentary Geology, v. 46, p. 67–75.

Allen, J.R.L., 1987, Desiccation of mud in the temperate intertidal zone: studies form the Severn Estuary and Eastern England: Royal Society of London, Philosophical Transactions, Series B, v. 315, p. 127–156.

Allen, J.R.L., and Banks, N.L., 1972, An interpretation and analysis of recumbent-folded deformed cross-bedding: Sedimentology, v. 19, p. 257–283.

Alsop, G.I., and Marco, S., 2011, Soft-sediment deformation within seismogenic slumps of the Dead Sea Basin: Journal of Structural Geology, v. 33, p. 433–457.

Alsop, G.I., and Marco, S., 2012, Tsunami and seiche-triggered deformation within offshore sediments: Sedimentary Geology, v. 261, p. 90–107.

Ambraseys, N., 1988, Engineering seismology: Earthquake Engineering and Structural Dynamics, v. 17, p. 1–105.

Anand, A., and Jain, A.K., 1987, Earthquakes and deformational structures (seismites) in Holocene sediments from the Himalayan–Andaman Arc, India: Tectonophysics, v. 133, p. 105–120.

Anketell, J.M., Cegła, J., and Dżułyński, S., 1970, On the deformational structures in systems with reversed density gradients: Société Géologique de Pologne, Annales, v. 40, p. 3–30.

Astin, T.R., and Rogers, D.A., 1991, Subaqueous shrinkage cracks in the Devonian of Scotland reinterpreted: Journal of Sedimentary Petrology, v. 61, p. 850–859.

Aswasereelert, W., Meyers, S.R., Carroll, A.R., Peters, S.E., Smith, M.E., and Feigl, K.L., 2013, Basin-scale cyclostratigraphy of the Green River Formation, Wyoming: Geological Society of America Bulletin, v. 125, p. 216–228.

Atwater, B.F., 1987, Evidence for great Holocene earthquakes along the outer coast of Washington State: Science, v. 236, p. 942–944.

Bachmann, G.H., and Aref, M.A.M., 2005, A seismite in Triassic gypsum deposits (Grabfeld Formation, Ladinian), southwestern Germany: Sedimentary Geology, v. 180, p. 75–89.

Bader, J.W., 2008, Structural and tectonic evolution of the Cherokee Ridge arch, south-central Wyoming: Implications for recurring strike-slip along the Cheyenne Belt suture zone: Rocky Mountain Geology, v. 43, p. 23–40.

Bader, J.W., 2009, Structural and tectonic evolution of the Douglas Creek Arch, the Douglas Creek fault zone, and environs, northwestern Colorado and northeastern Utah; implications for petroleum accumulation in the Piceance and Uinta Basins: Rocky Mountain Geology, v. 44, p. 121–145.

Beck, C., Mercier de Lépinay, B., Schneider, J.-L., Cremer, M., Çağatay, N., Wendenbaum, E., Boutareaud, S., Ménot, G., Schmidt, S., Weber, O., Eris, K., Armijo, R., Meyer, B., Pondard, N., Gutscher, M.-A., MARMACORE Cruise Party, Turon, J.-L., Labeyrie, L., Cortijo, E., Gallet, Y., Bouquerel, H., Gorur, N., Gervais, A., Castera, M.-H., Londeix, L., de

Rességuier, A., and Jaouen, A., 2007, Late Quaternary co-seismic sedimentation in the Sea of Marmara's deep basins: Sedimentary Geology, v. 199, p. 65–89.

Beck, C., 2011, Lake sediments as late Quaternary paleoseismic archives: Examples in the northwestern Alps and clues for earthquake-origin assessment of sedimentary disturbances, *in* Audemard, F.A., Michetti, A.M., and McCalpin, J.P., editors, Geological criteria for evaluating paleoseismicity revisited: Forty years of paleoseismic investigations and the natural record of past earthquakes: Geological Society of America, Special Paper 479, p. 159–179.

Becker, A., Colin, A., Davenport, C.A., and Giardini, D., 2002, Palaeoseismicity studies on end-Pleistocene and Holocene lake deposits around Basle, Switzerland: Geophysical Journal International, v. 149, p. 659–678.

Becker, A., Ferry, M., Schnellmann, M., and Giardini, D., 2005, Multiarchive paleoseismic record of late Pleistocene strong earthquakes in Switzerland: Tectonophysics, v. 400, p. 153–157.

Berra, F., and Felletti, F., 2011, Syndepositional tectonics recorded by soft-sediment deformation and liquefaction structures (continental Lower Permian sediments, Southern Alps, Northern Italy): Stratigraphic significance: Sedimentary Geology, v. 235, p. 249–263.

Bhattacharya, H.N., and Bandyopadhyay, S., 1998, Seismites in a Proterozoic tidal succession, Singhbhum, Bihar, India: Sedimentary Geology, v. 119, p. 239–252.

Biaggi, R.E., and Buchheim, H.P., 1999, Paleoecology and paleoenvironments during the initial stages of Eocene Fossil Lake, SW Wyoming, *in* Santucci, V.L., and McClelland, L., editors, National Park Service Paleontological Research, v. 4, p. 54–65.

Birgenheier, L., and Vanden Berg, M., 2011, Core-based integrated sedimentologic, stratigraphic, and geochemical analysis of the oil shale bearing Green River Formation, Uinta Basin, Utah: U.S. Department of Energy, Topical Report, 30 p.

Birnbaum, S.J., and Radlick, T.M., 1982, A textural analysis of trona and associated lithologies, Wilkins Peak Member, Eocene Green River formation, southwestern Wyoming, *in* Handford, C.R., Loucks, R.G., and Davies, G.R., editors, Depositional and diagenetic spectra of evaporites – a core workshop: Society of Economic Paleontologists and Mineralogists, Core Workshop No. 3, Calgary, Canada, p. 75–99.

Bøe, R., Longva, O., Lepland, A., Blikra, L.H., Sønstegaard, E., Haflidason, H., Bryn, P., and Lien, R., 2004, Postglacial mass movements and their causes in fjords and lakes in western Norway: Norwegian Journal of Geology, v. 84, p. 35–55.

Bohacs, K.M., Carroll, A.R. and Neal, J.E., 2003, Lessons from large lake systems—thresholds, nonlinearity, and strange attractors, *in* Chan, M.A., and Archer, A.W., editors, Extreme depositional environments: Mega end members in geologic time: Geological Society of America, Special Papers 370, p. 75–90.

Bohacs, K.M., Carroll, A.R., Neal, J.E. and Mankiewicz, P.J., 2000, Lake-basin type, source potential, and hydrocarbon character: an integrated sequence-stratigraphic–geochemical framework, *in* Gierlowski-Kordesch, E.H., and Kelts, K.R., editors, Lake basins through space and time: American Association of Petroleum Geologists, Studies in Geology 46, p. 3–34.

Borer, J., and McPherson, M., 1998, High-resolution stratigraphy of the Green River Formation, Raven Ridge, northeast Uinta Basin: American Association of Petroleum Geologists, Annual Convention, Field Trip 17, Guidebook, 117 p.

Bouchette, F., Seguret, M., and Moussine-Pouchkine, A., 2001, Coarse carbonate breccias as a result of water-wave cyclic loading (uppermost Jurassic–South-East Basin, France): Sedimentology, v. 48, p. 767–789.

Bowman, D., Korjenkov, A., and Porat, N., 2004, Late-Pleistocene seismites from Lake Issyk-Kul, the Tien Shan range, Kyrghyzstan: Sedimentary Geology, v. 163, p. 211–228.

Boyer, B.W., 1982, Green River laminites—does the playa-lake model really invalidate the stratified lake model?: Geology, v. 10, p. 321–324.

Bradley, M.D., 1995, Timing of the Laramide rise of the Uinta Mountains, Utah and Colorado, *in* Jones, R.W., editor, Resources of southwestern Wyoming: Wyoming Geological Association, 1995 Field Conference Guidebook, p. 31–44.

Bradley, W.H., 1926, Shore phases of the Green River formation in northern Sweetwater County, Wyoming: U.S. Geological Survey, Professional Paper 140-D, p. 121-131.

Bradley, W.H., 1929, The varves and climate of the Green River epoch: U.S. Geological Survey, Professional Paper 158-E, 110 p.

Bradley, W.H., 1930, The behaviour of certain mud crack casts during compaction: American Journal of Science, v. 20, p. 136–144.

Bradley, W.H., 1931, Origin and microfossils of the oil shale of the Green River formation of Colorado and Utah: U.S. Geological Survey, Professional Paper 168, 58 p.

Bradley, W.H., 1964, The geology of the Green River Formation and associated Eocene rocks in southwestern Wyoming and adjacent parts of Colorado and Utah: U.S. Geological Survey, Professional Paper 496-A, 86 p.

Bradley, W.H., 1970, Green River oil shale—concept of origin extended: An interdisciplinary problem being attacked from both ends: Geological Society of America Bulletin, v. 81, p. 985–1000.

Bradley, W.H., 1973, Oil shale formed in desert environment: Green River Formation, Wyoming: Geological Society of America Bulletin, v. 84, p. 1121–1124.

Bradley, W.H., and Eugster, H.P., 1969, Geochemistry and paleolimnology of the trona deposits and associated authigenic minerals of the Green River Formation of Wyoming: U.S. Geological Survey Professional Paper 496-B, 71 p.

Brenchley, P.J., and Newall, G., 1977, The significance of contorted bedding in Upper Ordovician sediments of the Oslo region, Norway: Journal of Sedimentary Petrology, v. 47, p. 819–833.

Buatois, L.A., and Mángano, M.G., 2011, Ichnology: Organism–Substrate Interactions in Space and Time. Cambridge, UK, Cambridge University Press, 358 p.

Buchheim, H.P., 1982, Breccias, mudflows, turbidites, fossil soils, or transposition structures: a case study from the Eocene Green River Formation, Wyoming [abstract]: American Association of Petroleum Geologists Bulletin, v. 66, p. 553.

Buchheim, H.P., 1994a, Eocene Fossil Lake, Green River Formation, Wyoming: A history of fluctuating salinity, *in* Renaut, R.W., and Last, W.M., editors, Sedimentology and Geochemistry of Modern and Ancient Saline Lakes: SEPM (Society for Sedimentary Geology), Special Publication 50, p. 239–247.

Buchheim, H.P., 1994b, Paleoenvironments, lithofacies and varves of the Fossil Butte Member of the Eocene Green River Formation, southwestern Wyoming: University of Wyoming, Contributions to Geology, v. 30, p. 3–14.

Buchheim, H.P., Cushman, R.A., and Biaggi, R.E., 2011, Stratigraphic revision of the Green River Formation in Fossil Basin, Wyoming: Rocky Mountain Geology, v. 46, p. 165–181.

Buchheim, H.P., and Eugster, H.P., 1998, Eocene Fossil Lake: The Green River Formation of Fossil Basin, southwestern Wyoming, *in* Pitman, J.K., and Carroll, A.R., editors., Modern and Ancient Lake Systems; New Problems and Perspectives: Utah Geological Association, Publication 26, p. 191–207.

Burst, J.F., 1965, Subaqueously formed shrinkage cracks in clay: Journal of Sedimentary Petrology, v. 35, p. 348–353.

Burton, D., Woolf, K., and Sullivan, B., 2014, Lacustrine depositional environments in the Green River Formation, Uinta Basin: Expression in outcrop and wireline logs: American Association of Petroleum Geologists Bulletin, v. 98, p. 1699–1715.

Calvo, J.P., Rodríguez-Pascua, M., Martín-Velázquez, S., Jiménez, S., and De Vicente, G., 1998, Microdeformation of lacustrine laminite sequences from Late Miocene formations of SE Spain: An interpretation of loop bedding: Sedimentology, v. 45, p. 279−292.

Carrillo, E., Audemard, F.A., Beck, C., Cousin, M., Jouanne, F., Cano, V., Castilla, R., Melo, L., and Villemin, T., 2006, A late Pleistocene natural seismograph along the Boconó fault (Mérida Andes, Venezuela): The moraine dammed Los Zerpa paleo-lake: Société Géologique de France, Bulletin, v. 177, p. 3–17.

Carroll, A.R., and Bohacs, K.M., 1999, Stratigraphic classification of ancient lakes: Balancing tectonic and climatic controls: Geology, v. 27, p. 99–102.

Carroll, A.R., Chetel, L.M., and Smith, M.E., 2006, Feast to famine: Sediment supply control on Laramide basin fill: Geology, v. 34, p. 197–200.

Carroll, A.R., Doebbert, A.C., Booth, A.L., Chamberlain, C.P., Rhodes-Carson, M.K., Smith, M.E., Johnson, C.M., and Beard, B.L., 2008, Capture of high-altitude precipitation by a low-altitude Eocene lake, western U.S.: Geology, v. 36, p. 791–794.

Cashion, W.B., 1967, Geology and fuel resources of the Green River Formation, southeastern Uinta Basin, Utah and Colorado: U.S. Geological Survey Professional Paper 548, 48 p.

Cashion, W.B., and Donnell, J.R., 1972, Chart showing correlation of selected key units in the organic-rich sequence of the Green River Formation, Piceance Creek Basin, Colorado, and Uinta Basin, Utah: U.S. Geological Survey Oil and Gas Investigations Chart OC-65, 1 plate.

Cashion, W.B., and Donnell, J.R., 1974, Revision of nomenclature of the upper part of the Green River Formation, Piceance Creek Basin, Colorado, and eastern Uinta Basin, Utah: U.S. Geological Survey Bulletin 1394-G, 9 p.

Castilla, R.A., and Audemard, F.A., 2007, Sand blows as a potential tool for magnitude estimation of pre-instrumental earthquakes: Journal of Seismology, v. 11, p. 483–487.

Castle, J.W., 1990, Sedimentation in Eocene Lake Uinta (lower Green River Formation), northeastern Uinta Basin, Utah, *in* Katz, B.J., editor, Lacustrine Basin Exploration—Case Studies and Modern Analogues: American Association of Petroleum Geologists, Memoir 50, p. 243–263.

Chapron, E., Beck, C., Pourchet, M., and Deconinck, J.-F., 1999, 1822 AD earthquake-triggered homogenite in Lake Le Bourget (NW Alps): Terra Nova, v. 11, p. 86–92.

Chen, J., Chough, S.K., Chun, S.S., and Han, Z., 2009, Limestone pseudoconglomerates in the Late Cambrian Gushan and Chaomidian Formations (Shandong Province, China): soft-sediment deformation induced by storm-wave loading: Sedimentology, v. 56, p. 1174–1195.

Chen, J., and Lee, H.S., 2013, Soft-sediment deformation structures in Cambrian siliciclastic and carbonate storm deposits (Shandong Province, China): differential liquefaction and fluidization triggered by storm-wave loading: Sedimentary Geology, v. 288, p. 81–94.

Chetel, L.M., and Carroll, A.R., 2010, Terminal infill of Eocene Lake Gosiute, Wyoming, USA: Journal of Sedimentary Research, v. 80, p. 492–514.

Cheel, R.J., and Rust, B.R., 1986, A sequence of soft-sediment deformation (dewatering) structures in Late Quaternary subaqueous outwash near Ottawa, Canada: Sedimentary Geology, v. 47, p. 77–93.

Chunga, K., Livio, F., Michetti, A.M., and Serva, L., 2007, Synsedimentary deformation of Pleistocene glaciolacustrine deposits in the Albese con Cassano Area (Southern Alps, Northern Italy), and possible implications for paleoseismicity: Sedimentary Geology, v. 196, p. 59–80.

Cohen, A.S., 2003, Paleolimnology: The History and Evolution of Lake Systems. Oxford University Press, Oxford, 528 p.

Cohen, A., McGlue, M.M., Ellis, G.S., Zani, H., Swarzenski, P.W., Assine, M.L. and Silva, A., 2015, Lake formation, characteristics, and evolution in retroarc deposystems: A synthesis of

the modern Andean orogen and its associated basins, *in* DeCelles, P.G., Ducea, M.N., Carrapa, B., and Kapp, P.A., editors, Geodynamics of a Cordilleran Orogenic System: The Central Andes of Argentina and Northern Chile: Geological Society of America, Memoir 212, p. 309–335.

Cole, R.D., and Picard, M.D., 1975, Primary and secondary sedimentary structures in oil shale and other fine-grained rocks, Green River Formation (Eocene), Utah and Colorado: Utah Geology, v. 2, p. 49–67.

Cole, R.D., and Picard, M.D., 1978, Comparative mineralogy of nearshore and offshore lacustrine lithofacies, Parachute Creek Member of the Green River Formation, Piceance Creek basin, Colorado, and eastern Uinta Basin, Utah: Geological Society of America Bulletin, v. 89, p. 1441–1454.

Coogan, J.C., 1992, Structural evolution of piggyback basins in the Wyoming-Idaho-Utah thrust belt, *in* Link, P.K., Kentz, M.A., and Platt, L.B., editors, Regional Geology of Eastern Idaho and Western Wyoming: Geological Society of America, Memoir 179, p. 55–81.

Cowan, C.A., and James, N.P., 1992, Diastasis cracks: Mechanically generated synaeresis-like cracks in Upper Cambrian shallow water oolite and ribbon carbonates: Sedimentology, v. 39, p. 1101–1118.

Cumming, V.M., Selby, D., and Lillis, P.G., 2012, Re–Os geochronology of the lacustrine Green River Formation: Insights into direct depositional dating of lacustrine successions, Re–Os systematics and paleocontinental weathering: Earth and Planetary Science Letters, v. 359–360, p. 194–205.

Daley, B., 1971, Diapiric and other deformational structures in an Oligocene argillaceous limestone: Sedimentary Geology, v. 6, p. 29–51.

Dalrymple, R.W., 1979, Wave-induced liquefaction—A modern example from the Bay of Fundy: Sedimentology, v. 26, p. 835–844.

Dalrymple, R.W., 1980, Wave-induced liquefaction: an addendum: Sedimentology, v. 27, p. 461.

Dane, C.H., 1954, Stratigraphic and facies relationships of the upper part of the Green River Formation and lower part of the Uinta Formation in Duchesne, Uintah, and Wasatch counties, Utah: American Association of Petroleum Geologists Bulletin, v. 38, p. 405–425.

Dasgupta, P., 1998, Recumbent flame structures in the Lower Gondwana rocks of the Jharia Basin, India—a plausible origin: Sedimentary Geology, v. 119, p. 253–261.

Davenport, C.A., and Ringrose, P.S., 1987, Deformation of Scottish Quaternary sediment sequences by strong earthquake motion, *in* Jones, M.E., and Preston, R.M.F., editors, Deformation of Sediments and Sedimentary Rocks: Geological Society of London, Special Publication 29, p. 299–314.

Davison, I., 1987, Normal fault geometry related to sediment compaction and burial: Journal of Structural Geology, v. 9, p. 393–401.

Davis, S.J., Wiegand, B.A., Carroll, A.R., and Chamberlain, C.P., 2008, The effect of drainage reorganization on paleoaltimetry studies: an example from the Paleogene Laramide foreland: Earth and Planetary Science Letters, v. 275, p. 258–268.

Davis, S.J., Mix, H.T., Wiegand, B.A., Carroll, A.R., and Chamberlain, C.P., 2009, Synorogenic evolution of large-scale drainage patterns: Isotope paleohydrology of sequential Laramide basins: American Journal of Science, v. 309, p. 549–602.

Deardorff, D.L., and Mannion, L.E., 1971, Wyoming trona deposits: University of Wyoming, Contributions to Geology, v. 10, p. 25–37.

DeCelles, P.G., 1994, Late Cretaceous–Paleocene synorogenic sedimentation and kinematic history of the Sevier thrust belt, northeast Utah and southwest Wyoming: Geological Society of America Bulletin, v. 106, p. 32–56.

DeCelles, P.G., 2004, Late Jurassic to Eocene evolution of the Cordilleran thrust belt and foreland basin system, western U.S.A.: American Journal of Science, v. 304, p. 105–168.

Demicco, R.V., 1985, Platform and off-platform carbonates of the Upper Cambrian of western Maryland, U.S.A.: Sedimentology, v. 32, p. 1–22.

Demicco, R.V., and Hardie, L.A., 1994, Sedimentary structures and early diagenetic features of shallow marine carbonate deposits: SEPM (Society for Sedimentary Geology) Atlas Series, v. 1., Tulsa, 265 p.

Desborough, G.A., 1978, A biogenic-chemical stratified lake model of the origin of oil shale of the Green River Formation: an alternative to the playa-lake model: Geological Society of America Bulletin, v. 89, p. 961–971.

Deville, E., Guerlais, S.-H., Lallemant, S., and Schneider, F., 2010, Fluid dynamics and subsurface sediment mobilization processes: an overview from Southeast Caribbean. Basin Research, v. 22, p. 361–379.

Deynoux, M., Proust, J.N., Durand, J., and Merino, E., 1990, Water-transfer cylindrical structures in the Late Proterozoic eolian sandstones in the Taoudeni Basin, West Africa: Sedimentary Geology, v. 66, p. 227–242.

Dickinson, W.R., Klute, M.A., Hayes, M.J., Janecke, S.U., Lundin, E.R., McKittrick, M.A., and Olivares, M.D., 1988, Paleogeographic and paleotectonic setting of Laramide sedimentary basins in the central Rocky Mountain region: Geological Society of America Bulletin, v. 100, p. 1023–1039.

Doebbert, A.C., Carroll, A.R., Mulch, A., Chetel, L.M., and Chamberlain, C.P., 2010, Geomorphic controls on lacustrine isotopic compositions: evidence from the Laney Member, Green River Formation, Wyoming: Geological Society of America Bulletin, v. 122, p. 236–252.

Doebbert, A.C., Johnson, C.M., Carroll, A.R., Beard, B.L., Pietras, J.T., Rhodes-Carson, M.K., Norsted, B., and Throckmorton, L.A., 2014, Controls on Sr isotopic evolution in lacustrine systems: Eocene Green River Formation, Wyoming: Chemical Geology, v. 380, p. 172–189.

Donovan, R.N., and Foster, R.J., 1972, Subaqueous shrinkage cracks from the Caithness Flagstone series (Middle Devonian) of northeast Scotland: Journal of Sedimentary Petrology, v. 42, p. 309–317.

Dorr, J.A., and Gingerich, P.D., 1980, Early Cenozoic mammalian paleontology, geologic structure, and tectonic history in the overthrust belt near LaBarge, western Wyoming: Rocky Mountain Geology, v. 18, p. 101–115.

Draganits, E., Grasemann, B., and Schmid, H.P., 2003, Fluidization pipes and spring pits in a Gondwanan barrier-island environment: groundwater phenomenon, palaeo-seismicity or a combination of both?, *in* Van Rensbergen, P., Hillis, R.R., Maltman, A.J., and Morley, C.K., editors, Subsurface Sediment Mobilization: Geological Society of London, Special Publication 216, p. 109–121.

Dyni, J.R., 1981, Geology of the nahcolite deposits and associ-ated oil shales of the Green River Formation in the Piceance Creek Basin, Colorado: Boulder, University of Colorado, Ph.D. Thesis, 144 p.

Dyni, J.R., 1996, Sodium carbonate resources of the Green River Formation: U.S. Geological Survey Open-File Report 96–729, 39 p.

Dyni, J.R., and Hawkins, J.E., 1981, Lacustrine turbidites in the Green River Formation, northwestern Colorado: Geology, v. 9, p. 235–238.

Dyni, J.R., Wiig, S.V., and Grundy, W.D., 1995, Trona resources in southwest Wyoming: Non-renewable Resources, v. 4, p. 340–352.

El-Isa, Z.H., and Mustafa, H., 1986, Earthquake deformations in the Lisan deposits and seismotectonic implications: Geophysical Journal of Royal Astronomical Society, v. 86, p. 413–424.

El Taki, H., and Pratt, B.R., 2012, Syndepositional tectonic activity in an epicontinental basin revealed by deformation of subaqueous carbonate laminites and evaporites: Seismites in Red River strata (Upper Ordovician) of southern Saskatchewan, Canada: Bulletin of Canadian Petroleum Geology, v. 60, p. 37–58.

Eriksson, P.G., Schieber, J., Bouougri, E., Gerdes, G., Porada, H., Banerjee, S., Bose, P.K., and Sarkar, S., 2007a, Classification of structures left by microbial mats in their host sediments, *in* Schieber, J., Bose, P.K., Eriksson, P.G., Banerjee, S., Sarkar, S., Altermann, W., and Catuneanu, O., editors, Atlas of Microbial Mat Features Preserved within the Siliciclastic Rock Record: Amsterdam, Elsevier, Atlases in Geoscience, v. 2., p. 39–52.

Eriksson, P.G., Porada, H., Banerjee, S., Bouougri, E., Sarkar, S., Bumby, A.J., 2007b, Mat destruction features, *in* Schieber, J., Bose, P.K., Eriksson, P.G., Banerjee, S., Sarkar, S., Altermann, W., and Catuneanu, O., editors, Atlas of Microbial Mat Features Preserved within the Siliciclastic Rock Record: Amsterdam, Elsevier, Atlases in Geoscience, v. 2. p. 76–105.

Ettensohn, F.R., Kulp, M.A., and Rast, N., 2002, Interpreting ancient marine seismites and apparent epicentral areas for paleo-earthquakes, Middle Ordovician Lexington Limestone, central Kentucky, *in* Ettensohn, F.R., Rast, N., and Brett, C.E., editors, Ancient Seismites: Geological Society of America, Special Paper 359, p. 177–190.

Ettensohn, F.R., Zhang, C., Gao, L., and Lierman, R.T., 2011, Soft-sediment deformation in epicontinental carbonates as evidence of paleoseismicity with evidence for a possible new seismogenic indicator: Accordion folds: Sedimentary Geology, v. 235, p. 222–233.

Eugster, H.P., and Hardie, L.A., 1975, Sedimentation in an ancient playa-lake complex: the Wilkins Peak Member of the Green River Formation of Wyoming: Geological Society of America Bulletin, v. 86, p. 319–334.

Eugster, H.P., and Surdam, R.C., 1973, Depositional environment of the Green River Formation of Wyoming: A preliminary report: Geological Society of America Bulletin, v. 84, p. 1115–1120.

Eyles, N., and Clark, B.M., 1985, Gravity-induced soft-sediment deformation in glaciomarine sequences of the Upper Proterozoic Port Askaig Formation, Scotland: Sedimentology, v. 32, p. 789–814.

Ferrill, D.A., and Morris, A.P., 2003, Dilational normal faults: Journal of Structural Geology, v. 25, p. 183–196.

Field, M.E., Gardner, V., Jennings, A.E., and Edwards, B.D., 1982, Earthquake-induced sediment failures on a 0.25° slope, Klamath River delta, California: Geology, v. 10, p. 542–546.

Fortuin, A.R., and Dabrio, C.J., 2008, Evidence for Late Messinian seismites, Níjar Basin, south-east Spain: Sedimentology, v. 55, p. 1595−1622.

Fouch, T.D, 1975, Lithofacies and related hydrocarbon accumulations in Tertiary strata of the western and central Uinta basin, Utah, *in* Bolyard, D.W., editor, Symposium on Deep Drilling Frontiers in the Central Rocky Mountains: Rocky Mountain Associations of Geologists, p. 163–173.

Fouch, T.D., Nuccio, V.F., Anders, D.E., Rice, D.D., Pitman, J.K., and Mast, R.F., 1994, Green River (!) petroleum system, Uinta Basin, Utah, USA, *in* Magoon, L.B., and Dow, W.G., editors, The Petroleum System—From Source to Trap: American Association of Petroleum Geologists, Memoir 60, p. 399–421.

Fouch, T.D., Nuccio, V.F., Osmond, J.C., MacMillan, L., Cashion, W.B., and Wandrey, C.J., 1992, Oil and gas in uppermost Cretaceous and Tertiary rock, Uinta Basin, Utah, *in* Fouch, T.D., Nuccio, V.F., and Chidsey, T.C., editors, Hydrocarbon and Mineral Resources of the Uinta Basin, Utah and Colorado: Utah Geological Association, Publication 20, p. 9–47.

Franczyk, K.J., Fouch, T.D., Johnson, R.C., Molenaar, C.M., and Cobban, W.A., 1992, Cretaceous and Tertiary paleogeographic reconstructions for the Uinta–Piceance basin study area: U.S. Geological Survey Bulletin B-1787-Q, p. 1–37.

Franczyk, K.J., Hanley, J.H., Pitman, J.K., and Nichols, D.J., 1991, Paleocene depositional systems in the western Roan Cliffs, Utah, *in* Chidsey, T.C., Jr., editor, Geology of East-Central Utah: Utah Geological Association, Publication 19, p. 111–127.

Frantz, C.M., Petryshyn, V.A., Marenco, P.J., Tripati, A., Berelson, W.M., and Corsetti, F.A., 2014, Dramatic local environmental change during the Early Eocene Climatic Optimum detected using high resolution chemical analyses of Green River Formation stromatolites: Palaeogeography, Palaeoclimatology, Palaeoecology, v. 405, p. 1–15.

Friedman, G.M., 1997, Dissolution-collapse breccias and paleokarst resulting from dissolution of evaporite rocks, especially sulfates: Carbonates and Evaporites, v. 12, p. 53–63.

García-Tortosa, F.J., Alfaro, P., Gibert, L., and Scott, G., 2011, Seismically induced slump on an extremely gentle slope (<1°) of the Pleistocene Tecopa paleolake (California): Geology, v. 39, p. 1055–1058.

Galli, P., 2000, New empirical relationships between magnitude and distance for liquefaction: Tectonophysics, v. 324, p. 169–187.

García-Tortosa, F.J., Alfaro, P., Gibert, L., and Scott, G., 2011, Seismically induced slump on an extremely gentle slope (<1°) of the Pleistocene Tecopa paleolake (California): Geology, v. 39, p. 1055–1058.

Goodwin, J.H., 1973, Analcime and K-feldspar in tuffs of the Green River Formation, Wyoming: American Mineralogist, v. 58, p. 93–105.

Goodwin, J.H., and Surdam, R.C., 1967, Zeolitization of tuffaceous rocks of the Green River Formation, Wyoming: Science, v. 157, p. 307–308.

Grabowski, G.J., Jr., and Pevear, D.R., 1985, Sedimentology and petrology of profundal lacustrine sediments, Mahogany Zone of the Green River Formation, Piceance Creek Basin, northwest Colorado, *in* Crevello, P.D., and Harris, P.M., editors, Deep-Water Carbonates: Buildups, Turbidites, Debris Flows and Chalk. A core workshop: Society of Economic Paleontologists and Mineralogists, Core Workshop 6, p. 386–430.

Greb, S.F., and Archer, A.W., 2007, Soft-sediment deformation produced by tides in a meizoseismic area, Trunagain Arm, Alaska: Geology, v. 35, p. 435–438.

Greb, S.F., and Dever, G., 2002, Critical evaluation of possible seismites; examples from the Carboniferous of the Appalachian Basin, *in* Ettensohn, F.R., Rast, N., and Brett, C.E., editors, Ancient Seismites: Geological Society of America, Special Paper 359, p. 109–125.

Griggs, R.L., 1968, Altered tuffaceous rocks of the Green River Formation in the Piceance Creek Basin, Colorado: U.S. Geological Survey Open-File Report 68-113, 38 p., 3 plates.

Grimm, K.A., and Orange, D.L., 1997, Synsedimentary fracturing, fluid migration, and subaqueous mass wasting: intrastratal microfractured zones in laminated diatomaceous sediments, Miocene Monterey Formation, California, USA: Journal of Sedimentary Research, v. 67, p. 601–613.

Groeger, A., and Bruhn, R., 2001, Structure and geomorphology of the Duchesne graben, Uinta Basin, Utah, and its enhancement of a hydrocarbon reservoir: American Association of Petroleum Geologists Bulletin, v. 85, p. 1661–1678.

Guhman, A.I., and Pederson, D.T., 1992, Boiling sand springs, Dismal River, Nebraska: Agents for formation of vertical cylindrical structures and geomorphic change: Geology, v. 20, p. 8–10.

Guiraud, M., and Plaziat, J.-C., 1993, Seismites in the fluviatile Bima sandstones: identification of paleoseisms and discussion of their magnitudes in a Cretaceous synsedimentary strike-slip basin (Upper Benue, Nigeria): Tectonophysics, v. 225, p. 493–522.

Guiraud, M., and Séguret, M., 1987, Soft-sediment microfaulting related to compaction within the fluvio-deltaic infill of the Soria strike-slip basin (northern Spain), *in* Jones, M., and Preston, R.M.F., editors, Deformation of Sediments and Sedimentary Rocks: Geological Society of London, Special Publication 29, p. 123–136.

Gulliver, T., 2006, Clastic dikes in the Parachute Creek Member, *in* Proceedings of the 26th Oil Shale Symposium, Colorado School of Mines, Golden, Colorado, 7 p.

Handford, C.R., Kendall, A.C., Prezbindowski, D.R., Dunham, J.B., and Logan, B.W., 1984, Salina-margin tepees, pisoliths, and aragonite cements, Lake MacLeod, Western Australia: their significance in interpreting ancient analogs: Geology, v. 12, p. 523–527.

Harazim, D., Callow, R.H.T., and McIlroy, D., 2013, Microbial mats implicated in the generation of intrastratal shrinkage ('synaeresis') cracks: Sedimentology, v. 60, p. 1621–1638.

Harris, R.C., 2004, Giant desiccation cracks in Arizona: Arizona Geology, v. 34, p. 1–4.

Hempton, M.R., and Dewey, J.F., 1983, Earthquake-induced deformational structures in young lacustrine sediments, East Anatolian Fault, southeast Turkey: Tectonophysics, v. 98, p. 7–14.

Hesselbo, J., and Trewin, N., 1984, Deposition, diagenesis and structures of the Cheese Bay shrimp bed, Lower Carboniferous, East Lothian: Scottish Journal of Geology, v. 20, p. 281–296.

Hibsch, C., Alvarado, A., Yepes, H., Perez, V.H., and Sébrier, M., 1997, Holocene liquefaction and soft-sediment deformation in Quito (Ecuador): A palaeoseismic history recorded by lacustrine sediments: Journal of Geodynamics, v. 24, p. 259–280.

Hildebrandt, C., and Egenhoff, S., 2007, Shallow-marine massive sandstone sheets and indicators of palaeoseismic liquefaction – An example from the Ordovician shelf of Central Bolivia: Sedimentary Geology, v. 202, p. 581–595.

Hiscott, R.N., and James, N.P., 1985, Carbonate debris flows, Cow Head Group, western Newfoundland: Journal of Sedimentary Petrology, v. 55, p. 735–745.

Holzer, T.M., and Clark, M.M., 1993, Sand boils without earthquakes: Geology, v. 21, p. 873–876.

Hurst, A., Cartwright, J.A., and Duranti, D., 2003, Fluidization structures in sandstone produced by upward injection through a sealing lithology, *in* Van Rensbergen, P., Hillis, R.R., Maltman, A.J., and Morley, C.K., editors, Subsurface Sediment Mobilization: Geological Society of London, Special Publication 216, p. 123–137.

Hurst, A., Scott, A., and Vigorito, M., 2011, Physical characteristics of sand injectites: Earth-Science Reviews, v. 106, p. 215–246.

Huuse, M., Jackson, C.A.-L., Van Rensbergen, P., Davies, R.J., Flemings, P.B., and Dixon, R.J., 2010, Subsurface sediment remobilization and fluid flow in sedimentary basins: an overview: Basin Research, v. 22, p. 342–360.

Iijima, A., and Hay, R.L., 1968, Analcime composition in tufts of the Green River Formation of Wyoming: American Mineralogist, v. 53, p. 184–200.

Ishihara, K., 1993, Liquefaction and flow failure during earthquakes: Géotechnique, v. 43, p. 351–415.

Jagniecki, E., Jenkins, D.M., Lowenstein, T.K., and Carroll, A.R., 2013, Experimental study of shortite ($Na_2Ca_2(CO_3)_3$) formation and application to the burial history of the Wilkins Peak Member, Green River Basin, Wyoming, USA: Geochimica et Cosmochimica Acta, v. 115, p. 31–45.

Johnson, R.C., 1981, Stratigraphic evidence for a deep Eocene Lake Uinta, Piceance Creek Basin, Colorado: Geology, v. 9, p. 55–62.

Johnson, R.C., and Finn, T.M., 1986, Cretaceous through Holocene history of the Douglas Creek arch, Colorado and Utah, *in* Stone, D. S., editor, New Interpretations of Northwest Colorado Geology: Rocky Mountain Association of Geologists, p. 77–95.

Johnson, R.C., Nichols, D.J., and Hanley, J.H., 1988, Stratigraphic sections of Lower Tertiary strata and charts showing palynomorph and mollusc assemblages, Douglas Creek arch area, Colorado and Utah: U.S. Geological Survey Miscellaneous Field Studies Map MF–1997, 2 sheets.

Johnson, R.C., Mercier, T.J., Brownfield, M.E., and Self, J.G., 2010a, Assessment of in-place oil shale resources in the Green River Formation, Uinta Basin, Utah and Colorado: U.S. Geological Survey Digital Data Series DDS–69–BB, chap. 1, 153 p.

Johnson, R.C., Mercier, T.J., Brownfield, M.E., Pantea, M.P., and Self, J.G., 2010b, An assessment of in-place oil shale resources in the Green River Formation, Piceance Basin, Colorado: U.S. Geological Survey Digital Data Series DDS–69–Y, chap. 1, 187 p.

Johnston, R.E., and Yin, A., 2001, Kinematics of the Uinta fault system (southern Wyoming and northern Utah) during the Laramide orogeny: International Geology Review, v. 43, p. 52–68.

Jolly, J.H.R., and Lonergan, L., 2002, Mechanisms and control on the formation of sand intrusions: Geological Society of London, Journal, v. 159, p. 605–617.

Jones, A.P., and Omoto, K., 2000, Towards establishing criteria for identifying trigger mechanisms for soft-sediment deformation: a case study of Late Pleistocene lacustrine sands and clays, Onikobe and Nakayamadaira Basins, northeastern Japan: Sedimentology, v. 47, p. 1211–1226.

Kahle, C.F., 2002, Seismogenic deformation structures in microbialites and mudstones, Silurian Lockport Dolomite, northwestern Ohio, U.S.A.: Journal of Sedimentary Research, v. 72, p. 201−216.

Karlin, R.E., and Abella, S.E.B., 1992, Paleoearthquakes in the Pugeot Sound Region recorded in sediments from lake Washington, U.S.A.: Science, v. 258, p. 1617–1619.

Kastens, K., and Cita, M.B., 1981, Tsunami-induced sediment transport in the abyssal Mediterranean Sea: Geological Society of America Bulletin, v. 92, p. 845–857.

Keefer, D.K., 1984, Landslides caused by earthquakes: Geological Society of America Bulletin, v. 95, p. 406–421.

Keighley, D., 2013, Outcrop chemostratigraphic correlation of the upper Green River Formation in the Uinta Basin, Utah – Mahogany oil shale zone to the Uinta Formation: Utah Geological Survey Miscellaneous Publication 13-01, 34 p.

Keighley, D., Flint, S., Howell, J., Andersson, D., Collins, S., Moscariello, A., and Stone, G., 2002, Surface and subsurface correlation of the Green River Formation in central Nine Mile Canyon, SW Uinta basin, Carbon and Duchesne counties, east-central Utah: Utah Geological Society Miscellaneous Publication 02-1, 66 p.

Keighley, D., Flint, S., Howell, J. and Moscariello, A., 2003, Sequence stratigraphy in lacustrine basins: a model of the Green River Formation (Eocene), southwest Uinta Basin, Utah, U.S.A.: Journal of Sedimentary Research, v. 73, p. 987–1006.

Keighley, D., and Vanden Berg, M., 2013, Where have the Mahogany Oil-Shale beds gone?: Possible evidence of large-scale slumping at Sand Wash, Uinta Basin, Utah [abs.]: American Association of Petroleum Geologists Database/Search and Discovery Article #90169.

Keighley, D., Törő, B., Vanden Berg, M., and Pratt, B.R., in press, Deformation within the Mahogany Oil Shale Zone of the Green River Formation at Sand Wash, eastern Utah, USA., *in* Birgenheier, L., Vanden Berg, M., and Ressetar, R., editors, The Uinta Basin and Uinta Mountains: Utah Geological Association Guidebook.

Kendall, C.G.St.C., and Warren, J., 1987, A review of the origin and setting of tepees and their associated fabrics: Sedimentology, v. 34, p. 1007–1027.

Kerr, M., and Eyles, N., 1991, Storm-deposited sandstones (tempestites) and related ichnofossils of the Late Ordovician Georgian Bay Formation, southern Ontario, Canada: Canadian Journal of Earth Sciences, v. 28, p. 266–282.

Kidder, D.L., 1990, Facies-controlled shrinkage-crack assemblages in Middle Proterozoic mudstones from Montana, USA: Sedimentology, v. 37, p. 943–951.

Klappa, C.F., 1980, Rhizoliths in terrestrial carbonates: classification, recognition, genesis and significance: Sedimentology, v. 27, p. 613–629.

Kleist, J.R., 1974, Deformation by soft-sediment extension in the coastal belt, Franciscan Complex: Geology, v. 2, p. 501–504.

Koç Taşgin, C., Orhan, H., Türkmen, I., and Aksoy, E., 2011, Soft-sediment deformation structures in the late Miocene Şelmo Formation around Adiyaman area, Southeastern Turkey: Sedimentary Geology, v. 235, p. 277–291.

Kuenen, P.H., 1953, Graded bedding with observations on the Lower Palaeozoic rocks of Britain: Koninklijke Nederlandsche Akademie van Wetenschappen, Verhandelingen, v. 20, p. 1–47.

Kuenen, P.H., 1958, Experiments in geology: Transactions of the Geological Society of Glasgow, v. 23, p. 1–37.

Lamerson, P.R., 1982, The Fossil Basin and its relationship to the Absaroka Thrust system, Wyoming and Utah, *in* Powers, R.B., editor, Geologic Studies of the Cordilleran Thrust Belt: Rocky Mountain Association of Geologists, 33rd Annual Field Conference, v. 1, p. 279–340.

Lan, Z.W., and Chen, Z.Q., 2012, Exceptionally preserved microbially induced sedimentary structures from the Ediacaran post-glacial successions in the Kimberley region, northwestern Australia: Precambrian Research, v. 200-203, p. 1–25.

Lan, Z.W., and Chen, Z.Q., 2013, Proliferation of MISS-forming microbial mats after the late Neoproterozoic glaciations: evidence from the Kimberley region, NW Australia: Precambrian Research, v. 224, p. 529–550.

Larsson, R., 1990, Behaviour of organic clay and gyttja: Rapport, Statens Geotekniska Institut, v. 38, 125 p.

Last, F.M., Last, W.M., and Halden, N.M., 2010, Carbonate microbialites and hardgrounds from Manito Lake, an alkaline, hypersaline lake in the northern Great Plains of Canada: Sedimentary Geology, v. 225, p. 34–49.

Ledésert, B., Buret, C., Chanier, F., Ferrière, J., and Recourt, P., 2003, Tubular structures of northern Wairarapa (New Zealand) as possible examples of ancient fluid expulsion in an accretionary prism: evidence from field and petrographical observations, *in* Van Rensbergen, P., Hillis, R.R., Maltman, A.J. and Morley, C.K., editors, Subsurface Sediment Mobilization: Geological Society of London, Special Publication 216, p. 95–107.

Lee, R.K.L., Owen, R.B., Renaut, R.W., Behrensmeyer, A.K., Potts, R. and Sharp, W., 2013, Facies, geochemistry and diatoms of late Pleistocene Olorgesailie tufas, southern Kenya Rift: Palaeogeography, Palaeoclimatology, Palaeoecology, v. 374, p. 197–217.

Leeder, M.R., 1987, Sediment deformation structures and palaeotectonic analysis of sedimentary basins, with a case-study from the Carboniferous of northern England, *in* Jones, M.E., and Preston, R.M.F., editors, Deformation of Sediments and Sedimentary Rocks: Geological Society of London, Special Publication 29, p. 137–146.

Leigh, R.T., 1991, Wyoming trona: an overview of the geology and economic utilization: Wyoming Geological Association Guidebook, 42nd Field Conference, p. 103–120.

Leroy, S., Kazanc, N., Ileri, O., Kibar, M., Emre, O., McGee, E., and Griffiths, H.I., 2002, Abrupt environmental changes within a late Holocene lacustrine sequence south of the Marmara Sea (Lake Manyas, N-W Turkey): possible links with seismic events: Marine Geology, v. 190, p. 531–552.

Lewis, K.B., 1971, Slumping on a continental slope inclined at 1°–4°: Sedimentology, v. 16, p. 97–110.

Li, Y., Craven, J., Schweig, S. and Obermeier, S.F., 1996, Sand boils induced by the 1993 Mississippi River food: could they one day be misinterpreted as earthquake-induced liquefaction?: Geology, v. 24, p. 171–174.

Love, J.D., 1970, Cenozoic geology of the Granite Mountains area, central Wyoming: U.S. Geological Survey Professional Paper 495-C, 154 p.

Lowe, D.R., 1975, Water-escape structures in coarse-grained sediments: Sedimentology, v. 22, p. 157–204.

Lundell, L.L., and Surdam, R.C., 1975, Playa lake deposition: Green River Formation, Piceance Creek Basin, Colorado: Geology, v. 3, p. 493–497.

M'Gonigle, J.W., and Dover, J.H., 1992, Geologic map of the Kemmerer 30' x 60' Quadrangle, Lincoln, Uinta, and Sweetwater Counties, Wyoming: U.S. Geological Survey, Miscellaneous Investigations Series, Map I-2079, scale 1: 100,000.

Machlus, M.L., Olsen, P.E., Christie-Blick, N., and Hemming, S.R., 2008, Spectral analysis of the lower Eocene Wilkins Peak Member, Green River Formation, Wyoming: Support for Milankovitch cyclicity: Earth and Planetary Science Letters, v. 268, p. 64–75.

Maltman, A., 1984, On the term 'soft-sediment deformation': Journal of Structural Geology, v. 6, p. 589–592.

Maltman, A., 1994, Editor's preface, *in* Maltman, A., editor, The geological deformation of sediments: London, Chapman and Hall, p. xi-xiii.

Maltman, A.J., and Bolton, A., 2003, How sediments become mobilized, *in* Van Rensbergen, P., Hillis, R.R., Maltman, A.J., and Morley, C.K., editors, Subsurface Sediment Mobilization: Geological Society of London, Special Publication 216, p. 9–20.

Marco, S., and Agnon, A., 1995, Prehistoric earthquake deformations near Masada, Dead Sea graben: Geology, v. 23, p. 695–698.

Marco, S., and Agnon, A., 2005, High-resolution stratigraphy reveals repeated earthquake faulting in the Masada Fault Zone, Dead Sea Transform: Tectonophysics, v. 408, p. 101–112.

Martel, A.T., and Gibling, M.R., 1993, Clastic dikes of the Devono-Carboniferous Horton Bluff Formation, Nova Scotia: storm-related structures in shallow lakes: Sedimentary Geology, v. 87, p. 103–119.

Martín-Chivelet, J., Palma, R.M., López-Gómez, J., and Kietzmann, D.A., 2011, Earthquake-induced soft-sediment deformation structures in Upper Jurassic open-marine microbialites (Neuquén Basin, Argentina): Sedimentary Geology, v. 235, p. 210–221.

Mason, G.M., 1983, An examination of mineralogic data for the Mahogany Marker tuff of the Green River Formation, Piceance Creek Basin, Colorado, *in* Gary, J.H., editor, Proceedings of the Sixteenth Oil Shale Symposium, Golden, Colorado, p. 124–131.

Massari, F., Ghibaudo, G., D'Alessandro, A., and Davaud, E., 2001, Water-upwelling pipes and soft-sediment deformation structures in Lower Pleistocene calcarenites (Salento, southern Italy): Geological Society of America Bulletin, v. 113, p. 545–560.

Mastrogiacomo, G., Moretti, M., Owen, G., and Spalluto, L., 2012, Tectonic triggering of slump sheets in the Upper Cretaceous carbonate succession of the Porto Selvaggio area (Salento peninsula, southern Italy): Synsedimentary tectonics in the Apulian Carbonate Platform: Sedimentary Geology, v. 269–270, p. 15–27.

Matsuda, J.I., 2000, Seismic deformation structures of the post-2300 a BP muddy sediments in Kawachi lowland plain, Osaka, Japan: Sedimentary Geology, v. 135, p. 99–116.

McCalpin, J., 2009, Paleoseismology (2nd Edition): San Diego, USA, Elsevier, 613 p.

McGlue, M.M., Soreghan, M.J., Michel, E., Todd, J.A., Cohen, A.S., Mischler, J., O'Connell, C.S., Castañeda, O.S., Hartwell, R.J., Lezzar, K.E. and Nkotagu, H.H., 2010, Environmental controls on shell-rich facies in tropical lacustrine rifts: a view from Lake Tanganyika's littoral: Palaios, v. 25, p. 426–438.

McLaughlin, P.I., and Brett, C.E., 2004, Eustatic and tectonic controls on the distribution of marine seismites: examples from the Upper Ordovician of Kentucky, USA: Sedimentary Geology, v. 168, p. 165–192.

Migowski, C., Agnon, A., Bookman, R., Negendank, J.F.W., and Stein, M., 2004, Recurrence pattern of Holocene earthquakes along the Dead Sea transform revealed by varve-counting and radiocarbon dating of lacustrine sediments. Earth and Planetary Science Letters, v. 222, p. 301–314.

Mills, P.C., 1983, Genesis and diagnostic value of soft-sediment deformation structures—A review: Sedimentary Geology, v. 35, p. 83–104.

Milroy, P.G., and Wright, V.P., 2002, Fabrics, facies control and diagenesis of lacustrine ooids and associated grains from the Upper Triassic, southwest England: Geological Journal, v. 37, p. 35–53.

Mohindra, R., and Bagati, T.N., 1996, Seismically induced soft-sediment deformation structures (seismites) around Sumdo in the lower Spiti valley (Tethys Himalaya): Sedimentary Geology, v. 101, p. 69–83.

Molina, J.M., Alfaro, P., Moretti, M., and Soria, J.M., 1998, Soft-sediment deformation structures induced by cyclic stress of storm waves in tempestites (Miocene, Guadalquivir Basin, Spain): Terra Nova, v. 10, p. 145–150.

Moncure, G., and Surdam, R.C., 1980, Depositional environment of the Green River Formation in the vicinity of the Douglas Creek Arch, Colorado and Utah: University of Wyoming, Contributions to Geology, v. 19, p. 9–24.

Monecke, K., Anselmetti, F.S., Becker, A., Sturm, M., and Giardini, D., 2004, The record of historic earthquakes in lake sediments of Central Switzerland: Tectonophysics, v. 394, p. 21–40.

Monecke, K., Anselmetti, F.S., Becker, A., Schnellmann, M., Sturm, M., and Giardini, D., 2006, Earthquake-induced deformation structures in lake deposits: A Late Pleistocene to Holocene paleoseismic record for Central Switzerland: Eclogae Geologicae Helvetiae, v. 99, p. 343–362.

Montenat, C., Barrier, P., Ott d'Estevou, P., and Hibsch, C., 2007, Seismites: an attempt at critical analysis and classification: Sedimentary Geology, v. 196, p. 5–30.

Moretti, M., Alfaro, P., Caselles, O., and Canas, J.A., 1999, Modelling seismites with a digital shaking table: Tectonophysics, v. 304, p. 369–383.

Moretti, M., 2000, Soft-sediment deformation structures interpreted as seismites in middle–late Pleistocene aeolian deposits (Apulian foreland, southern Italy): Sedimentary Geology, v. 135, p. 167–179.

Moretti, M., and Ronchi, A., 2011, Liquefaction features interpreted as seismites in the Pleistocene fluvio-lacustrine deposits of the Neuquén Basin (Northern Patagonia): Sedimentary Geology, v. 235, p. 200–209.

Moretti, M., and Sabato, L., 2007, Recognition of trigger mechanisms for soft-sediment deformation in the Pleistocene lacustrine deposits of the Sant'Arcangelo Basin (Southern Italy): Seismic shocks vs. overloading: Sedimentary Geology, v. 196, p. 31–45.

Moretti, M., Soria, J.M., Alfaro, P., and Walsh, N., 2001, Asymmetrical soft-sediment deformation structures triggered by rapid sedimentation in turbiditic deposits (Late Miocene, Guadix Basin, Southern Spain): Facies, v. 44, p. 283–294.

Morgan, C.D., Chidsey, T.C., McClure, K.P., Bereskin, S.R., and Deo, M.D., 2003, Reservoir characterization of the Lower Green River Formation, Uinta Basin, Utah: Utah Geological Survey Open File Report 441, 140 p.

Mörner, N.-A., 2005, An interpretation and catalogue of paleoseismicity in Sweden: Tectonophysics, v. 408, p. 265–307.

Morris, T.H., and Richmond, D.R., 1992, A predictive model of reservoir continuity in fluvial sandstone bodies of a lacustrine deltaic system, Colton Formation, Utah, *in* Fouch, T.D., Nuccio, V.F., and Chidsey, T.C., Jr., editors, Hydrocarbon and Mineral Resources of the Uinta Basin, Utah and Colorado: Utah Geological Association, Publication 20, p. 227–236.

Morsilli, M., and Pomar, L., 2012, Internal waves vs. surface storm waves: A review on the origin of hummocky cross-stratification: Terra Nova, v. 24, p. 273–282.

Mulder, T., and Alexander, J., 2001, The physical character of subaqueous sedimentary density flows and their deposits: Sedimentology, v. 48, p. 269–299.

Mulder, T., and Cochonat, P., 1996, Classification of offshore mass movements: Journal of Sedimentary Research, v. 66, p. 43–57.

Nataraja, M.S., and Gill, H.S., 1983, Ocean wave-induced liquefaction analysis: Journal of the Geotechnical Engineering, v. 109, p. 573–590.

Neal, J.T., Langer, A.M., and Kerr, P.F., 1968, Giant desiccation polygons of Great Basin playas: Geological Society of America Bulletin, v. 79, p. 69–90.

Needham, R.S., 1978, Giant-scale hydroplastic deformation structures formed by the loading of basalt onto water-saturated sand, Middle Proterozoic, Northern Territory, Australia: Sedimentology, v. 25, p. 285–295.

Nemec, W., 1990, Aspects of sediment movement on steep delta slopes, *in* Colella, A., and Prior, D.B., editors, Coarse-Grained Deltas: International Association of Sedimentologists, Special Publication 10, p. 29–73.

Neuwerth, R., Suter, F., Guzman, C.A., and Gorin, G.E., 2006, Soft-sediment deformation in a tectonically active area: The Plio-Pleistocene Zarzal Formation in the Cauca Valley (Western Colombia): Sedimentary Geology, v. 186, p. 67–88.

Nyman, S.L., Nelson, C.S., Campbell, K.A., Schellenberg, F., Pearson, M.J., Kamp, P.J.J., Browne, G.H., and King, P.R., 2006, Tubular carbonate concretions as hydrocarbon migration pathways? Examples from North Island New Zealand: Proceedings of New Zealand Petroleum Conference, Auckland, 6–8 March 2006, 10 p.

Nyman, S.L., Nelson, C.S., and Campbell, K.A., 2010, Miocene tubular concretions in East Coast Basin, New Zealand: analogue for the subsurface plumbing of cold seeps: Marine Geology, v. 272, p. 319–336.

Obermeier, S.F., 1996, Use of liquefaction-induced features for paleoseismic analysis—An overview of how seismic liquefaction features can be distinguished from other features and how their regional distribution and properties of source sediment can be used to infer the location and strength of Holocene paleo-earthquakes: Engineering Geology, v. 44, p. 1–76.

Ohsumi, T., and Ogawa, Y., 2008, Vein structures, like ripple marks, are formed by short-wavelength shear waves: Journal of Structural Geology, v. 30, p. 719–724.

Oliveira, C.M.M., Hodgson, D.M., and Flint, S.S., 2009, Aseismic controls on in situ soft-sediment deformation processes and products in submarine slope deposits of the Karoo Basin, South Africa: Sedimentology, v. 56, p. 1201–1225.

Onasch, C.M., and Kahle, C.F., 2002, Seismically induced soft-sediment deformation in some Silurian carbonates, eastern U.S. Midcontinent, *in* Ettensohn, F.R., Rast, N., and Brett, C.E., editors, Ancient Seismites: Geological Society of America, Special Paper 359, p. 165−176.

Oriel, S.S., and Tracey, J.I., Jr., 1970, Uppermost Cretaceous and Tertiary stratigraphy of Fossil Basin, southwestern Wyoming: U.S. Geological Survey, Professional Paper 635, 53 p.

Osleger, D.A., Heyvaert, A.C., Stoner, J.S., and Verosub, K.L., 2009, Lacustrine turbidites as indicators of Holocene storminess and climate: Lake Tahoe, California and Nevada: Journal of Paleolimnology, v. 42, p. 103–122.

Osmond, J.C., 1992, Greater Natural Buttes Gas Field, Uintah County, Utah, *in* Fouch, T.D., Nuccio, V.F., and Chidsey, T.C., Jr., editors, Hydrocarbon and mineral resources of the Uinta Basin, Utah and Colorado: Utah Geological Association, Publication 20, p. 143–163.

Owen, G., 1987, Deformation processes in unconsolidated sands, *in* Jones, M.E., and Preston, R.M.F., editors, Deformation of Sediments and Sedimentary Rocks: Geological Society of London, Special Publication 29, p. 11–24.

Owen, G., 1995, Soft-sediment deformation in Upper Proterozoic Torridonian sandstones (Applecross Formation) at Torridon, northwest Scotland: Journal of Sedimentary Research, v. A65, p. 495–504.

Owen, G., 1996a, Anatomy of water-escape cusp in Upper Proterozoic Torridon Group sandstones, Scotland: Sedimentary Geology, v. 103, p. 117–128.

Owen, G., 1996b, Experimental soft-sediment deformation: structures formed by the liquefaction of unconsolidated sands and some ancient examples: Sedimentology, v. 43, p. 279–293.

Owen, G., 2003, Load structures: gravity-driven sediment mobilization in the shallow subsurface, *in* Van Rensbergen, P., Hillis, R.R., Maltman, A.J., and Morley, C.K., editors, Subsurface Sediment Mobilization: Geological Society of London, Special Publication 216, p. 21–34.

Owen, G., and Moretti, M., 2008, Determining the origin of soft-sediment deformation structures: a case study from Upper Carboniferous delta deposits in south-west Wales, UK: Terra Nova, v. 20, p. 237–245.

Owen, G., and Moretti, M., 2011, Identifying triggers for liquefaction-induced soft-sediment deformation in sands: Sedimentary Geology, v. 235, p. 141–147.

Owen, G., Moretti, M., and Alfaro, P., 2011, Recognising triggers for soft-sediment deformation: current understanding and future directions: Sedimentary Geology, v. 235, p. 133–140.

Owen, R.A., Owen, R.B., Renaut, R.W., Scott, J.J., Jones, B., and Ashley, G.M., 2008, Mineralogy and origin of rhizoliths on the margins of saline, alkaline Lake Bogoria, Kenya Rift Valley: Sedimentary Geology, v. 203, p. 143–163.

Owen, R.B., Renaut, R.W., and Stamatakis, M.G., 2011, Late Miocene lacustrine sedimentation in the Mytilinii Basin, Samos Island, Greece: Journal of Paleolimnology, v. 46, p. 151–166.

Parize, O., and Friès, G., 2003, The Vocontian clastic dykes and sills: A geometric model, *in* Van Rensbergen, P., Hillis, R.R., Maltman, A.J., and Morley, C.K., editors, Subsurface Sediment Mobilization: Geological Society of London, Special Publication 216, p. 51–72.

Parize, O., Beaudoin, B., Eckert, S., Friès, G., Hadj-hassen, F., Schneider, F., Su, K., Tijani, A., Trouliller, A., De Fouquet, C., and Vandromme, R., 2007, The Vocontian Aptian and Albian syndepositional clastic sills and dikes: A field-based mechanical approach to predict and model the early fracturing of marly-limy sediments, *in* Hurst, A., and Cartwright, J., editors, Sand Injectites: Implications for Hydrocarbon Exploration and Production: American Association of Petroleum Geologists, Memoir 87, p. 163–173.

Parizot, M., Eriksson, P.G., Aifa, T., Sarkar, S., Banerjee, S., Catuneanu, O., Altermann, W., Bumby, A.J., Bordy, E.M., Louis van Rooy, J., and Boshoff, A.J., 2005, Suspected microbial

mat-related crack-like sedimentary structures in the Palaeoproterozoic Magaliesberg Formation sandstones, South Africa: Precambrian Research, v. 138, p. 274–296.

Paz, J.D.S., Rossetti, D.F., 2005, Linking lacustrine cycles with syn-sedimentary tectonic episodes: an example from the Codo Formation (late Aptian) northeastern Brazil. Geological Magazine, v. 142, p. 269–285.

Paz, J.D.S., and Rossetti, D.F., 2006, Paleohydrology of an Upper Aptian lacustrine system from northeastern Brazil: Integration of facies and isotopic geochemistry: Palaeogeography, Palaeoclimatology, Palaeoecology, v. 241, p. 247–266.

Picard, M.D., 1955, Subsurface stratigraphy and lithology of Green River Formation in Uinta Basin, Utah: American Association of Petroleum Geologists Bulletin, v. 39, p. 75–102.

Picard, M.D., 1966, Oriented, linear-shrinkage cracks in Green River Formation (Eocene), Raven Ridge area, Uinta Basin, Utah: Journal of Sedimentary Petrology, v. 36, p. 1050–1057.

Picard, M.D., and High, L.R., 1968, Sedimentary cycles in the Green River Formation (Eocene), Uinta Basin, Utah: Journal of Sedimentary Petrology, v. 38, p. 378–383.

Picard, M.D., and High, L.R., Jr., 1972, Paleoenvironmental reconstructions in an area of rapid facies change, Parachute Creek Member of Green River Formation (Eocene), Uinta Basin, Utah: Geological Society of America Bulletin, v. 83, p. 2689–2708.

Pietras, J.T., and Carroll, A.R., 2006, High-resolution stratigraphy of an underfilled lake basin: Wilkins Peak Member, Eocene Green River Formation, Wyoming, U.S.A.: Journal of Sedimentary Research, v. 76, p. 1197–1214.

Pietras, J.T., Carroll, A.R., and Rhodes, M.K., 2003, Lake basin response to tectonic drainage diversion: Eocene Green River Formation, Wyoming: Journal of Paleolimnology, v. 30, p. 115–125.

Pitman, J.K., 1982, Regional stratigraphic and depositional analysis of rock units in the upper Garden Gulch and Parachute Creek Members of the Green River Formation, Piceance Creek basin, Colorado, *in* Proceedings of the 15th Oil Shale Symposium, Colorado School of Mines, Golden, Colorado, p. 79–100.

Pitman, J.K., Fouch, T.D., and Goldhaber, M.B., 1982, Depositional setting and diagenetic evolution of some Tertiary unconventional reservoir rocks, Uinta Basin, Utah: American Association of Petroleum Geologists Bulletin, v. 66, p. 1581–1596.

Plaziat, J.-C., Purser, B.H. and Philobbos, E., 1990, Seismic deformation structures (seismites) in the syn-rift sediments of the NW Red Sea (Egypt): Société Géologique de France, Bulletin, v. 8, p. 419−434.

Plint, A.G., 1985, Possible earthquake-induced soft-sediment faulting and remobilization in Pennsylvanian alluvial strata, southern New Brunswick, Canada: Canadian Journal of Earth Sciences, v. 22, p. 907–912.

Plummer, P.S., and Gostin, V.A., 1981, Shrinkage cracks: desiccation or synaeresis: Journal of Sedimentary Petrology, v. 51, p. 1147–1156.

Pope, M.C., Read, J.F., Bambach, R.K., and Hofmann, H.J., 1997, Late Middle to Late Ordovician seismites of Kentucky, southwest Ohio and Virginia: sedimentary recorders of earthquakes in the Appalachian basin: Geological Society of America Bulletin, v. 109, p. 489–503.

Postma, G., 1983, Water escape structures in the context of a depositional model of a mass flow dominated conglomeratic fan-delta (Abrioja Formation, Pliocene, Almeria Basin, Spain): Sedimentology, v. 30, p. 91–103.

Pratt, B.R., 1994, Seismites in the Mesoproterozoic Altyn Formation (Belt Supergroup), Montana: A test for tectonic control of peritidal carbonate cyclicity: Geology, v. 22, p. 1091–1094.

Pratt, B.R., 1998a, Syneresis cracks: subaqueous shrinkage in argillaceous sediments caused by earthquake-induced dewatering: Sedimentary Geology, v. 117, p. 1–10.

Pratt, B.R., 1998b, Molar-tooth structure in Proterozoic carbonate rocks: Origin from synsedimentary earthquakes, and implications for the nature and evolution of basins and marine sediments: Geological Society of America Bulletin, v. 110, p. 1028–1045.

Pratt, B.R., 1999, Gas bubble and expansion crack origin of “molar-tooth” calcite structures in the middle Proterozoic Belt Supergroup, western Montana—Discussion: Journal of Sedimentary Research, v. 69, p. 1136–1140.

Pratt, B.R., 2001, Oceanography, bathymetry and syndepositional tectonics of a Precambrian intracratonic basin: integrating sediments, storms, earthquakes and tsunamis in the Belt Supergroup (Helena Formation, ca. 1.45 Ga), western North America: Sedimentary Geology, v. 141–142, p. 371−394.

Pratt, B.R., 2002a, Storms versus tsunamis: Dynamic interplay of sedimentary, diagenetic, and tectonic processes in the Cambrian of Montana: Geology, v. 30, p. 423–426.

Pratt, B.R., 2002b, Tepees in peritidal carbonates: origin via earthquake-induced deformation, with example from the Middle Cambrian of western Canada: Sedimentary Geology, v. 153, p. 57–64.

Pratt, B.R., 2011, Molar-tooth structure, *in* Reitner, J., and Thiel, V., editors, Encyclopedia of Geobiology. Springer, Dordrecht, p. 662–666.

Price, N.J., 1966, Fault and Joint Development in Brittle and Semi-brittle Rock: Oxford, UK, Pergamon Press, 176 p.

Prior, D.B., Bornhold, B.D., Coleman, J.M., and Bryant, W.R., 1982, Morphology of a submarine slide, Kitimat Arm, British Columbia: Geology, v. 10, p. 588–592.

Pruss, S.B., Bosak, T., Macdonald, F., McLane, M., and Hoffman, P., 2010, Microbial facies in an early Cryogenian (Sturtian) cap carbonate, the Rasthof Formation, Otavi Group, northern Namibia: Precambrian Research, v. 181, p. 187–198

Ratterman, N.G., and Surdam, R.C., 1981, Zeolite mineral reactions in a tuff in the Laney Member of the Green River Formation, Wyoming: Clays and Clay Minerals, v. 29, p. 365–377

Remy, R., 1989, Lacustrine hummocky cross-stratification in Green River Formation, southern Uinta basin, Utah [abs.]: American Association of Petroleum Geologists Bulletin, v. 73, p. 1171.

Remy, R., 1992, Stratigraphy of the Eocene part of the Green River Formation in the south-central part of the Uinta basin, Utah [abs.]: U.S. Geological Survey Bulletin B-1787-BB, p. 1–69.

Renaut, R.W., and Gierlowski-Kordesch, E.H., 2010, Lakes, *in* James, N.P., and Dalrymple, R.W., editors, Facies Models (4th Edition): Geological Association of Canada, GEOtext 6, p. 541–575.

Rhodes, M.K., Carroll, A.R., Pietras, J.T., Beard, B.L., and Johnson, C.M., 2002, Strontium isotope record of paleohydrology and continental weathering, Eocene Green River Formation, Wyoming: Geology, v. 30, p. 167–170.

Ricci Lucchi, F., 1995, Sedimentological indicators of paleoseismicity, *in* Serva, L., and Slemmons, D.B., editors, Perspectives in Paleoseismology: Association of Engineering Geologists, Special Publication 6, p. 7–17.

Rider, M.H., 1978, Growth faults in Carboniferous of western Ireland: Geological Society of America Bulletin, v. 62, p. 2191–2213.

Ringrose, P.S., 1989, Paleoseismic (?) liquefaction event in late Quaternary lake sediment at Glen Roy, Scotland: Terra Nova, v. 1, p. 57–62.

Rodríguez-López, J.P., Meléndez, N., Soria, A.R., Liesa, C.L., and van Loon, A.J., 2007, Lateral variability of ancient seismites related to differences in sedimentary facies (the synrift Escucha Formation, mid-Cretaceous, eastern Spain): Sedimentary Geology, v. 201, p. 461–484.

Rodríguez-Pascua, M.A., Calvo, J.P., De Vicente, G., and Gómez-Gras, D., 2000, Soft-sediment deformation structures interpreted as seismites in lacustrine sediments of the Prebetic Zone, SE Spain, and their potential use as indicators of earthquake magnitudes during the Late Miocene: Sedimentary Geology, v. 135, p. 117–135.

Rodríguez Pascua, M.A., De Vicente, G., Calvo, J.P., and Pérez-López, R., 2003, Similarities between recent seismic activity and paleoseismites during the late miocene in the external Betic Chain (Spain): relationship by the 'b' value and the fractal dimension: Journal of Structural Geology, v. 25, p. 749–763.

Røe, S.-L., and Hermansen, M., 2006, New aspects of deformed cross-strata in fluvial sandstones: examples from Neoproterozoic formations in northern Norway: Sedimentary Geology, v. 186, p. 283–293.

Roehler, H.W., 1965, Early Tertiary depositional environments in the Rock Springs uplift area, *in* DeVoto, RH., and Bitter, P.K., editors, Sedimentation of Late Cretaceous and Tertiary outcrops, Rock Springs uplift: Wyoming Geological Association Guidebook, 19th Field Conference, p. 140–150.

Roehler, H.W., 1972, Zonal distribution of montmorillonite and zeolites in the Laney Shale Member of the Green River Formation in the Washakie Basin: U.S. Geological Survey Professional Paper 800-B, p. 123–126.

Roehler, H.W., 1974, Depositional environments of rocks in the Piceance Creek Basin, Colorado, *in* Murray, D.K., editor, Guidebook to the energy resources of the Piceance Creek Basin, Colorado: Rocky Mountain Association of Geologists, 25th Annual Field Conference, p. 57–64.

Roehler, H.W., 1990. Sedimentology of freshwater lacustrine shorelines in the Eocene Scheggs Bed of the Tipton Tongue of the Green River Formation, Sand Wash Basin, Northwest Colorado. Geological Survey, Bulletin 1911, 49 p.

Roehler, H.W., 1992, Correlation, composition, areal distribution, and thickness of Eocene stratigraphic units, greater Green River basin, Wyoming, Utah, and Colorado: U.S. Geological Survey, Professional Paper 1506-E, 49 p.

Roehler, H.W., 1993, Eocene climates, depositional environments, and geography, greater Green River basin, Wyoming, Utah, and Colorado: U.S. Geological Survey, Professional Paper 1506-F, 74 p.

Roehler, H. W., Hanley, J.H., and Honey, J.G., 1988, Geology and paleoecology of the Cottonwood Creek delta in the Eocene Tipton Tongue of the Green River Formation and a mammalian fauna from the Eocene Cathedral Bluffs Tongue of the Wasatch Formation, Southeast Washakie Basin, Wyoming: U.S. Geological Survey, Bulletin 1669-A-C, 47 p.

Rossetti, D.F., 1999, Soft-sediment deformation structures in late Albian to Cenomanian deposits, São Luís Basin, northern Brazil: evidence for palaeoseismicity: Sedimentology, v. 46, p. 1065–1081.

Rossetti, D.F., and Góes, A.M., 2000, Deciphering the sedimentological imprint of paleoseismic events: an example from the Aptian Codó Formation, northern Brazil: Sedimentary Geology, v. 135, p. 137–156.

Rossetti, D.F., and Santos, A.E., Jr, 2003, Events of sediment deformation and mass failure in Upper Cretaceous estuarine deposits (Cametá Basin, northern Brazil) as evidence for seismic activity: Sedimentary Geology, v. 161, p. 107–130.

Rothwell, R.G., Reeder, M.S., Anastasakis, G., Stow, D.A.V., Thomson, J., and Kähler, G., 2000, Low sea-level stand emplacement of megaturbidites in the western and eastern Mediterranean Sea: Sedimentary Geology, v. 135, p. 75–88.

Rubey, W.W., Oriel, S.S., and Tracey, J.I., Jr., 1975, Geology of the Sage and Kemmerer 15-minute Quadrangles, Lincoln County, Wyoming: U.S. Geological Survey, Professional Paper 855, 18 p.

Ruble, T.E., and Philp, R.P., 1998, Stratigraphy, depositional environments, and organic geochemistry of source rocks in the Green River Petroleum System, Uinta Basin, Utah, *in* Pitman, J.K., and Carroll, A.R., editors, Modern and Ancient Lake Systems; New Problems and Perspectives: Utah Geological Association, Publication 26, p. 289–328.

Ryder, R.T., Fouch, T.D., and Elison, J.H., 1976, Early Tertiary sedimentation in the western Uinta Basin, Utah: Geological Society of America Bulletin, v. 87, p. 496–592.

Samaila, N.K., Abubakar, M.B., Dike, E.F.C., and Obaje, N.G., 2006, Description of soft-sediment deformation structures in the Cretaceous Bima Sandstone from the Yola Arm, Upper Benue Trough, northeastern Nigeria: Journal of African Earth Sciences, v. 44, p. 66–74.

Sangrey, D.A., Henkel, D.J., and Esrig, M.I., 1969, The effective stress response of a saturated clay soil to repeated loading: Canadian Geotechnical Journal, v. 6, p. 241–252.

Sarg, J.F., Suriamin, Tänavsuu-Milkeviciene, K., and Humphrey, J.D., 2013, Lithofacies, stable isotopic composition, and stratigraphic evolution of microbial and associated carbonates, Green River Formation (Eocene), Piceance basin: American Association of Petroleum Geologists Bulletin, v. 97, p. 1937–1966.

Sauerbrey, M.A., Juschus, O., Gebhardt, A.C., Wennrich, V., Nowaczyk, N.R., and Melles, M., 2013, Mass movement deposits in the 3.6 Ma sediment record of Lake El'gygytgyn, Far East Russian Arctic: classification, distribution and preliminary interpretation: Climate of the Past, v. 9, p. 1949–1967.

Schieber, J., 1999, Microbial mats in terrigenous clastics: the challenge of identification in the rock record: Palaios, v. 14, p. 3–12.

Schieber, J., Bose, P.K., Eriksson, P.G., Banerjee, S., Sarkar, S., Altermann, W., and Catuneanu, O., editors, 2007, Atlas of microbial mat features preserved within the siliciclastic rock record: Amsterdam, Elsevier, Atlases in Geoscience, v. 2, 311 p.

Schnellmann, M., Anselmetti, F.S., Giardini, D., and McKenzie, J.A., 2007, 15 000 Years of mass- movement history in Lake Lucerne: implications for seismic and tsunami hazards: Eclogae Geologicae Helvetiae, v. 99, p. 409–428.

Schomacker, E.R., Kjemperud, A.V., Nystuen, J.P. and Jahren, J.S., 2010, Recognition and significance of sharp-based mouth-bar deposits in the Eocene Green River Formation, Uinta Basin, Utah: Sedimentology, v. 57, p. 1069–1087.

Schroeder, S., Beukes, N.J., and Sumner, D.Y., 2009, Microbialite-sediment interactions on the slope of the Campbellrand carbonate platform (Neoarchean, South Africa): Precambrian Research, v. 169, p. 68–79.

Scott, B., and Price, S., 1988, Earthquake-induced structures in young sediments: Tectonophysics, v. 147, p. 165–170.

Seed, H.B., and Lee, K.L., 1966, Liquefaction of saturated sands during cyclic loading. Journal of Soil Mechanics and Foundations Division, v. 92, p. 105–134.

Seed, H.B., and Rahman, M.S., 1977, Wave-induced pore pressure in relation to ocean floor stability of cohesionless soils: Marine Geotechnology, v. 3, p. 123–150.

Seilacher, A., 1969, Fault-graded beds interpreted as seismites: Sedimentology, v. 13, p. 155–159.

Seilacher, A., 1984, Sedimentary structures tentatively attributed to seismic events: Marine Geology, v. 55, p. 1–12.

Shelton, J.W., 1962, Shale compaction in a section of Cretaceous Dakota Sandstone, northwestern North Dakota: Journal of Sedimentary Petrology, v. 32, p. 873–877.

Simonson, B.M., and Carney, K.E., 1999, Roll-up structures: evidence of in-situ microbial mats in Late Archean deep shelf environments: Palaios, v. 14, p. 13–24.

Sims, J.D., 1973, Earthquake-induced structures in sediments of Van Norman Lake, San Fernando, California: Science, v. 182, p. 161–163.

Sims, J.D., 1975, Determining earthquake recurrence intervals from deformational structures in young lacustrine sediments: Tectonophysics, v. 29, p. 141–152.

Smith, M.E., Carroll, A.R., Jicha, B.J., Cassel, E.J., and Scott, J.J., 2014a, Paleogeographic record of Eocene Farallon slab rollback beneath western North America: Geology, v. 42, p. 1039–1042.

Smith, M.E., Carroll, A.R., Scott, J.J., and Singer, B.S., 2014b, Early Eocene carbon isotope excursions and landscape destabilization at eccentricity minima: Green River Formation of Wyoming: Earth and Planetary Science Letters, v. 403, p. 393–406.

Smith, M.E., Carroll, A.R., and Singer, B.S., 2008, Synoptic reconstruction of a major ancient lake system: Eocene Green River Formation, western United States: Geological Society of America Bulletin, v. 120, p. 54–84.

Smith, M.E., Chamberlain, K.R., Singer, B.S., and Carroll, A.R., 2010, Eocene clocks agree: Coeval $^{40}Ar/^{39}Ar$, U-Pb, and astronomical ages from the Green River Formation: Geology, v. 38, p. 527–530.

Smoot, J.P., 1978, Origin of the carbonate sediments in the Wilkins Peaks Member of the lacustrine Green River Formation (Eocene), Wyoming, U.S.A., *in* Matter, A., and Tucker, M.E., editors, Modern and ancient lake sediments: International Association of Sedimentologists, Special Publication 2, p. 215–240.

Smoot, J.P., 1983, Depositional subenvironments in an arid closed basin; the Wilkins Peak Member of the Green River Formation (Eocene), Wyoming, U.S.A.: Sedimentology, v. 30, p. 801–827.

Spalluto, L., Moretti, M., Festa, V. and Tropeano, M., 2007, Seismically-induced slumps in Lower-Maastrichtian peritidal carbonates of the Apulian Platform (southern Italy): Sedimentary Geology, v. 196, p. 81–98.

Steidtmann, J.R., McGee, L.C., and Middleton, L.T., 1983, Laramide sedimentation, folding, and faulting in the southern Wind River Range, Wyoming, *in* Lowell, J.D., editor, Rocky Mountain Foreland Basins and Uplifts: Rocky Mountain Association of Geologists, 9th Annual Field Conference Guidebook, p. 161–167.

Stollhofen, H., 1998, Facies architecture variations and seismogenic structures in the Carboniferous-Permian Saar–Nahe Basin (SW Germany): evidence for extension-related transfer fault activity: Sedimentary Geology, v. 119, p. 47–83.

St-Onge, G., Chapron, E., Mulsow, S., Salas, M., Viel, M., Debret, M., Foucher, A., Mulder, T., Winiarski, T., Desmet, M., Costa, P.J.M., Ghaleb, B., Jaouen, A., and Locat, J., 2012, Comparison of earthquake-triggered turbidites from the Saguenay (Eastern Canada) and

Reloncavi (Chilean margin) Fjords: Implications for paleoseismicity and sedimentology: Sedimentary Geology, v. 243–244, p. 89–107.

St-Onge, G., Mulder, T., Piper, D.J.W., Hillaire-Marcel, C., and Stoner, J.S., 2004, Earthquake and flood-induced turbidites in the Saguenay Fjord (Québec): a Holocene paleoseismicity record: Quaternary Science Reviews, v. 23, p. 283–294.

Strachan, L.J., 2002, Slump-initiated and controlled syndepositional sandstone remobilization: an example from the Namurian of County Clare, Ireland: Sedimentology, v. 49, p. 25–41.

Strasser, M., Monecke, K., Schnellmann, M., and Anselmetti, F.S., 2013, Lake sediments as natural seismographs: A compiled record of late Quaternary earthquakes in central Switzerland and its implication for Alpine deformation: Sedimentology, v. 60, p. 319–341.

Stromberg, S.G., and Bluck, B., 1997, Turbidite facies, fluid-escape structures and mechanisms of emplacement of the Oligo-Miocene Aljibe Flysch, Gibraltar Arc, Betics, southern Spain: Sedimentary Geology, v. 115, p. 267–288.

Sumner, D.Y., 1997, Late Archean calcite-microbe interactions: two morphologically distinct microbial communities that affected calcite nucleation differently: Palaios, v. 12, p. 302–318.

Surdam, R.C., and Parker, R.D., 1972, Authigenic aluminosilicate minerals in the tuffaceous rocks of the Green River Formation, Wyoming: Geological Society of America Bulletin, v. 83, p. 689–700.

Surdam, R.C., and Stanley, K.O., 1979, Lacustrine sedimentation during the culminating phase of Eocene Lake Gosiute, Wyoming (Green River Formation): Geological Society of America Bulletin, v. 90, p. 93–110.

Surdam, R.C., and Stanley, K.O., 1980, Effects of changes in drainage-basin boundaries on sedimentation in Eocene Lakes Gosiute and Uinta of Wyoming, Utah, and Colorado: Geology, v. 8, p. 135–139.

Surdam, R.C. and Wolfbauer, C.A., 1975, Green River Formation, Wyoming: A playa-lake complex: Geological Society of America Bulletin, v. 86, p. 335–345.

Surlyk, F., Gjelberg, J., and Noe-Nygaard, N., 2007, The Upper Jurassic Hareelv Formation of East Greenland: A giant sedimentary injection complex, *in* Hurst, A., and Cartwright, J.A., editors, Sand Injectites: Implications for Hydrocarbon Exploration and Production: American Association of Petroleum Geologists, Memoir 87, p. 141–149.

Talbot, M.R., and Allen, P.A., 1996, Lakes, *in* Reading, H.G., editor, Sedimentary environments: processes, facies and stratigraphy: Blackwell Science, Oxford, p. 83–124.

Tänavsuu-Milkeviciene, K., and Sarg, F.J., 2011, Evolution of the Green River Formation, Piceance Creek Basin: Implications for Eocene lake history, Colorado, Utah and Wyoming: Proceedings of the 31st Oil Shale Symposium, Colorado School of Mines, Golden, Colorado, poster presentation, 1 p.

Tänavsuu-Milkeviciene, K., and Sarg, F.J., 2012, Evolution of an organic-rich lake basin – stratigraphy, climate and tectonics: Piceance Creek basin, Eocene Green River Formation: Sedimentology, v. 59, p. 1735–1768.

Tank, R.W., 1972, Clay minerals of the Green River Formation (Eocene) of Wyoming: Clay Minerals, v. 9, p. 297–308.

Tanner, P.W.G., 1998, Interstratal dewatering origin for polygonal patterns of sand-filled cracks: a case study from late Proterozoic metasediments of Islay, Scotland: Sedimentology, v. 45, p. 71–89.

Taylor, A.M., and Goldring, R., 1993, Description and analysis of bioturbation and ichnofabric: Geological Society of London, Journal, v. 150, p. 141–148.

Thomas, R.G., Williams, B.P.J., Morrissey, L.B., Barclay, W.J. and Allen, K.C., 2006, Enigma variations: the stratigraphy, provenance, palaeoseismicity and depositional history of the Lower Old Red Sandstone Cosheston Group, southern Pembrokeshire, Wales. Geological Journal, v. 41, p. 481–536.

Törő, B., and Pratt, B.R., in press, Eocene paleoseismic record in the Green River Formation, Fossil Basin, Wyoming – implications of synsedimentary deformation structures in lacustrine carbonate mudstones: Journal of Sedimentary Research.

Törő, B., and Pratt, B.R., in press, Characteristics and implications of sedimentary deformation features in the Green River Formation (Eocene) in Utah and Colorado, *in* Birgenheier, L., Vanden Berg, M., and Ressetar, R., editors, The Uinta Basin and Uinta Mountains: Utah Geological Association Guidebook.

Törő, B., Pratt, B.R., and Renaut, R.W., 2014, Indicators of Paleoseismicity in the Lacustrine Sediments of the Eocene Green River Formation, Wyoming, Colorado and Utah (USA): AAPG Datapages/Search and Discovery Article #51005.

Törő, B., Pratt, B.R., and Renaut, R.W., 2015, Tectonically induced change in lake evolution recorded by seismites in the Eocene Green River Formation, Wyoming: Terra Nova, v. 27, p. 218–224.

Tsuchida, H., and Hayashi, S., 1971, Estimation of liquefaction potential of sandy soils: Proceedings of the Third Joint Meeting, US-Japan Panel on Wind and Seismic Effects, UJNR, Tokyo, May 1971, p. 91–109.

Tweddle, D., and Crossley, R., 1991, Effects of an earthquake on demersal cichlid fishes of southern Lake Malawi: Journal of Fish Biology, v. 38, p. 305–308.

Vanden Berg, M.D., Lehle, D.R., Carney, S.M., and Morgan, C.D., 2013, Geological characterization of the Birds Nest aquifer, Uinta Basin, Utah: Assessment of the aquifer's potential as a saline water disposal zone: Utah Geological Survey Special Study 147, 47 p.

Van Houten, F.B., 1964, Cyclic lacustrine sedimentation, Upper Triassic Lockatong Formation, central New Jersey and adjacent Pennsylvania, *in* Merriam, D.E., editor, Symposium on cyclic sedimentation: Kansas Geological Survey Bulletin 169, p. 497–531.

van Loon, A.J., 1992, The recognition of soft-sediment deformations as early-diagenetic features—a literature review, *in* Chilingarian, G.V., and Wolf, K.H., editors, Diagenesis, III: Amsterdam, Elsevier, Developments in Sedimentology, v. 47, p. 135–189.

van Loon, A.J., 2009, Soft-sediment deformation structures in siliciclastic sediments: an overview: Geologos, v. 15, p. 3–55.

van Loon, A.J., and Brodzikowski, K., 1987, Problems and progress in the research on soft-sediment deformations: Sedimentary Geology, v. 50, p. 167–193.

van Loon, A.J., Brodzikowski, K., and Zieliński, T., 1995, Shock-induced resuspension deposits from a Pleistocene proglacial lake (Kleszców Graben, central Poland): Journal of Sedimentary Research, v. 65, p. 417–422.

van Loon, A.J. and Wiggers, A.J., 1976, Metasedimentary 'graben' and associated structures in the lagoonal Almere member (Groningen Formation, the Netherlands): Sedimentary Geology, v. 16, p. 237–254.

Visher, G.S., and Cunningham, R.D., 1981, Convolute laminations—A theoretical analysis: example of a Pennsylvanian sandstone: Sedimentary Geology, v. 28, p. 175–188.

Waldmann, N., Anselmetti, F.S., Ariztegui, D., Austin J.A., Jr., Pirouz, M., Moy, C.M., and Dunbar, R., 2010, Holocene mass wasting events in Lago Fagnano, Tierra del Fuego (54°S): implications for paleoseismicity of the Magallanes-Fagnano transform fault: Basin Research, v. 23, p. 171–190.

Warren, J.K., 1983, Tepees, modern (southern Australia) and ancient (Permian—Texas and New Mexico)—a comparison: Sedimentary Geology, v. 34, p. 1–19.

Weaver, J.D., and Jeffcoat, R.E., 1978, Carbonate ball and pillow structures: Geological Magazine, v. 115, p. 245–253.

Weidlich, O., and Bernecker, M., 2004, Quantification of depositional changes and paleoseismic activities from laminated sediments using outcrop data: Sedimentary Geology, v. 166, p. 11–20.

Weiss, M.P., 1969, Oncolites, paleoecology and Laramide tectonics, central Utah: American Association of Petroleum Geologists Bulletin, v. 53, p. 1105–1120.

Weiss, M.P., Witkind, I.J., and Cashion, W.B., 1990, Geologic map of the Price 30’ x 60’ quadrangle, Carbon, Duchesne, Uintah, Utah, and Wasatch counties, Utah: U.S. Geological Survey Miscellaneous Investigations Series Map I-1981, scale 1:100,000.

Wells, J.T., Prior, D.B., and Coleman, J.M., 1980, Flowslides in muds on extremely low angle tidal flats, northeastern South America: Geology, v. 8, p. 272–275.

Wells, N.A., Richards, S.S., Peng, S., Keattch, S.E., Hudson, J.A., and Copsey, C.J., 1993, Fluvial processes and recumbently folded crossbeds in the Pennsylvanian Sharon Conglomerate in Summit County, Ohio, U. S. A.: Sedimentary Geology, v. 85, p.63–83.

Wheeler, R.L., 2002, Distinguishing seismic from nonseismic soft-sediment structures: criteria from seismic-hazard analysis, *in* Ettensohn, F.R., Rast, N., and Brett, C.E., editors, Ancient seismites: Geological Society of America, Special Paper 359, p. 1–11.

Whitmore, J.H., and Strom, R., 2010, Sand injectites at the base of the Coconino Sandstone, Grand Canyon, Arizona: Sedimentary Geology, v. 230, p. 46–59.

Wiig, S.V., Grundy, W.D., and Dyni, J.R., 1995, Trona resources in the Green River basin, southwest Wyoming: U.S. Geological Survey Open-File Report 95-476, 88 p.

Wilf, P., 2000, Late Paleocene–early Eocene climate changes in southwestern Wyoming: Paleobotanical analysis: Geological Society of America Bulletin, v. 112, p. 292–307.

Williamson, C.R., and Picard, M.D., 1974, Petrology of carbonate rocks of the Green River Formation (Eocene): Journal of Sedimentary Petrology, v. 44, p. 738–759.

Wing, S.L., and Greenwood, D.R., 1993, Fossils and fossil climate: The case for equable continental interiors in the Eocene: Royal Society of London Philosophical Transactions, series B, v. 341, p. 243–252.

Woodhall, R.J., 1980, Engineering problems of Great Salt Lake, Utah, marine oil drilling operation, *in* Gwynn, J.W., editor, Great Salt Lake: A Scientific, Historical, and Economic Overview: Utah Geological and Mineral Survey Bulletin 116, p. 377–392.

Yonkee, W.A., and Weil, A.B., 2010, Reconstructing the kinematic evolution of curved mountain belts: Internal strain patterns in the Wyoming salient, Sevier thrust belt, U.S.A.: Geological Society of America Bulletin, v. 122, p. 24–49.

Young, R.G., 1995, Stratigraphy of green River Formation in Piceance Creek Basin, Colorado, *in* Averett, W.R., editor, The Green River Formation in Piceance Creek and Eastern Uinta Basins: Grand Junction Geological Society, 1995 Field Trip Guidebook, p. 1–13.

Zachos, J.C., Dickens, G.R., and Zeebe, R.E., 2008, An early Cenozoic perspective on greenhouse warming and carbon-cycle dynamics: Nature, v. 451, p. 279–283.

Zachos, J., Pagani, M., Sloan, L., Thomas, E., and Billups, K., 2001, Trends, rhythms, and aberrations in global climate 65 Ma to present: Science, v. 292, p. 685–693.

APPENDIX A.

LIST OF DEFORMATION FEATURES (UT, CO)

**Appendix A.** List of locations studied in the Uinta and Piceance Creek Basins (Chapter 4), name of deformation features, host lithology with interpreted depositional environment, and figure number(s).

| Location | Deformation features | Host lithology (Depositional environment) | Figure no. |
|---|---|---|---|
| Willow Creek–Indian Canyon | Load structure | Cross-stratified sandstone (deltaic/littoral) | 4.3A |
| | Folding | Stromatolite (sublittoral) | 4.6C |
| | Sedimentary dike (Type 1) | Wave-ripple cross-laminated sandstone (deltaic/littoral) | 4.13A |
| | Sedimentary dike (Type 2) | Massive mudstone (deltaic) | 4.15B |
| | | Wavy- to lenticular-laminated silty carbonate mudstone (sublittoral) | 4.15C–G |
| | | Laminated organic-poor carbonate mudstone (sublittoral) | 4.16A |
| | | Laminated organic-rich carbonate mudstone (profundal) | 4.15A, 4.18A–D |
| | Carbonate breccia | Cross-stratified sandstone and massive mudstone (deltaic/littoral) | 4.25A, B |
| Nine Mile Canyon | Load structure | Organic-poor laminated carbonate mudstone (profundal) | 4.4G, H |
| | Convolution | Channelized trough cross-stratified sandstone (fluvial) | 4.5A, B |
| | Sedimentary dike (Type 1) | Cross-laminated sandstone to laminated sandy siltstone (Horse Bench Sandstone) (littoral) | 4.13B, C, E–H, 4.14D, E |
| | Sedimentary dike (Type 2) | Laminated organic-rich carbonate mudstone (profundal) | 4.16B, C |
| | Sedimentary dike (Type 4) | Laminated organic-rich to organic-poor carbonate mudstone (profundal to sublittoral) | 4.20A–H |
| | Sedimentary dike (Type 5) | Laminated to lenticular-laminated silty carbonate mudstone (profundal to sublittoral) | 4.22A–D |
| Gate Canyon | Load structure | Cross-laminated calcareous sandstone (littoral) | 4.3B |
| | Convolution | Calcareous tabular to trough cross-stratified sandstone (littoral) | 4.5D, E |
| | Folding | Tabular cross-stratified sandstone (littoral) | 4.6A |
| | Shear structures | Laminated organic-rich carbonate | 4.8A |

| | | | |
|---|---|---|---|
| | | mudstone (profundal) | |
| | Sedimentary dike (Type 1) | Cross-laminated to laminated calcareous sandstone and siltstone (sublittoral) | 4.13D, 4.14A |
| | Sedimentary dike (Type 2) | Laminated organic-poor silty carbonate mudstone (sublittoral) | 4.17A |
| North Franks Canyon | Sedimentary dike (Type 1) | Cross-laminated calcareous sandstone (S2 marker) (littoral) | 4.14B |
| | | Wavy- and lenticular-laminated calcareous siltstone (sublittoral) | 4.14C |
| | Sedimentary dike (Type 6) | Laminated organic-rich carbonate mudstone to silty mudstone (profundal to sublittoral) | 4.23A, B |
| | Carbonate breccia | Laminate organic-poor carbonate mudstone (profundal to sublittoral) | 4.25C, D |
| Sand Wash/ Green River | Load structures | Tabular to hummocky cross-stratified sandstone (Horse Bench Sandstone) (littoral) | 4.3C, D |
| | | Tabular to hummocky cross-stratified sandstone (S2 marker) (littoral) | 4.3E, F |
| | Convolution | Channelized tabular to trough cross-stratified sand (fluvial) | 4.5F, G |
| | Folding | Tabular cross-stratified sandstone (Horse Bench Sandstone) (littoral) | 4.6B |
| | Mass-transport deposit | Laminated to massive organic-rich carbonate mudstone (profundal) | Keighley et al., 2015 |
| Bitter Creek | Load structures | Laminated organic-poor silty carbonate mudstone (profundal to sublittoral) | 4.4A, B |
| | Sedimentary dike (Type 2) | Laminated organic-rich carbonate mudstone (profundal) | 4.17B, C |
| | Sedimentary dike (Type 3) | Laminated organic-rich carbonate mudstone (profundal) | 4.18A, B |
| Evacuation Creek / White River | Load structure | Tabular to trough cross-stratified sandstone (fluvial) | 4.4C |
| | | Cross-laminated calcareous sandstone (littoral) | 4.3G |
| | Convolution | Trough cross-stratified sandstone (fluvial) | 4.4C |
| | Fold | Laminated organic-poor carbonate mudstone (profundal) | 4.6D |
| | | Laminated organic-rich carbonate mudstone (profundal) | 4.6H |
| | Shear structure | Laminated organic-rich carbonate | 4.8C–E, |

| | | | |
|---|---|---|---|
| | | mudstone (profundal) | 4.9A–F |
| | Sedimentary dike (Type 2) | Laminated organic-poor carbonate mudstone (sublittoral) | 4.16D, 4.17D |
| | | Laminated organic-rich carbonate mudstone (profundal) | 4.18E–G |
| | Sedimentary dike (Type 3) | Laminated organic-poor carbonate mudstone (profundal) | 4.19C, D |
| | Carbonate breccia | Domal stromatolite (sublittoral) | 4.25F |
| | | Laminate organic-poor carbonate mudstone (profundal to sublittoral) | 4.25A |
| Hells Hole Canyon | Fold | Laminated organic-rich carbonate mudstone (profundal) | 4.6E– G |
| | Pinch-and-swell structure | Laminated organic-rich carbonate mudstone (profundal) | 4.7A–D |
| | Brecciated oil shale | Laminated organic-rich carbonate mudstone (profundal) | 4.12A–D |
| | Sedimentary dike (Type 4) | Laminated organic-rich carbonate mudstone (profundal) | 4.21A–F |
| | Microfaults | Laminated organic-rich carbonate mudstone (profundal) | 4.24A, B |
| Douglas Pass | Load structure | Massive to laminated calcareous muddy siltstone (sublittoral) | 4.4D |
| | | Massive to laminated organic-poor carbonate mudstone (sublittoral) | 4.4E, F |
| | Mass-transport deposit | Cross-stratified sandstone to laminated organic-rich carbonate mudstone (deltaic to profundal) | 4.11A–F |
| | Sedimentary dike (Type 1) | Wavy- and lenticular-laminated calcareous siltstone (sublittoral) | 4.14G, H |
| | Sedimentary dike (Type 2) | Lenticular-laminated calcareous silty mudstone (sublittoral) | 4.18H |
| | | Laminated organic-poor carbonate mudstone (sublittoral) | 4.16E |
| | Carbonate breccia | Domal stromatolite and grainstone (littoral) | 4.25G |
| | | Laminated calcareous siltstone (sublittoral to littoral) | 4.25H, I |
| | | Laminated organic-rich to silty carbonate mudstone (sublittoral) | 4.26A–D |
| Piceance Creek Basin | Oil shale breccias | Laminated organic-rich carbonate mudstone (profundal) | 4.12E, F |
| | Sedimentary dike (Type 1) | Laminated organic-poor carbonate mudstone (sublittoral) | 4.14F |
| | Microfaults | Laminated organic-rich carbonate mudstone (profundal) | 4.24C, D |

APPENDIX B.

SUMMARY OF DEFORMATION FEATURES (UT, CO)

**Appendix B.** Summary of deformation features in the Uinta and Piceance Creek Basins (Chapter 4), showing the name of deformation features, the interpreted depositional environment and host lithology in which they occur, and possible trigger(s).

| Name/Classification | Depositional Setting and Host Lithology | Possible Trigger(s) |
|---|---|---|
| Load Structures | Deltaic mouthbar sandstone | Groundwater seepage |
| | Littoral sandstones | Wave-action; Earthquake |
| | Littoral/sublittoral siltstone | Earthquake |
| | Littoral/sublittoral carbonates | Overloading; Earthquake |
| Convolution | Fluvial/deltaic sandstone | Earthquake |
| | Littoral sandstone | Wave-action; Earthquake |
| Folding | Littoral sandstone | Wave-action; Earthquake |
| | Sublittoral microbial carbonate | Earthquake |
| | Profundal carbonate mudstone | Earthquake |
| Pinch-and-Swell Structure | Profundal carbonate mudstone | Compaction; Earthquake |
| Shear Structure | Profundal carbonate mudstone | Earthquake/Tectonic stress |
| Mass-Transport Deposits | Debris flow deposit in sublittoral carbonate mudstone | Earthquake |
| Brecciated Oil Shale | Profundal organic-rich carbonate mudstone | Earthquake |
| Type 1 Sedimentary Dikes | Littoral/deltaic sandstone | Salinity fluctuations; Earthquake |
| | Littoral to sublittoral carbonate mudstone | Earthquake |
| Type 2 Sedimentary Dikes | Deltaic sandstone and mudstone | Earthquake |
| | Littoral to sublittoral silty carbonate mudstone | Earthquake |
| | Profundal carbonate mudstone | Earthquake |
| Type 3 Sedimentary Dikes | Profundal carbonate mudstone | Earthquake |
| Type 4 Sedimentary Dikes | Profundal/sublittoral carbonate mudstone | Diagenetic alteration; Earthquake |
| Type 5 Sedimentary Dikes | Sublittoral to profundal (silty) carbonate mudstone | Disequilibrium compaction; Earthquake |

| | | |
|---|---|---|
| Type 6 Sedimentary Dikes | Sublittoral to profundal (silty) carbonate mudstone | Earthquake/Tectonic stress |
| Microfaults | Profundal carbonate mudstone | Compaction; Earthquake |
| Carbonate Breccia | Deltaic to littoral siliciclastics | Wave-action; Currents |
| | Littoral to sublittoral microbial carbonate and grainstone | Wave-action; Earthquake |
| | Sublittoral siltstone to profundal carbonate mudstone | Earthquake |

# APPENDIX C.
# COPYRIGHT PERMISSIONS

The copyright information of the following papers:

Törő, B., and Pratt, B.R., in press, Eocene paleoseismic record in the Green River Formation, Fossil Basin, Wyoming – implications of synsedimentary deformation structures in lacustrine carbonate mudstones: Journal of Sedimentary Research.

Törő, B., Pratt, B.R., and Renaut, R.W., 2015, Tectonically induced change in lake evolution recorded by seismites in the Eocene Green River Formation, Wyoming: Terra Nova, v. 27, p. 218–224.

are included in the following pages.

**PLEASE RETURN SCANNED FORM TO:**

Melissa Lester, JSR Editorial Office
3300 Penrose Place 100
P.O. Box 9140
Boulder, CO 80301-9140
jsedres@gmail.com

To: Authors who have submitted a manuscript or material for publication. Because of current international copyright laws you are being asked to complete and return this form to the Editor of the publication in which your work will appear.

# TRANSFER OF COPYRIGHT AGREEMENT

**Copyright to the article entitled:**

"*Eocene paleoseismic record of the Green River Formation, Fossil Basin, Wyoming - implications of synsedimentary deformation structures in lacustrine carbonate mudstones*"

**Authored by:**

Balázs Törő and Brian Pratt

is hereby transferred to SEPM, to the extent transferable for publication in the Journal of Sedimentary Research.

To be signed by at least one of the authors (senior or corresponding, who agrees to have the authority and is responsible to inform the others, if any, or, in the case of a "work made for hire," the employer).

| | |
|---|---|
| Signature | Signature |
| Print Name | Print Name |
| Title, if not author | Title, if not author |
| Company or Institution | Company or Institution |
| Date | Date |

You must return this form granting SEPM the legal right to publish your work. Failure to assign copyright to SEPM prohibits us from publishing your work. SEPM is aware that, if you work for a government agency, or your work is publicly funded, it may be in the public domain and copyright is not transferable. That is why the form reads that copyright is "hereby transferred to SEPM to the extent transferable." You still must sign this form to give us permission to publish your work. If you have any questions, please contact the editor of the publication involved, or the SEPM Business Office.

By signing this document the author(s) acknowledges that he or she has obtained permission for any previously published content included in the article and that he or she must obtain written permission from SEPM before re-publishing any of the material or figures from the copyrighted article described above. If the author fails to obtain written permission the SEPM reserves the right to prohibit the author from publishing with SEPM in the future.

**Terra Nova**

**Published by Wiley (the "Owner")**

**COPYRIGHT TRANSFER AGREEMENT**

Date: 2015-03-12

Contributor name: Balázs Törő

Contributor address: Department of Geological Sciences, University of Saskatchewan, 114 Science Place, Saskatoon, SK S7N 5E2, Canada

Manuscript number: TER-2014-0107.R1

Re: Manuscript entitled Tectonically induced change in lake evolution recorded by seismites in the Eocene Green River Formation, Wyoming (the "Contribution")

for publication in Terra Nova (the "Journal")

published by John Wiley & Sons Ltd ("Wiley")

Dear Contributor(s):

Thank you for submitting your Contribution for publication. In order to expedite the editing and publishing process and enable the Owner to disseminate your Contribution to the fullest extent, we need to have this Copyright Transfer Agreement executed. If the Contribution is not accepted for publication, or if the Contribution is subsequently rejected, this Agreement shall be null and void.
**Publication cannot proceed without a signed copy of this Agreement.**

---

## A. COPYRIGHT

**1.** The Contributor assigns to the Owner, during the full term of copyright and any extensions or renewals, all copyright in and to the Contribution, and all rights therein, including but not limited to the right to publish, republish, transmit, sell, distribute and

otherwise use the Contribution in whole or in part in electronic and print editions of the Journal and in derivative works throughout the world, in all languages and in all media of expression now known or later developed, and to license or permit others to do so.

**2.** Reproduction, posting, transmission or other distribution or use of the final Contribution in whole or in part in any medium by the Contributor as permitted by this Agreement requires a citation to the Journal suitable in form and content as follows: (Title of Article, Contributor, Journal Title and Volume/Issue, Copyright © [year], copyright owner as specified in the Journal, Publisher). Links to the final article on the publisher website are encouraged where appropriate.

**B. RETAINED RIGHTS**

Notwithstanding the above, the Contributor or, if applicable, the Contributor's employer, retains all proprietary rights other than copyright, such as patent rights, in any process, procedure or article of manufacture described in the Contribution.

**C. PERMITTED USES BY CONTRIBUTOR**

**1. Submitted Version.** The Owner licenses back the following rights to the Contributor in the version of the Contribution as originally submitted for publication:

> **a.** The right to self-archive on the Contributor's personal website, place in a not for profit subject-based preprint server or repository, or in the Contributor's company/ institutional repository or archive. This right extends to both intranets and the Internet. The Contributor may not update the submitted version or replace it with the accepted or the published Contribution. The version posted must acknowledge acceptance for publication and, following publication of the final Contribution, contain a legend as follows: This is the pre-peer reviewed version of the following article: FULL CITE, which has been published in final form at [Link to final article]. Contributors are not required to remove preprints posted to not for profit preprint servers prior to submission of the Contribution.
>
> **b.** The right to transmit, print and share copies with colleagues, provided that there is no systematic distribution of the submitted version, e.g. posting on a listserve, network (including scientific social networks) or automated delivery.

**2. Accepted Version.** The Owner licenses back the following rights to the Contributor in the version of the Contribution accepted for publication:

**a.**The right to self-archive the peer-reviewed (but not final) version of the Contribution on the Contributor's personal website, in the Contributor's company/institutional repository or archive, and in certain not for profit subject-based repositories such as PubMed Central as listed at the following website:http://olabout.wiley.com/WileyCDA/Section/id-820227.html, subject to an embargo period of 12 months for scientific, technical and medical (STM) journals and 24 months for social science and humanities (SSH) journals following publication of the final Contribution. There are separate arrangements with certain funding agencies governing reuse of this version as set forth at the following website:http://www.wiley.com/go/funderstatement. The Contributor may not update the accepted version or replace it with the published Contribution. The version posted must contain a legend as follows: This is the accepted version of the following article: FULL CITE, which has been published in final form at [Link to final article].

**b.**The right to transmit, print and share copies with colleagues, provided that there is no systematic distribution of the accepted version, e.g. posting on a listserve, network (including scientific social networks) or automated delivery.

**3. Final Published Version.** The Owner hereby licenses back to the Contributor the following rights with respect to the final published version of the Contribution:

**a.** Copies for colleagues. The personal right of the Contributor only to send or transmit individual copies of the final published version in any format to colleagues upon their specific request provided no fee is charged, and further provided that there is no systematic distribution of the Contribution, e.g. posting on a listserve, network or automated delivery.

**b.** Re-use in other publications. The right to re-use the final Contribution or parts thereof for any publication authored or edited by the Contributor (excluding journal articles) where such re-used material constitutes less than half of the total material in such publication. In such case, any modifications should be accurately noted.

**c.** Teaching duties. The right to include the Contribution in teaching or training duties at the Contributor's institution/place of employment including in course packs, e-reserves, presentation at professional conferences, in-house training, or distance learning. The Contribution may not be used in seminars outside of normal teaching obligations (e.g. commercial seminars). Electronic posting of the

final published version in connection with teaching/training at the Contributor's company/institution is permitted subject to the implementation of reasonable access control mechanisms, such as user name and password. Posting the final published version on the open Internet is not permitted.

**d.** Oral presentations. The right to make oral presentations based on the Contribution.

**4. Article Abstracts, Figures, Tables, Data Sets, Artwork and Selected Text (up to 250 words).**

**a.** Contributors may re-use unmodified abstracts for any non-commercial purpose. For online uses of the abstracts, the Owner encourages but does not require linking back to the final published versions.

**b.** Contributors may re-use figures, tables, data sets, artwork, and selected text up to 250 words from their Contributions, provided the following conditions are met:

(i) Full and accurate credit must be given to the Contribution.

(ii) Modifications to the figures, tables and data must be noted. Otherwise, no changes may be made.

(iii) The re-use may not be made for direct commercial purposes, or for financial consideration to the Contributor.

(iv) Nothing herein shall permit dual publication in violation of journal ethical practices.

**D. CONTRIBUTIONS OWNED BY EMPLOYER**

**1.** If the Contribution was written by the Contributor in the course of the Contributor's employment (as a "work-made-for-hire" in the course of employment), the Contribution is owned by the company/institution which must execute this Agreement (in addition to the Contributor's signature). In such case, the company/institution hereby assigns to the Owner, during the full term of copyright, all copyright in and to the Contribution for the full term of copyright throughout the world as specified in paragraph A above.

For company/institution-owned work, signatures cannot be collected electronically and so instead please print off this Agreement, ask the appropriate person in your company/institution to sign the Agreement as well as yourself in the space provided below, and email a scanned copy to the Journal production editor. For production editor contact details, please visit the Journal's online author guidelines.

**2.** In addition to the rights specified as retained in paragraph B above and the rights granted back to the Contributor pursuant to paragraph C above, the Owner hereby grants back, without charge, to such company/institution, its subsidiaries and divisions, the right to make copies of and distribute the final published Contribution internally in print format or electronically on the Company's internal network. Copies so used may not be resold or distributed externally. However, the company/institution may include information and text from the Contribution as part of an information package included with software or other products offered for sale or license or included in patent applications. Posting of the final published Contribution by the company/institution on a public access website may only be done with written permission, and payment of any applicable fee(s). Also, upon payment of the applicable reprint fee, the company/institution may distribute print copies of the published Contribution externally.

## E. GOVERNMENT CONTRACTS

In the case of a Contribution prepared under U.S. Government contract or grant, the U.S. Government may reproduce, without charge, all or portions of the Contribution and may authorize others to do so, for official U.S. Government purposes only, if the U.S. Government contract or grant so requires. (U.S. Government, U.K. Government, and other government employees: see notes at end.)

## F. COPYRIGHT NOTICE

The Contributor and the company/institution agree that any and all copies of the final published version of the Contribution or any part thereof distributed or posted by them in print or electronic format as permitted herein will include the notice of copyright as stipulated in the Journal and a full citation to the Journal.

## G. CONTRIBUTOR'S REPRESENTATIONS

The Contributor represents that the Contribution is the Contributor's original work, all individuals identified as Contributors actually contributed to the Contribution, and all individuals who contributed are included. If the Contribution was prepared jointly, the Contributor has informed the co-Contributors of the terms of this Agreement and has

obtained their written permission to execute this Agreement on their behalf. The Contribution is submitted only to this Journal and has not been published before. (If excerpts from copyrighted works owned by third parties are included, the Contributor will obtain written permission from the copyright owners for all uses as set forth in the Journal's Instructions for Contributors, and show credit to the sources in the Contribution.) The Contributor also warrants that the Contribution contains no libelous or unlawful statements, does not infringe upon the rights (including without limitation the copyright, patent or trademark rights) or the privacy of others, or contain material or instructions that might cause harm or injury. The Contributor further warrants that there are no conflicts of interest relating to the Contribution, except as disclosed.

☐ I agree to the COPYRIGHT TRANSFER AGREEMENT as shown above and have obtained written permission from all other contributors to execute this Agreement on their behalf.

Contributor's signature (type name here): BALAZS TORO

Date: 2015/03/12

**SELECT FROM OPTIONS BELOW:**

◉ **Contributor-owned work**

○ U.S. Government work

*Note to U.S. Government Employees*
*A contribution prepared by a U.S. federal government employee as part of the employee's official duties, or which is an official U.S. Government publication, is called a "U.S. Government work", and is in the public domain in the United States. In such case, Paragraph A.1 will not apply but the Contributor must type his/her name (in the Contributor's signature line) above. Contributor acknowledges that the Contribution will be published in the United States and other countries. If the Contribution was not prepared as part of the employee's duties or is not an official U.S. Government publication, it is not a U.S. Government work.*

**[ ] U.K. Government work (Crown Copyright)**

*Note to U.K. Government Employees*

**For Crown Copyright this form cannot be completed electronically and should be printed off, signed in the Contributor's signatures section above by the appropriately authorised individual and returned to the Journal production editor by email.** For production editor contact details please visit the Journal's online author guidelines. *The rights in a contribution prepared by an employee of a UK government department, agency or other Crown body as part of his/her official duties, or which is an official government publication, belong to the Crown. Contributors must ensure they comply with departmental regulations and submit the appropriate authorisation to publish. If your status as a government employee legally prevents you from signing this Agreement, please contact the Journal production editor.*

**[ ] Other**

Including Other Government work or Non-Governmental Organisation work

*Note to Non-U.S., Non-U.K. Government Employees or Non-Governmental Organisation Employees*

**For Other Government or Non-Governmental Organisation work this form cannot be completed electronically and should be printed off, signed in the Contributor's signatures section above by the appropriately authorised individual and returned to the Journal production editor by email.** For production editor contact details please visit the Journal's online author guidelines. *If you are employed by the Department of Veterans Affairs in Australia, the World Bank, the World Health Organization, the International Monetary Fund, the European Atomic Energy Community, the Jet Propulsion Laboratory at California Institute of Technology, or are a Canadian Government civil servant, please download a copy of the license agreement from*http://authorservices.wiley.com/bauthor/faqs_copyright.asp *and return it to the Journal Production Editor. If your status as a government or non-governmental organisation employee legally prevents you from signing this Agreement, please contact the Journal production editor.*Name of Government/Non-Governmental Organisation:

_____

**[ ] Company/institution owned work (made for hire in the course of employment)**

**For "work made for hire" this form cannot be completed electronically and should be printed off, signed and returned to the Journal production editor by email.** For production editor contact details please visit the Journal's online author guidelines. *If you are an employee of Amgen, please download a copy of the company addendum from*http://authorservices.wiley.com/bauthor/faqs_copyright.asp *and return your signed*

*license agreement along with the addendum.*Name of Company/Institution:

_____

Authorized Signature of Employer:_____
Date:_____
Signature of Employee:_____
Date:_____

---

**Note to Contributors on Deposit of Accepted Version**

**Funder arrangements**

Certain funders, including the NIH, members of the Research Councils UK (RCUK) and Wellcome Trust have specific requirements for the deposit of the Accepted Version in a repository after an embargo period. Details of funding arrangements are set out at the following website: http://www.wiley.com/go/funderstatement. Please contact the Journal production editor if you have additional funder requirements.

Unless otherwise specified, the accepted version of the contribution must be self-archived in accordance with Wiley's Terms and Conditions for Self-Archiving at http://olabout.wiley.com/WileyCDA/Section/id-817011.html.